

**Some pages of this thesis may have been removed for copyright restrictions.**

If you have discovered material in Aston Research Explorer which is unlawful e.g. breaches copyright, (either yours or that of a third party) or any other law, including but not limited to those relating to patent, trademark, confidentiality, data protection, obscenity, defamation, libel, then please read our [Takedown policy](#) and contact the service immediately (openaccess@aston.ac.uk)

# Development of a passive MEG stimulus for measurement of the binaural masking level difference

LAUREN ELIZABETH GASCOYNE

Doctor of Philosophy

ASTON UNIVERSITY

June 2014

©Lauren Elizabeth Gascoyne, 2014

Lauren Elizabeth Gascoyne asserts her moral right to be identified as the  
author of this thesis

This copy of the thesis has been supplied on condition that anyone who consults it is understood to recognise that its copyright rests with its author and that no quotation from the thesis and no information derived from it may be published without appropriate permission or acknowledgement.

**Aston University**

**Development of a passive MEG stimulus for measurement of the binaural masking level difference**

**Lauren Elizabeth Gascoyne**

**Doctor of Philosophy**

**2014**

The ability to hear a target signal over background noise is an important aspect of efficient hearing in everyday situations. This mechanism depends on binaural hearing whenever there are differences in the inter-aural timing of inputs from the noise and the signal. Impairments in binaural hearing may underlie some auditory processing disorders, for example temporal-lobe epilepsies. The binaural masking level difference (BMLD) measures the advantage in detecting a tone whose inter-aural phase differs from that of the masking noise. BMLD's are typically estimated psychophysically, but this is challenging in children or those with cognitive impairments. The aim of this doctorate is to design a passive measure of BMLD using magnetoencephalography (MEG) and test this in adults, children and patients with different types of epilepsy. The stimulus consists of Gaussian background noise with 500-Hz tones presented binaurally either in-phase or 180° out-of-phase between the ears. Source modelling provides the N1m amplitude for the in-phase and out-of-phase tones, representing the extent of signal perception over background noise. The passive BMLD stimulus is successfully used as a measure of binaural hearing capabilities in participants who would otherwise be unable to undertake a psychophysical task.

Key words: Magnetoencephalography, binaural unmasking, auditory development, epilepsy.

## **Acknowledgements**

I would firstly like to thank my main supervisor Dr Caroline Witton for her excellent supervision, patience and encouragement throughout. I would also like to thank my Associate Supervisor Professor Paul L. Furlong for his valuable insight and feedback throughout the course of this PhD. Further thanks go to Professor Bruce Henning for his valuable contributions and participation during the stimulus development phase.

Lastly I want to say a big thanks to everyone who supported me along the way, from the postgraduate office, to the ABC, and to my husband and family who have always been encouraging and helped me keep my perspective. I am very grateful to everyone who helped me with my research.

# Contents

Acknowledgements.....	3
List of Figures .....	9
List of tables .....	13
List of abbreviations.....	14
<a href="#">Chapter 1: Introduction.....</a>	<a href="#">15</a>
1.1 Binaural perception and spatial hearing.....	15
1.1.2 Scene analysis.....	15
1.1.3 Cocktail party effect .....	16
1.1.4 Binaural unmasking.....	17
1.1.5 Binaural masking level difference (BMLD) .....	18
1.2 Masking .....	21
1.2.1 Masking mechanisms .....	22
1.3 The auditory brain.....	23
1.4 Measuring neuronal responses.....	24
1.4.1 Evoked and induced activity .....	24
1.4.2 The M100 .....	25
1.5 Masking effects on neurophysiological responses .....	26
1.6 Pitch salience and perception .....	26
1.6.1 Salience and masking .....	27
1.7 Aims.....	28
<a href="#">Chapter 2: General Methods .....</a>	<a href="#">29</a>
2.1 Introduction to psychophysics .....	29
2.1.1 Thresholds and signal detection .....	29
2.1.3 Staircase method .....	30
2.1.3 Correlational research.....	31
2.2 Magnetoencephalography.....	33
2.2.1 SQUIDS.....	34
2.2.2 Advantages and limitations of MEG.....	34
2.2.3 MEG systems.....	35
2.2.4 Data processing in Elekta system.....	35
2.2.5 Data processing in CTF system.....	36
2.2.6 MEG data collection.....	36
2.2.7 MEG and MRI co-registration.....	37
2.2.8 Source modelling.....	37
2.2.9 Normalisation of source model data .....	41

<a href="#">Chapter 3:</a> Exploring the N1m-P2m complex using different source localisation techniques .....	42
3.1 Introduction.....	42
3.1.1 Characteristics of the auditory N1-P2 response. ....	42
3.1.2 Component separation .....	43
3.1.3 Cortical sources .....	44
3.1.4 Measurement of the N1-P2 complex.....	45
3.1.5 Aim .....	46
3.2 Method.....	46
3.2.1 Participants .....	46
3.2.2 Auditory stimulus .....	46
3.2.3 MEG data collection and preprocessing .....	47
3.2.4 Analysis methods .....	47
3.3 Results.....	49
3.3.1 Evoked response example.....	49
3.3.2 Dipole fit example .....	50
3.3.3 ER beamformer example.....	51
3.3.4 Minimum Norm Estimation example.....	52
3.3.5 Talairach localisations .....	53
3.4 Discussion.....	63
<a href="#">Chapter 4:</a> Developing a MEG stimulus for passive measurement of the BMLD .....	66
4.1 Introduction .....	66
4.1.2 Signal .....	66
4.1.4 Factors for consideration .....	70
4.1.2 Aim .....	71
4.2 Method.....	71
4.2.1 Calibration of stimulus .....	71
4.2.2 Validity of N1m and N1 .....	71
4.2.3 The masked M100.....	72
4.2.4 Number of averages.....	72
4.3 Results.....	72
4.3.1 Calibration of stimulus .....	72
4.3.2 Validity of M100 .....	72
4.3.3 The masked N1m.....	75
4.3.4 Number of averages.....	76
4.4 Discussion.....	77
4.4.1 Calibration of stimulus .....	77

4.4.2	Validity of tone .....	77
4.4.3	The masked M100 .....	78
4.4.4	Number of averages .....	78
4.4.5	Further considerations: Inter-stimulus interval .....	79
4.4.6	Stimulus details .....	79
<b>Chapter 5:</b> Investigating a neural correlate of the psychophysical BMLD with an adult cohort .....		81
5.1	Introduction .....	81
5.1.1	The value of a neural correlate of the BMLD .....	81
5.1.2	Physiological considerations .....	82
5.1.3	The psychophysical BMLD .....	87
5.1.4	Aims .....	87
5.2	Method .....	87
5.2.1	Participants .....	87
5.2.2	Stimuli .....	88
5.2.3	Psychophysical assessment .....	89
5.2.4	MEG data collection .....	89
5.2.5	Psychophysics analysis .....	90
5.2.6	MEG sensor data analysis .....	90
5.2.7	MEG source data analysis .....	90
5.3	Results .....	92
5.3.1	Psychophysics .....	92
5.3.2	MEG sensor data .....	94
5.3.3	MEG source estimates .....	99
5.3.4	Computing the BMLD .....	107
5.4	Discussion .....	109
5.4.1	Key findings .....	109
5.4.2	Measuring the BMLD .....	110
5.4.3	Overall effects of hemisphere .....	110
5.4.4	Response morphology .....	111
5.4.5	The BMLD .....	112
5.4.6	Limitations of the analysis method .....	113
5.4.7	Limitations of the study design .....	114
5.4.8	Recommendations for further research .....	115
<b>Chapter 6:</b> Measuring the neural BMLD in typically developing children .....		116
6.1	Introduction .....	116
6.1.1	Auditory response development .....	116

6.1.2	Auditory system development.....	120
6.1.3	Factors affecting children’s performance .....	120
6.1.4	Stimulus effects on the auditory response .....	122
6.1.5	Practical considerations when recording children using MEG.....	124
6.1.6	Finding the BMLD .....	125
6.1.7	Aim .....	125
6.2	Method.....	125
6.2.1	Participants .....	125
6.2.2	Psychophysics procedure .....	126
6.2.3	MEG procedure .....	126
6.2.4	Stimulus.....	127
6.3	Results.....	127
6.3.1	Sensor data.....	127
6.3.2	Inverse estimates .....	133
6.3.3	Computing the BMLD.....	143
6.4	Discussion.....	144
6.4.1	Morphology.....	144
6.4.2	Group data .....	145
6.4.4	Neural BMLD validity.....	147
<a href="#">Chapter 7</a>	Binaural hearing in epilepsy: 10 case studies.....	149
7.1	Introduction .....	149
7.1.1	Epilepsies.....	150
7.1.2	Medications.....	152
7.1.3	M100 in epilepsy .....	153
3.1.4	Aim .....	154
3.2	Method.....	154
3.2.1	Participants .....	154
3.2.2	Stimulus.....	155
3.2.3	MEG data collection.....	155
3.2.4	Analysis.....	155
3.3	Results.....	155
3.4	Summary of patient data .....	176
3.5	Discussion.....	177
3.5.1	Evoked responses.....	177
3.5.2	Hemispheric effects .....	178
3.5.3	Types of epilepsy.....	179

3.5.4	Effects of medication .....	180
3.5.5	Potential effects of attention.....	180
3.5.6	Evaluation of methods .....	181
<a href="#">Chapter 8</a>	Discussion .....	182
	List of References.....	187
	Appendix 1 .....	207
	Appendix 2 .....	208
	Appendix 3 .....	209

## List of Figures

## Page

Figure 1.1	Illustration of the shape of the auditory filter, adapted from Wikimedia Commons.....	21
Figure 1.2	The auditory pathway, taken from Access Science, 2014.....	23
Figure 2.1	The relationship between stimulus, neural activity and perception, adapted from Ehrenstein & Ehrenstein (1999) p1212.....	31
Figure 2.2	The magnetoencephalography system.....	33
Figure 3.1	The main component peaks of the auditory evoked potential. Taken from Shahin et al. (2011) with permission.....	43
Figure 3.2	An example sensor level evoked response to a train of clicks, using a CTF MEG system.....	49
Figure 3.3	Dipole fit example for the N1m in left and right hemispheres.....	50
Figure 3.4	Dipole fit example for the P2m in left and right hemispheres.....	50
Figure 3.5	Half-head ER beamformer example for the N1m in left and right hemispheres.....	51
Figure 3.6	Half-head ER beamformer example for the P2m in left and right hemispheres.....	51
Figure 3.7	MNE example for the N1m in left and right hemispheres.....	52
Figure 3.8	MNE example for the P2m in left and right hemispheres.....	52
Figure 3.9	Mean co-ordinate values for dipole, ER beamformer and MNE for the N1m response in the left hemisphere.....	55
Figure 3.10	Plot of mean Talairach localisations for the dipole, ER beamformer and MNE in coronal and axial plane for N1m in left hemisphere.....	56
Figure 3.11	Mean co-ordinate values for dipole, ER beamformer and MNE for the N1m response in the right hemisphere.....	57
Figure 3.12	Plot of mean Talairach localisations for the dipole, ER beamformer and MNE in coronal and axial plane for N1m in right hemisphere.....	58
Figure 3.13	Mean co-ordinate values for dipole, ER beamformer and MNE for the P2m response in the left hemisphere.....	59
Figure 3.14	Plot of mean Talairach localisations for the dipole, ER beamformer and MNE in coronal and axial plane for P2m in left hemisphere.....	60
Figure 3.15	Mean co-ordinate values for dipole, ER beamformer and MNE for the P2m response in the right hemisphere.....	61

Figure 3.16	Plot of mean Talairach localisations for the dipole, ER beamformer and MNE in coronal and axial plane for P2m in right hemisphere.....	62
Figure 4.1	The binaural masking level difference.....	68
Figure 4.2	EEG and MEG response validity, example one.....	73
Figure 4.3	EEG and MEG response validity, example two.....	74
Figure 4.4	An evoked average timeseries demonstrating the differences between masked and unmasked dichotic and diotic tones when presented at the same level.....	75
Figure 4.5:	Evoked responses of different numbers of averages.....	76
Figure 5.1	Evoked response from one group of channels taken from the left temporal lobe from an example participant showing the M100 responses to each intensity of the tone.....	94
Figure 5.2	Scaled group mean N1m evoked amplitudes for the left hemisphere...	95
Figure 5.3	Scaled group mean N1m evoked amplitudes for the right hemisphere.	95
Figure 5.4	Group mean N1m evoked latencies for the left hemisphere.....	97
Figure 5.5	Group mean N1m evoked latencies for the right hemisphere.....	97
Figure 5.6	Mean Talairach localisations taken from the activations shown in the dSPM estimate for the largest dichotic trigger.....	100
Figure 5.7	Distribution of activation using the dSPM estimate for each participant for the largest dichotic trigger.....	101-3
Figure 5.8	Scaled group mean N1m timeseries amplitudes for the left hemisphere.....	104
Figure 5.9	Scaled group mean N1m timeseries amplitudes for the right hemisphere.....	104
Figure 5.10	Group mean N1m timeseries latencies for the left hemisphere.....	106
Figure 5.11	Group mean N1m timeseries latencies for the left hemisphere.....	106
Figure 5.12	Graph showing the linear trend of the correlation between the psychophysically derived BMLD and the neural BMLD extracted from the amplitude values at source.....	109
Figure 6.1	Evoked average for an example younger child showing the difference between the loudest dichotic and diotic responses.....	128
Figure 6.2	Evoked average for an example older child showing the difference between the loudest dichotic and diotic responses.....	128

Figure 6.3.	Evoked amplitude values for four younger children, showing values for the loudest dichotic and diotic tone stimulus over noise for both hemispheres.....	130
Figure 6.4	Evoked amplitude values for four older children, showing values for the loudest dichotic and diotic tone stimulus over noise for both hemispheres.....	131
Figure 6.5	Mean evoked latency values for the loudest dichotic and diotic tone stimulus over noise, taken from both hemispheres.....	132
Figure 6.6.	dSPM estimates for the younger group of participants (1, 2, 3 & 8), in response to the loudest dichotic trigger, shown for both hemispheres.....	133
Figure 6.7.	dSPM estimates for the older group of participants (4, 5, 6, & 7), in response to the loudest dichotic trigger, shown for both hemispheres.....	134
Figure 6.8	Overlaid timeseries data extracted from MNE for the left and right hemispheres of the group of younger children.....	135
Figure 6.9	Sensor level evoked response taken from the right temporal lobe for participant 3, using MNE software.....	136
Figure 6.10	Overlaid timeseries data extracted from MNE for the left and right hemispheres of the group of older children.....	137
Figure 6.11	Sensor level evoked response taken from the right temporal lobe for participant 7, using MNE software.....	138
Figure 6.12	Timeseries amplitude values for four younger children, showing values for the loudest dichotic and diotic tone stimulus over noise for both hemispheres.....	139
Figure 6.13	Timeseries amplitude values for four older children, showing values for the loudest dichotic and diotic tone stimulus over noise for both hemispheres.....	140
Figure 6.14	Mean raw latency values for the younger and older children taken from the MNE timeseries data.....	141
Figure 7.1	Patient sensor averages (top), Matlab timeseries plots (middle) and dSPM estimates (bottom) for the left (left column) hemisphere and right (right column) hemisphere responses to the loudest dichotic and diotic triggers.....	157
Figure 7.2	Patient sensor averages (top), Matlab timeseries plots (middle) and dSPM estimates (bottom) for the left (left column) hemisphere and right (right column) hemisphere responses to the loudest dichotic and diotic triggers.....	159

Figure 7.3	Patient sensor averages (top), Matlab timeseries plots (middle) and dSPM estimates (bottom) for the left (left column) hemisphere and right (right column) hemisphere responses to the loudest dichotic and diotic triggers.....	161
Figure 7.4	Patient sensor averages (top), Matlab timeseries plots (middle) and dSPM estimates (bottom) for the left (left column) hemisphere and right (right column) hemisphere responses to the loudest dichotic and diotic triggers.....	163
Figure 7.5	Patient sensor averages (top), Matlab timeseries plots (middle) and dSPM estimates (bottom) for the left (left column) hemisphere and right (right column) hemisphere responses to the loudest dichotic and diotic triggers.....	165
Figure 7.6	Patient sensor averages (top), Matlab timeseries plots (middle) and dSPM estimates (bottom) for the left (left column) hemisphere and right (right column) hemisphere responses to the loudest dichotic and diotic triggers.....	167
Figure 7.7	Patient sensor averages (top), Matlab timeseries plots (middle) and dSPM estimates (bottom) for the left (left column) hemisphere and right (right column) hemisphere responses to the loudest dichotic and diotic triggers.....	169
Figure 7.8	Patient sensor averages (top), Matlab timeseries plots (middle) and dSPM estimates (bottom) for the left (left column) hemisphere and right (right column) hemisphere responses to the loudest dichotic and diotic triggers.....	171
Figure 7.9	Patient sensor average (top), Matlab timeseries plots (middle) and dSPM estimates (bottom) for the right hemisphere responses to the loudest dichotic and diotic triggers.....	173
Figure 7.10	Patient sensor averages (top), Matlab timeseries plots (middle) and dSPM estimates (bottom) for the left (left column) hemisphere and right (right column) hemisphere responses to the loudest dichotic and diotic triggers.....	175

## List of tables

## Page

Table 3.1	Numbers of acceptable fits for dipole fitting, ER beamformer and MNE for both N1m and P2m responses.....	53
Table 3.2	Mean Talairach co-ordinates for N1m and P2m for dipole fitting, ER beamformer and MNE.....	54
Table 5.1	Psychophysics thresholds and BMLD values.....	93
Table 5.2	Talairach co-ordinates extracted for the dSPM estimate using the M100 response to the largest dichotic trigger.....	99
Table 5.3	Correlation table of the psychophysical BMLD value with the computed BMLD values from the timeseries amplitude and latency data.....	108
Table 6.1	Participant demographics and data acquisition.....	126
Table 6.2	Amplitude and latency values extracted from the timeseries data for the younger child group, demonstrating the difference between the largest dichotic and largest diotic tones.....	142
Table 6.3	Amplitude and latency values extracted from the timeseries data for the older child group, demonstrating the difference between the largest dichotic and largest diotic tones.....	142
Table 6.4	Psychophysical BMLD values of the whole sample population with available data compared with the amplitude and latency unmasking values extracted from sensor and source data.....	143
Table 7.1	Typical epilepsy medications and side effects.....	152
Table 7.2	Summary of patient data showing demographics, epilepsy and medication, and amplitude and latency values for N1m.....	176

## List of abbreviations

2AFC	2 alternative forced choice
ABR	auditory brainstem response
ASSR	auditory steady state response
BMLD	binaural masking level difference
CMR	comodulation masking release
EEG	electroencephalography
ERF	event-related field
ERP	event-related potential
HG	Heschl's gyrus
IID	inter-aural intensity difference
ILD	inter-aural level difference
IPD	inter-aural phase difference
ISI	inter-stimulus interval
ITD	inter-aural time difference
LEP	late evoked potential
MEG	magnetoencephalography
MLD	masking level difference
MLR	middle latency response
MSR	magnetically shielded room
SNR	signal – to –noise ratio
SQUIDS	super-conducting quantum interference device
SRT	speech reception threshold
SSP	signal space projection
SSS	signal space separation
STG	superior temporal gyrus
tSSS	temporal signal space separation

# Chapter 1:

---

## Introduction

Listening with two ears is an important ability which allows humans to identify from where sounds originate. Part of this ability also allows detection of a sound amongst background noise, known as binaural unmasking. Binaural unmasking capabilities vary between individuals, and may be affected by abnormalities in the auditory pathway, from the ear to the cortex. Disruption of the binaural unmasking mechanism may have a detrimental impact on a person's overall auditory perceptual abilities, hence it is important to gain an indication of the extent of the impairment. This thesis describes the development of a stimulus designed to objectively measure binaural unmasking at the cortical level, specifically in young people with neuronal abnormalities.

This introductory chapter begins with a description of binaural hearing and an explanation of the binaural masking level difference (BMLD), which measures the extent of binaural unmasking. Following this, a critical summary of how neuroimaging methods have been used to measure these mechanisms via specific brain activity will be presented. Lastly, a summary of the aims of this thesis will be presented.

### 1.1 Binaural perception and spatial hearing

#### 1.1.2 Scene analysis

When a sound signal reaches the ears, the brain uses two measures to distinguish from which direction a sound originates. These are called inter-aural time difference (ITD) and inter-aural level difference (ILD, also known as inter-aural intensity difference - IID).

ITD: As the sound signal reaches one ear before the other, specialised neurons within the brain can discriminate which ear received the sound first, which would indicate that the localisation of the sound is originating from that direction as it takes less time to travel to that ear. Conversely, the ear

that receives the sound later is the ear that is furthest away from the origin of the noise. Each potential sound location on the azimuth plane has a different ITD, for example a sound coming at 90 degrees to the head has an ITD of about 0.7ms, whereas a sound coming directly towards the front of the head has an ITD of 0ms (Litovsky et al., 1999). Although the time delays between the ears are tiny, coincidence detectors can detect the delays and then accurately localise the sound. ITDs are particularly effective at low frequencies, below about 1500Hz (Blauert 1985).

ILD: ILDs are highly frequency dependent and are significantly affected by the physiology of the head and shoulders, known as an 'acoustic shadow' (Litovsky et al., 1999) through attenuation of the waves before they can reach the ear farthest from the origin of the sound. Unlike light waves, sound waves are able to bend due to their longer wavelength, so when they reach the farthest ear from the source their intensity is reduced. This phenomenon is particularly effective at high frequencies, meaning the inter-aural level difference is greater above about 3000Hz (Litovsky et al., 1999) with ILDs reaching levels of 20dB for sounds originating from the side of the head (Litovsky et al., 1999). Like ITDs, specialized groups of neurons are 'tuned' to specific levels of intensity difference in the ears, which then translate into a localisation signal. In the natural free field, the ITDs and ILDs covary, and moving the head can alter the relationship between the auditory pathways to clarify the phase relationship and hence the source localisation (Bronkhorst & Plomp, 1988). Hawley et al., (2004) estimate that the binaural improvement is 3dB when the noise interferer is spatially separated by 90 degrees.

### **1.1.3 Cocktail party effect**

There are more ways to measure binaural hearing than those already mentioned. Hearing in noisy environments, also known as 'the cocktail party effect' (Cherry, 1953), is a subject that has been widely studied. This refers to how it can be tricky to distinguish voices from background noise due to masking effects. From a perceptual grouping perspective, the mechanism by which we separate a target noise or speech from the background interfering noise has been termed auditory scene analysis (Bregman 1990) and relies on the grouping of similar sounds into auditory streams. One

criterion of this grouping is spatial location of the sounds, so sounds that come from the same origin are grouped together and considered a stream (Bregman, 1990). Perceptual grouping can occur in two ways; simultaneous grouping or sequential grouping, depending on how the auditory system classifies the sound streams according to their similarities (Bregman, 1990).

#### **1.1.4 Binaural unmasking**

According to Hawley et al. (2004), the binaural advantage is 'robust in all spatial situations'. This could be largely due to binaural unmasking: the ability to hear a signal within noise. The major advantage of binaural unmasking is the ability to discern speech from a noisy background. This ability is important as it allows us to communicate effectively in everyday life, for example in environments such as busy classrooms.

It is difficult to hear a target sound at one ear when it is occluded by a masker, however if the masker is simultaneously presented to the other ear, the target sound then becomes audible (Egan, 1965). This is known as binaural unmasking or release from masking. Binaural unmasking relies on a difference in phase between the signal and the masker, which allows for easier identification of the signal (Hirsh, 1950; Jeffress et al., 1952). The notation used to identify these conditions are as follows: NOS0 represents the masker and signal being in-phase (homophasic) at both ears; NOS $\pi$  represents the signal at one ear being 180° out-of-phase (antiphasic). The antiphasic condition provides a percept of the sound widening (Licklider, 1948), making it the most intelligible phase relation for detecting a signal within noise. The phase relationships show there is more taking place than simply spatial localisation cues (Licklider, 1948).

The outer ear (pinna) is shaped to funnel the sound waves into the ear canal. The shape of the pinna is also very important for creating 'notches' in the sound, meaning that some spectral frequencies are attenuated while others are amplified, allowing the listener to identify the direction of the sound source (Hofman et al., 1998). The head, shoulders and body also create notches in the spectral frequencies of the sound, contributing further information about the location of the sound, particularly in the vertical plane (Blauert, 1985). This modulation of the sound wave by the head and

body is unique to each individual and is known as the 'head-related transfer function' (Middlebrooks et al., 1989).

#### **1.1.5 Binaural masking level difference (BMLD)**

Release from masking can be explained most easily with the idea of a signal, e. g. a tone, presented alongside a masking noise; the amplitude threshold at which the signal is just masked by the noise is called the masked threshold. The binaural masking level difference is a way of measuring the masked threshold as a function of the phase difference of signal and masker (Licklider, 1948). The masked threshold for hearing the signal when it is out-of-phase can be as low as 15dB in comparison to when in-phase (Durlach, 1963). According to Zwicker & Henning (1985) there are four factors which contribute to BMLDs; just noticeable differences (JNDs), binaural interaction and temporal effects in both simultaneous and non-simultaneous masking. By studying these factors, the authors revealed that there is a high degree of correlation between a participant's sensitivity to changes in inter-aural delay and changes in inter-aural level.

The binaural masking level difference can be easily measured in a lab situation, as the stimulus parameters are controllable. Zwicker & Henning (1984) found that the BMLD was highly dependent on the relative spectra of the signal and noise, and that the MLD was highest when within the narrowband of the masker. In one experiment, the narrowband masker was 100Hz wide, centred on a 250Hz frequency. The BMLD was 25dB when the signal was inside the masker band, and reduced to 3dB for a signal just 30Hz outside the masker band. The effect was more pronounced for the NoSpi condition than for the NoSo condition (Zwicker & Henning, 1984).

Historically, there are two main theories that attempt to explain the BMLD. Durlach's (1963) E-C model, and Jeffress' (1971) inter-aural difference model.

Perhaps the most widely known theory of binaural unmasking was Durlach's (1963) equalization-cancellation (E-C) theory. This theory states that the auditory system proportionally adjusts the levels of masker and signal until the masker is cancelled out and only the signal remains. Durlach's

model consists of three stages, these being initial filtering, E-C and decision. The E-C mechanism is activated by a binaural stimulus, and the decision stage involves a signal detector which operates on the input with the largest signal-to-noise ratio (SNR). However, E-C theory relies on certain assumptions, such as 'perfect precision' of the auditory system, and the existence of a 'selector mechanism' for stimulus modes. Importantly, the E-C mechanism will not work if the signal and masker are in the same inter-aural relation because the signal gets cancelled out as well as the masker (Durlach, 1963). To explain this, Durlach (1963) also assumes the E-C model is limited by small random errors, therefore justifying how it can account for data in most BMLD studies that use a Gaussian noise masker (Wightman, 1969).

The second model of binaural hearing is Jeffress' (1971) inter-aural difference model. Binaural cues result in perception of spatial separation of the signal and noise, and the noise on its own. The masking level difference is largest below 1500Hz where inter-aural phase difference is the prominent cue. When there is no inter-aural phase difference, it is presumed that the auditory system operates monaurally. In fact, Jeffress' model suggests there are two mechanisms of binaural hearing. One operates on time differences alone and relies on the firing rates of phase-locked neural fibres below about 1500Hz. The other is effective over the whole frequency range, utilises differences in time and intensity, and is likely to be affected by the total neural activity difference between the two ears. A major benefit of this model over Durlach's (1963) E-C model is that it not only accounts for inter-aural phase differences but also accounts for spatial localisation.

Wightman (1969) found that neither model fully accounted for his result of a negative BMLD. This occurred when the signal was less detectable when out-of-phase than when in-phase with the masker. Wightman suggested that this unusual result was due to an error in the experimental design and was not an auditory phenomenon per se, however this case demonstrates the difficulties that can be encountered when designing a suitable experiment to test binaural hearing.

More recent models of binaural hearing tend to focus on the neural firing mechanisms, and involve both the characteristic frequencies and coincidence detectors of neurons in the auditory cortex (e.g.

Stern & Trahiotis, 1996). These models are able to account for a greater variety of data including binaural sluggishness, localization and lateralization of sounds, as well as MLDs (Moore, 2008). Traditional models are also being merged with research from other more specific areas, for example Beutelmann et al. (2010) combined the E-C model with the standard speech intelligibility index (SII) (ANSI, 1997) to produce a binaural speech intelligibility model. The model predicted 'speech reception threshold' (SRT) in steady state noise very well for different noise source locations, degrees of hearing of loss, and various room types. Similarly Brandewie & Zahorik (2010) found that the speech reception threshold is improved if a person is accustomed to the specific acoustics of a room.

Within the field of binaural hearing there have been some discrepancies and disagreements. On the subject of a binaural advantage afforded by binaural unmasking, Hawley et al. (2004) mention their surprise that the binaural advantage was robust against interferers that were spatially separated when the binaural unmasking models used depend on a coherent masker. An example would be Durlach's E-C model (1963) which has the capacity to only cancel one interferer, however Culling et al. (2003) claim that models of binaural unmasking are in fact more robust to lower coherence than might be expected. On the other hand, Yost (1997) points out that binaural unmasking works in theory, however real-life sounds do not enter the ears already inter-aurally phase-reversed.

There may be other cues to localisation than binaural ones. The inner ear encodes sounds by their frequencies (Moore, 2008) which may have an influence over differentiation of sources of sound. However, one problem with this is that two sound sources might have frequency spectra that overlap. Hall et al. (1984) suggest the auditory system might compare the outputs of different filters in order to enhance signal detection. It is known, however, that the auditory system does use the amplitude fluctuations of a masker to assist in detection of a signal through auditory separation (Festen & Plomp, 1990). This is known as comodulation masking release and has been studied in terms of whether the mechanism is related to that for the BMLD (Cohen & Schubert, 1991). In a study by Feston & Plomp (1990), it was found that both speech-shaped noise and competing voice maskers lead to a lower threshold for speech reception when compared to steady-state noise due to masker amplitude fluctuations which allow the auditory system to separate the signals. Similarly, Hawley et

al. (2004) found that with a single interferer, as opposed to complex interferers, the signal becomes more exposed if the masker amplitude regularly fluctuates by large amounts.

## 1.2 Masking

Masking occurs when a background noise prevents the detection of a target signal. In the auditory system, frequency selectivity of a signal takes place in an overlapping array of band-pass filters in the cochlea. Each filter is centred on a particular frequency, however the sloping shape of the filter allows closely surrounding frequencies through, cutting them off at an intensity level of 3dB below the centre frequency. The bandwidth of the frequencies allowed through is known as the 'critical bandwidth'. The auditory system uses the filter with the same centre frequency as the signal for perception of the stimulus (see Figure 1.1 for an illustration of the auditory filter). Masking of the signal occurs when frequencies of noise that fall within the critical bandwidth also enter the filter.

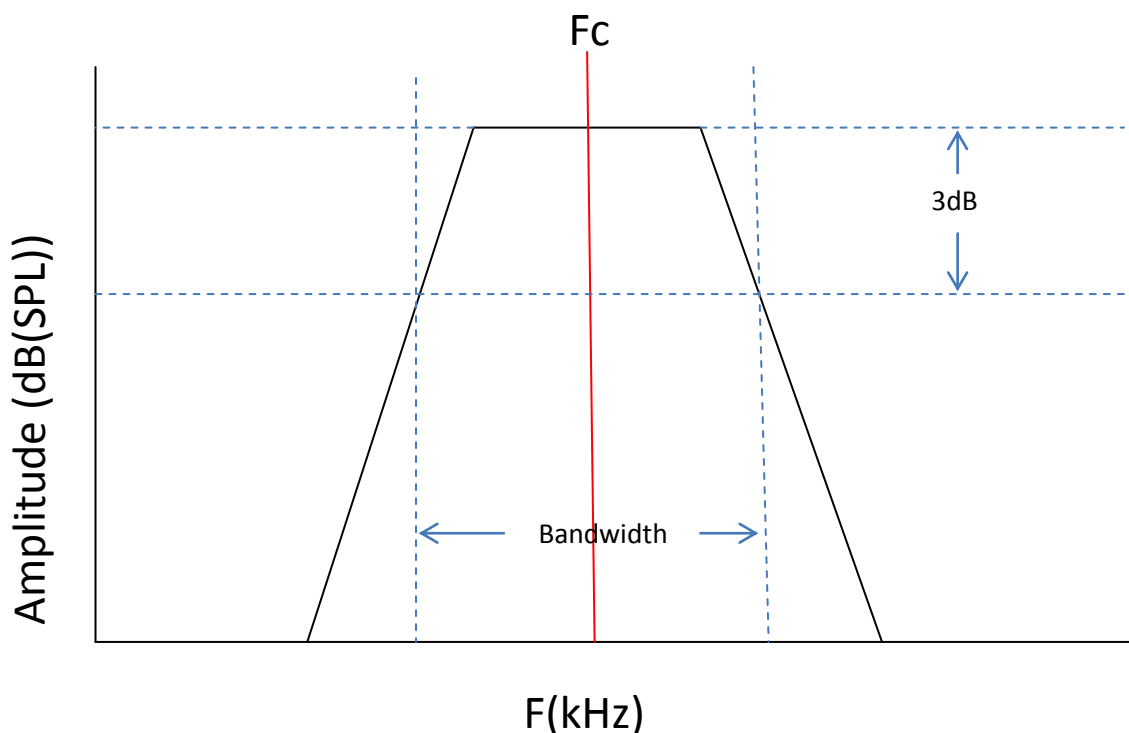


**Figure 1.1** Illustration of the shape of the auditory filter. Retrieved and adapted from Wikimedia Commons, 06.02.14. The bandwidth represents the upper and lower limits at which the signal entering the filter falls 3dB below the peak intensity at the characteristic frequency ( $F_c$ ), and so is not included in the signal output of the filter.

### 1.2.1 Masking mechanisms

Two possible mechanisms are thought to cause the masking effect in the auditory filter.

1. Excitation: The masker and signal energy are summed within the filter. If the amount of energy at this filter output is not above a certain level it may go undetected.
2. Suppression: The masker suppresses the signal energy which would be evoked if the signal was presented alone, particularly at masker frequencies far from the signal frequency (Oxenham & Plack, 1998).

When a signal and masker are presented at the same time and frequency, the signal will not be detected unless the summed amount of energy reaches a certain threshold level for detection in the auditory filter at that characteristic frequency. However, this effect can also be seen when the masker and signal are presented at the same time but at different frequencies, known as simultaneous masking. If the masker is close to the frequency of the signal, a 'spread of excitation' of the masker into the filter containing the signal still occludes it (Fletcher, 1940). If the masker is far away from the signal frequency, particularly if the masker has a lower frequency than the signal, there is an effect of suppression of the signal with excitatory activity at the signal location (Wightman et al., 1977; Weber, 1983). Originally the ideas of excitation and suppression of neural activity in masking were alternative theories, however more recently research has suggested that a combination of excitation and suppression occur depending on the frequencies of signal and masker (Delgutte, 1990; Moore & Vickers, 1997; Moore, 2004).

Further, there is an effect of non-simultaneous masking, involving a signal and masker that are presented at different points in time. The masker can still occlude the signal even if they are not simultaneous, taking the form of forward- or backward-masking. For a review of non-simultaneous masking please see Moore (2007).

### 1.3 The auditory brain

Auditory processing allows humans to discern different characteristics of sound waves and subsequently convert them into relevant information about the source and nature of the sound in the form of neuronal signals travelling to the primary auditory cortex and beyond. The central auditory pathway is shown in Figure 1.2, binaural processing takes place in the inferior colliculus and medial superior olive where the neurons cross hemispheres, creating both ipsilateral and contralateral pathways (Moore, 1991).

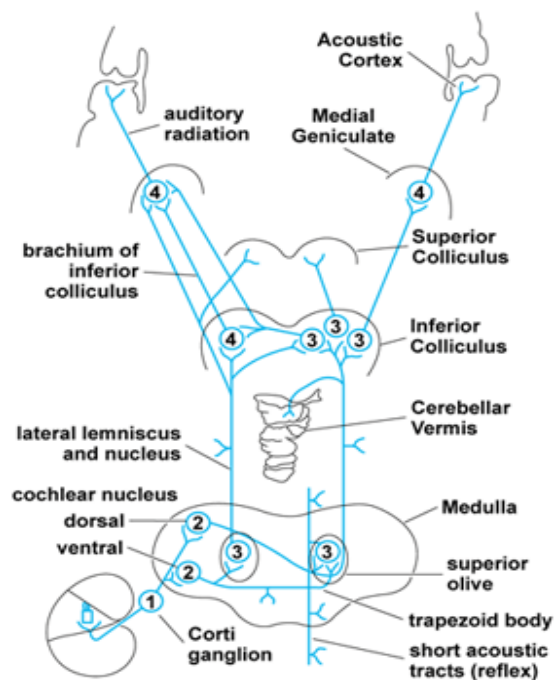


**Fig. 1.2** The central auditory pathway. Taken from accessscience.com, with permission.

The primary auditory cortex is thought to be organized tonotopically to mirror the structure of the cochlea. This means that neurons respond maximally to certain frequencies, known as their characteristic, or best, frequency, in the form of a tuning curve. A tuning curve is a threshold of hearing curve for a neuron (Hartmann, 1998). The tuning curve shows the smallest amplitude necessary to stimulate the neuron to fire 10% more than its spontaneous firing rate for its characteristic frequency (Hartmann, 1998).

## **1.4 Measuring neuronal responses**

The brain is made up of white matter, grey matter and cerebro-spinal fluid. The neurons comprising the grey matter include pyramidal cells, stellate cells and glial cells and are formed into long-range and short-range networks throughout the brain. Communication between neurons occurs via electrical and chemical transmission across synapses between neuronal axons and dendrites.

Neurons fire through a rapid change in potential in the synapse of the nerve. When a number of neurons fire simultaneously, this change in electrical potential can be detected using imaging techniques. Techniques to measure this electrical potential, (electroencephalography, EEG) or the magnetic field associated with this electrical potential, (magnetoencephalography, MEG) can be used to identify different features of the activity, including strength, neuronal orientation, location, and oscillatory speed. Further information about these techniques can be found in Chapter 2.

### **1.4.1 Evoked and induced activity**

Event-related brain activity in MEG or EEG is phase-locked to a stimulus and can be either induced or evoked. Induced signals constitute a change in the overall oscillatory pattern of the ongoing activity, and areas of neurons either synchronise or desynchronise depending on the stimulus (Pfurtscheller & Lopes Da Silva, 1999). Evoked responses are characterised by activity which is both phase and time-locked to the stimulus onset, for example responses to auditory stimuli such as clicks are usually well described in the literature as they tend to occur at similar times in different people. These evoked responses are visualised by averaging numerous trials of the same stimulus allowing the uncorrelated background noise to be removed and for the time-locked components of the response to be visualised (David et al., 2005). This approach relies heavily on the idea that an invariant stimulus will elicit an invariant neural response, and any variability between trials is taken as an effect of noise. There is debate in the EEG/MEG literature regarding the nature of evoked activity to unchanging stimuli. The traditional model of evoked responses states that the evoked activity occurs as a summation of the background noise and the additional energy generated as a result of stimulus detection. According to this model the amount of energy increase and decrease over time is what

constitutes evoked activity, and the amplitude and latency of the peak of this activity is what is measured as the evoked response (Coles & Rugg, 1995).

An alternative view is that there is no increase or decrease in power/energy at the onset of a stimulus, but instead the stimulus incites the neurons to align themselves in-phase (Jansen et al., 2003; Makeig et al., 2002). The averaged evoked response that we observe is simply a result of the phase 'resetting' of oscillators. The model does not support the idea of a focal localised source of activity, as it is a possibility that the response travels across the cortex like a wave. Additionally, it can be argued that phase-alignment is inherently frequency-dependent, due to the fact that if there was completely random or completely unified alignment across frequencies, then the response would not look like an event-related potential (ERP). Instead, each frequency band has its own speed of phase-alignment, with lower frequencies taking longer to align than higher ones (Burgess, 2012). So the amplitude and latency of the response in this case depends on the phase alignment process as opposed to the energy increase in the neuronal population.

#### **1.4.2 The M100**

The most basic cortical auditory response is known as the N1-P2 complex in EEG, and M100 (N1m) and M200 (P2m) responses in MEG. It occurs in response to the auditory cortex detecting the presence of a sound, and appears within the primary auditory cortex. The N1-P2 is so named because there is a deflection at approximately 100ms and another in the opposite polarity at 200ms. The N1-P2 has been widely studied in regard to its developmental trajectory. The P1 and a slow N2 response are the first to mature, around the age of two years (Martin et al., 2008; Ponton et al., 2002). These responses flank the N1-P2 response in latency. The N1 appears at around 7-9 nine years, and the P2 follows at early adolescence (Martin et al., 2008) when it becomes mature. Another study claims that the full N1-P2 response is mature by the age of 9 (Tonquist-Uhlen et al., 2003), showing some discrepancies within the literature. Further information on the N1/m and P2/m responses and their subsequent development can be found in Chapters 3 and 6 respectively.

## **1.5 Masking effects on neurophysiological responses**

Despite the masking effect occluding a signal at high noise levels, there is evidence to suggest that low levels of noise can actually improve signal detection (Zeng et al., 2000; Chatterjee & Robert., 2001; Schneider & Parker, 1990). This phenomenon is known as stochastic resonance (Moss et al., 2004; Ward et al., 2006) and the mechanism occurs by boosting the signal of a previously undetectable target through the addition of white noise. The noise provides a signal boost at all frequencies, including the signal frequency, meaning that the noise now reaches detection threshold and the extra energy at the signal frequency can be detected and isolated to unmask the signal.

The N1 auditory evoked response is thought to reflect signal detection (Hillyard et al., 1971; Alain & Tremblay, 2007). When a low-level masking noise is added to a tone, the amplitude (Alain et al., 2009; Okamoto et al., 2007; Galambos & Makeig, 1992a) and latency (Chueden, 1972) of the evoked N1 can increase. Alain et al. (2009) showed that low-level noise increased the amplitude of the N1m dipole response to high and low pitched tones compared to when they were presented alone, the effect was larger for lower pitched than high pitched tones. Alain et al. (2009) showed a larger noise-related change in the right hemisphere than the left.

Suggestions of mechanisms that might explain the effect of an increase in signal amplitude when paired with background noise include an increase in phase synchrony (Galambos & Makeig, 1992b) or reduction in latency jitter in N1m generation (Stufflebeam et al., 2000). Alain et al. (2009) suggest the possibility that background noise modulates activity from the efferent system, protecting the auditory system from loud noises (Huffman & Henson, 1990).

## **1.6 Pitch salience and perception**

Pitch is one of the main percepts in audition and is a direct result of the frequency, or periodicity, of a sound; an increase in the frequency leads to a perceived increase in pitch. The pitch onset response (POR) is an auditory evoked potential which arises when the periodicity of a sound goes

from being temporally unregular to regular without altering the other characteristics of the sound (Seither-Preisler et al., 2004). The POR has been shown to arise from the same neural generators as the N1-P2, and elicits a larger amplitude evoked response when the pitch is more salient (Seither-Preisler et al., 2004). The percept of pitch may be derived from different stimuli, such as complex harmonic pitches, and also binaural interaction such as Huggin's pitch (Cramer & Huggins, 1958) but sinusoidal waveforms provide the purest evocation of pitch, and so are commonly used to measure pitch salience (e.g. Penagos et al., 2004; Gutschalk et al., 2004). Salience can be defined as pitch strength or perceptibility. Since perceptibility is a subjective measure, some work has been undertaken to link the salience with the actual neuronal correlate of the sound (e. g. Sasaki et al., 2005) through comparison with behavioural measures. The measurement of evoked responses have shown that the perceptibility of a tone is directly related to the amplitude (Keidel & Spreng, 1965; Adler & Adler, 1989) and latency (Picton et al., 1977; Forss et al., 1993; Roberts, 2000) of the N1. So, the more perceptible the tone to the individual, the larger and earlier is the N1 evoked response peak. Hence, using these response variables, it is possible to measure the perceptibility of a tone in terms of its loudness through both the timing and size of the N1 peak.

### **1.6.1 Salience and masking**

The absolute intensity level of a tone is not the only way to measure its salience. The classical psychophysics study by Hawkins & Stevens (1950) shows that the SNR of the signal and masker is directly related to the salience of the signal, with a higher SNR leading to greater salience. Further, Phillips & Kelly, (1992) used cats to show that it was the relationship between the signal and masker that determined the size of the evoked potential rather than the absolute tone level. In this experiment, the ERP amplitude increased and latency decreased with increasing SNR as opposed to actual signal level, indicating that the morphology of the N1-P2 complex was driven primarily by SNR. Importantly, this study showed an effect on the N1 but not the P2 component of the N1-P2 complex (see Chapter 3 for further information on the N1-P2 complex).

Earlier work by this group (Phillips & Hall, 1986; Phillips, 1990) showed that the salience of the masked signal is greater in the auditory cortex than in the auditory nerve, which could be due to the

larger SNR in the cortex. The cochlear nerve fibres continuously discharge to the masker (Phillips & Kelly, 1992), but this does not occur in the cortex, thereby increasing the SNR of the masked signal at cortical level (Gibson et al., 1985). This could be because the neuron's dynamic firing range is available at the cortical level to encode the target signal without interference by the background masker (Billings et al., 2010).

## **1.7 Aims**

The main aims of this thesis are as follows:

1. Develop passive stimuli for use in MEG, designed to elicit evoked responses of varying salience according to their phase presentation over background noise.
2. Test the stimuli on an adult cohort and typically developing children.
3. Use the stimuli with a participant group with abnormal cortical function who would otherwise be unable to undertake a psychophysical task, to measure their binaural unmasking abilities.

# Chapter 2:

---

## **General Methods**

This chapter describes the methods and analysis techniques presented in this thesis. First is an introduction to psychophysics, followed by an explanation of the MEG system and the techniques used to analyse the neuronal responses. It will include a general description and evaluation of each method, including advantages and limitations, followed by a more detailed account of the data acquisition parameters and analysis techniques used.

### **2.1 Introduction to psychophysics**

The research discipline of psychophysics was first contrived by (Fechner 1860) as a quantitative method to measure the relationship between a stimulus and the subjective perception of that stimulus. Systematic variation of the characteristics of a sensory stimulus can result in a difference in perception which is then measured and quantified through the participant response. This behavioural response measurement can be used to characterise individual differences in experience between participants presented with the same stimuli, and conclusions and predictions about the link between perception and an objective stimulus can be drawn (Kingdom & Prins, 2010). Psychophysics is a broad field and consists of various methods to measure different aspects of perception and perceptual systems. This section will focus on measuring the perceptual threshold of a signal, and the uncertainty associated with this measurement.

#### **2.1.1 Thresholds and signal detection**

A sensory threshold value is defined as the amount of stimulus energy needed for detection of a stimulus 50% of the time (Bi & Ennis, 1998). Detection of a stimulus presence is known as the 'detection' or 'absolute' threshold, and detection of a stimulus change occurs at the 'discrimination' threshold (Kingdom & Prins, 2010). Signal detection theory begins with the assumption that the

inherent decision making required in perception involves a degree of uncertainty, and that this uncertainty can be empirically measured through the use of probabilities (Hartmann, 1998).

The aim of psychophysics is to provide an objective measure of perception, which can only be achieved if the participant is not able to use their subjective threshold. According to high-threshold theory (see Wickens, 2002), participants will naturally engage an internal threshold mechanism, whereby the signal must reach a subjective threshold before the participant will indicate a detection. Random fluctuations in either the stimulus or perception of the stimulus mean that the measure must be repeated a number of times and the average taken over a number of trials before conclusions can be drawn about a threshold. If the stimulus exceeds the criterion, the subject will respond 'yes', whereas if the stimulus falls below the criterion, the subject responds 'no'. This concept is useful when only one subject is used, however when comparing individuals each is likely to have a different criterion, hence a different idea of what constitutes a 'yes' response. In order to compare individual responses equivocably, it is important to use a task designed to avoid the involvement of the subject's threshold criterion. Rather than presenting a signal to which the participant is required to respond if they heard it or not, two alternative intervals are presented, with only one interval containing the signal. By obliging the participant to choose which interval they perceive to contain the signal, the problem of comparing individual internal thresholds is removed. By increasing and decreasing the intensity of the signal as a function of whether or not the participant heard it, the threshold can be found.

### **2.1.3 Staircase method**

The up-down staircase paradigm (Levitt, 1971), relies on the assumption that a signal with a larger intensity is more likely to be detected by the participant. This method is known as an adaptive procedure, as it increases the stimulus intensity when the participant makes an incorrect response, and decreases it when the participant makes a correct response, providing an estimation of the detection threshold relatively quickly. In this thesis, the 1-up 2-down staircase will be employed (Levitt, 1971). The participant starts the staircase with a signal that is suprathreshold, to which they

should respond correctly. At this point the signal intensity decreases in a step-wise fashion, with two steps down for every right answer, but then one step back up if the participant makes a wrong answer. The participant will make right answers until they reach their threshold, defined as a certain number of reversals, at which point they will no longer be able to hear the stimulus so if they guess their chances of getting a correct answer will fall to 50%. Once they give a wrong response, the program will increase the level of the signal again by one step, continuing in this fashion until they are making a right response 75% of the time. The signal intensity at this level is taken to be their absolute threshold. A number of difficulties may arise from using a paradigm such as this, for example using step sizes that are too large or too small can be too imprecise or can take too long. Also step-wise procedures can introduce the problem of the participant anticipating the steps and adjusting their responses (Levitt, 1971).

### 2.1.3 Correlational research

Modern psychophysics is widely used in conjunction with neuroscience methods, as a type of correlational research. Objective neuroscience methods are well-suited to studying neurophysiology, which can provide a useful complement to the study of behavioural psychophysics (e. g. Spillman & Ehrenstein, 1996; Gazzaniga, 1995; Epp et al., 2013). This partnership yields a robust insight into the interplay between stimulus, neural activity and perception, see Figure 2.1.

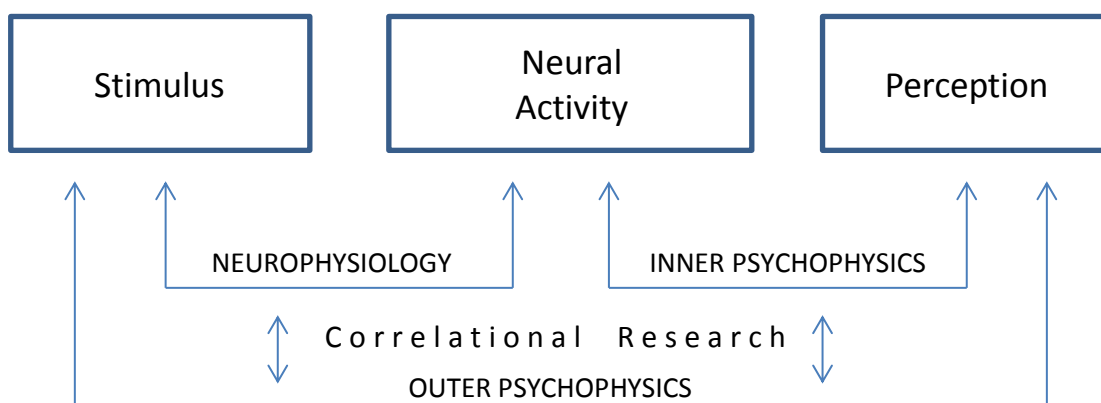


**Figure 2.1** The relationship between the stimulus, neural activity and perception. Adapted from Ehrenstein & Ehrenstein, (1999).

Neurophysiology is the basic neural response to a stimulus, inner psychophysics refers to the relationship between this neural activity and participant perception, while outer psychophysics shows the relationship between the stimulus and perception derived from the behavioural responses (this is psychophysics in the traditional sense). When these separate concepts are triangulated in their measurement, they are sometimes termed correlational research.

With the link between neuroscience and psychophysics strengthening, correlational research can be used to tap exclusively into mechanisms within a certain location in the brain, including evaluating poor perceptual performance in subjects with specific brain lesions. Fechner believed that the bodily responses, and the mental interpretation and perception of that response, are two facets of the same process, the measurement of which reflects a key goal of modern neuroscience. The techniques that will be used to measure the neural responses are described below.



### **2.2.1 SQUIDS**

The MEG system consists of an array of sensors arranged within a helmet, within which a participant places their head while sitting in a moveable chair. The sensors are known as superconducting quantum interference devices (SQUIDS). SQUIDS comprise superconducting loops that can acquire magnetic data at a temporal resolution high enough to study even the smaller responses of interest in the brain. To achieve this, the SQUIDS are surrounded by liquid helium inside the dewar to keep them at a temperature low enough to function efficiently. There are two types of sensor typically used; magnetometers and gradiometers. Each type is able to collect magnetic field data in a different way, allowing for a wider range of activity detection.

This degree of sensitivity means that the MEG system is susceptible to magnetic interference from the surrounding environment, and thus needs to be kept within a magnetically shielded room (MSR) to prevent interference from environmental magnetic noise.

### **2.2.2 Advantages and limitations of MEG**

**Advantages:** The SQUIDS are super-cooled using liquid helium inserted into the dewar to allow acquisition of data at low SNRs. The SQUIDS provide an excellent level of temporal resolution of neural activity akin to EEG. MEG also has superior spatial localisation capacity as opposed to EEG, due to the fact that responses are not subject to interference and distortion by the skull and scalp.

**Limitations:** MEG is only able to provide data from sources that are tangential to the surface of the cortex, leading to selective measurement of sulci-focussed activity. EEG provides more data, as it also is able to detect radial sources of activity. However, EEG has the disadvantage of distortion of the signal due to interference from the skull and scalp, therefore has poorer spatial localisation than MEG.

Historically, MEG also had the disadvantage of the participant having to sit very still throughout the recording in order for the spatial localisation to be accurate. However, new MEG systems, such as the

one used in the data collection for this thesis, are able to correct for any head motion during the recording.

### **2.2.3 MEG systems**

The studies in this thesis have been conducted on two different MEG systems. The first experimental study was conducted on the CTF MEG system (CTF, Vancouver), and the remaining studies were conducted using the Elekta Neuromag MEG system (Elekta Neuromag, Oy).

#### ***CTF***

This system had a sensor arrangement consisting of 275 axial gradiometer channels, and employed 3<sup>rd</sup> order noise cancellation. The system did not have any movement correction compensation, so any head movements that were 5mm from the starting position adversely affected the resulting coregistration and data. In these circumstances, if movements above 5mm were made, the data was discarded and re-recorded.

#### ***Elekta Neuromag***

This system had 306 channel sensors arranged in groups of three consisting of two planar gradiometers and one magnetometer. This system had the option of interference suppression called Internal Active Shielding (IAS), however this was not used in the course of these studies. This system also utilised an online movement tracking tool, known as continuous MaxMove which tracked head movements throughout the recording so they could be compensated for in the data reconstruction. These extra offline processes meant that the processing of the data post-recording was more complicated than the CTF system, for example it was necessary to run Maxfilter. These online and post-recording processes are described in more detail below.

### **2.2.4 Data processing in Elekta system**

#### ***Internal active shielding***

The shielding inside the door of the magnetically shielded room allows the subtraction of the signal from within the sphere around the helmet with the signal from inside the room. This means that any

signal outside the helmet is automatically cancelled out by the programme, so many artifacts from other body parts will not affect the data gathered from within the helmet.

### ***Maxfilter***

MaxFilter is a necessary processing step prior to visualisation of Elekta data. The step involves processing the data to remove any continuous head position information, and also to apply signal space separation (Taulu & Kajola, 2005). 'tSSS' (temporal Signal Space Separation) (Taulu & Simola, 2006) is a temporal and spatial filter which is able to suppress interference from both outside the dewar helmet, and also from very close to the sensors themselves, allowing for suppression of bodily sources of magnetic interference such as dental braces.

### ***Signal Space Projection (SSP)***

SSP is a tool used to suppress the varying amplitudes of magnetic disturbance that occur externally to the MEG scanner (Uusitalo & Ilmoniemi, 1997). The SSP vectors can be adjusted until the amplitudes are suppressed uniformly. These external background disturbances tend to be unchanging, meaning that the SSP vectors do not need to be altered at each recording as long as the SQUIDs are in the same position.

## **2.2.5 Data processing in CTF system**

### ***3<sup>rd</sup> order noise cancellation***

The higher order noise cancellation allows the sensors of the CTF system to be sensitive to the weak magnetic signals from the brain, while excluding larger interfering signals from outside the head. This process is undertaken in real time, during the recording, and alongside magnetic shielding enhances the noise reduction during the recording.

## **2.2.6 MEG data collection**

The participants were introduced into the MSR after being carefully screened for metal. Once settled in the MSR, a silent video was played for the participant while the channels were heated to reduce trapped flux. Just before the recording started, the participants were informed and notified that they would receive the sounds. They were reminded to stay as still as they could during the recording, and

were instructed to relax and continue to watch the silent video during the recording. This was to reduce fatigue and also visual stimulation was employed to reduce the amount of resting alpha activity which could produce artefacts in the resulting data. Data were collected at a sample rate of 1000Hz (Elekta) or 600Hz (CTF) and in the Elekta system an online average was also collected to check an auditory response was being elicited during the recording. In the Elekta system, the head position of the participant was continuously monitored throughout the recording. In the CTF system, any participant head movement of more than 5mm was signalled via a warning message, as this was the recommended maximum movement to ensure reliable source localisation of data.

### **2.2.7 MEG and MRI co-registration**

In order to measure exactly where activity is occurring within an individual's brain, an anatomical MRI of that individual's head is required. By using the digital headshape acquired before the MEG recording takes place, the MEG and MRI can be co-registered through a multiple-iteration least-error method of fitting the two headshapes together using a process based on an algorithm by Adjamian et al. (2004). For this process to be effective, distinctive landmarks such as the nose, inion and eyebrows need to be well defined during the head digitisation, as it is these which allow the MEG and MRI headshapes to be linked correctly. Sensors inside the MEG dewar record the position of the coils at all times during the recording, allowing the activity to be localised to a neural source within the anatomical MRI. The depth of the source is determined by the strength of the activity.

### **2.2.8 Source modelling**

Analysis of sensor data is useful as a way to discover certain response characteristics such as response timing and amplitude as well as providing a magnetic field pattern of the neural activity. An approximation of the general cortical area of the response can be made from the location of the MEG channels, however it is often useful to determine the depth or exact location of the source. Magnetic activity detected by sensors generally represents the location of the activity relative to the scalp, however there is always detection of activity by surrounding sensors not directly over the source which prevents the true source of the activity being determined in this way. By exploiting this spatial

filtering advantage, a timecourse of activity at a particular region within a specified time window can be extracted from a region of interest. Source space analysis can utilise a generic spherical head model to visualise the source of activity, or can use the individual's own brain structure by combining the MEG data with an anatomical MRI via coregistration.

Source modelling utilises recorded surface data to approximate the underlying source activity within the brain (Hämäläinen et al., 1993). The search for a solution to the 'inverse problem' is the definitive goal of MEG, as it allows a reasonable interpretation of the activity occurring within the brain without direct measurement of activity at the source. However, Helmholtz (1853) asserted that there are an infinite number of solutions to the inverse problem, so it is necessary to apply the limiting assumptions of a predetermined model, as discussed in the next section. More recently, Barnes et al. (2006) found that it is possible to get a good estimation of activity if sufficient information is provided.

#### ***2.2.8.1 Equivalent current dipole estimation***

Fitting equivalent current dipoles (ECD) to MEG data is a commonly-used technique to localise neural activity peaks to their original source. ECDs are fitted using an algorithm which determines the direction, strength and orientation of an evoked response. The dipole aligns to the strongest magnetic field pattern in the local vicinity, and by adhering to Fleming's 'right hand rule' determines the direction of the electrical activity associated with the neuronal firing in response to a stimulus. Dipole fitting is useful as they can give an accurate representation of the source location and strength of an evoked response (Lutkenhoner et al., 2003), and have been frequently used for this purpose in auditory analysis (e. g. Fujiki et al., 2002; Pang et al., 2003). However, certain limitations make them unsuitable for certain types of analysis. Dipoles cannot be used to visualise spectral power, making them suitable to localise evoked but not induced changes in activity. In addition to this, the technique has difficulties in localising extended sources, as the assumption is made that underlying sources of activity must be focal (Huang et al., 2006). Further, ECD models require some a priori

knowledge of the number of dipoles in advance of fitting, and can be susceptible to depth estimation errors in low SNR conditions (Ogura & Sekihara, 1993).

This example is useful to show that MEG is a more suitable technique to use when localising sources than EEG particularly for auditory responses. The auditory response occurs within the supratemporal plane on the Sylvian fissure, which lies tangentially to the skull (Lütkenhöner & Steinsträter, 1998). As MEG only detects sources tangential to the skull, the activity detected is restricted to this type of orientation, making MEG more suitable for detection of activity at the cortex, whereas EEG can detect deeper more radial sources which then become impeded by the skull and scalp surface (Virtanen et al., 1998).

#### ***2.2.8.2 Beamforming and virtual electrodes***

Beamforming is a technique used to spatially filter the signal from a sensor array. It is a commonly used technique in other fields, but has only been applied to MEG data relatively recently in the form of synthetic aperture magnetometry (SAM) (Robinson & Vrba., 1998). The source space, i. e. the brain volume, is divided into a 3D voxel grid. The beamformer amplifies the signal in each voxel individually, while also repressing the signal from the remaining voxels (Van Veen et al., 1997). This effectively cleans the data and reduces noise and other artefacts by ensuring that interference from surrounding voxels does not affect the signal in one individual voxel. When the beamformer is applied through a chosen time-frequency window to all the voxels in the grid, a reconstruction of the neuronal activity throughout the cortex can be created and the spectral power can be seen (Van Veen et al., 1997).

A further application of beamforming involves a reconstruction of the data within a single voxel or area of interest, showing the change in activity over a set period of time for that single location. This is known as virtual electrode analysis, as it resembles placing an electrode into the brain and recording the neuronal activity in that location. Virtual electrodes have been shown to be good models of auditory evoked responses (Sedley et al., 2012) and have the added advantage of being effective in low SNR circumstances.

### **2.2.8.3 Minimum Norm Estimation**

Minimum norm estimation (MNE) is an alternative method of localising activity by measuring the underlying current distribution comprising the primary and associated volume currents (Hämäläinen & Ilmoniemi, 1994). MNE employs a distributed source model by segmenting the cortical surface space into 6000-10000 vertices, each with a 3-dimensional current dipole fixed in location and orientation, but allowed to vary in amplitude. The forward solution is determined, which indicates how the underlying current distribution on the brain surface produces the pattern of activity in the sensor data. An inverse solution is then created by altering the amplitudes of the dipoles in the grid until a solution which matches the measured data and represents the least overall power is found. By requiring the solution to represent the least overall power, the method ensures the resulting current distribution estimation involves the minimal amount of neuronal energy possible.

Classical MNE (Hämäläinen & Ilmoniemi, 1994) has been criticised for having a superficial bias; meaning that activity distributions are biased towards the cortical surface. However, Hauk (2004) found this method to be particularly suitable for certain types of stimuli, such as more complex cognitive tasks, and noisy single-trial data involving unpredictable source locations. More modern versions of MNE (e. g. dSPM (Dale et al., 2000), sLORETA (Pascual-Marqui, 2002)) have countered the superficial bias using depth-weighting, and have also incorporated noise-normalisation, allowing visualisation of the activity significantly above background noise (Dale et al., 2000). One of the main advantages of MNE is that little a priori knowledge of the location and extent of sources is necessary as the activity distribution includes both focal and extended sources. Both MNE and ECD methods are able to approximate the location of the source (Hämäläinen and Hari, 2002), however ECDs do not take into account the possibility of extended sources. MNE has further advantages over dipole models as there is a much lower location bias with minimal modelling assumptions, and there is also the inclusion of noise normalisation.

### **2.2.9 Normalisation of source model data**

Data normalisation involves mapping a data range onto another scale. This is necessary for comparison of source model data from a number of different participants. This can be achieved through a normalised brain co-ordinate system known as the Talairach Co-ordinate system (Talairach & Tournoux, 1988). The data is scaled using a set of fixed points in the brain, which define the outside brain boundary as well as medial points known as the anterior and posterior commissure. These co-ordinates are identified individually for each subject, allowing the whole brain volume to be scaled into the Talairach co-ordinate system.

# Chapter 3:

---

## Exploring the N1m-P2m complex using different source localisation techniques

### 3.1 Introduction

This chapter will act as a brief introduction to the N1m and P2m in terms of definition and localisation of the response complex. Three techniques are used to analyse the same set of data with regards to the average localisation of the N1m and P2m in a group of participants. The chapter begins with an introduction to the nature and characteristics of the separate components of the response, and then is followed by a description and evaluation of the methods and analysis techniques used in the context of the results. Implications of these results will be discussed with regards to further studies involving analysis of this response complex.

#### 3.1.1 Characteristics of the auditory N1-P2 response

First described by Wolpaw & Penry (1975), the N1-P2 complex is an obligatory, temporal component of the cortical auditory response. In a conventional EEG setup, the N1-P2 consists of a negative deflection at ~100ms and a positive deflection at ~200ms in response to an onset of sound energy at 0ms (Davis et al., 1966; Näätänen & Picton, 1987). In MEG the response components are referred to as N1m (M100) and P2m (M200). These labels are used interchangeably.

The complete auditory evoked response is made up of a series of components occurring at different times and at different points throughout the auditory pathway after the onset of a stimulus. These components comprise auditory brainstem responses (ABRs), middle latency responses (MLRs) and late evoked potentials (LEPs). The N1-P2 complex is a late evoked potential, in contrast to the P1, a. k. a. P50 (M50 or P1m in MEG) which is a middle latency response, occurring at 50ms after the stimulus onset. The P1, N1 and P2 response components are labelled below.

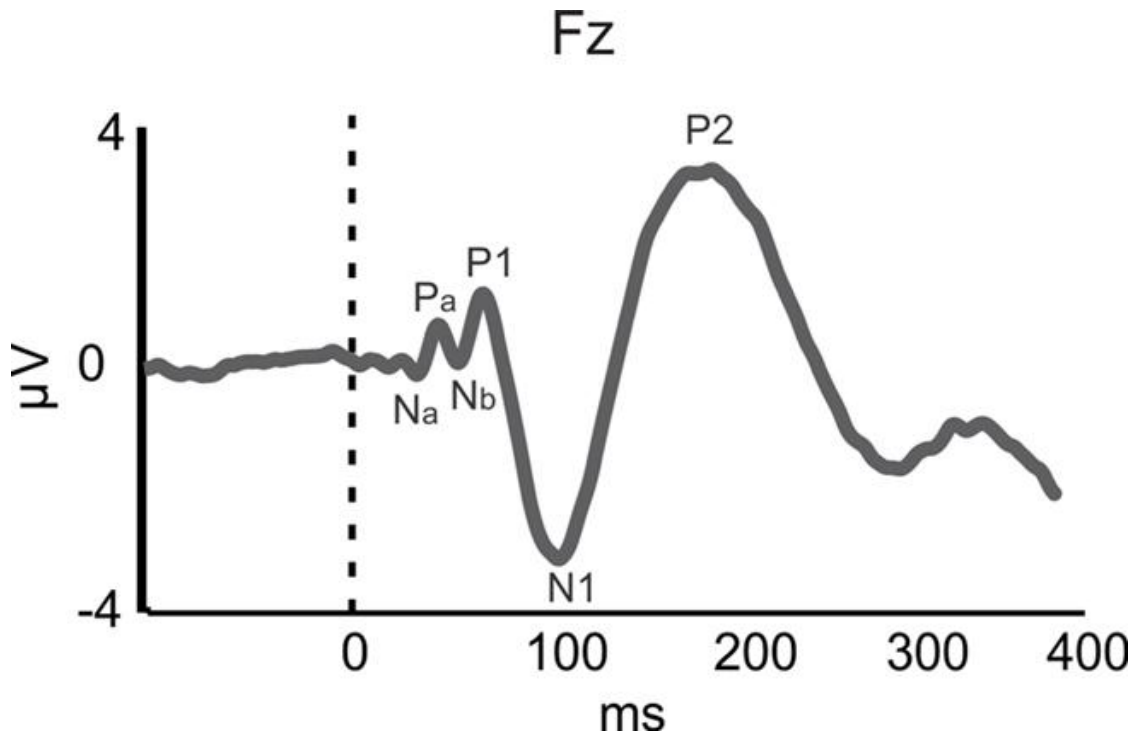


**Figure 3.1** The main component peaks of the auditory evoked potential. Taken from (Shahin 2011) with permission.

It is possible to manipulate the morphological characteristics of the N1-P2 complex in EEG and MEG through alteration of the stimulus attributes such as intensity and frequency. Stimulus attributes are integrated within the first 35ms after stimulus onset, leading to the visible modulation in the M100 at cortical level (Jenkins et al., 2011; Gage & Roberts, 2000). For example, a stimulus shorter than about 40ms will lead to an M100 of smaller amplitude (Gage & Roberts, 2000).

### 3.1.2 Component separation

The N1-P2 complex is elicited in response to a sound, however the N1 and P2 components are separable in terms of generators (Martin et al., 2008). The P2 is less well understood than the N1; they co-vary in latency and amplitude but are not necessarily linked (Martin et al., 2008). Further, there is research to suggest that N1 and P2 can be separated from each other in terms of their location (Lütkenhöner & Steinsträter, 1998), and also in the time course of their developmental trajectory (Crowley & Colrain, 2004). There have also been shown to be differences between these

response components in the context of sleep, as the N1 decreases in amplitude with sleep onset, whereas the P2 increases in amplitude (see Crowley & Colrain, 2004).

### **3.1.3 Cortical sources**

Some early MEG studies identified the source of the N1m to within both primary and secondary auditory cortex (e. g. Elberling et al., 1982; Hari, 1983; Reite et al., 1994). More recently, the N1m sources are thought to include supratemporal sources located in the planum temporale (PT) in MEG (Pantev et al., 1995; Lütkenhöner & Steinsträter, 1998), corroborated with intracranial measurements (Liégeois-Chauvel et al., 1994; Howard et al., 2000). Howard et al. (2000) used intracranial recordings to show that a binaural click train activates a number of inter-connected auditory areas extending into the posterior lateral superior temporal area. Further, both Lavikainen et al. (1994) in MEG and Giard et al. (1994) in EEG found additional frontal and parietal generators of the N1m/N1 component.

The study by Lutkenhoner & Steinstrater (1998) involved extensive analysis of the N1m-P2m response in one human subject. It was confirmed that the planum temporale (PT) is the dominant contributor to the N1m, however a number of generators are involved in this process. The study also revealed that P2m originates from, or near to, Heschl's gyrus (HG). This study has been very influential in the literature due to its depth of analysis, however the drawback to this is the fact that only one subject was used to find these data.

It is well-known that the N1-P2 complex produces an evoked response in both hemispheres, even when the stimulus is presented monaurally, with the contralateral response being larger and earlier than the ipsilateral response (Mäkelä, 1988). This response pattern has also been seen when using binaural stimuli (Tiihonen, Hari et al., 1989), and in responses to binaural tone signals under different monaural masking conditions, such as continuous speech, music and intermittent noise (Hari & Mäkelä, 1988).

### 3.1.4 Measurement of the N1-P2 complex

The N1-P2 complex has most frequently been localised using the dipole fitting technique in both EEG (Ponton et al., 2002) and MEG (Albrecht et al., 2000; Lutkenhoner et al., 2003; Fujiki et al., 2002). Dipoles have also been used to measure the auditory N1m response in children (Pang et al., 2003) and to determine language dominance alongside later AEF components (Merrifield et al., 2007).

Despite their prevalence in past literature there are number of drawbacks to using dipoles for localisation, some of which have been outlined in Chapter 2. As the cortical auditory response consists of two simultaneous evoked responses, one in each hemisphere, a simultaneous two-dipole model has been utilised successfully (Herdman, et al., 2003; Ponton et al., 2002), however some methods involved fitting a dipole to one hemisphere at a time, and/or restricting the location to a subset of channels in each hemisphere (e. g. Pekkonen et al., 1995). Drawbacks to this technique include a requirement of a priori estimation of the number and location of dipole sources and an assumption of focality.

Other analysis methods that have recently been used in analysing the N1-P2 response include event-related beamformers (Cheyne et al., 2007). This is a method of spatially filtering the data, and provides a good source model of spectral power, also providing superior artefact reduction than dipole models (for further information on beamformers please see Chapter 2). One potential drawback to the whole-head beamformer method is that any correlated sources may be suppressed, making it potentially unsuitable for the auditory cortical response which consists of two correlated hemispheric sources. Despite this theoretical drawback, studies have shown that under some circumstances, such as high SNR (Quraan et al., 2011) beamformers are resistant to spatially separated correlated sources. Alternatively, applying a beamformer to each hemisphere separately is another method of using this technique, and has previously been used successfully in localisation (Herdman et al., 2003; Witton et al., 2012).

Another alternative technique used to localise the N1-P2 complex is minimum-norm estimation (MNE). See Chapter 2 for a summary of the theoretical basis behind classical MNE and its later

advancements including noise normalisation and depth-weighting (Dale et al., 2000). This method uses a distributed dipole model to identify the range of activation in a cortical area, and like the beamformer method requires no a priori knowledge of the location of the sources. MNE has been successfully used to localise and characterise evoked responses in the auditory cortex (Gilmore et al., 2009) as well as other brain areas (von Leupoldt et al., 2010; Cicmil et al., 2014). MNE is useful for visualisation of the response timeseries at every vertex within a cortical region of interest, negating the problem of overly constraining the source localisation (Hämäläinen & Hari, 2002).

### **3.1.5 Aim**

The overall aim of this study is to evaluate the equivalency of the localisation abilities of each of three analysis methods; dipole fitting, event-related beamformers, and minimum-norm estimation when localising the N1m and P2m auditory evoked responses.

## **3.2 Method**

### **3.2.1 Participants**

Eleven adults (seven females) took part in the study. The age range was 26-71. No participants reported a history of hearing impairment or neurological problems, although two participants would be considered experienced listeners.

### **3.2.2 Auditory stimulus**

The MEG auditory stimulus consisted of a train of clicks comprising 200 trials presented diotically. The duration of each click was 5ms, with a 1ms rise and fall time, with an interstimulus interval of 1200ms which was jittered randomly by up to 200ms.

### **3.2.3 MEG data collection and preprocessing**

MEG data were acquired using a 275-channel whole-head CTF MEG system (Vancouver) with axial gradiometers and 3<sup>rd</sup> order noise cancellation. Data were sampled at a rate of 600Hz. The participants were asked to remain alert but still during the recording.

After the recording, the data were powerline-filtered with a notch filter at 50Hz, off-line corrected for baseline drift and subdivided into epochs of 1000ms each, comprising 500ms pre- and post-trigger. The epochs were carefully visually screened and any epochs containing artefacts such as eye movements were removed from the dataset. An average of 32 epochs per dataset were removed in this manner. Evoked averages were computed, which were then band-pass filtered between 1-30Hz.

### **3.2.4 Analysis methods**

All participants had a structural MRI available for the dipole fitting and ER beamformer methods, two participants did not have an MRI available for the MNE analysis. The structural MRI was spatially coregistered with the participant's MEG data using a modified version of the programme created by Adjamian et al. (2004).

#### ***3.2.4.1 Dipole source modelling***

The dipole fitting program used was the CTF DipoleFit software, which utilises a least-square minimisation method. The dipole field pattern was used to decide at what latency the response should be modelled, both the N1m and P2m responses were modelled separately. The N1m was chosen as the strongest field pattern within the range of 70-140ms and the P2m was chosen as the strongest opposite field pattern between 140-250ms. Where possible both hemispheres were modelled simultaneously. Dipole model fits were accepted according to their location and error value. Only dipole activations which fell within the superior temporal gyrus, near to or posterior to Heschl's gyrus, and had <15% error value were accepted. The dipole co-ordinates and error values were noted, and the co-ordinates were converted into Talairach space for each participant.

### **3.2.4.2 ER beamformer**

Event-related beamformer analysis was undertaken using a similar method to that reported by Cheyne et al. (2007). The CTF beamformer software and Matlab were used to perform the computations. The time windows chosen for the beamformer analysis were based on pilot spectrograms of evoked activity (see Appendix 1 for examples). The spectrograms showed that the power was mostly based in the lower frequencies, so the beamformer was performed within the 4-30Hz frequency band, encompassing the theta (4-8Hz), alpha (8-12Hz) and beta (13-30Hz) activations. The time windows chosen from the pilot spectrograms were 0-200ms for the N1m and 50-250ms for the P2m responses. ER beamformer was performed on the datasets using half-head channels, computing each hemisphere separately. A multi-sphere head model for each participant was derived from their outer skull surface (Huang et al., 1999). The ER beamformer peaks were computed using the latency of the average sensor data, filtered into the frequency band of choice. Beamformer peaks were accepted as the source closest to Heschl's Gyrus within the first 5 peaks of activation identified by the program within each hemisphere. Sources were included unless they were outside the temporal or parietal lobe. The co-ordinates for the ER beamformer were noted and converted into Talairach space (Talairach & Tournoux, 1988) for each participant.

### **3.2.4.3 Minimum Norm Estimation**

An anatomical MRI reconstruction was created. The surfaces were rendered using Freesurfer (Fischl, 2012; Dale et al., 1999; Fischl et al., 1999) and a headshape was created using Elekta software (Elekta Neuromag, Helsinki, Finland). The headshape was coregistered with the MEG polhemus points using a modified version of a surface-matching technique (Adjamian et al., 2004). MNE was used to define the inverse solution to the measured MEG data using the reconstructed MRI, and the dSPM activity distribution was visualised on the inflated cortex (Dale et al., 2000). A noise covariance of the pre-trigger baseline data was used to threshold the MEG data so only activity that was significantly larger than background noise was displayed. Each hemisphere was visualised separately, and the strength of the activity in the primary auditory cortex over time was used as a guide to the latency of the

M100 and M200 evoked components. When a suitable latency was decided for each component, the vertex containing the largest amplitude response for each component at that latency was identified. The Talairach co-ordinates for that vertex were identified. Two fewer participant MRIs were available than for the ER beamformer and dipole fit analyses due to unsuitable MRI file formats, totalling 9 participants for the MNE analysis.

### 3.3 Results

#### 3.3.1 Evoked response example

In Figure 3.2, the M50, M100 and M200 components represent the magnetic counterparts of the auditory evoked potentials of P1, N1 and P2 respectively, as shown in Figure 3.1.

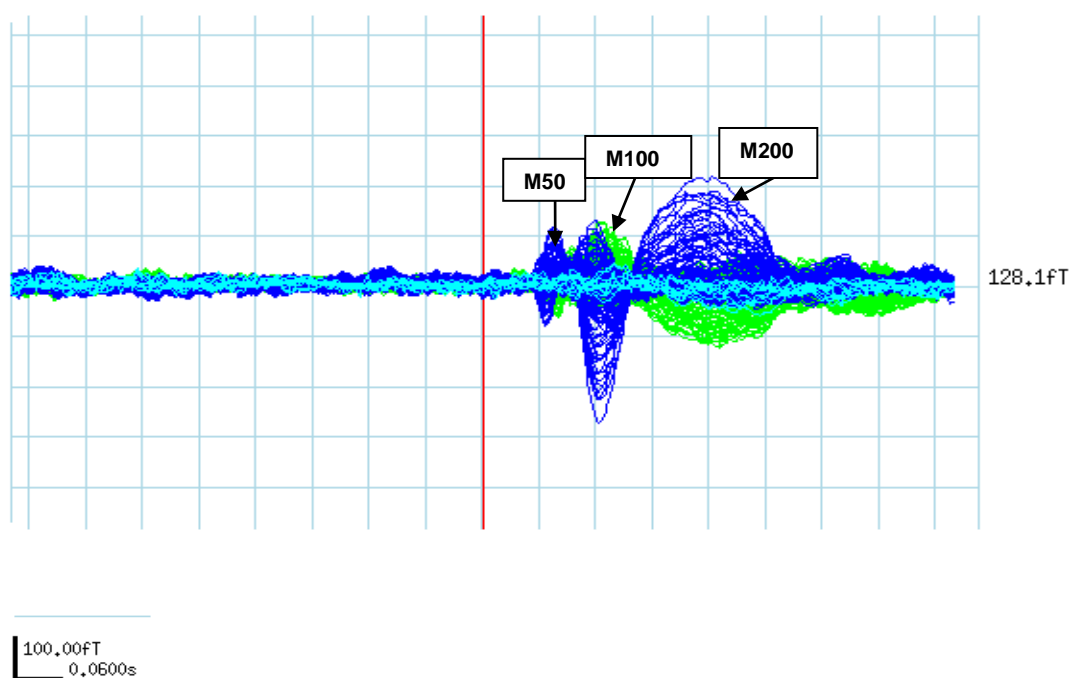


**Figure 3.2** A typical evoked response at sensor level. The figure includes all the channels from the CTF MEG system. The red line indicates the trigger onset, the blue channel overlays represent the left hemisphere and the green overlays represent the right hemisphere channels. The turquoise channels overlays represent the vertex channels. The M50, M100 and M200 components are labelled.

### 3.3.2 Dipole fit example

Figures 3.3 and 3.4 show an example dipole fit for one typical participant.

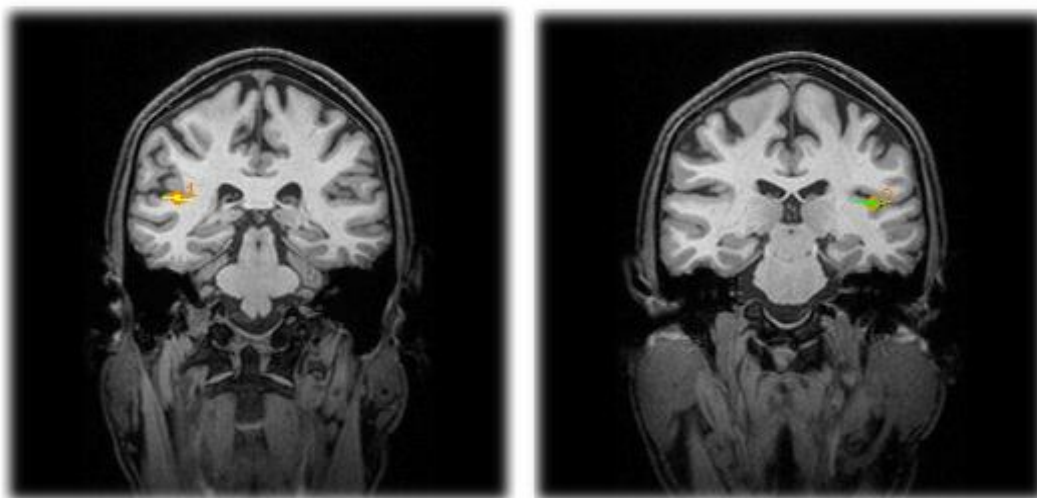


**Figure 3.3** Dipole fit example for the N1m in left and right hemispheres. Created using DipoleFit software as part of the CTF software package and shown in the coronal plane. Dipoles were fit simultaneously in both hemispheres, N1m latency is 120ms, dipole fit error is 9.2% (shown).

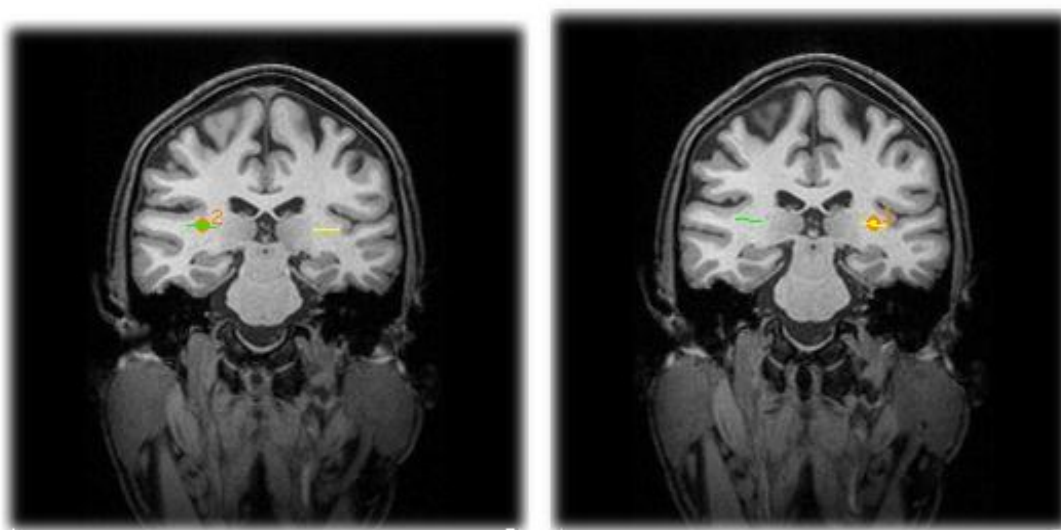


**Figure 3.4** Dipole fit example for the P2m in left and right hemispheres. Created using DipoleFit software as part of the CTF software package and shown in the coronal plane. Dipoles were fit first for the right hemisphere and second for the left hemisphere, P2m latency is 220ms, dipole fit error is 7.8% (shown).

### 3.3.3 ER beamformer example

Figures 3.5 and 3.6 show an example half-head ER beamformer result for one typical participant.



**Figure 3.5** Half-head ER beamformer example for the N1m in left and right hemispheres. Created using the CTF beamformer software and shown in the coronal plane. Beamformer activations were computed separately for each hemisphere, at the latency of 125ms, within a window of 4-30Hz. The beamformer window used was 0-200ms.

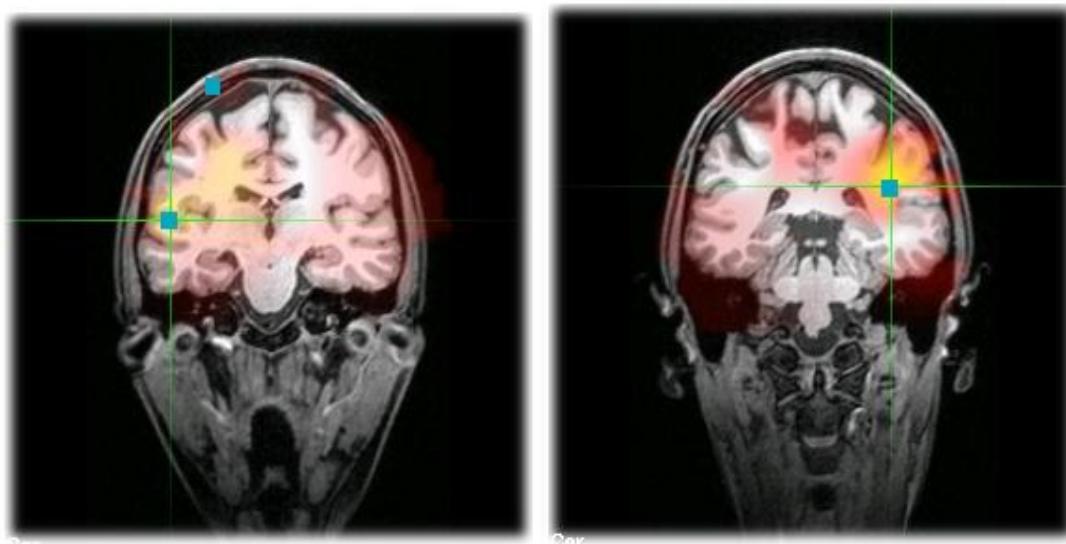


**Figure 3.6** Half-head ER beamformer example for the P2m in left and right hemispheres. Created using the CTF beamformer software and shown in the coronal plane. Beamformer activations were computed separately for each hemisphere, at the latency of 200ms on the left and 203ms on the right, within a window of 4-30Hz. The beamformer window used was 50-250ms.

### 3.3.4 Minimum Norm Estimation example

Figures 3.7 and 3.8 show an example MNE result for one typical participant

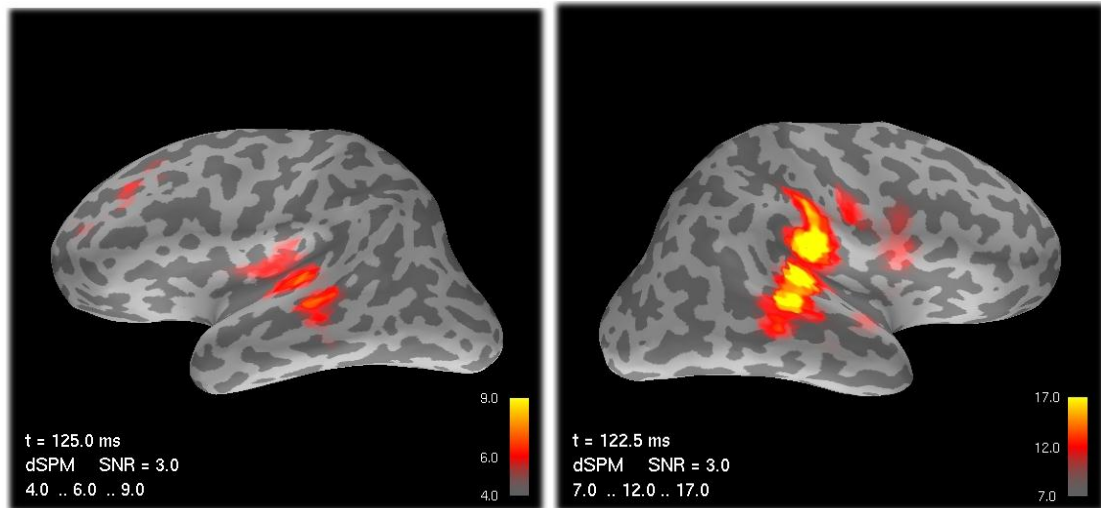


**Figure 3.7** MNE example for the N1m in left and right hemispheres. Created using Freesurfer and MNE software and shown on an inflated cortex. MNE activations were computed for the whole distributed dipole model. Latencies are shown, thresholds are chosen to optimise visualisation of the activity.

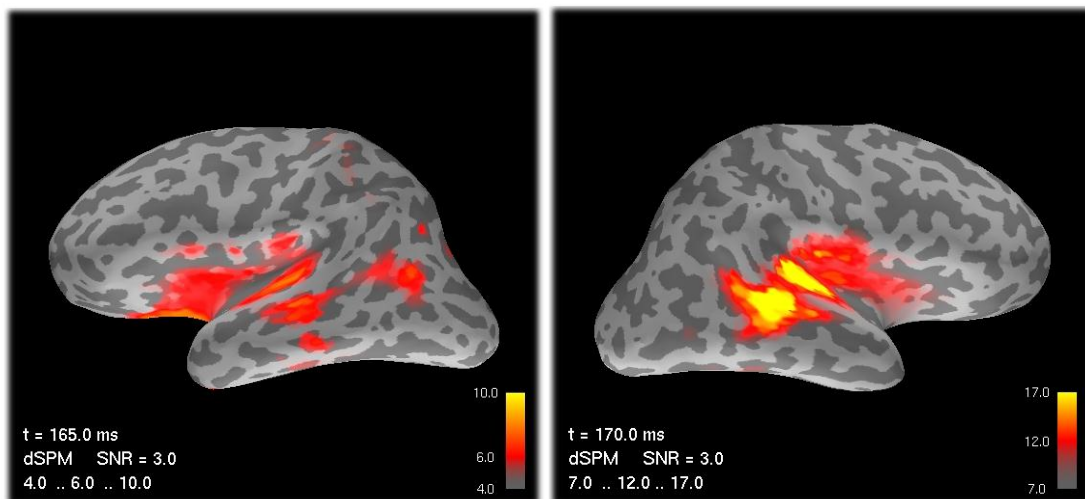


**Figure 3.8** MNE example for the P2m in left and right hemispheres. Created using Freesurfer and MNE software and shown on an inflated cortex. MNE activations were computed for the whole distributed dipole model. Latencies are shown, thresholds are chosen to optimise visualisation of the activity.

As described in subsection 3.1.3, the N1m and P2m sources are distributed, with some secondary generators located within the parietal lobe, this spread of activity can be seen in the beamformer and MNE methods as they are able to visualise the distribution of activity.

### 3.3.5 Talairach localisations

The Talairach co-ordinates were computed for the acceptable fits for each method for each individual. Table 3.1 shows the number of acceptable fits found for each method and response component.

Response component	Hemisphere	Dipole (N=11)	ERBF (N=11)	MNE (N=9)
N1m	Left	7	9	9
	Right	5	9	9
P2m	Left	6	9	9
	Right	7	9	9

**Table 3.1** Numbers of acceptable fits for dipole fitting, ER beamformer and MNE for both N1m and P2m responses. See relevant Method subsections for the definition of an acceptable fit for each method.

The mean Talairach co-ordinates for each method are shown in Table 3.2 for each hemisphere, analysis method and response component separately.

	LEFT HEMISPHERE			RIGHT HEMISPHERE		
<b>N1</b>	<b>X</b>	<b>Y</b>	<b>Z</b>	<b>X</b>	<b>Y</b>	<b>Z</b>
Dipole	-47.74	-23.46	14.58	52.54	-27.39	17.54
ERBF	-46.4	-33.66	13.18	53.23	-27.03	34.98
MNE	-46.23	-31.71	10.88	51.48	-23.19	5.89
<b>P2</b>	<b>X</b>	<b>Y</b>	<b>Z</b>	<b>X</b>	<b>Y</b>	<b>Z</b>
Dipole	-42.66	-20.31	15.9	40.63	-22.27	9.57
ERBF	-54.77	-20.96	12.87	52.97	-26.67	16.38
MNE	-49.8	-26.81	3.9	47.44	-16.2	7.67

**Table 3.2** Mean Talairach co-ordinates for N1m and P2m for each source localisation method. X represents the left-right direction, Y represents the anterior-posterior direction, Z represents the superior-inferior direction.

The mean Talairach localisations and their respective 95% confidence intervals are considered for each response component and hemisphere separately. Figures 3.9 and 3.10 show the mean localisations for the N1m in the left hemisphere, Figures 3.11 and 3.12 show the mean localisations for the N1m in the right hemisphere, Figures 3.13 and 3.14 show the mean localisations for the P2m in the left hemisphere, and Figures 3.15 and 3.16 show the mean localisations for the P2m in the right hemisphere.

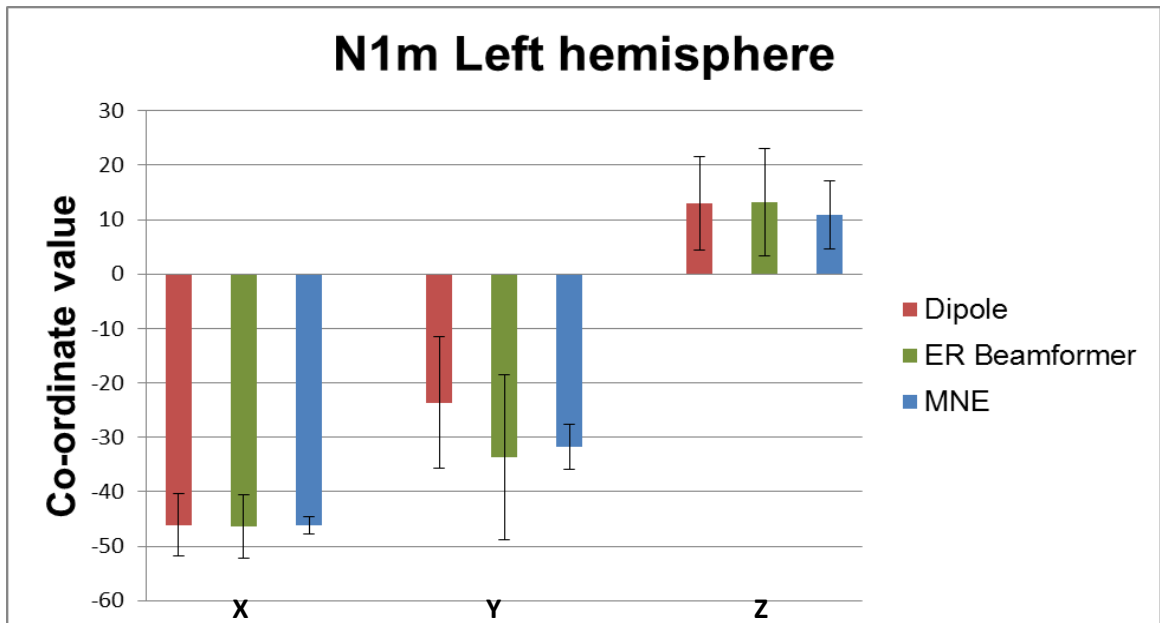
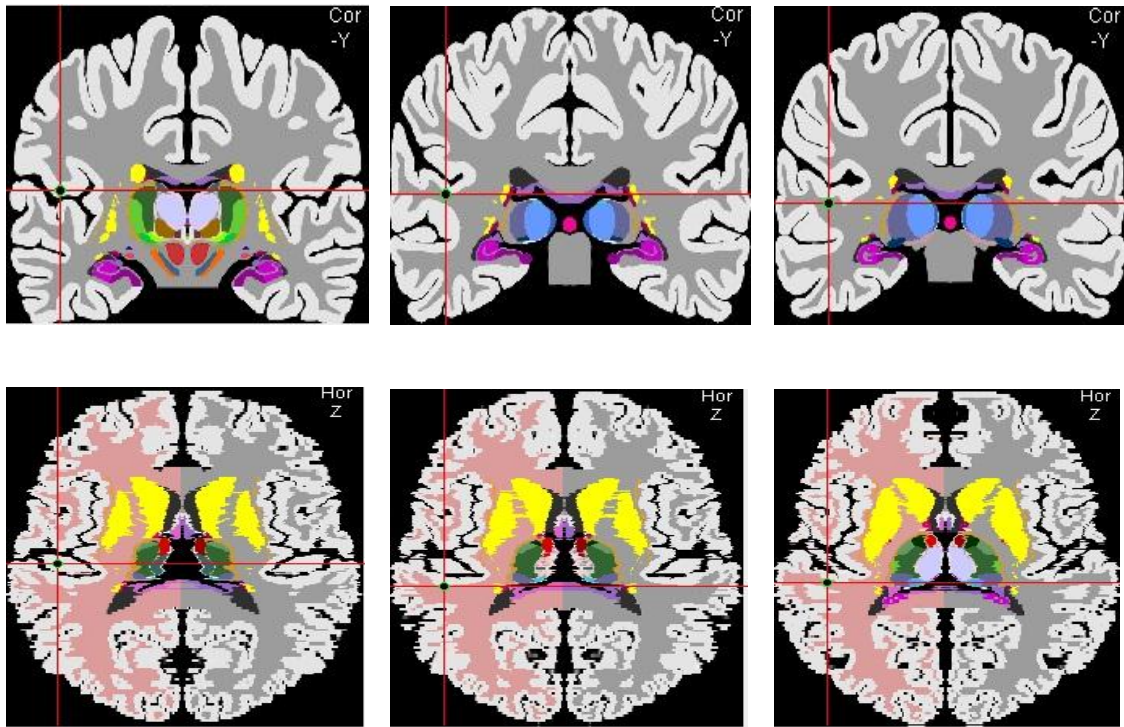


**Figure 3.9** Mean co-ordinate values for dipole, ER beamformer and MNE for the N1m response in the left hemisphere. The error bars indicate the 95% confidence intervals. The X-axis labels indicate the co-ordinate groups of X, Y and Z co-ordinates.

As can be seen from Figure 3.9, the comparison between the co-ordinate values in all dimensions (X, Y and Z) direction are similar and no overlap of 95% confidence intervals indicates that there is no significant difference in the localisations within each co-ordinate grouping. The Y dimension shows the largest degree of difference between the three analysis methods. MNE shows the smallest degree of variance in every co-ordinate grouping.



**Dipole**

**Beamformer**

**MNE**

**Figure 3.10** Plot of mean Talairach localisations for the dipole, ER beamformer and MNE in coronal and axial plane for N1m in left hemisphere. The top row shows the coronal plane and the bottom row shows the axial plane. The localisations are displayed on the template brain provided by humanbrain.info with permission.

As can be seen from these sources, the dipole localisation is more anterior and superior than the beamformer and MNE localisations.

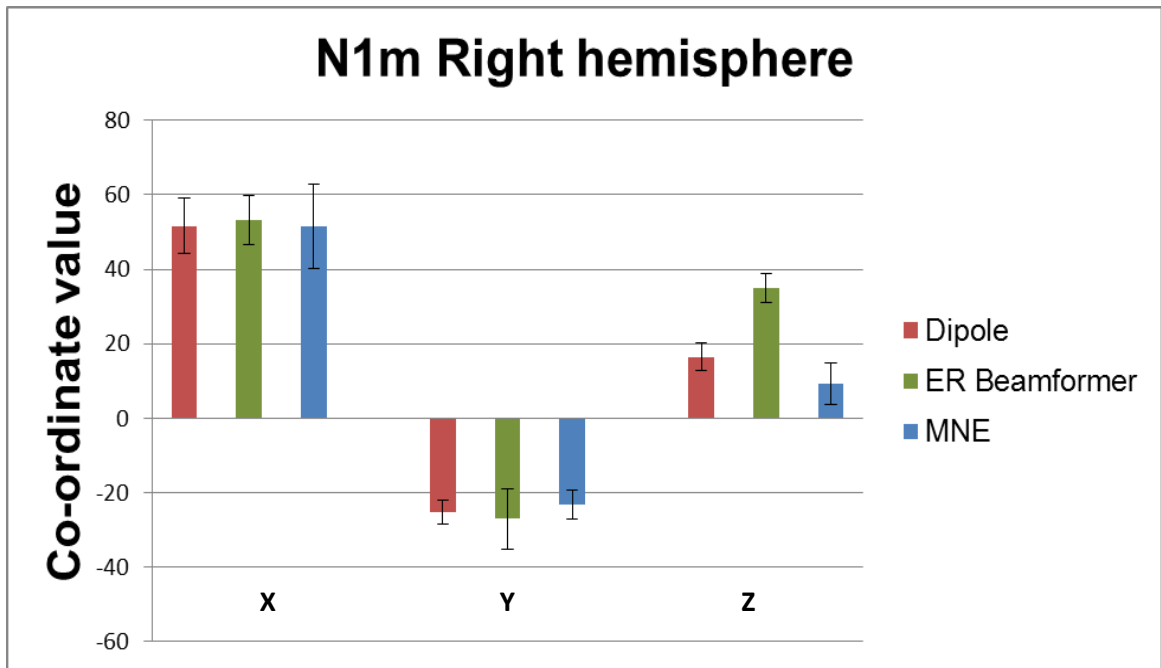
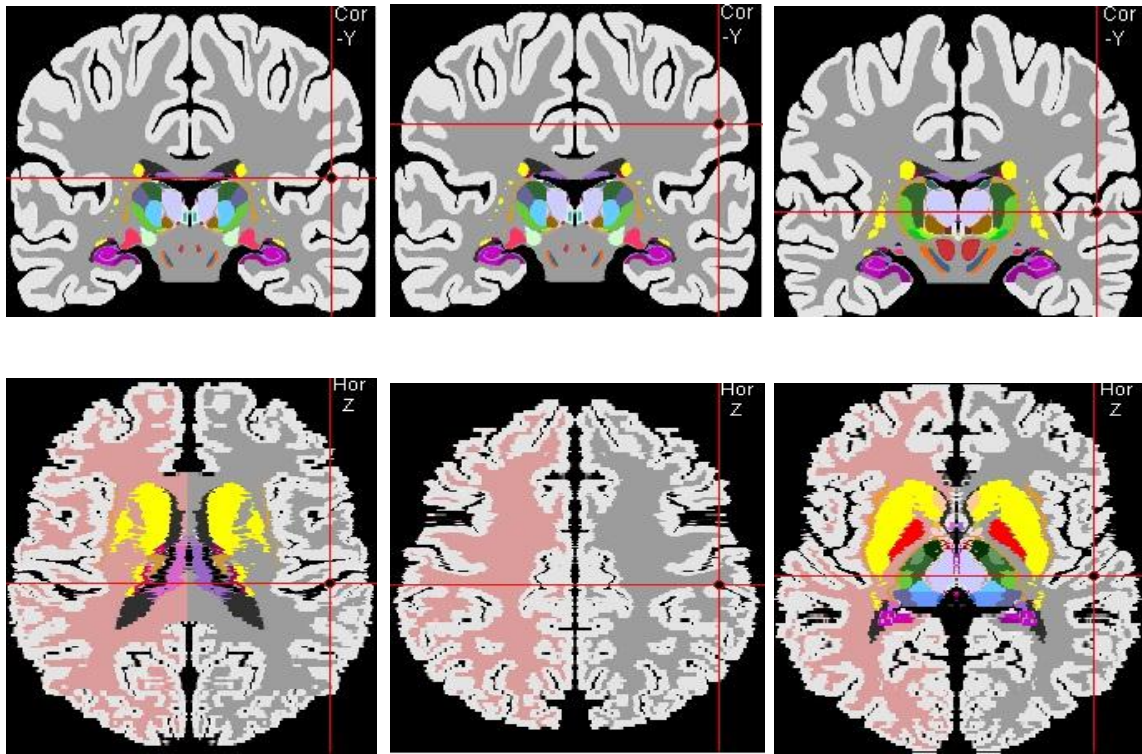


**Figure 3.11** Mean co-ordinate values for dipole, ER beamformer and MNE for the N1m response in the right hemisphere. The error bars indicate the 95% confidence intervals. The X-axis labels indicate the co-ordinate groups of X, Y and Z co-ordinates.

Figure 3.11 shows that the X and Y co-ordinate groupings show no significant differences in terms of localisation between the three analysis methods. However, the Z co-ordinate grouping shows a different pattern, as the ER beamformer value is significantly different to the dipole and MNE values in this co-ordinate dimension. This graph also shows a different pattern of variance when compared to the previous graph showing the opposite hemisphere for this response component. Here, the dipole method seems to show the least variance, with MNE showing the largest variance in both the X and Z co-ordinate groupings.



**Dipole**

**Beamformer**

**MNE**

**Figure 3.12** Plot of mean Talairach localisations for the dipole, ER beamformer and MNE in coronal and axial plane for N1m in right hemisphere. The top row shows the coronal plane and the bottom row shows the axial plane. The localisations are displayed on the template brain provided by humanbrain.info with permission.

As can be seen from Figures 3.11 and 3.12, the ER beamformer localisation is more superior than the dipole and MNE sources, with the 95% confidence intervals indicating this is a significant effect.

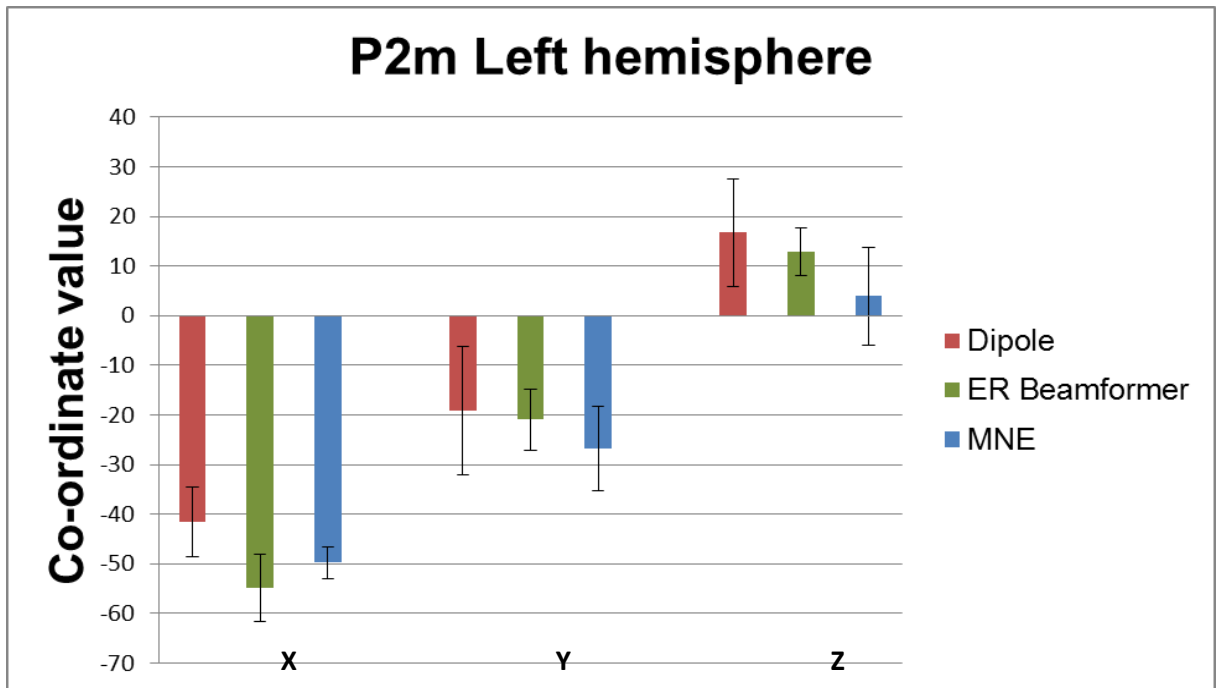
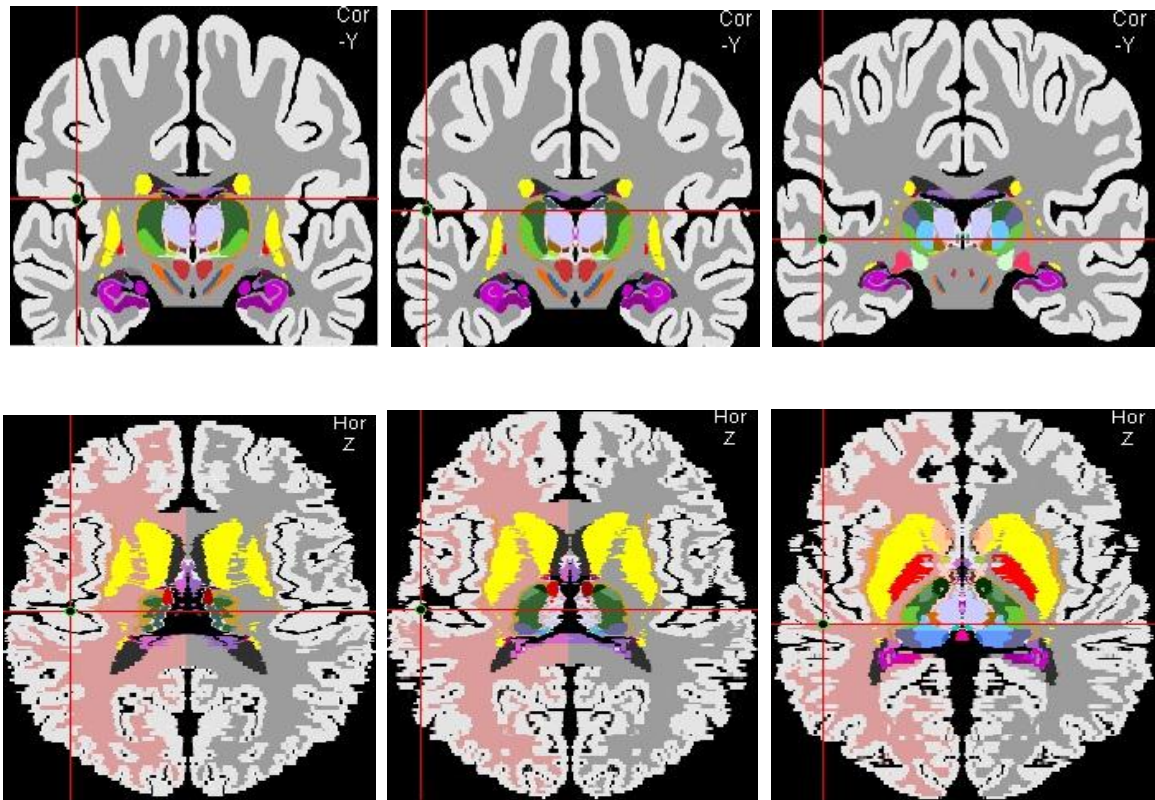


**Figure 3.13** Mean co-ordinate values for dipole, ER beamformer and MNE for the P2m response in the left hemisphere. The error bars indicate the 95% confidence intervals. The X-axis labels indicate the co-ordinate groups of X, Y and Z co-ordinates.

The graph (Figure 3.13) shows that there are no significant differences between the dipole, ER beamformer and MNE values in any of the co-ordinate groupings, indicated by the overlap of the confidence intervals within each co-ordinate grouping.



**Dipole**

**Beamformer**

**MNE**

**Figure 3.14** Plot of mean Talairach localisations for the dipole, ER beamformer and MNE in coronal and axial plane for P2m in left hemisphere. The top row shows the coronal plane and the bottom row shows the axial plane, using the template brain available from humanbrain.info with permission.

As can be seen in Figures 3.13 and 3.14, each technique yielded a clearly different localisation for the P2m. The dipole fit yielded the most medial and superior localisation, the beamformer showed the most lateral localisation, and MNE yielded a localisation that was inferior.

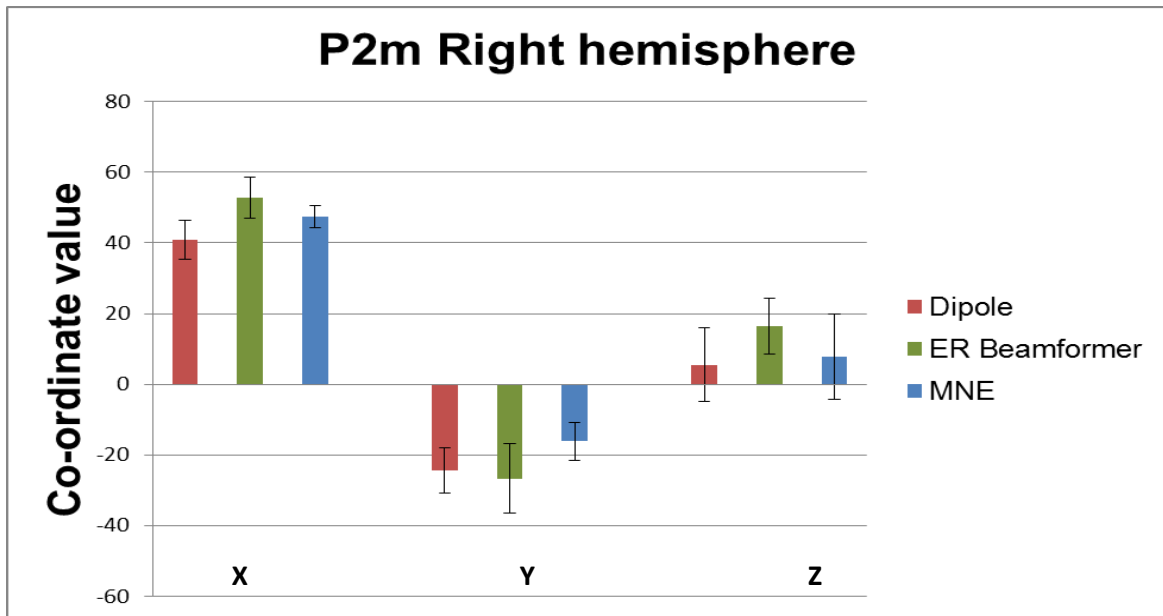
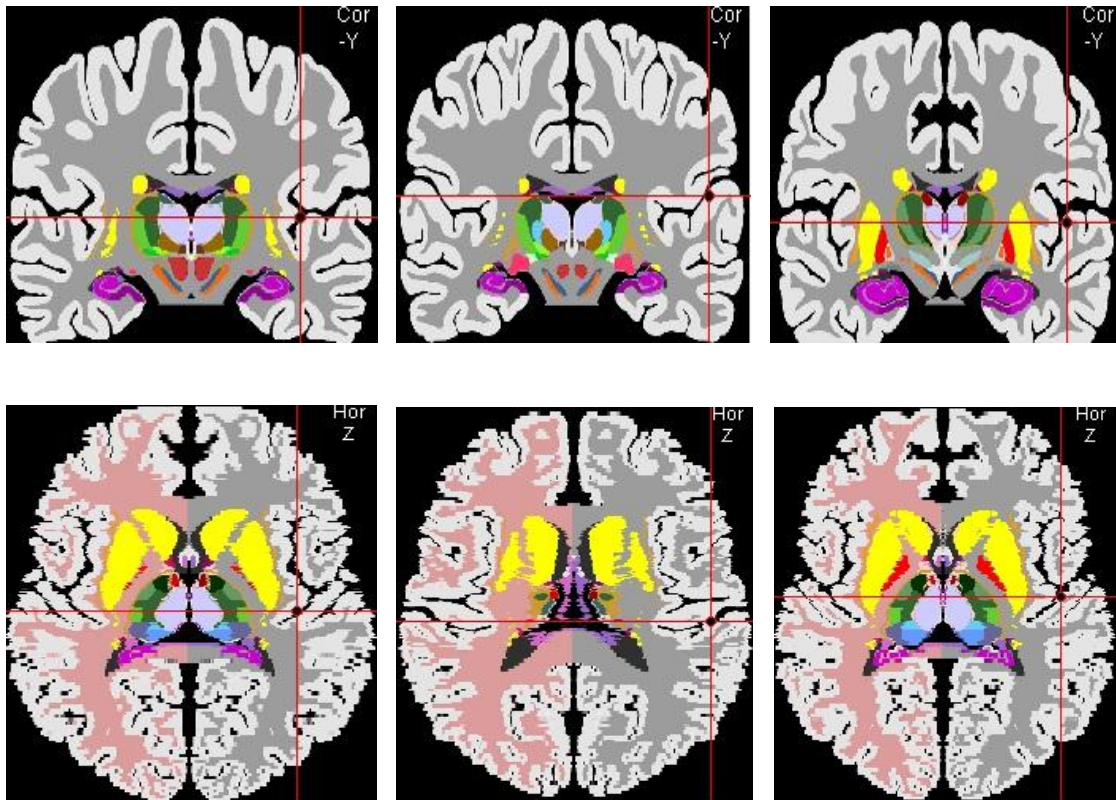


**Figure 3.15** Mean co-ordinate values for dipole, ER beamformer and MNE for the P2m response in the right hemisphere. The error bars indicate the 95% confidence intervals. The X-axis labels indicate the co-ordinate groups of X, Y and Z co-ordinates.

Here, Figure 3.15 shows that again there were no significant differences between the co-ordinate values for each method within each co-ordinate grouping. There is a large degree of variance within each method in the Z co-ordinate grouping, however the X and Y groupings showed smaller amounts of variance within each method.



**Dipole**

**Beamformer**

**MNE**

**Figure 3.16** Plot of mean Talairach localisations for the dipole, ER beamformer and MNE in coronal and axial plane for P2m in right hemisphere. The top row shows the coronal plane and the bottom row shows the axial plane. The localisations are displayed on the template brain provided by humanbrain.info with permission.

As can be seen in the images, again the dipole localisation was the most medial localisation, and MNE provided the most anterior localisation.

Overall, neither the N1m nor the P2m responses yielded an acceptable source model fit in every participant in either hemisphere. The MNE method showed an activity distribution in the respective expected regions for the N1m response (planum temporale) for all participants, however the localisation of the mean P2m localisation in the left hemisphere was very inferior. The dipole fits tended to be medial, with the beamformer fits for the N1m in the right hemisphere being superior.

### 3.4 Discussion

The aim of this study was to consider the relative equivalency of three analysis techniques in terms of localising the N1m and P2m auditory evoked responses. The data in this study indicate that in most cases, there is no significant difference between the localisations of each technique for either the N1m or P2m responses in either hemisphere. The only exception to this is when measuring the Z coordinate in the right hemisphere for the N1m response, which shows a significant difference in localisation between the ER beamformer and the other two methods, with the beamformer showing a localisation that is significantly more superior in cortical location, determined by no overlap of the 95% confidence intervals.

The N1m and P2m auditory evoked responses are known to be dynamic responses originating from the planum temporale and Heschl's Gyrus respectively (Näätänen & Picton, 1987; Godey et al., 2001; Lütkenhöner & Steinsträter, 1998; Lutkenhoner et al., 2003). Although dipole fitting has traditionally been used to localise this response complex, this technique relies on a priori knowledge of the location and number of sources. However, a distributed source model such as MNE shows that there are a number of dipole activations for each response component in each hemisphere, without needing a priori knowledge of the number or location of sources (Lee et al., 2012). ER beamforming is another distributed source model method, which yields a peak voxel of activation within the time window and frequency band specified (Cheyne et al., 2007). One advantage of the dipole method over the beamformer is that it is able to localise two correlated sources at once. Some studies have used dipole fitting successfully as the technique provides a good approximation of activity (Kiebel et al., 2007). However, commonly cited drawbacks of this technique include the potential for mislocalisation, especially in children (Pang et al., 2003). Children's heads are smaller and further from the sensors, leading to a smaller SNR for the evoked activity (Pang et al., 2003). Also, smaller heads introduce a greater likelihood of interference from the source in the opposite hemisphere, which can lead to difficulties in fitting the dipole in the lateral direction (Pang et al., 2003). Dipole fitting is more affected by noisy channel data than the other techniques (Turetsky et al., 1990), which

could be a reason why some fits were found to be unacceptable, despite epochs containing large artefacts being removed prior to fitting. As further studies in this thesis involve source localisation of the auditory evoked field in children, dipole fitting may not be the most suitable method.

Cheyne et al. (2007) compared ER beamformers and dipole fitting in their study looking at presurgical functional mapping of the auditory cortex. Unlike the results presented here, they found no systematic differences in location for the ER beamformer and dipole fits. However, they also found that using a restricted sensor range within which to fit their dipoles provides a better goodness-of-fit when compared to a 2-dipole model, but they also mislocalised the response to outside of the primary auditory cortex more frequently.

All the techniques showed localisations within the primary auditory cortex. Although there is little difference between the localisations in each method, there is a great deal of inter-subject variability, as shown by the 95% confidence intervals. Variability between individuals can be due to a number of factors, including differences in anatomy, which is particularly common in the temporal lobe (Mäkelä et al., 1993). Also, factors such as artefacts in the channels can contaminate the average, causing localisation error, even when due care is taken to ensure the removal of these artefacts. Minimum norm estimation holds an advantage here as it is able to take into account different noise levels at different sensors and measure their covariance in relation to the signal (Hauk, 2004). With regards to the response components, the N1m always showed a clear response and was observed more often than the P2m (Jacobson et al., 1992), hence the N1m will be used in the future studies in the remainder of this thesis.

Overall, the three analysis techniques confer different advantages and drawbacks in the measurement of the auditory response. Pang et al. (2003) recommend finding an alternative localisation method to dipole fitting in order to incorporate the wider spread of activity for auditory responses. MNE and beamformer are able to incorporate a wider spread of activity along with a lack of localisation bias, and also theoretically provide superior noise reduction, providing an advantage over dipole fitting. According to the results in this chapter, the beamformer localisation for the right

hemisphere N1m is located superior to planum temporale, which could indicate that the peak of activity is reflecting the spread of activity into the secondary auditory areas. Additionally, the MNE result shows a very deep source on average for the P2m in the left hemisphere, showing that neither method localises the responses exactly in line with previous findings. MNE has been shown to be effective in localisation of auditory areas (Lee, et al., 2012, 2014). Further, Work by Cicmil et al. (2014) suggests MNE is more accurate than beamformer when accurately representing the retinotopic map, illustrating its ability to localise distributed sources more effectively in comparison to spatial accuracy of fMRI.

A further benefit of MNE over the ER beamformer method is that it allows the user to select a vertex of interest according to the highest amplitude of the timeseries in each individual within a region of activity. For this reason, MNE will be used for the remainder of this thesis to measure timeseries' of auditory evoked responses in different stimulus conditions. Please see Chapter 5 for further details of how this is implemented in this study.

# Chapter 4:

---

## Developing a MEG stimulus for passive measurement of the BMLD

### 4.1 Introduction

This is a relatively short chapter considering the factors that need to be taken into account when developing a stimulus to measure the BMLD. The chapter consists of a summary of the stimulus components that make up the BMLD stimulus, as well as a consideration of the validity of the resulting evoked responses to masked tones.

There are a number of auditory paradigms which can potentially be used to show a binaural unmasking effect in psychophysics. The binaural masking level difference (BMLD), comodulation masking release (CMR) (Hall et al., 1984), binaural edge pitch (Klein & Hartmann, 1981) and Huggin's pitch (Cramer & Huggins, 1958) are all examples of a stimulus paradigm that will engage the binaural hearing mechanism. The BMLD was chosen as the most suitable paradigm for purpose, the reasoning for this will be explained in the following sections. The component parts of these stimuli will now be considered.

#### 4.1.2 Signal

The unmasking mechanism can be engaged either through the use of a pure tone signal presented out-of-phase (e. g. the BMLD and CMR) or alternatively through a noise phase alteration between the ears (e. g. Huggin's pitch and binaural edge pitch). Phase-reversing a narrow section of the masking noise in one ear can cause the listener to perceive a tone at the frequency of the centre of the phase-reversed section of masking noise, this is known as Huggin's pitch (Cramer & Huggins, 1958). When using a pure sinusoidal tone signal, the signal represents an addition of energy to the masking noise at that frequency, as opposed to when a section of the masking noise is phase-reversed. A tone-in-noise paradigm would be suitable when analysing a simple evoked response using neuroimaging

methods as a pure tone elicits a clear M100 and varying the intensity of the tone will lead to predictable amplitude and latency changes in the response which can be easily measured (see Chapter 3 for information on the M100 morphology). The BMLD is derived from the difference in threshold between a diotic and inter-aurally phase-reversed dichotic tone, both of which are masked by background noise.

#### **4.1.2.1 *Tone characteristics***

Choosing a range of tones of different intensities will show the M100 amplitude and latency sizes at different tone levels, which will indicate whether or not the response is a valid M100. In addition, the range of tones chosen should be wide enough to show the range of the maximum and minimum neural responses to the tones.

Tone frequency is important in the elicitation of the BMLD, as tones of higher frequencies have previously been shown to elicit smaller BMLDs (Durlach & Colburn, 1978), with the most pronounced BMLD of between 12-15dB being elicited using a tone of 500Hz (Hirsh, 1948).

#### **4.1.2.2 *Phase ratio***

Previous work examining the BMLD has shown that the maximum inter-aural phase ratio possible of  $180^\circ$  will yield the largest BMLD (Durlach & Colburn, 1978). See Figure 4.1 for a visual explanation of the signal and noise relationship in the BMLD. If the dichotic tone is presented to each ear simultaneously and the phase relation is above or below  $180^\circ$ , the auditory system does not have a precedence cue for localisation and so would not be able to localise the sound (Litovsky et al., 1999). In real-life situations, other auditory cues such as head shadow or altering the phase difference between the ears through movement of the head would be available to resolve this problem. For the purposes of simply separating the signal from the background masking noise, this effect would not be a hindrance. However, for the purposes of maximising the BMLD, the largest phase-ratio of  $180^\circ$  will be used in the current research.

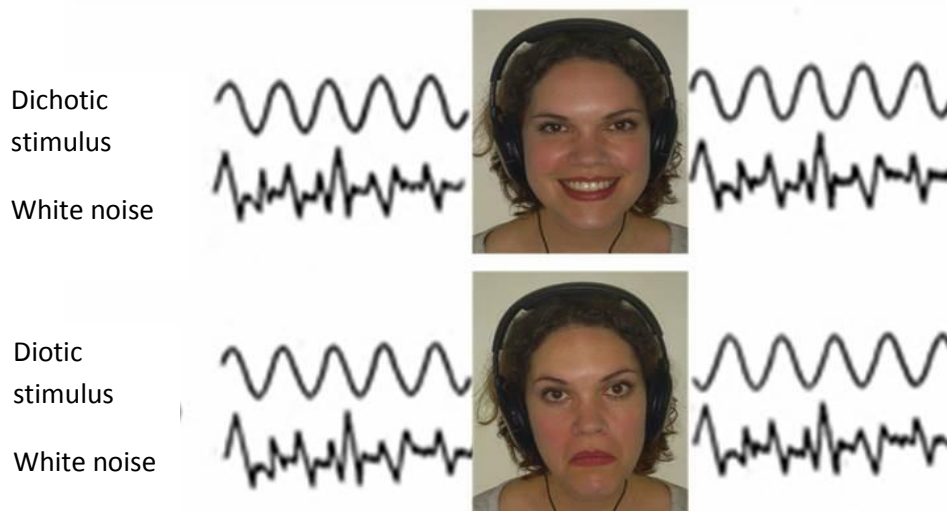


**Figure 4.1:** The binaural masking level difference. The dichotic stimulus can be heard more easily over the background noise as it perceived to be spatially separated from the noise.

#### 4.1.3 Noise

Noise is a stimulus component that can take a number of different forms. Noise can be broadband or narrowband, and centred on various different frequencies. As a masker, white Gaussian noise is useful as it provides a flat distribution of frequency power over the whole spectrum. ‘Low-noise’ noise is a type of noise with small amplitude fluctuations (Pumplin, 1985) and has been investigated as a potential masker in a paradigm of this nature (Hall et al., 1998) with the finding that the smaller degree of fluctuation in the masker compared to Gaussian white noise did not enhance the MLD as predicted. It seems that the high degree of masker fluctuations found in white Gaussian noise are necessary for effective unmasking (Hall et al., 1998).

Gaussian noise has prominent frequency fluctuations and so yields a higher threshold for out-of-phase signals and a lower threshold for in-phase signals according to the envelope masking minima hypothesis (Buss et al., 2003), whereby the binaural system is able to exploit the improved SNR at envelope masking minima. This improvement in SNR remains related to binaural unmasking as the noise may still be of a higher amplitude than the signal even at the lowest points of the noise envelope. In general, a narrow bandwidth of noise has been shown to increase the behavioural

BMLD (Bourbon & Jeffress, 1965, Wightman, 1971) and also the electrophysiological BMLD (Fowler & Mikami, 1992b). However a narrow bandwidth for masking noise can lead to the participant utilising extra binaural cues for localisation from the fluctuations in the masker envelope which are not related to binaural unmasking. This effect is linked to comodulation masking release whereby the participant is able to extract extra binaural cues for detection from increasing the number of noise bands in the surrounding masker envelope (Hall et al., 1984) as opposed to the phase-relation of the signal per se. Comodulation masking noise has been utilised by Epp et al. (2013) to elicit an unmasking effect for a tone signal. In this paradigm it is not the intensity of the signal which is altered to reveal the unmasking effect but the addition of flanking noise bands which are then amplitude modulated coherently across the bandwidth of the noise. The results of this study show that the N1 was not sensitive to changes in the comodulation of the masker, but was sensitive to inter-aural phase disparity in the BMLD which was also tested by Epp et al., (2013).

It is possible to use either continuous masking noise, or to use intermittent masking noise when presenting the target signal. It has been shown that intermittent noise can cause an evoked response to the onset and offset of the noise, which could potentially cause an artifact in the evoked response to the target (Seither-Preisler et al., 2004). Research has shown that continuous background noise does not elicit an M100, so would not interfere with the evoked response elicited by the target signal (Chait et al., 2004). Other BMLD studies have successfully used continuous masking noise, for example Hari & Mäkelä (1988) presented continuous background masking noise at 84dB SPL to mask their target signals.

For this thesis a continuous 500Hz wideband masker was chosen, centred on the signal of interest, to ensure that the spectra of the signal could not be detected outside the bandwidth of the masker. This will preclude any extraction of binaural cues unrelated to the dichotic phase of the signal.

#### **4.1.4 Factors for consideration**

##### **4.1.4.1 Calibration of stimulus**

The stimuli sound files were created using Matlab (version R2012a) and presented using Presentation (version 15.1). The sound files were calibrated to test the level at presentation to the participant, using an artificial ear. It was found that the tones were distorted at the highest level due to an effect of the external amplifier used in the presentation equipment. Hence the tones were presented in an intensity range from the highest volume possible without distortion, down to a level where an evoked response is still visible over the background baseline noise. All tones were presented suprathreshold so that the differences between the amplitudes and latencies could be examined.

##### **4.1.4.2 Validity of M100**

To contribute to the validity of the M100 responses, concurrent EEG data were recorded on a small number of participants. It is shown that both EEG and MEG are measuring the same neuronal discharge in response to a sound, albeit using different processes (Virtanen et al., 1998), so triangulating the MEG measured response with a well-established literature using another method will provide further support for the validity of the M100.

##### **4.1.4.3 The masked M100**

The BMLD stimulus involves presentation of a masked tone. As described in Chapter 1, previous findings have shown that masked tones yield N1 and N1m responses with larger amplitudes and longer latencies than unmasked tones (Alain et al., 2009; Okamoto et al., 2007).

##### **4.1.4.4 Number of averages**

An evoked response is built up as more trials are included in the average. Averaging increases the SNR of the signal over the background masking noise, according to rule of the thumb that states that the SNR is the square root of the number of trials averaged. It is important to include a larger

number of trials in the average than this in auditory work, due to the fact that some trials are highly likely to contain artefacts, such as eye blinks, and may need removing from the analysis.

#### **4.1.2 Aim**

The aim of this chapter was to validate and explore the different characteristics of a BMLD stimulus to ultimately develop a suitable paradigm for use in MEG.

## **4.2 Method**

A number of pilot trials were recorded testing out various aspects of the stimulus, of which some are reported here. Data presented here were taken from subjects between the ages of 28-73, all of whom were recruited from within the Aston Brain Centre as pilot subjects. Data were recorded on the Elekta Neuromag Triux system, using a sample rate of 1kHz. The participants' headshape was first collected using the Elekta polhemus system before the participants were introduced into the scanner.

### **4.2.1 Calibration of stimulus**

The program and equipment used to present the auditory stimuli were calibrated by an external specialist using an artificial ear. The tone and noise stimuli was generated in Matlab, and presented using Presentation. The stimuli were presented via a LG Flatron W2253TQ computer attached to a Behringer MicroAMP HA400 amplifier which presented the sounds through Etymotic transducers and eartubes suitable for use inside the magnetically shielded room. The tone stimulus was calibrated at a number of different frequencies to ensure that there was no effect of distortion to the sinusoidal wave. The noise stimulus was also calibrated to gauge the intensity level.

### **4.2.2 Validity of N1m and N1**

Using the Elekta MEG-compatible EEG equipment, three electrodes were placed on the participants' head prior to entering the scanner. The skin was first prepared to reduce electrical impedance by the skin. One electrode was placed on the scalp vertex, and another placed on the earlobe of the participant. This montage was chosen to avoid the possibility of scalp electrodes being disrupted by the action of the polhemus pen. The MEG coils were placed on the forehead and ears after the EEG

electrodes were in place. This order was chosen so that the MEG coils were not accidentally moved when applying the EEG electrodes. Once in the scanner the impedance of the EEG electrodes was checked to ensure the impedance was within an acceptable range as specified by the acquisition program. The auditory stimulus was presented as a series of 50ms pure tones of 500Hz presented at an ISI of 1 second with 100ms jitter. The tones at each level were presented 100 times at each level of 20.3, 17.6, 15.2 and 9.1dB above the continuous 500Hz-wide, Gaussian, background noise level, which was presented at 70dB SPL.

#### **4.2.3 The masked M100**

To measure the difference between the masked and unmasked tones, the paradigm described above was used, however after presenting the full stimulus another recording was undertaken with the background noise muted so only the tones at the same levels were presented.

#### **4.2.4 Number of averages**

The number of averages required for an evoked response were examined using the evoked response to the loudest dichotic tone over noise for one participant, acquired using the same method as previously described.

### **4.3 Results**

#### **4.3.1 Calibration of stimulus**

The background noise intensity used was 70dB SPL, and the 4 tone levels above this were for both the dichotic and diotic tones were chosen as follows: 90.3dB, 87.6dB, 85.2dB and 79.1dB. The tone levels may initially seem to be at unusual levels, however the intensity was measured according to the step-wise attenuation properties of the program used to present them (Presentation v.15.1). A biological test of validity ensured that the tones and noise were presented at a comfortable listening level.

#### **4.3.2 Validity of M100**

Figures 4.2 and 4.3 show EEG and MEG traces for the M100 in two participants. The M100 is labelled in the EEG trace and a vertical line shows how it lines up with the MEG trace. The morphologies of the EEG and MEG responses in both participants suggest that these are the same responses being measured in each participant.

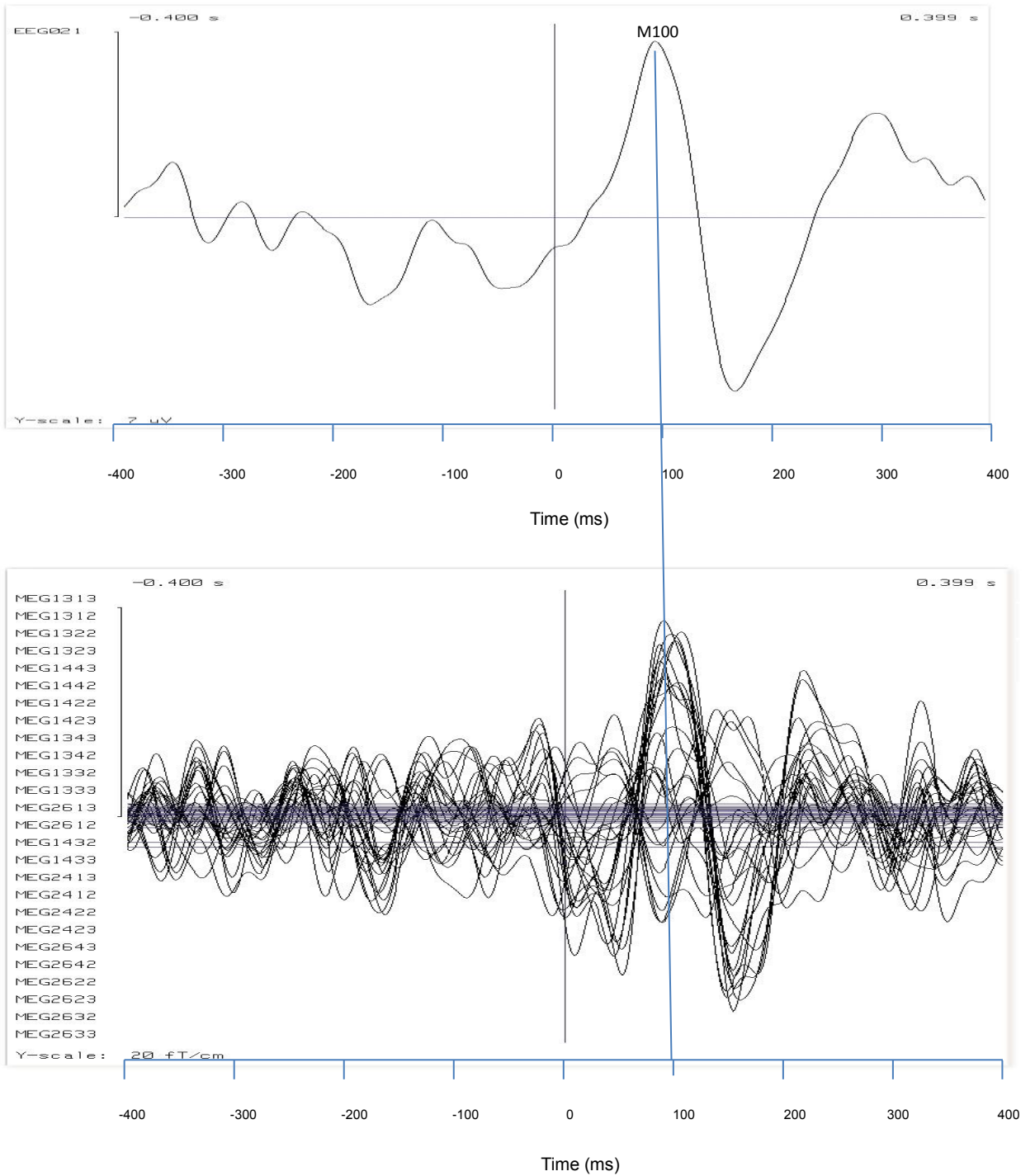


**Figure 4.2** EEG and MEG response validity, example one. The figure shows the EEG trace (above) and MEG trace (below) obtained from a concurrent recording. The M100 is labelled and can be shown to be the same latency in both modalities.

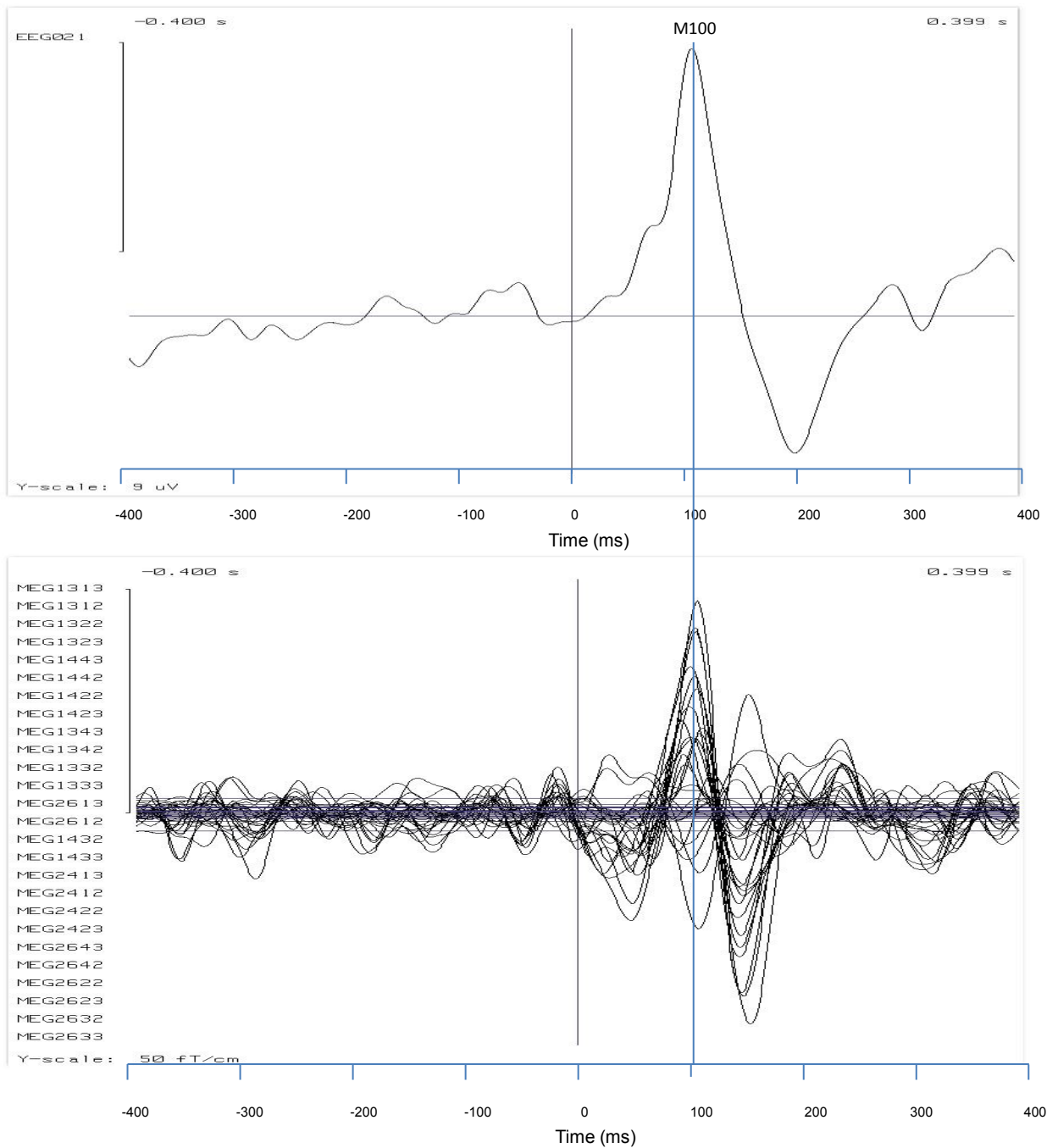


**Figure 4.3** EEG and MEG response validity, example two. The figure shows the EEG trace (above) and MEG trace (below) obtained from a concurrent recording. The M100 is labelled and can be shown to be the same latency in both modalities.

### 4.3.3 The masked N1m

When masked by a background noise, the M100 evoked response appears to be larger and the latency is slightly later than a tone that is completely unmasked. The larger amplitude of the masked tone demonstrates the effect of energy summation in the mechanism of auditory masking. The masking noise provides additional energy in the frequency region of the sinusoidal tone, so the additional energy will be manifested as a larger amplitude in the evoked response. This is in contrast to the increase in amplitude of the dichotic tone compared to the diotic tone, which is not related to energy summation but instead is a binaural mechanism of unmasking. Figure 4.4 does not show a significant effect for masking, however this is expected in sensor data as artefacts and noise reduce the signal to noise ratio.

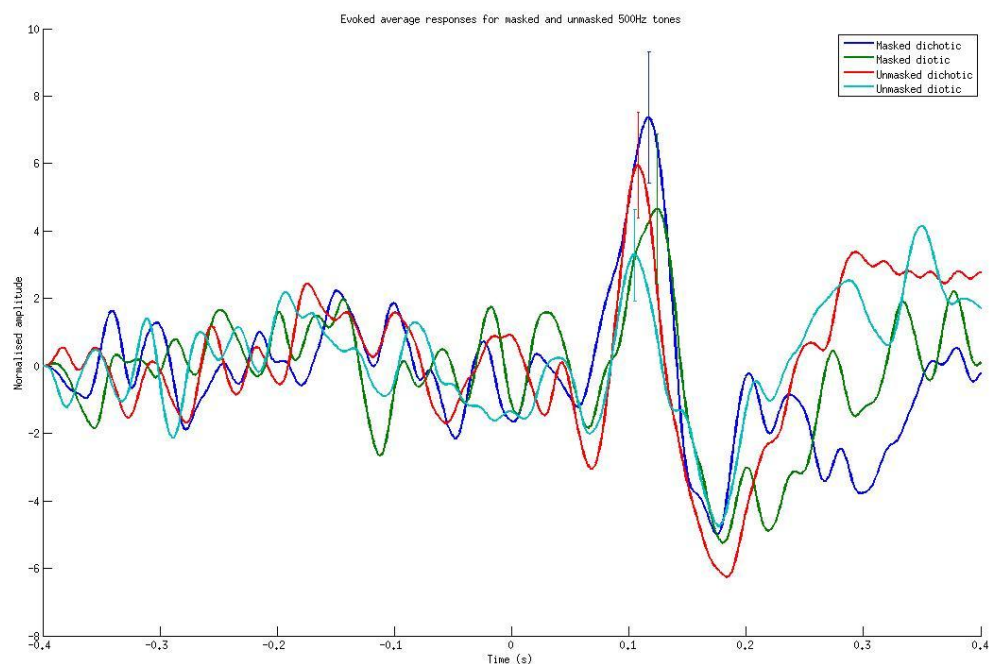


**Figure 4.4** An average evoked timeseries for one participant demonstrating the masked and unmasked dichotic and diotic tones when presented at the same level. The 500Hz dichotic and diotic tones are presented for 50ms duration with a rise and fall time of 5ms, at 90dB SPL, and in the masked condition the background Gaussian noise is presented at 70dB SPL. Each condition is shown using the same MEG sensor over the right temporal lobe. Error bars show standard deviation for 79 trials per condition. A paired t-test shows there is no significant difference between error variance in the masked and unmasked tones in the dichotic condition,  $t(78) = 1.666$ ,  $p > 0.05$ , or the diotic condition,  $t(78) = 1.081$ ,  $p > 0.05$ .

#### 4.3.4 Number of averages

Figure 4.5 below shows the same auditory evoked M100 when averaged using a different number of trials, namely, 20, 40, 60 and 80 trials.

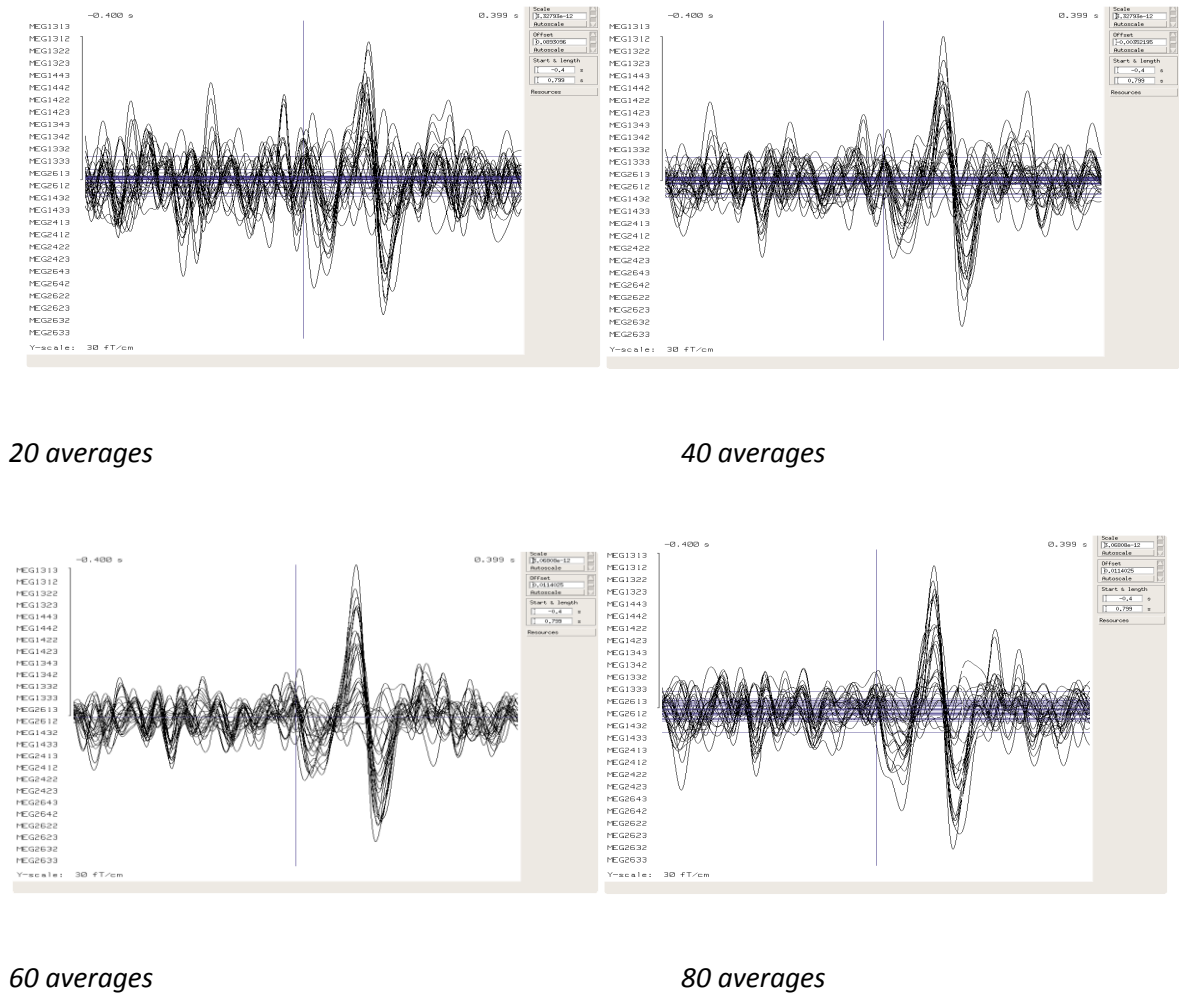


**Figure 4.5:** Evoked responses of different numbers of averages. This figure shows overlays of averages of 20, 40, 60 and 80 trials of the same auditory evoked response to a masked tone, using Elekta software. The 500Hz dichotic tone is presented for 50ms duration with a rise and fall time of 5ms, at 90dB SPL, with a 500Hz background Gaussian masking noise of 70dB SPL.

As can be seen in Figure 4.5, the evoked response becomes clearer as the SNR increases with an increasing number of averages.

## **4.4 Discussion**

### **4.4.1 Calibration of stimulus**

After calibration of the auditory equipment, it was decided to use a set range of tones over background noise for all participants due to constraints on the amplitude of the tones. Over a certain level, the loudest tone was distorted out of a sinusoidal shape so was not suitable for use in the paradigm. Ideally, the number of tone intensities used would be as few as possible in order to keep the recording short while maintaining a long enough ISI and large enough number of trials. Noise had to be loud enough to engage the binaural unmasking mechanism, however in order to measure evoked responses at threshold there would have to be a very large number of trials due to the signal to noise ratio being so low. The stimulus intensity level was kept supraliminal to show clearly marked different amplitudes on increasing and decreasing intensity level steps. 100 repetitions of each tone were used to make sure that a clear evoked response could be averaged following artefact trial removal.

Ultimately the stimulus will be used with children, so a very large number of trials would not be suitable for this age group as the signal-to-noise ratio would be likely to decrease further with fatigue leading to increased movement. For this reason, it was decided not to measure the evoked response at threshold, and instead to investigate the possibility of computing a BMLD value simply from supra-threshold measurements of differences in the dichotic and diotic values. The range of tones used then had to be loud enough over the background noise to elicit an evoked response but not so quiet that the response signal would become 'lost' within the background sensor noise.

### **4.4.2 Validity of tone**

The EEG responses shown here have strong face validity in terms of their equivalency to the MEG responses with regards to the latency, morphology and amplitude. According to examples shown in the well-established EEG literature, the AEPs shown here are typical N1 responses (see Hyde, 1997 for a review).

#### **4.4.3 The masked M100**

When directly comparing the masked and the unmasked tones, the masked tones show a larger amplitude and longer latency than the unmasked tones, as is predicted according to the literature (Alain et al., 2009; Okamoto et al., 2007). This phenomenon is thought to occur as a result of a summation of energy within the auditory filter at the characteristic frequency of the signal, leading to a larger amplitude of evoked response.

#### **4.4.4 Number of averages**

Averaging of evoked responses is a necessary step in the processing of MEG and EEG data to average out the non-time locked activity (i. e. the background noise) and enhance the time locked activity (i. e. the auditory response). Slight variations in neuronal firing between trials can be cancelled out by averaging the full range of trials sample point by sample point. The neural activity will not always be exactly time-locked as there may be differences between trials in the timing of neuronal firing, however the averaging process removes this variation by calculating the mean at each sample point within a specified averaging time window.

As evoked responses rely on averaging multiple presentations of the same stimulus, the number of averages can have an effect on the size of the evoked response, particularly in a low SNR situation. To explore this, the same stimulus was averaged a different number of times to see at what point the evoked response size stayed the same. In previous literature, researchers have used averages ranging from 40 to 200, however it is generally agreed that 40 is the minimum required to elicit the evoked response and 70 is ample. For the purposes of this thesis, the interest lies in the amplitude difference between the peaks of the diotic and dichotic responses. As this is a relative measure, the absolute number of averages does not affect the relative differences as long as each stimulus has the same number of averages.

Automatic artefact reduction can remove trials containing artefacts that exceed a certain threshold, which may affect the number of averages. However, the tones are presented randomly which means

there should be no systematic bias towards removal of trials containing any one trigger over the others. The only instance in which this could present a difference is that it could affect relative amplitudes between individuals if one dataset contains more baseline noise than others, but the BMLD is computed on an individual basis so as long as the intra-individual averages are consistent then the noise in the data should not pose a problem.

#### **4.4.5 Further considerations: Inter-stimulus interval**

The amplitude of the ERF is affected by the inter-stimulus interval, (Cheuden, 1972). In this study, the authors used four seconds or more to elicit an auditory evoked response in children. It has been shown that child responses require a long ISI to be able to view all of the different components present in the N1. Imada et al. (1997) showed that in children, the N1 amplitude increases as the stimulus interval increases. Strikingly, Davis et al. (1966) undertook a study showing that the N1P2 amplitude decreased by 50% when the ISI was shortened from three seconds to one second, and again reduced to a third when it was decreased to 0.5 seconds using EEG. Ideally, the ISI would be 10 seconds or more to show the full response (Davis et al., 1966) however this size of ISI would not be realistic when trying to record participant groups for whom the paradigm should ideally be kept as short as possible. Interestingly, the latencies are not affected despite the amplitude changes (Davis et al., 1966). Using MEG, Hari et al. (1982) measured the N1m using maximum ISIs of 4-8 seconds which agreed with the EEG results in terms of ISI reported above. In contrast to these findings, Loveless et al. (1989) showed in their MEG study that the N1m in fact increased when the ISI was shorter than 0.5 seconds. As these findings do not concur with the majority of the other literature on ISI length and response amplitude, the authors suggested the reason for this related to the frequency spectra of the response being increased through a number of different channels.

#### **4.4.6 Stimulus details**

After trialling a variety of stimulus parameters, including tone and noise level, tone frequency, number of averages and checking the validity of the response through comparison with another neurological measure, the BMLD paradigm was refined to ensure that the maximum BMLD possible

would be elicited. The paradigm consists of a Gaussian white noise stimulus, 500Hz wide, centred on 500Hz, presented at 70dB SPL. The tone stimulus consists of a 500Hz sinusoidal tone with a duration of 50ms and a 5ms rise and fall time. The tone is presented in two binaural conditions: in-phase (diotic) or 180 degrees out-of-phase (dichotic). Each tone condition is presented randomly at 4 different tone levels of 20.3, 17.6, 15.2 and 9.1dB above the background noise level, for 100 trials each, with an ISI of 1000ms, with up to 100ms random jitter.

# Chapter 5:

---

## **Investigating a neural correlate of the psychophysical BMLD with an adult cohort**

### **5.1 Introduction**

This chapter will present data recorded from a cohort of adults using a stimulus designed to measure the BMLD passively in MEG, and behavioural measurements using psychophysics. An exploration into whether or not there is a correlation between these two methods in terms of finding the BMLD will be undertaken and the results reported.

#### **5.1.1 The value of a neural correlate of the BMLD**

By utilising stimulus cues such as phase and intensity of sounds, humans can discern from which direction they originate through timing and level differences between the inputs at the ears (Rayleigh, 1907). We also use this mechanism to differentiate a target signal from background noise by perceptually separating the signal through localisation (see Chapter 1 for a full description of the binaural unmasking mechanism). Timing differences in signal between the ears can be easily created in a laboratory environment by altering the phase relation of a stimulus, with the localisation cues provided by out-of-phase signals making them more perceptible in noise than in-phase signals (Hirsh, 1948; Licklider, 1948). Controlled alteration of the relation between stimulus inputs at each ear can form the basis of psychophysical paradigms designed to study various aspects of auditory perception (e.g. Wetherill & Levitt, 1965; Kawase et al., 2000).

Under optimal conditions, the psychophysical method is an excellent technique to measure binaural hearing using the BMLD paradigm (Hirsh, 1948; Jeffress, Blodgett & Deatherage, 1952; Grantham, 1995). However, psychophysics requires a behavioural response to indicate perception of a stimulus,

so its usefulness is limited if participants are unable to respond appropriately and reliably. There is need to measure the binaural hearing of children hearing a teacher or parent talking in a noisy environment. Sometimes these people are unaware or unable to verbally express that they cannot hear, and also are unable to complete a psychophysical task. In these cases, a passive measure of the BMLD is a useful tool to discern the spatial hearing abilities in potentially any participant. One way to measure if a stimulus has been perceived without relying on behavioural responses is to measure the evoked neural response to a sound (Sasaki et al., 2005). Monaurally, tonal perceptibility is related to the amount of energy contained within a sound source (Green & Swets, 1966), however the auditory binaural mechanism allows tones to be more perceptible (have an increased salience) over a masker when they are phase-inverted at one ear. The salience of a sound is reflected in the morphology of the M100 response, and increasing the salience results in increased amplitude and decreased latency of this evoked response. Measuring the evoked response characteristics in MEG should therefore provide a direct measure of the perceptibility of tones with different phase relations over a background masking noise. If the level of the out-of-phase tone is perceived to be greater than the in-phase tone over masking noise as measured by the neural evoked responses, this is an indication of engagement of the binaural mechanism.

### **5.1.2 Physiological considerations**

#### ***5.1.2.1 Hemispheric differences***

It is well established that a sound presented to either ear will elicit an evoked response in both auditory cortices (see Moore, 1991). However, further studies have shown that asymmetries exist between the hemispheres in response to auditory stimulation. Hine & Debener (2007) showed a larger amplitude and shorter latency of the tangential N100 component in the right hemisphere in response to monaurally-presented 1000Hz tones and noise in EEG. Each hemisphere was analysed separately and both contralateral and ipsilateral hemispheres showed the same lateralization to the right in all conditions, which the authors interpreted as an asymmetry in processing as opposed to an asymmetry in structural connections. Hine & Debener did evaluate the data at source level in this study, however there are more effective methods of localising a monaural response in order to

derive source waveform data than EEG (see Chapter 2 for further details on techniques). Using MEG, Howard & Poeppel (2009) have shown that the right hemisphere exhibits shorter latencies and larger amplitudes in response to single clicks presented binaurally, and combined with previous work, have attributed this to the sharp onset of the sound. MEG studies have shown a right hemisphere lateralisation for responses to tones with a rise time of 2ms (e.g. Gabriel et al., 2004; Huotilainen et al., 1998; Jin et al., 2007), which is shorter than the conventionally used tone rise time of 5-10ms (Phillips, 1988). Interestingly, (Pardo et al., 1999) showed a left hemisphere lateralization for tones with gradual onsets (300ms), which the authors suggest could be linked to hemispheric differences related to speech perception (Pardo et al., 1999). Related to this is the concept that there is a bilateral pitch centre, which appears more distributed using unresolved harmonic stimuli (Hall & Plack, 2007) and more focally in the anterior regions of the primary auditory cortex using resolved harmonic stimuli (Norman-Haignere et al., 2013). Evidence for a right hemisphere advantage for tones is mirrored by evidence for a left hemisphere advantage for speech (Eulitz et al., 1995). Further, speech and tone responses have been shown to originate from separate sources in primary auditory cortex (Kuriki & Murase, 1989), particularly in the left hemisphere (Eulitz et al., 1995). These data highlight the importance of rise-time of a stimulus and also the importance of analysing the hemispheres separately in response to a binaural stimulus, for which MEG is an ideal technique as previously described. This study will look at the effects of hemisphere, with a prediction that the right hemisphere may show a larger amplitude and shorter latency evoked response than the left hemisphere in the majority of participants.

#### **5.1.2.2 *The masked M100***

Studies have demonstrated that an ongoing background stimulus can affect the M100 (Hari & Mäkelä, 1988; Woods et al., 1984). When studying the effects of masking on the M100 and M50, Levanen & Sams, (1997) found that the masker decreased the amplitude of the M100 responses in contralateral masking conditions, whereas the M50 amplitude showed no effect of masking. They found that the larger number of different frequency and amplitude transient components the masker contained, the more effective it was in reducing the auditory evoked response, for example speech

and music maskers were more effective than continuous white noise due to their more salient fluctuations. Hari & Mäkelä (1988) suggested that maskers containing sounds fluctuating in intensity and frequency may be processed more in the central auditory pathway, as opposed to masking noise which may be processed more in the peripheral auditory pathway. In their study, Hari & Mäkelä (1988) presented 25ms tones randomly to the left or right ear, with different types of maskers presented to the left ear. It was shown that intermittent noise, speech and music all diminished the M100 amplitude in both hemispheres without any effect on the sensation level of the target. In contrast, when continuous masking noise was presented to the left ear with a left ear target tone, the M100 in the left hemisphere was diminished in amplitude and sensation, with no significant change to the right hemisphere response. The authors concluded that the M100 response amplitude is not linked to sensation when the masking noise fluctuates in intensity and frequency, however a continuous masking noise will yield a reduced M100 amplitude and sensation level on the same side as the target. In contrast to this type of energetic masking, informational masking occurs when the masker occludes or distracts from the target signal even when it is not within the same frequency range (Kidd et al., 1998; Durlach et al., 2003).

### ***5.1.2.3 BMLD in the auditory cortex***

Physiologically, binaural interaction takes place in the inferior colliculus and medial superior olive, but the actual perception of a binaural sound takes place in the primary auditory cortex (Moore, 1991). The behavioural MLD has been shown to be disrupted in brainstem studies of patients with central auditory processing disorders (e.g. Ferguson et al., 1998; Gravel et al., 1996; Hannley et al., 1983). Indeed, Noffsinger et al. (1982) found that the MLD was directly linked to particular elements of the auditory brainstem potential, with abnormal I, II and III ABR waves yielding little to no MLD, while abnormal IV and V waves yielded a normal MLD in their subjects. Despite the behavioural evidence for BMLD processing at this level, direct neural measurements of the N1 at the medial superior olive in the human (Langford, 1984), and inferior colliculus in the cat (Caird et al., 1980) do not show binaural unmasking, nor does the ASSR at brainstem level in the human (Wong & Stapells 2004). Neural measurements of binaural unmasking have been shown at the cortical level for the

M100 (Sasaki et al., 2005), and also the ASSR (Wong & Stapells, 2004). Other N1-P2 associated responses have also demonstrated a BMLD at the cortical but not brainstem level (e.g. Fowler & Mikami, 1992a, 1992b, 1995, 1996; Kevanishvili & Lagidze, 1987). These collective results would initially suggest that binaural information is not extracted until the higher cortical level. However, this conclusion would seem to be unlikely as the binaural unmasking mechanism has a reliance on phase-locking which gradually degrades up to the cortical level (Litovsky & McAlpine, 2010). Wong & Stapells (2004) suggest that a more likely answer is that the BMLD is created at the brainstem but is only demonstrated in the cortical evoked responses. In their study, Wong & Stapells (2004) also interestingly found that, unlike their measured N1-P2 cortical ERPs, the ASSR cortical responses did not show a BMLD when the noise was phase-inverted.

A theory as to why the BMLD only manifests itself in the cortex was put forward by Jiang et al. (1997b). The authors suggest that unmasking may depend on small groups of neurons increasing and decreasing in activity relative to whichever signal and masker condition is presented. Jiang et al., (1997b) go on to report that the techniques employed in whole-head sensor measurement of neural activity are relatively insensitive, and an amount of amplification of the neural signals at the cortex is the reason they are detectable. However, modern techniques analysing evoked fields permit more sensitive and precise measurement of neural activity at the cortical source (see General Methods for more information on these techniques).

#### **5.1.2.4 Effects of tone pitch**

A number of studies have investigated the effects of pitch on tone processing. Measuring the N1-P2, Roberts et al. (2000) showed that low frequency sounds (i. e. 100Hz) elicit N100s with longer latencies than high frequency sounds (i. e. 1kHz). When studying the effect on N100s of different pitches of tones in noise both monaurally and binaurally, Chait et al. (2006) showed that binaural mechanisms above the level of the SOC may become engaged for pitch created by the binaural 'missing fundamental' effect (Houtsma, 1972), but not monaural pitch stimuli occurring above the

level of the SOC indicating that there may be different mechanisms for binaural and monaural pitch processing (see also Carlyon et al., 2001; Moore, 1997; de Cheveigné, 2005).

#### **5.1.2.5 *Effects of tone intensity***

The stimulus incorporates tones of different levels, so it is important to assess whether there is an effect of amplitude in the auditory cortex. The idea of the tonotopic map in the auditory cortex is well established within the animal (Kosaki et al., 1997; Merzenich & Brugge, 1973) and human literature (Liegeois-Chauvel et al., 1991; Romani et al., 1982; Talavage et al., 2004), unlike the prospect of an amplitude map. Amplitude refers to the variations in brain responses that occur as a result of changes in stimulus amplitude (Cansino, 2006). The literature looking into amplitude of the auditory cortex in humans is sparse and no firm conclusions can be drawn as to its existence or nature. A number of animal experiments have been undertaken to investigate auditory amplitude (e. g. Suga & Manabe, 1982; Taniguchi & Nasu, 1993; Heil et al., 1994), which ultimately have influenced further work on human processing. The first MEG study to look at amplitude in human A1 was undertaken by Pantev et al. (1989) who found that fitted dipoles moved from medial to lateral positions and source depth decreased as intensity increased. However, further MEG studies failed to find amplitude variation in human A1; Vasama et al. (1995) could not replicate the findings of Pantev et al. (1989) despite using similar intensity values, but they did find the expected intensity effect of a decrease in latency and increase in amplitude of the N1 with increasing stimulus intensity. Other work has used MEG and fMRI to investigate amplitude in both animals and humans (e.g. Bilecen et al., 2002; Romani et al., 1982; Liegeois-Chauvel et al., 1991). From these studies it can be concluded that an increase in stimulus intensity leads not to a movement of the source of activity, but rather a spread of activation through the auditory cortex. The exact meaning of the activation spread is not known, however it is possible that it could imply recruitment of further neurons or could be related to draining veins due to increased metabolic demands in the same number of neurons (Cansino, 2006). Ultimately the evidence for an amplitude map in A1 is inconclusive in both MEG and fMRI, in contrast to the robust findings associated with tonotopicity (for a review of these please see Cansino, 2006).

### **5.1.3 The psychophysical BMLD**

As described in Chapter 2, the psychophysical BMLD can be extrapolated into an integer value depicting the dB difference in threshold between the diotic and dichotic tones over masking noise. What has not been previously determined is whether or not it is possible to identify this unmasking effect using a neural correlate derived exclusively from the M100 at a single source location.

### **5.1.4 Aims**

1. Evaluate whether taking a measure of the difference between the M100 amplitudes or latencies for the dichotic and diotic tones will indicate the presence of a BMLD that is comparable to a psychophysical measure.
2. Confirm whether the M100 evoked responses have a shorter latency and larger amplitude for tones that are perceived to be louder over background noise.
3. Confirm whether or not the right hemisphere has a larger response overall than the left hemisphere.
4. Consider the effects of latency and amplitude for the dichotic compared to the diotic tones of the same intensity.

## **5.2 Method**

### **5.2.1 Participants**

17 participants took part (9F) aged between 24 – 73 years. All participants undertook the behavioural psychophysical task, and the passive MEG recording. Anatomical MRI scans were acquired for those individuals who had not already had one. Participants were recruited from the Aston Brain Centre and also the postgraduate population within the School of Life and Health Sciences. Participants gave informed consent and were screened carefully for metal and health-

related contra-indications to being scanned, such as pacemakers. Participants were not paid to take part in this study.

## **5.2.2 Stimuli**

### **5.2.2.1 Psychophysical stimulus**

Each participant undertook a psychophysics task created using Python 2.7.1, designed to determine their BMLD threshold value. The task involved first establishing their noise threshold using a threshold detection paradigm, followed by a 10 reversal 1 up 2 down 2 Alternative Forced Choice (2AFC) task (Levitt, 1971). The first task involved finding the hearing threshold of the participant. A psychophysical paradigm was set up in order to determine the quietest noise that could be heard by the participant. A noise sound was played and the participant had 3 seconds to respond with a click if they perceived the noise. The ISI between the stimuli was jittered from 1000-5000ms in between the trials. Participants were given visual feedback to show that their response had been registered with the program. Once the stimulus had gone below threshold, the participant had to wait until they could hear the noise return once more and then click to register their perception of the noise. This continued for 10 reversals and the geometric mean of the last 8 of these was taken as the threshold.

The participants then undertook the BMLD paradigm using a 5ms tone pip centred on 500Hz over the 500Hz-wide Gaussian noise masker. They first completed the task using the dichotic tone, then repeated the task using the diotic tone. The dichotic task took longer due to the fact that the tone was more easily heard above the noise, so the masked threshold was lower and therefore took longer to reach. This order of presentation was chosen so that the task that took the longest was presented first, and the shorter one second. The difference in length and order of presentation of the two tasks is a limitation as it was not counterbalanced, meaning that there may be order effects. However, the task is designed so that it accurately finds the threshold in each condition by a large number of repeated trials, and the attention and memory load needed to complete this task accurately is well within the capabilities of a typical adult. The BMLD was calculated from the 10 threshold values obtained for each condition, which consisted of the geometric mean of the masked threshold value

for the last 8 reversals for each condition. The first two reversals were discarded as they were designed to be suprathreshold to allow the participant to become accustomed to the task each time.

#### **5.2.2.2 MEG stimulus**

The MEG stimulus was produced using Presentation using tone and noise files created in Matlab. The stimulus consisted of continuous 500Hz wide Gaussian noise centred on 500Hz, presented binaurally at a comfortable listening level (70dB SPL). The tones were presented at 500Hz and had a duration of 50ms with a 5ms rise and fall time. There were 8 tone triggers, with intensities of 20.3, 17.6, 15.2 and 9.1 dB above the background noise level in both the dichotic and diotic conditions. The tone intensities were determined by the step-size of the attenuation levels in Presentation. The tone stimulus ISI was 1 second with a random jitter of up to 100ms and each 500Hz tone lasted 50ms with 5ms rise and fall times. The paradigm lasted approximately 14 minutes in total.

#### **5.2.3 Psychophysical assessment**

The psychophysical assessments took place inside a soundproof chamber within the Aston Brain Centre. The paradigm was presented on a Dell Inspiron mini 10 laptop, using Etymotic insert eartubes with transducers. The values at each reversal for the dichotic and diotic threshold tasks were recorded and checked for face validity.

#### **5.2.4 MEG data collection**

The data were collected on the Elekta Neuromag system. The participants' headshape was first collected using the Elekta polhemus system. Then the participants were introduced into the scanner after being carefully screened for metal. Once settled in the scanner, a silent video was played for the participant while any bad channels were heated to reduce trapped flux. Just before the recording started, the participants were informed and notified that they would receive the sounds. They were reminded to stay as still as they could during the recording, and were instructed to relax and continue to watch the silent video throughout. This was to reduce fatigue and also visual stimulation was employed to reduce the amount of resting alpha activity which could produce artefacts in the

resulting data. Participants were not asked to attend to the stimuli. Data were collected at a sample rate of 1000Hz and an on-line average was also collected to check an auditory response was being elicited during the recording. The head position of the participant was continuously monitored throughout the recording.

### **5.2.5 Psychophysics analysis**

The thresholds for the perception of the dichotic and diotic tones over the masking noise were found and the BMLD value calculated using Equation 5.1.

$$20 \times \log_{10}(S_{ONO}/S_{piNO}) \quad (5.1)$$

$S_{ONO}$  and  $S_{piNO}$  here refer to the threshold values for the diotic and dichotic stimuli respectively.

### **5.2.6 MEG sensor data analysis**

The data were preprocessed using tSSS (Taulu & Simola, 2006) with movement correction using a sphere with origin derived from the cardinal points. The data were then digitally filtered between 0.5-30Hz. Following this the data were visually inspected and epochs associated with each trigger averaged separately using MNE software (Dale et al., 2000). Epochs were obtained over the time period of 400ms to 400ms surrounding each trigger. Averages were visually inspected as overlays of groups of channels using MNE software to identify the channel with the largest amplitude. Matlab was used to take sample point data depicting the M100 amplitude and latency of each trigger average from the channel which had the largest amplitude of evoked response within each hemisphere between 0–200ms. The values for amplitude and latency for each trigger were scaled within each individual to obtain a measure of the variance in the response sizes.

### **5.2.7 MEG source data analysis**

#### **5.2.7.1 *Freesurfer reconstruction***

The anatomical MRI was prepared and checked according to the Freesurfer reconstruction protocol freely available online (Fischl, 2012) and a headshape was created from the reconstructed MRI using

Elekta software. This headshape was coregistered with the MEG polhemus points using a modified version of a surface matching coregistration program previously described by Adjamian et al. (2004).

#### **5.2.7.2 Inverse estimate**

The noise-normalized and depth-weighted dSPM estimate (Dale et al., 2000) available in the MNE software (Hämäläinen & Ilmoniemi, 1994) was used to find the inverse solution reflecting the measured data for each participant in the reconstruction of their inflated cortex. The averaged data were loaded into the MNE software and viewed using the derived inverse operator. The noise-normalized and depth-weighted dSPM activity distribution was displayed on the inflated cortex (Dale et al., 2000). The noise covariance file from the raw data was used to threshold the image to only show activity that was significantly larger than the background noise. Each hemisphere was viewed separately. The data for the loudest dichotic trigger was used in subsequent analysis to localise the peak response, as this elicited the largest M100 response in all participants. The location of a peak voxel in the ROI was selected for the biggest dichotic stimulus, and timeseries for all triggers were reconstructed at this location.

To do this, examination of the strength of activity 20ms before and after the sensor level evoked M100 latency for this trigger for each participant was used to check the spread of activity was occurring in the expected location of the superior temporal gyrus (STG). The latency at which the strength of activity was observed to be strongest within this time range was used as the latency from which to choose a suitable vertex for localisation.

A vertex within the peak activation located halfway between the lateral and medial edges of the STG in the coronal plane and within the posterior half of the STG in the sagittal plane was chosen using the participant anatomical MRI as a guide. Within this ROI, the vertex displaying the timeseries with the largest N100 response amplitude was chosen. The Talairach co-ordinates of this location were recorded for each hemisphere. Once the latency and vertex of interest were identified for the largest dichotic trigger, timeseries data (-400 to 400ms) were computed for all of the remaining triggers in

the same location for both types of masked tone. This protocol was used in each hemisphere separately.

The timeseries data were loaded into Matlab and the sample point containing the largest amplitude of activity within 50-150ms post-trigger was identified as the latency of interest for each trigger separately. The amplitudes and latencies for each trigger were established in this manner. The amplitudes of each M100 were plotted against the associated dB tone level above noise for both types of tone.

Additionally, the latency of the maximum amplitude for each trigger timeseries were found separately, within the window of 50-130ms using Matlab. This reduced window was due to the fact that as the M100 amplitudes became smaller with decreasing tone intensity, the M200 would sometimes be the largest peak within the 50-150ms range. The latencies and amplitudes of the M100 for each trigger separately were found.

## **5.3 Results**

### **5.3.1 Psychophysics**

The psychophysical thresholds for noise, dichotic stimulus and diotic stimulus are shown in Table 5.1. Also shown is the calculated BMLD value for each participant.

Participant	Noise threshold	Dichotic threshold	Diotic threshold	BMLD value
1	0.00046	0.0079	0.051	16.1
2	0.00066	0.034	0.049	18.1
3	0.00043	0.0036	0.0215	15.5
4	0.00228	0.0097	0.1934	26
5	0.00038	0.0083	0.07702	19.4
6	0.0004	0.00864	0.0629	17.3
7	0.00037	0.0139	0.0594	12.6
8	0.00048	0.01104	0.06118	14.9
9	0.00025	0.0089	0.0479	14.6
10	0.00018	0.00649	0.01259	5.8
11	0.00118	0.02054	0.07182	10.9
12	0.00046	0.01274	0.032	7.9
13	0.00040	0.01153	0.07065	15.8
14	0.00057	0.00749	0.06964	19.4
15	0.00047	0.0147	0.0657	13
16	0.00030	0.01073	0.05776	14.6
17	0.00752	0.01042	0.05776	14.9
<b>MEAN</b>	<b>0.00099</b>	<b>0.0118</b>	<b>0.0621</b>	<b>15.1</b>
<b>STD DEV</b>	<b>0.00175</b>	<b>0.0069</b>	<b>0.0386</b>	<b>4.59</b>

**Table 5.1** Psychophysical thresholds and BMLD values. The table shows the initial noise threshold, and dichotic and diotic thresholds for each participant. The table also shows the BMLD value calculated from these thresholds. The mean dichotic threshold is 0.0118 and standard deviation is 0.0069. The mean diotic threshold is 0.0621 and standard deviation is 0.0386. The mean BMLD value is 15.1dB with a standard deviation of 4.59.

### 5.3.2 MEG sensor data

An example sensor average is shown in Figure 5.1.

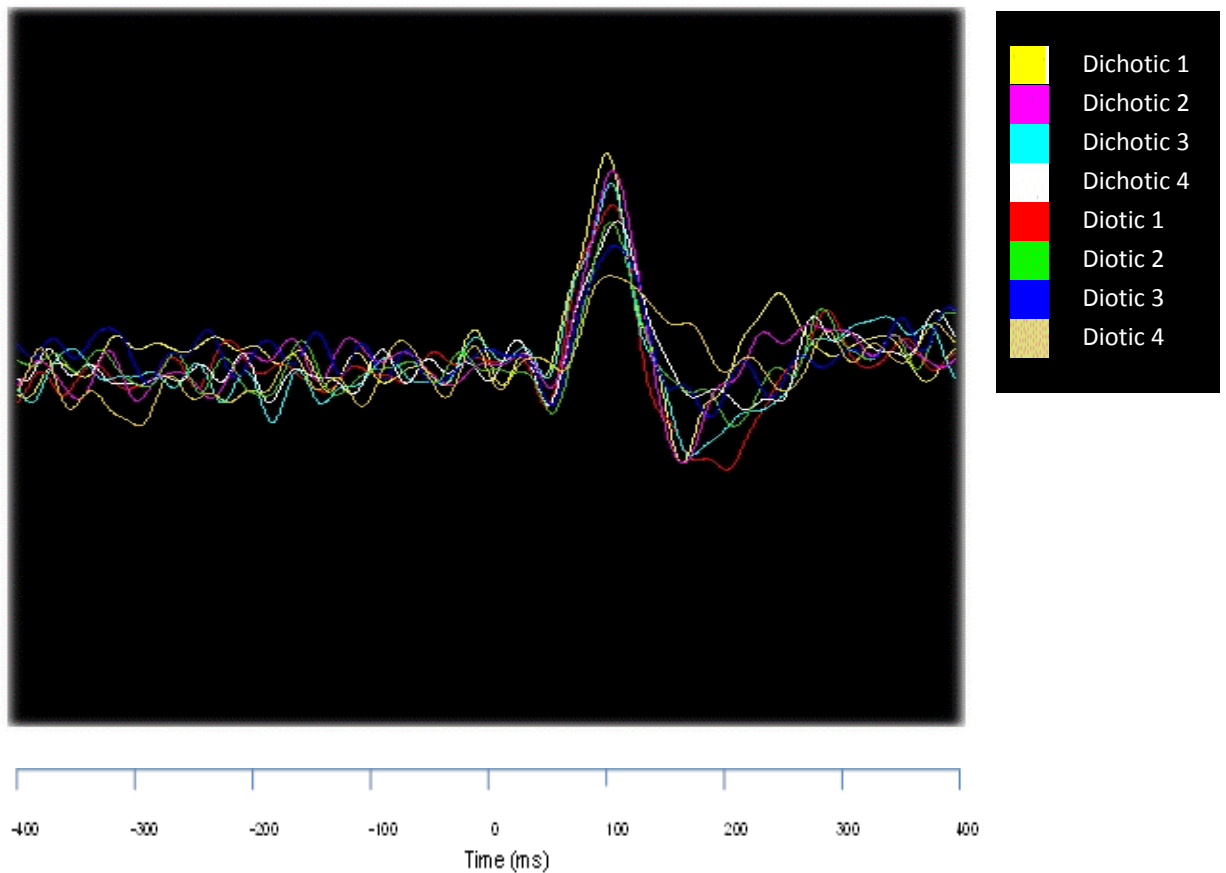


**Figure 5.1** Evoked response from one group of channels taken from the left temporal lobe from an example participant showing the M100 responses to each intensity of the tone. The sensor data is visualised using MNE software. This participant was an adult female who was an experienced listener. The key denotes the colours related to the loudest (1) to quietest (4) dichotic and diotic tone stimuli. The evoked responses are shown here for relative purposes.

As can be seen from Figure 5.1, sensor level averages showed the expected decrease in amplitude and increase in latency as the tones became less salient over the background noise. The effect is also seen in the group data. Figures 5.2 and 5.3 show the scaled group level mean amplitudes for each trigger condition. The amplitude values need to be scaled when viewed at the group level because individual differences in head position, channel noise and anatomy may all contribute to a large difference in the amplitude of the evoked responses between people and between recordings. Here, only the relative differences between the tone stimulus intensity and tone stimulus phase are important, so scaling provides a useful measure of visualisation between a group of individuals.

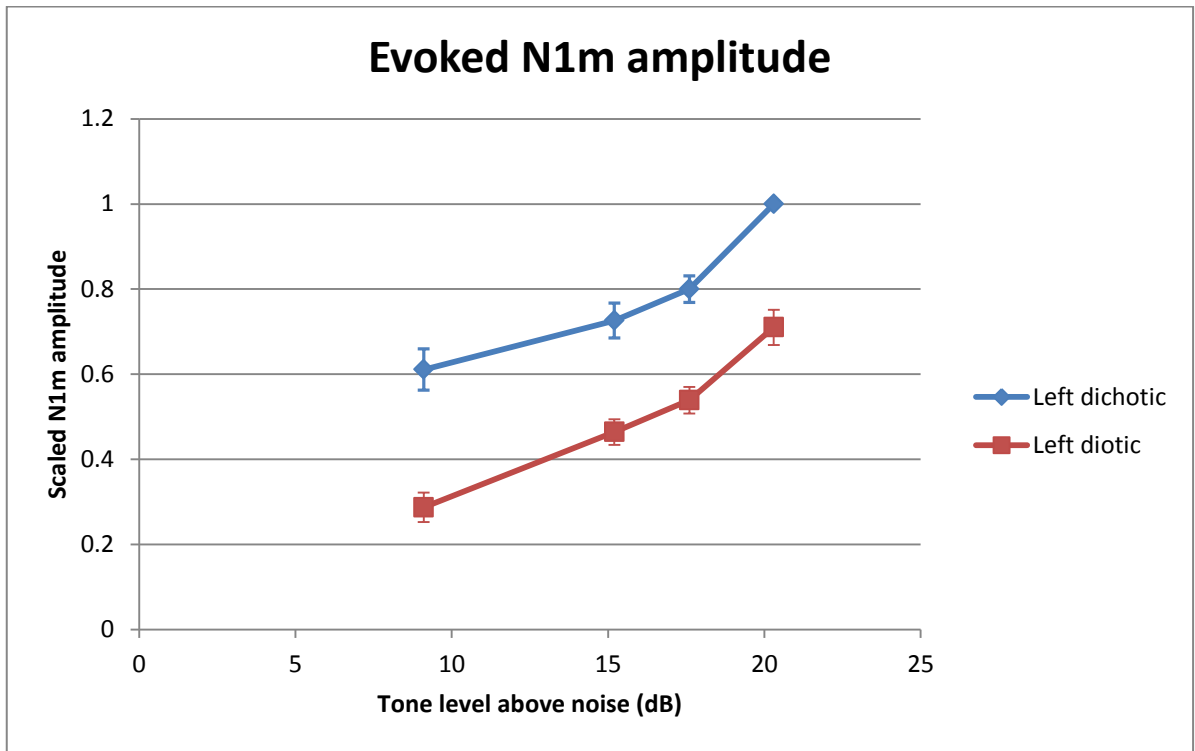


**Figure 5.2** Scaled group mean N1m evoked amplitudes for the left hemisphere. The error bars indicate 95% confidence intervals. (N=17). Responses are scaled to the loudest dichotic trigger.

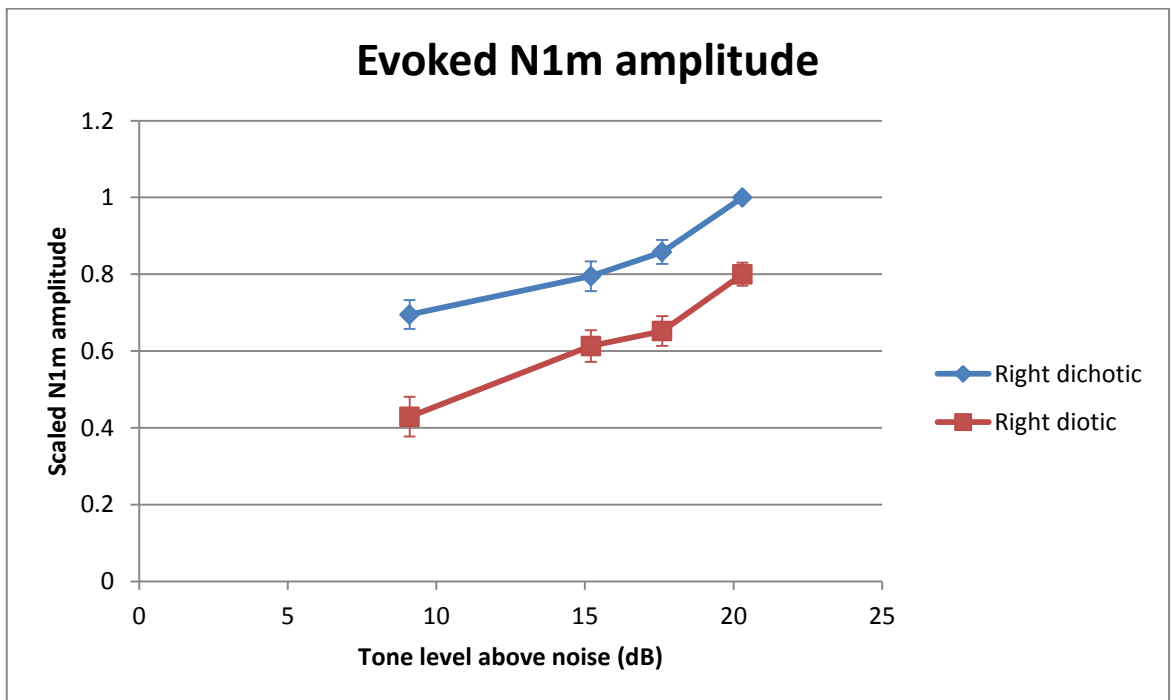


**Figure 5.3** Scaled group mean N1m evoked amplitudes for the right hemisphere. The error bars indicate 95% confidence intervals. (N=17). Responses are scaled to the largest dichotic trigger.

A repeated measures ANOVA was performed to study the effects of hemisphere, phase and intensity on N1m amplitude at sensor level. The results reported with a Greenhouse-Geisser correction show there was a significant main effect of phase,  $F(1, 17) = 86.214$ ,  $p < .001$ , and intensity,  $F(1.4, 17) = 43.196$ ,  $p < .001$ , but no significant main effect of hemisphere,  $F(1, 17) = .234$ ,  $p = .635$  on the amplitude of the N1m at sensor level. There was a significant interaction between phase and intensity,  $F(3, 17) = 3.456$ ,  $p = .046$ . No other interactions were significant.

Post hoc testing using the Bonferroni correction revealed a significant difference in means of evoked responses between all tone intensities, ( $p < 0.05$ ), with the exception of between the two middle tone intensities ( $p = 0.07$ ). These results suggest that the amplitude values were not significantly different between the hemispheres, but were significantly different between the dichotic and diotic tone responses. The response amplitudes are significantly different between the different intensities, except for between the 15.2 and 17.6dB tone levels over the background noise.

Overall the scaled amplitude data from the evoked responses has shown the expected decrease in response to a decrease in tone intensity, with a significant difference between the dichotic and diotic tone values at each level. Unlike amplitude, latency values do not need to be scaled when compared as a group in MEG due to its excellent temporal resolution. Figures 5.4 and 5.5 show the mean latency values for the group population for each stimulus condition.

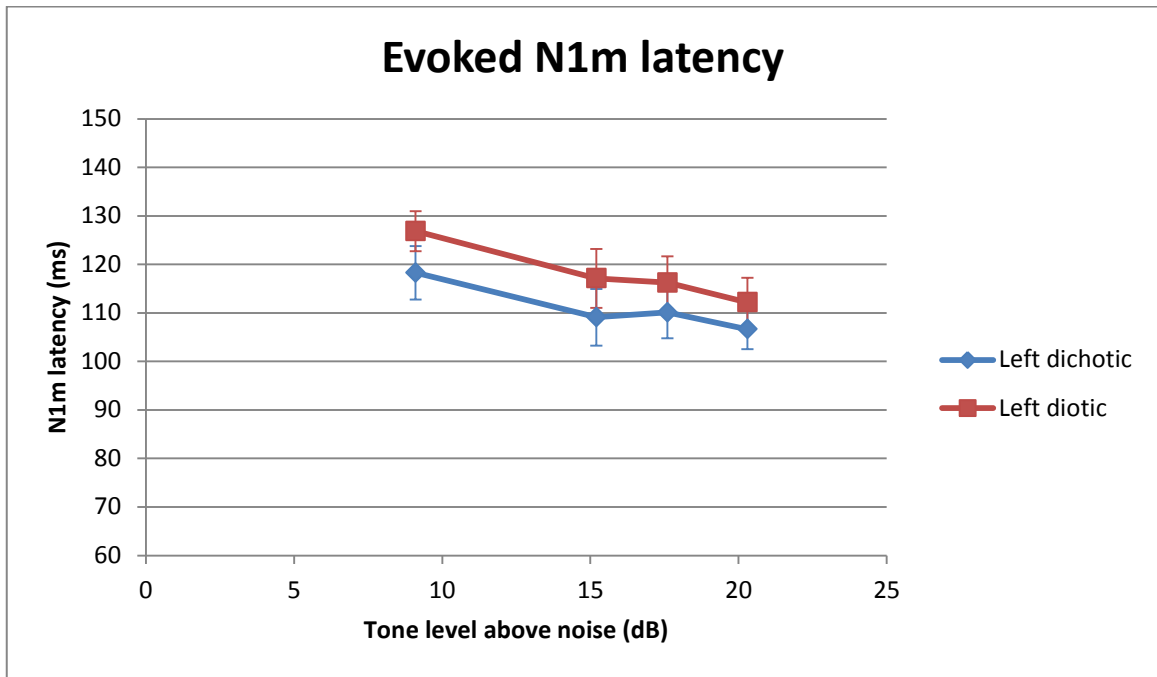


**Figure 5.4** Group mean N1m evoked latencies for the left hemisphere. The error bars indicate 95% confidence intervals. (N=17).

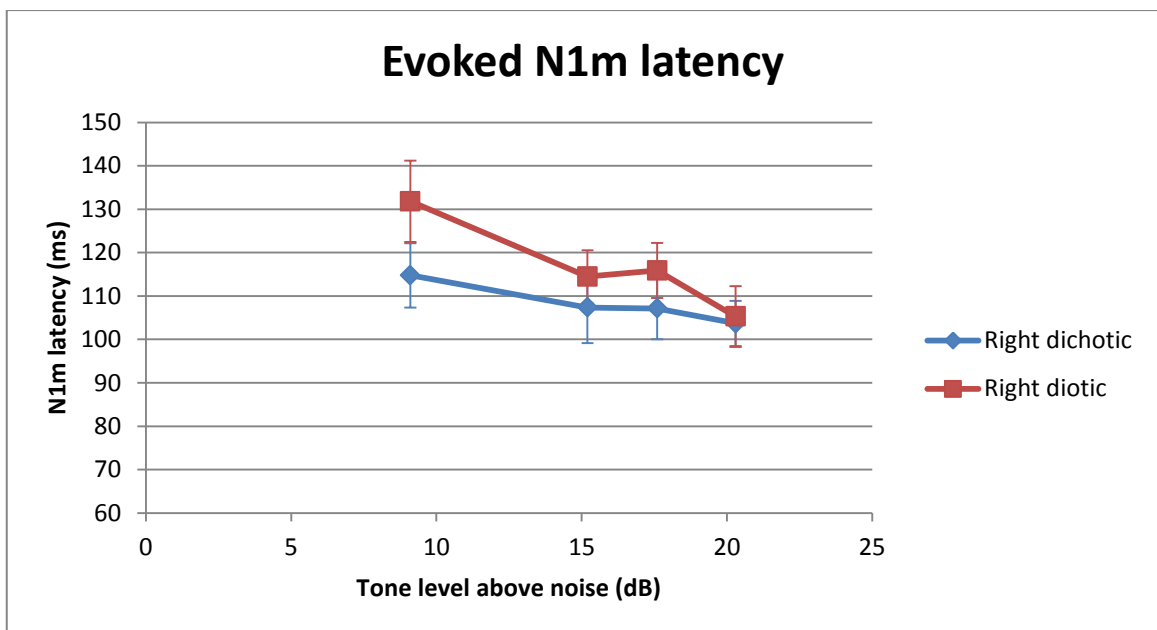


**Figure 5.5** Group mean N1m evoked latencies for the right hemisphere. The error bars indicate 95% confidence intervals. (N=17).

The graphs in Figures 5.4 and 5.5 indicate that there is no significant difference between the dichotic and diotic latency values in either the left or right hemispheres as there is an overlap between the 95% confidence interval error bars.

A repeated measures ANOVA was performed to study the effects of hemisphere, phase and intensity on N1m amplitude at sensor level. The results reported with a Greenhouse-Geisser correction show there was a significant main effect of phase,  $F(1, 14) = 28.362$ ,  $p < .001$  and intensity,  $F(1.892, 14) = 33.188$ ,  $p < .001$ , with no significant main effect of hemisphere,  $F(1, 14) = 1.362$ ,  $p = .264$  on the latency of the N1m at sensor level. There was a significant interaction between phase and intensity,  $F(3, 14) = 3.783$ ,  $p = .044$ .

Post hoc testing using the Bonferroni correction revealed a significant difference in means between all intensities, apart from between the two middle intensities ( $p = .07$ ). Overall, these results suggest that the latency values are not significantly different between the hemispheres, but are significantly different between the dichotic and diotic tone responses. The response latencies are significantly different between the different intensities, except for between the 15.2 and 17.6dB tone levels over the background noise.

### 5.3.3 MEG source estimates

#### 5.3.3.1 Localisations

The Talairach co-ordinates were extracted from the chosen vertex in each individual's inverse estimate. The Talairach co-ordinates for each individual are shown in Table 5.2, and the mean localisation is demonstrated on a template brain in Figure 5.6.

Participant	Left hemisphere			Right hemisphere		
	X	Y	Z	X	Y	Z
1	-46.7	-15.8	4.6	53.3	-30.2	10
2	-53.6	-27.3	5.9	49.6	-28.1	9.1
3	-53.5	-21.2	-5.4	51.6	-22.8	8.7
4	-53	-28.6	6.2	48.3	-20.5	12.1
5	-57	-30.7	5.8	51.5	-17.4	4.5
6	-44.8	-26.6	5.7	52.3	-25.4	8.4
7	-55	-30.3	10.6	60.7	-9.4	3.7
8	-54.3	-17.9	4.1	46.3	-18.7	2.1
9	-49.2	-27.2	2.3	47.3	-20.1	4.4
10	-47.4	-22.6	2.6	51.4	-27.8	8.3
11	-48.3	-29.1	7.4	44.9	-21.2	5.3
12	-52.8	-14.1	0.7	44.3	-21.6	7
13	-46.5	-30	11.4	45.2	-26.7	19.6
14	-48.5	-31.2	3	49.8	-21.9	2.4
15	-52.8	-23	-0.6	48.1	-25.4	8.1
16	-58.1	-24.8	-0.1	51.7	-18.1	6.6
17	-55.1	-34.6	4.8	49.3	-28.1	4.8
<b>Mean</b>	<b>-51.6</b>	<b>-25.6</b>	<b>4.1</b>	<b>49.7</b>	<b>-22.6</b>	<b>7.4</b>
<b>Std Dev</b>	<b>3.9</b>	<b>5.8</b>	<b>4.1</b>	<b>3.9</b>	<b>5.2</b>	<b>4.2</b>

**Table 5.2** Talairach co-ordinates extracted for the dSPM estimate using the M100 response to the largest dichotic trigger. The mean and standard deviation for each co-ordinate in each hemisphere are shown.

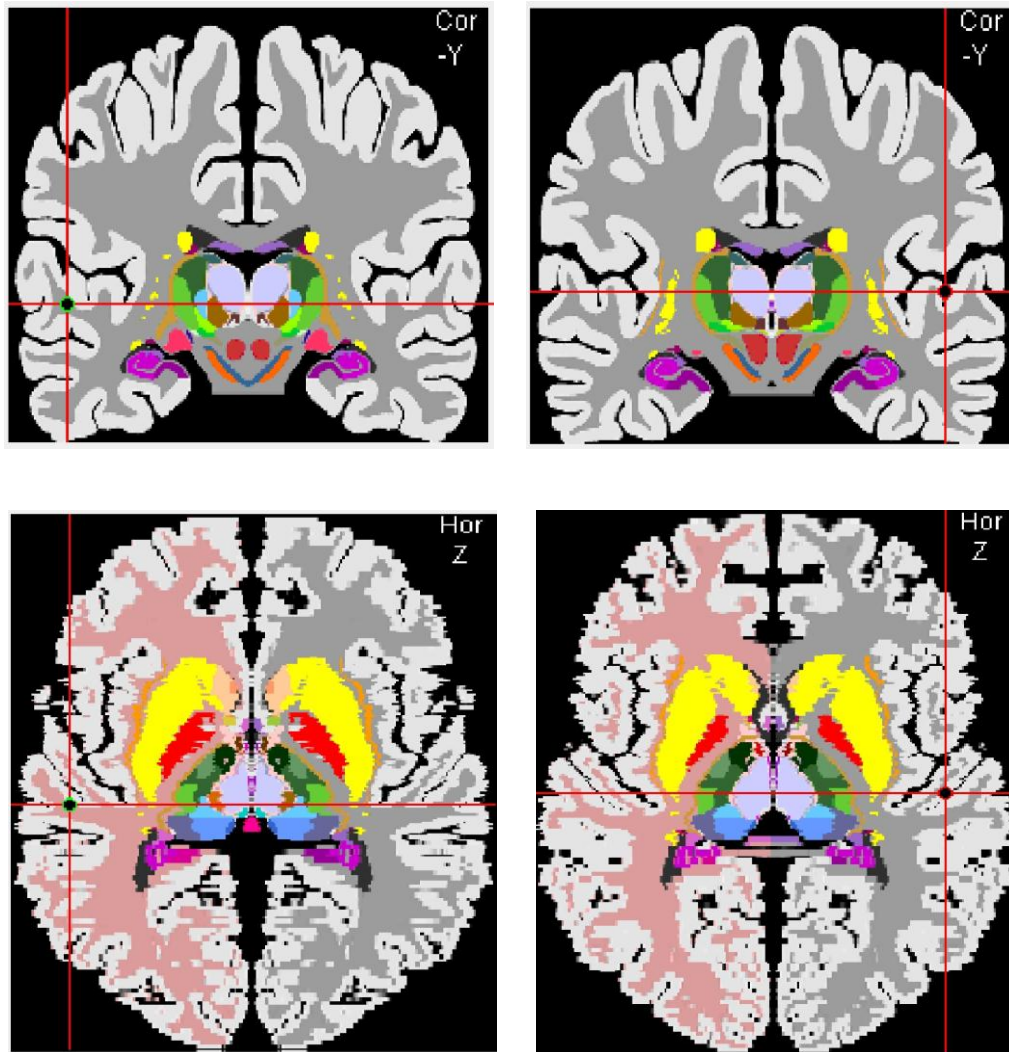
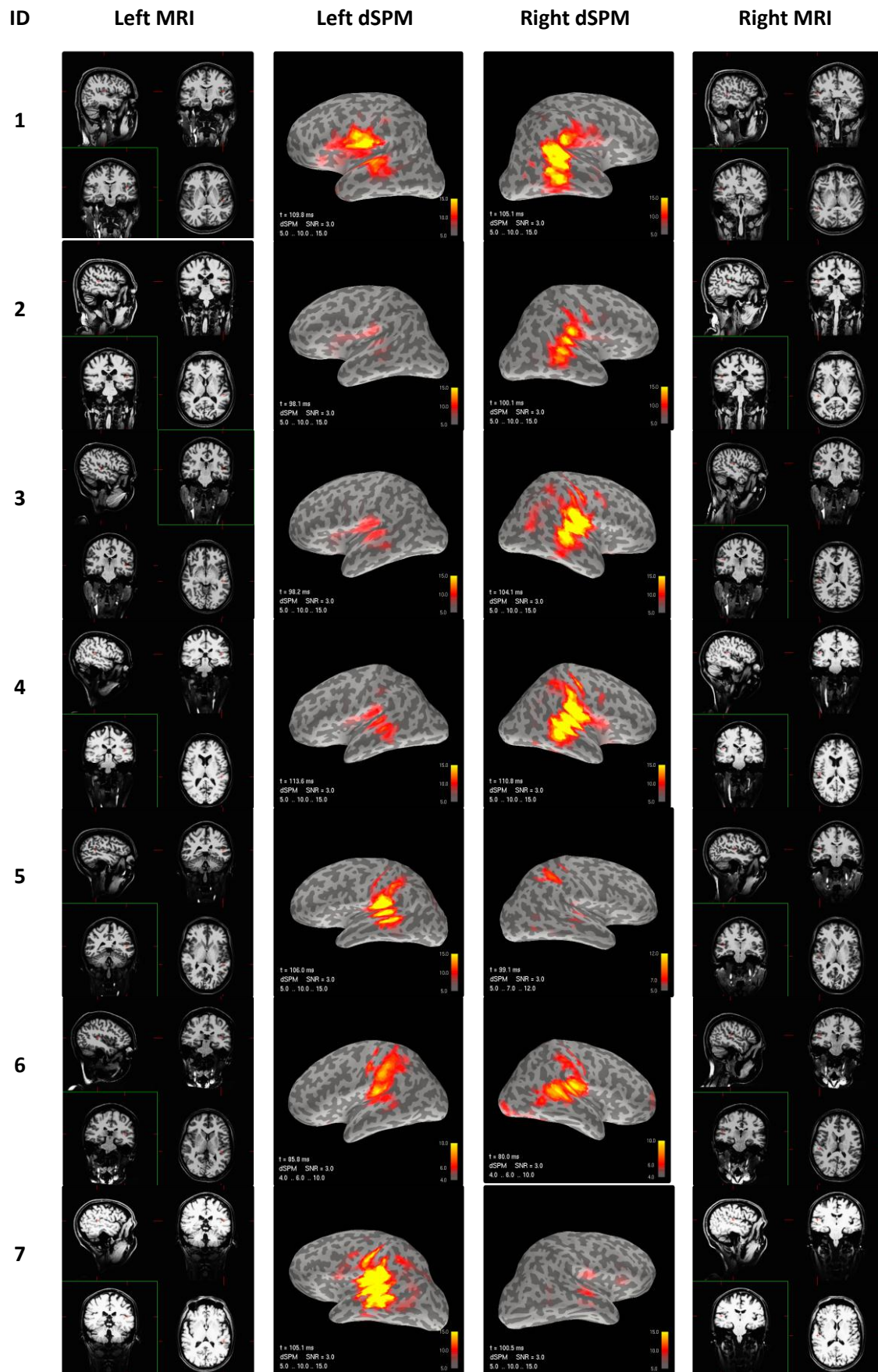
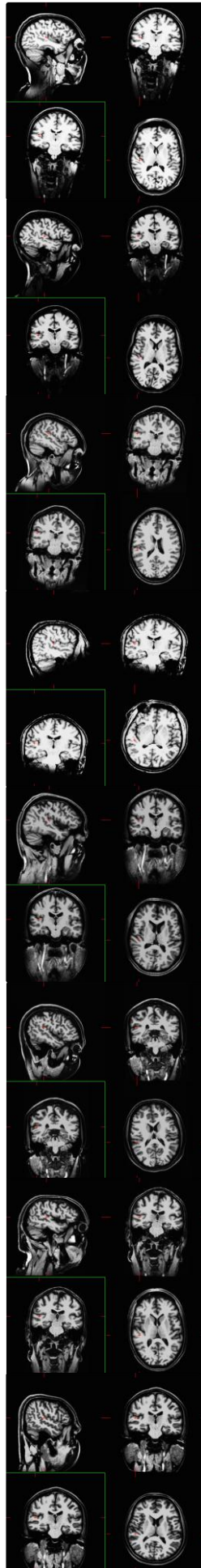
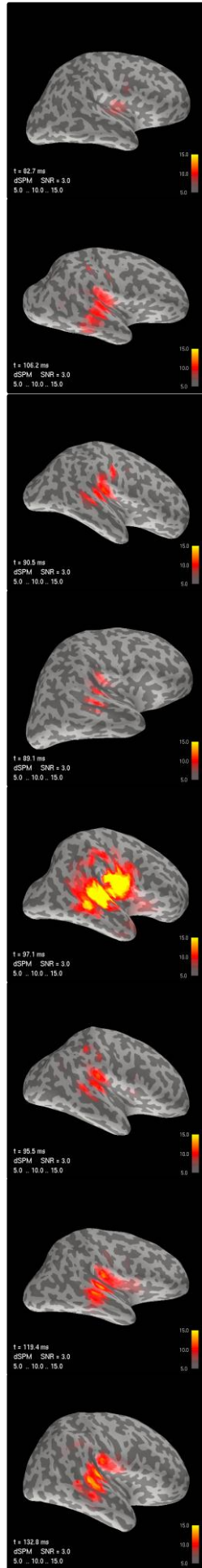
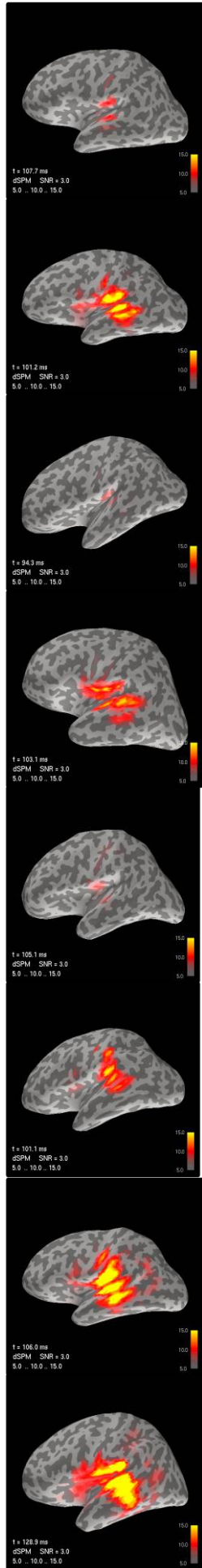
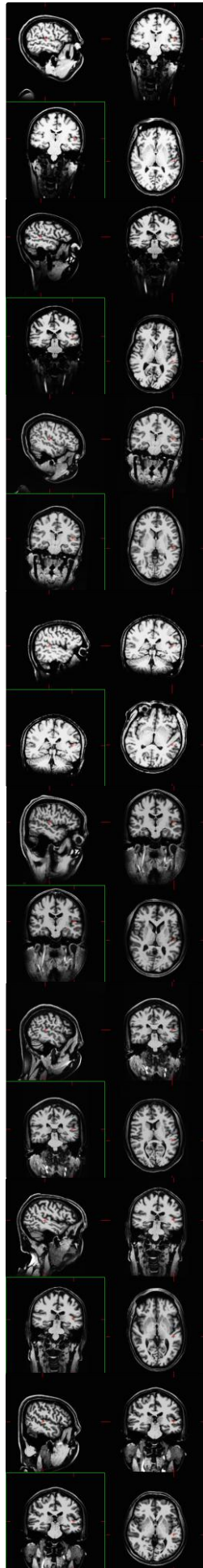


**Figure 5.6** Mean Talairach localisations taken from the activations shown in the dSPM estimate for the largest dichotic trigger. The top row shows the coronal plane and the bottom row shows the sagittal plane. The localisations are displayed on the template brain provided by humanbrain.info with permission.

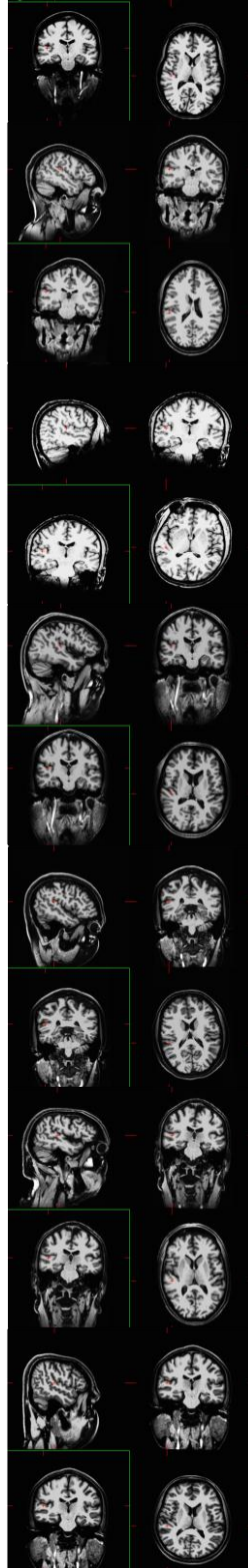
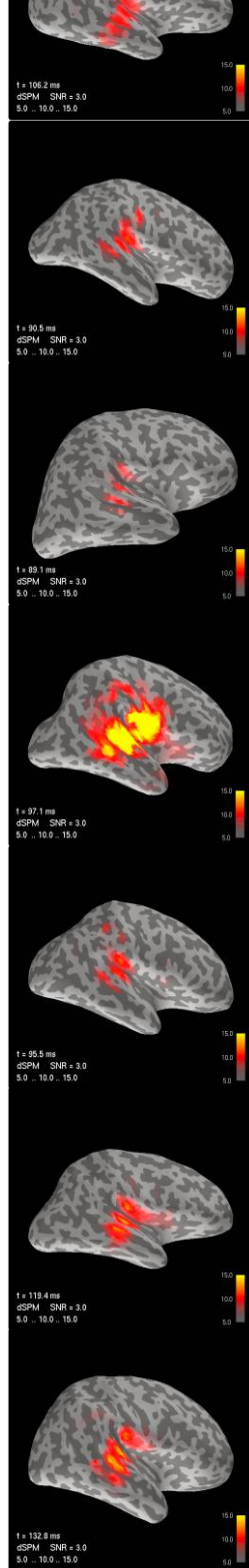
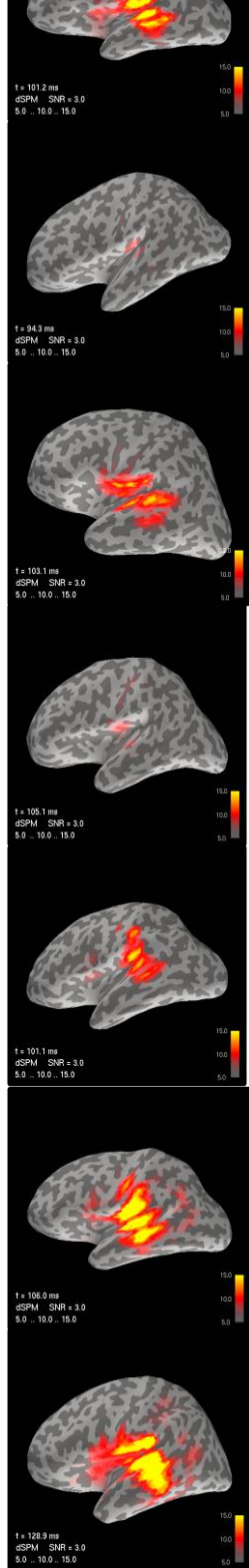
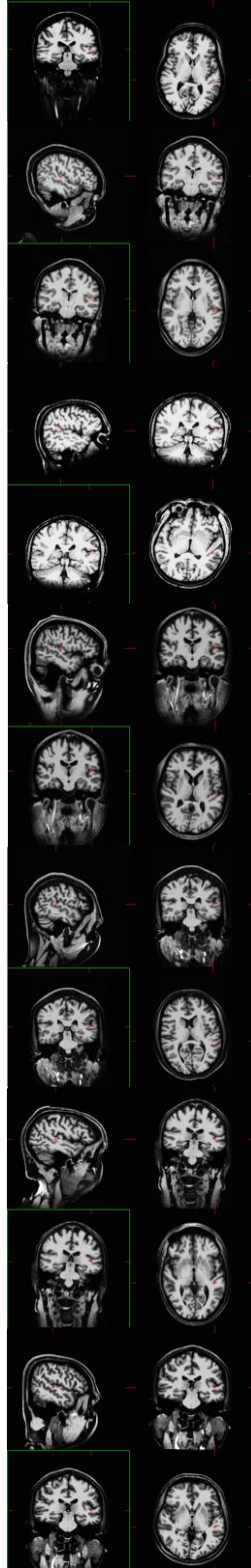
As can be seen from Figure 5.6, the mean localisations for the largest response amplitude is slightly more inferior and posterior in the left than the right hemisphere. Each individual has one hemisphere with a stronger dSPM than the other, as can be seen in Figure 5.7. The images are thresholded individually for easy visualisation of the spread of activity.



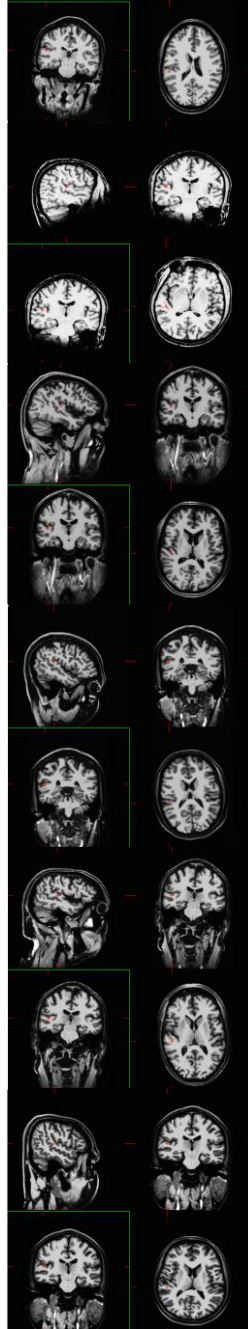
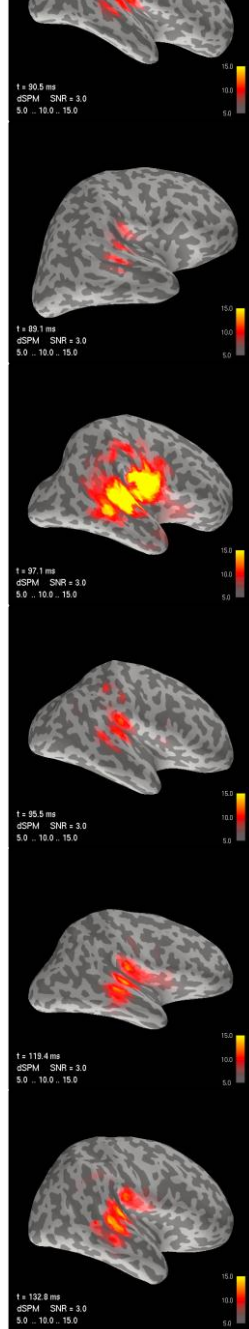
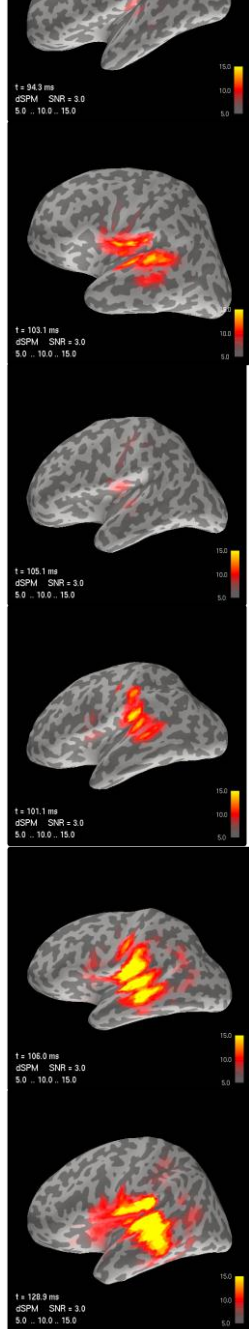
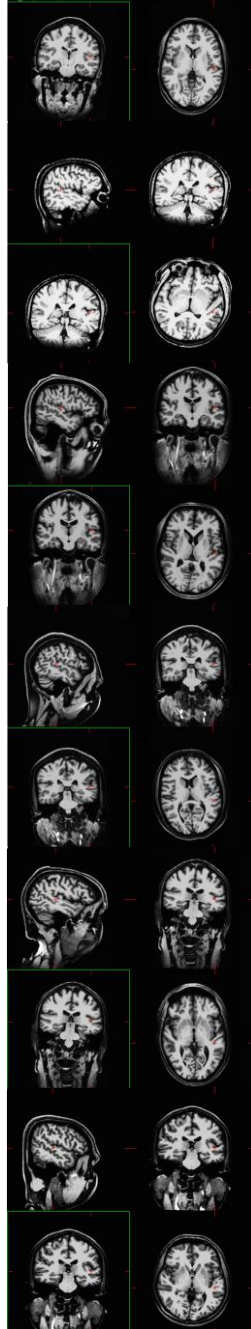
8



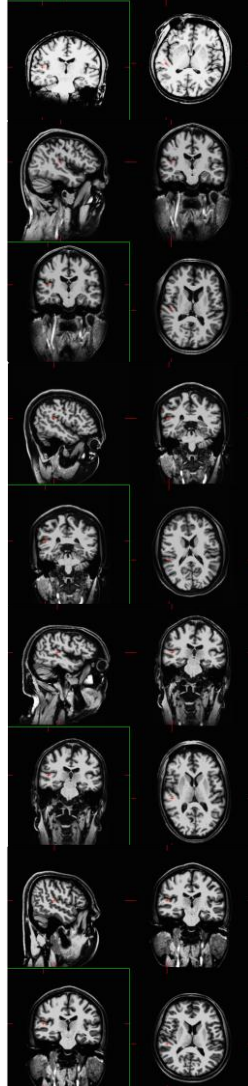
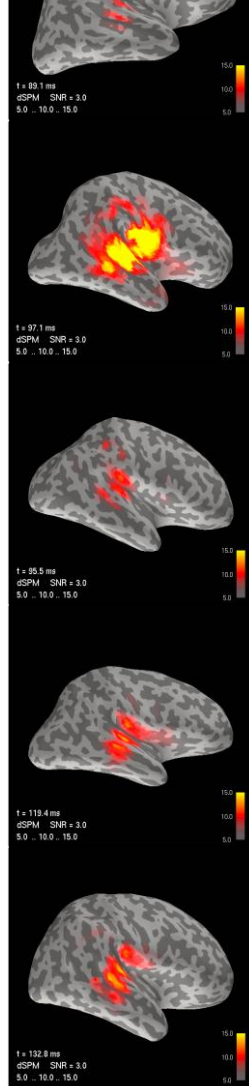
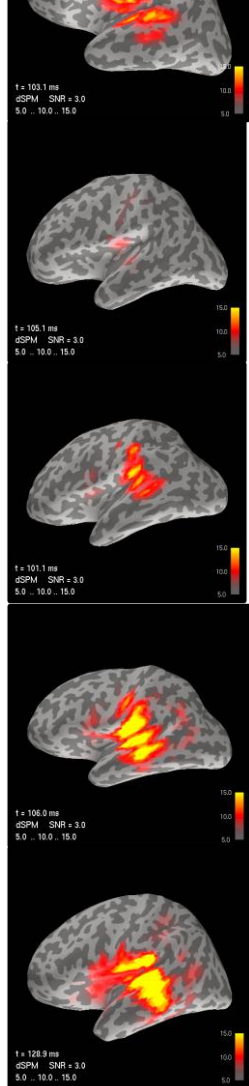
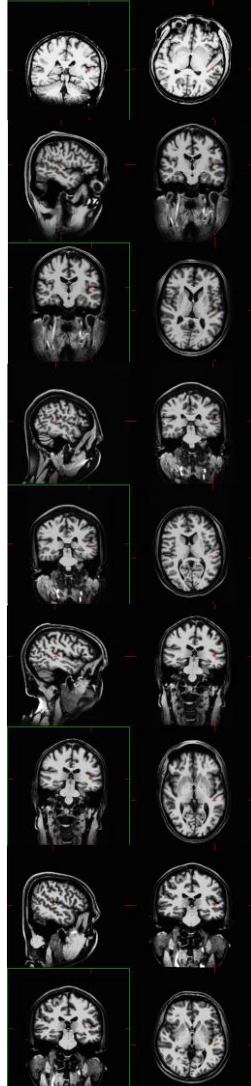
9



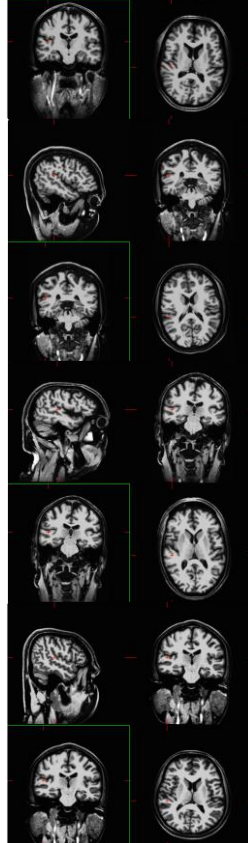
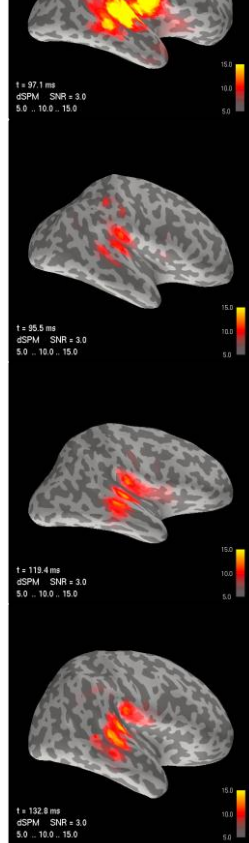
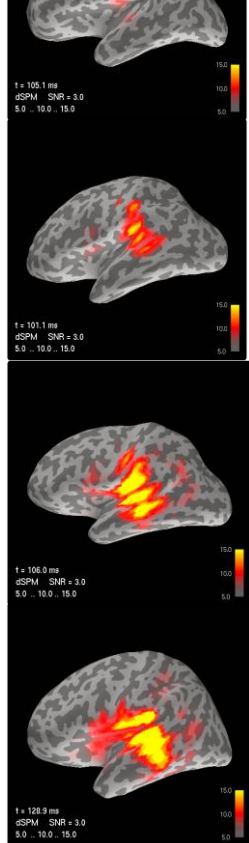
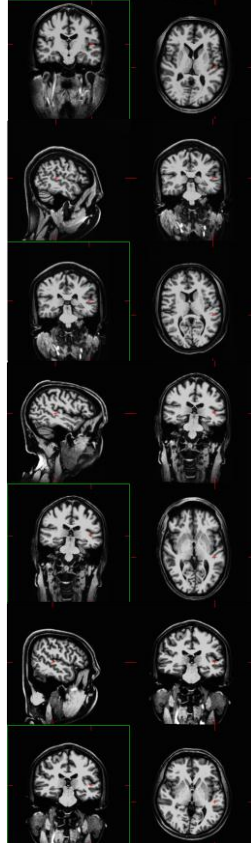
10



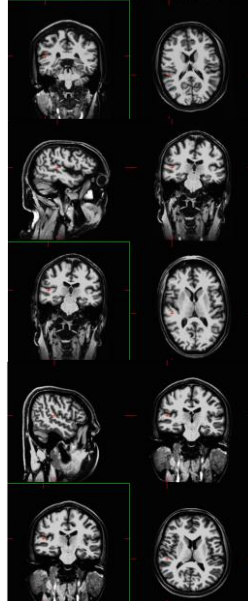
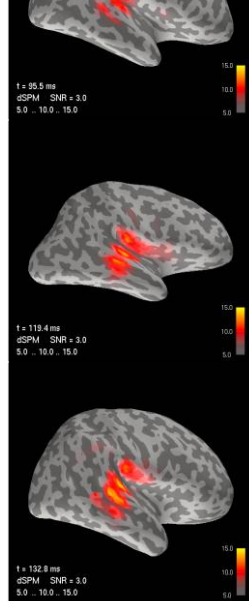
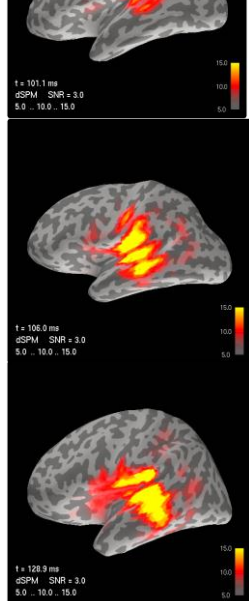
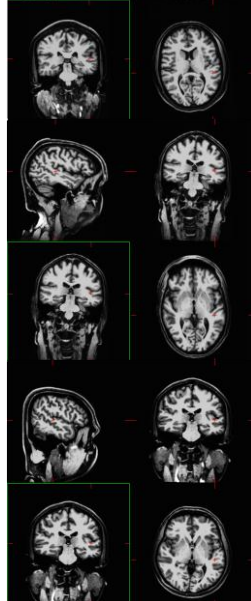
11



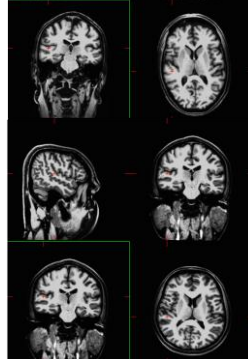
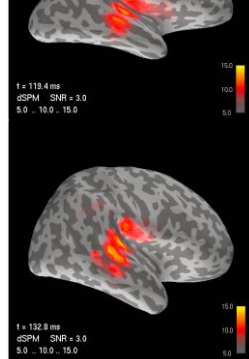
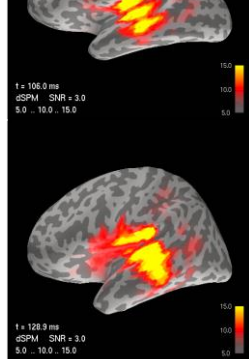
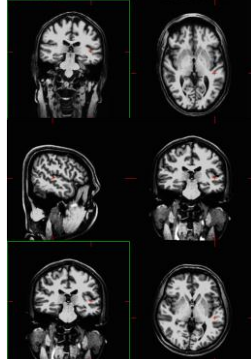
12



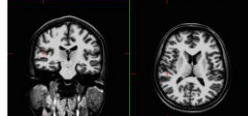
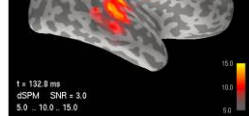
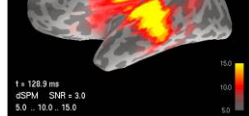
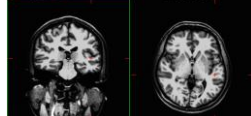
13



14



15



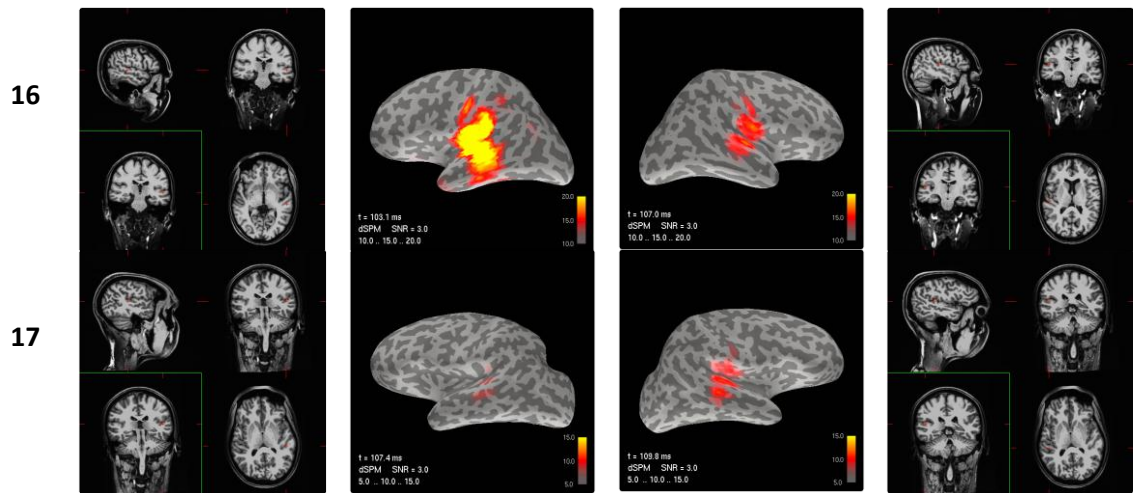


**Figure 5.7** Distribution of activation using the dSPM estimate for each participant for the largest dichotic trigger. The dSPM estimate is shown in the two central columns, with the corresponding anatomical MRI shown in the outer columns showing the location of the chosen vertex. The MRIs are presented in radiological view. Latencies and threshold values are shown on the images.

### 5.3.3.2 Timeseries amplitudes

The timeseries amplitudes for the N1m are displayed in Figures 5.8 and 5.9 as a group mean. The amplitudes have been scaled to the largest dichotic trigger. The amplitudes show the expected pattern of increase with an increase in tone intensity above the background masking noise, and the 95% confidence intervals suggest a significant difference between the dichotic and diotic tone values. The graphs show a similar pattern of results compared to the sensor amplitude data (Figures 5.2 and 5.3), however in the timeseries data there is a difference, as the right hemisphere diotic response for the second data point (15.2dB) shows an unexpected increase in response amplitude compared to the next loudest stimulus.

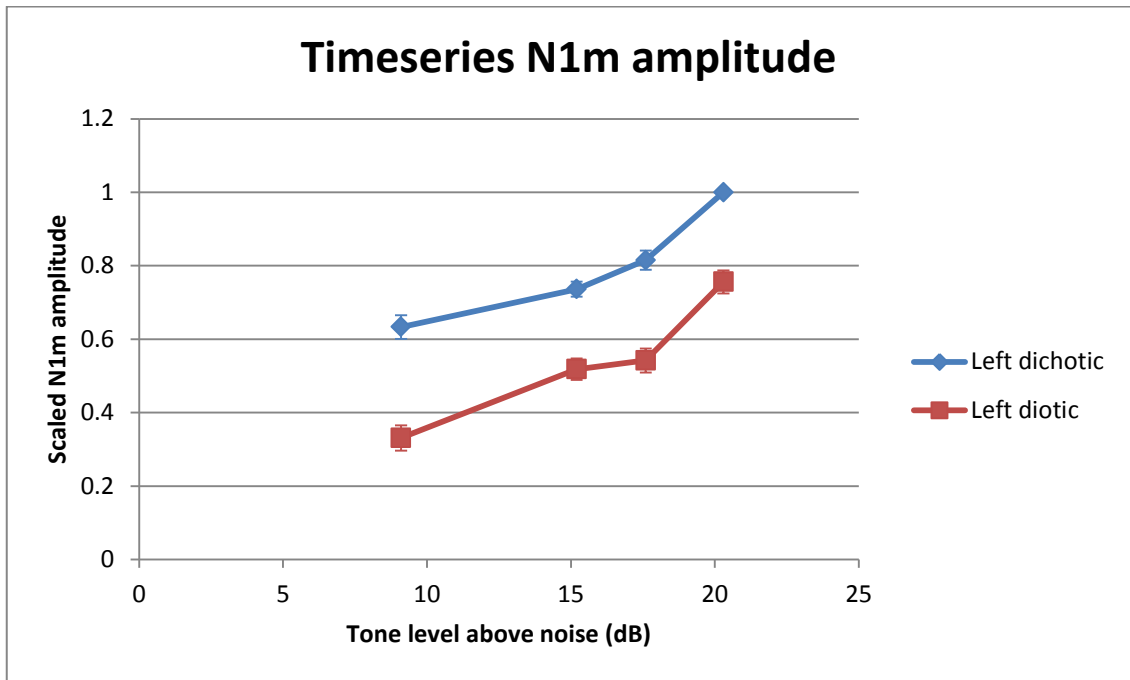


**Figure 5.8** Scaled group mean N1m timeseries amplitudes for the left hemisphere. The error bars indicate 95% confidence intervals. (N=17). Amplitudes are scaled to the largest dichotic trigger.

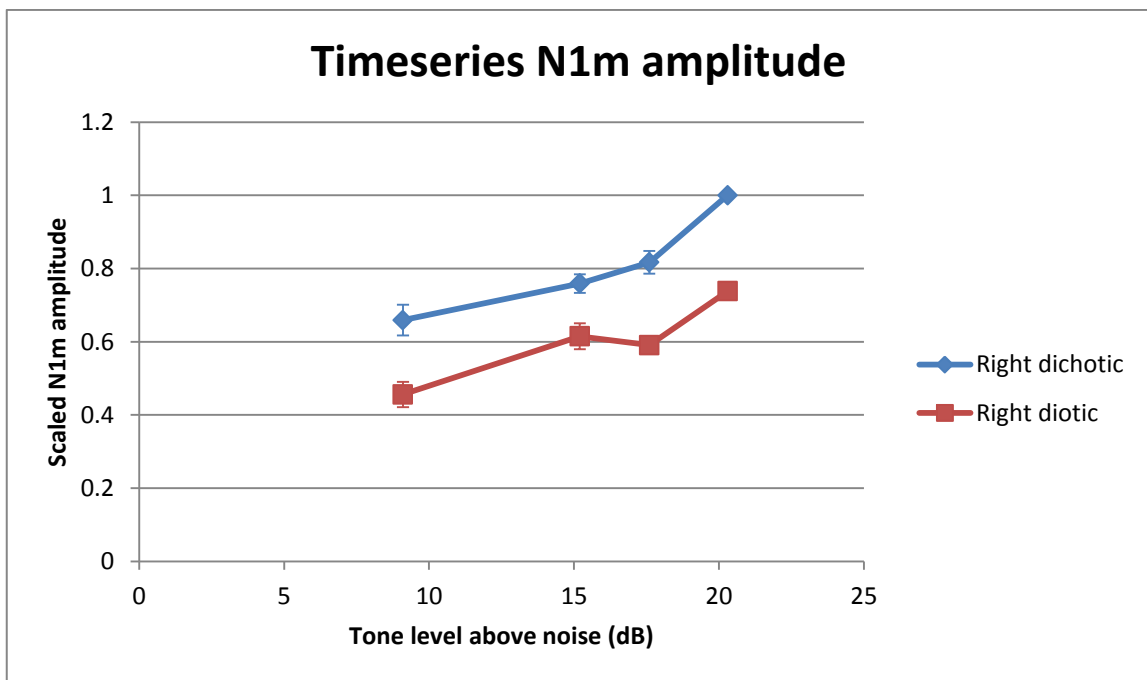


**Figure 5.9** Scaled group mean N1m timeseries amplitudes for the right hemisphere. The error bars indicate 95% confidence intervals. (N=17). Amplitudes are scaled to the largest dichotic trigger.

A repeated measures ANOVA was performed to study the effects of hemisphere, phase and intensity on N1m amplitude. The results reported with a Greenhouse-Geisser correction show there was no significant main effect of hemisphere on the amplitude of the N1m,  $F(1, 17) = .003$ ,  $p = .958$ . There was a significant effect of phase,  $F(1, 17) = 156.303$ ,  $p = .000$ , and intensity,  $F(1.28, 17) = 41.66$ ,  $p = .000$  on the N1m amplitude. There were no significant interactions between hemisphere, phase and intensity. Post hoc testing using the Bonferroni correction revealed a significant difference in means between all intensities, apart from between the two middle intensities ( $p = .594$ ). These results suggest that the amplitude values are not significantly different between the hemispheres, but are significantly different between the dichotic and diotic tone responses. The response amplitudes are significantly different between the different intensities, except for between the 15.2 and 17.6dB tone levels over the background noise.

### ***5.3.3.3 Timeseries latencies***

The timeseries latencies for the N1m are displayed in Figures 5.10 and 5.11 as a group mean. The latencies show the expected pattern of decrease with an increase in tone intensity above the background masking noise, and the 95% confidence intervals suggest no significant difference between the dichotic and diotic tone values, with the exception of the third data point in Figure 5.11 which would suggest a significant difference between the dichotic and diotic values at this intensity.

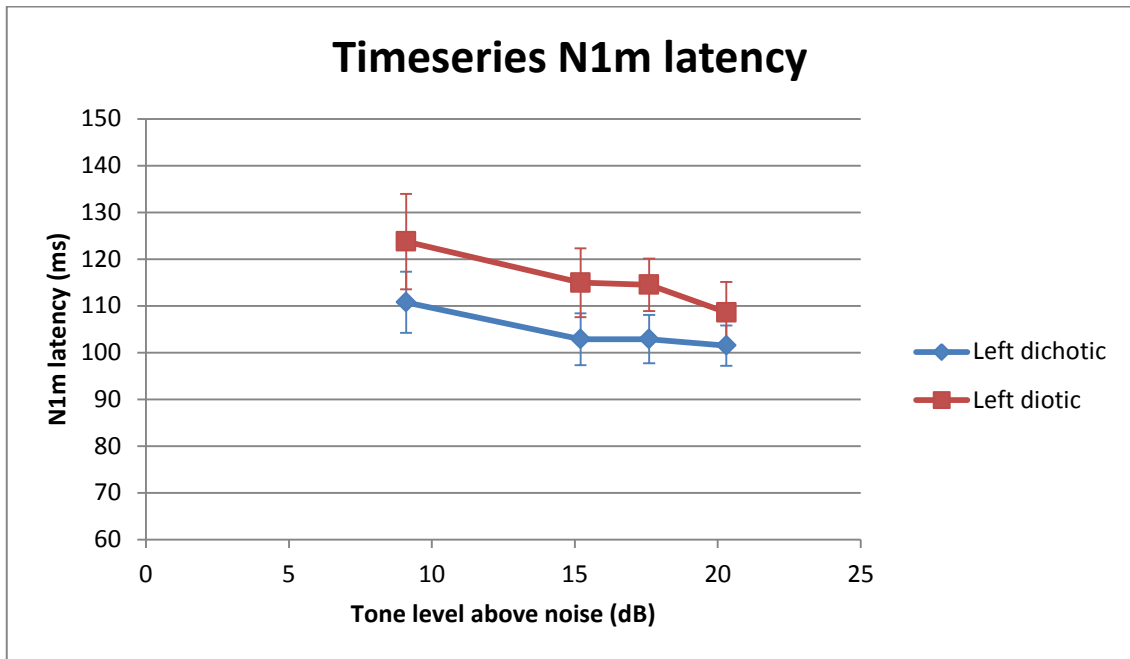


**Figure 5.10** Group mean N1m timeseries latencies for the left hemisphere. The error bars indicate 95% confidence intervals. (N=17).

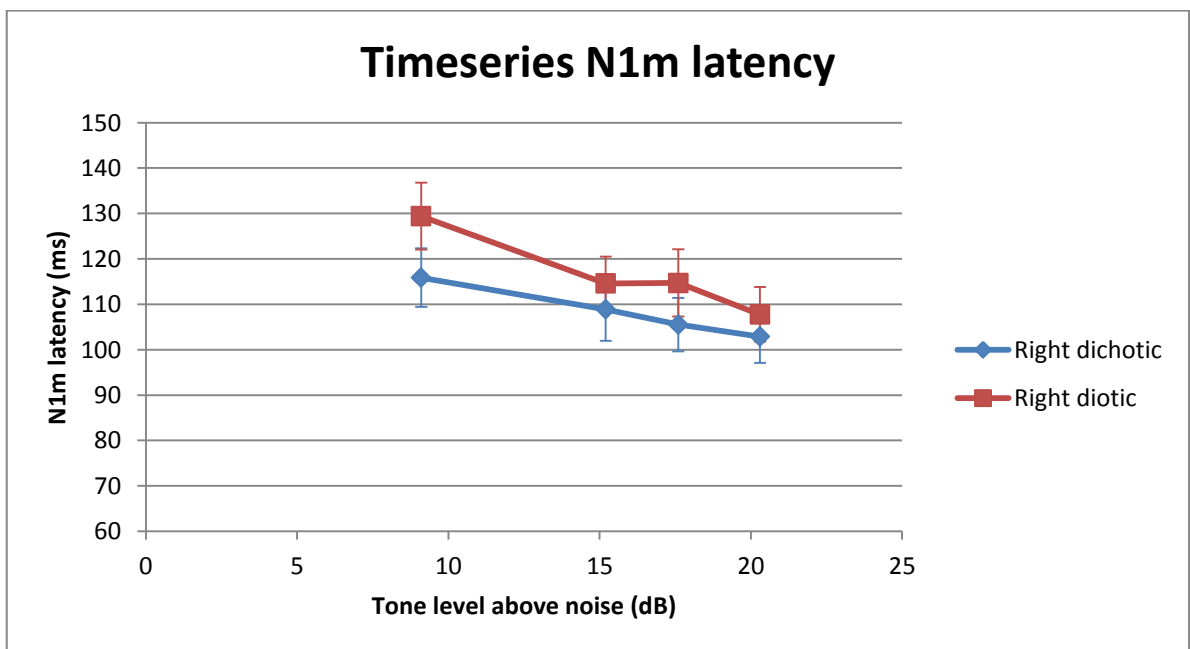


**Figure 5.11** Group mean N1m timeseries latencies for the right hemisphere. The error bars indicate 95% confidence intervals. (N=17).

A repeated measures ANOVA was performed to study the effects of hemisphere, phase and intensity on N1m latency. The results reported with a Greenhouse-Geisser correction show there was no significant main effect of hemisphere on the latency of the N1m,  $F(1, 15) = .000$ ,  $p = .984$ . There was

a significant effect of phase,  $F(1, 15) = 19.81$ ,  $p = .001$ , and intensity,  $F(1.4, 15) = 47.82$ ,  $p = .000$  on the N1m latency. There were no significant interactions between hemisphere, phase and intensity. Post hoc testing using the Bonferroni correction revealed a significant difference in means between all intensities, apart from between the two middle intensities ( $p = .357$ ). These results suggest that the latency values are not significantly different between the hemispheres, but are significantly different between the dichotic and diotic tone responses. The response latencies are significantly different between the different intensities, except for between the 15.2 and 17.6dB tone levels over the background noise.

#### **5.3.4 Computing the BMLD**

The statistical results already presented indicate that there was a significant difference between the dichotic and diotic values for both amplitude and latency conditions for sensor data and inverse estimate timeseries data. The results show the expected morphology changes of the N1m as a function of tone intensity overall, with a significant difference between the tone intensity levels occurring between the loudest and second loudest, and the third loudest and the quietest tone intensities three of the four triggers. The error bars in all conditions were small, indicating that the trajectories for each condition were broadly comparable across stimulus values.

Two different methods for computing the BMLD were used. For amplitude, the raw diotic value was subtracted from the raw dichotic value for each trigger intensity, and these values were then summed for each individual. The resulting value was used as a correlate of binaural unmasking. The same method was employed using evoked response latency values, with the dichotic evoked response value being subtracted from the diotic value for each trigger intensity and summed for each individual.

In addition, a value was computed between the dichotic and diotic evoked responses for the loudest trigger only, for amplitude and latency separately in each individual. The values for both sensor and source level evoked N1ms were used and the correlations with the psychophysical BMLD are presented in Table 5.3.

		Psychophysical BMLD	
	Neural BMLD	Pearson's correlation coefficient	Significance (2-tailed)
Sensor data	Amplitude (4 triggers)	.199	.443
	Amplitude (loudest dichotic trigger)	-.111	.670
	Latency (4 triggers)	.320	.211
	Latency (loudest dichotic trigger)	-.108	.680
Source timeseries	Amplitude (4 triggers)	.586	.013**
	Amplitude (loudest dichotic trigger)	.323	.205
	Latency (4 triggers)	.042	.874
	Latency (loudest dichotic trigger)	-0.8	.761

**Table 5.3** Correlation table of the psychophysical BMLD value with the computed BMLD values from the timeseries amplitude and latency data. The table contains the Pearson's correlation coefficient and the two-tailed significance value ( $p < 0.05$ ). Significance is highlighted with \*\*.

As can be seen from the table, the only significant correlation between the psychophysical BMLD value and the neural binaural unmasking value occurs the difference between the dichotic and diotic timeseries amplitude values summed from all the triggers.

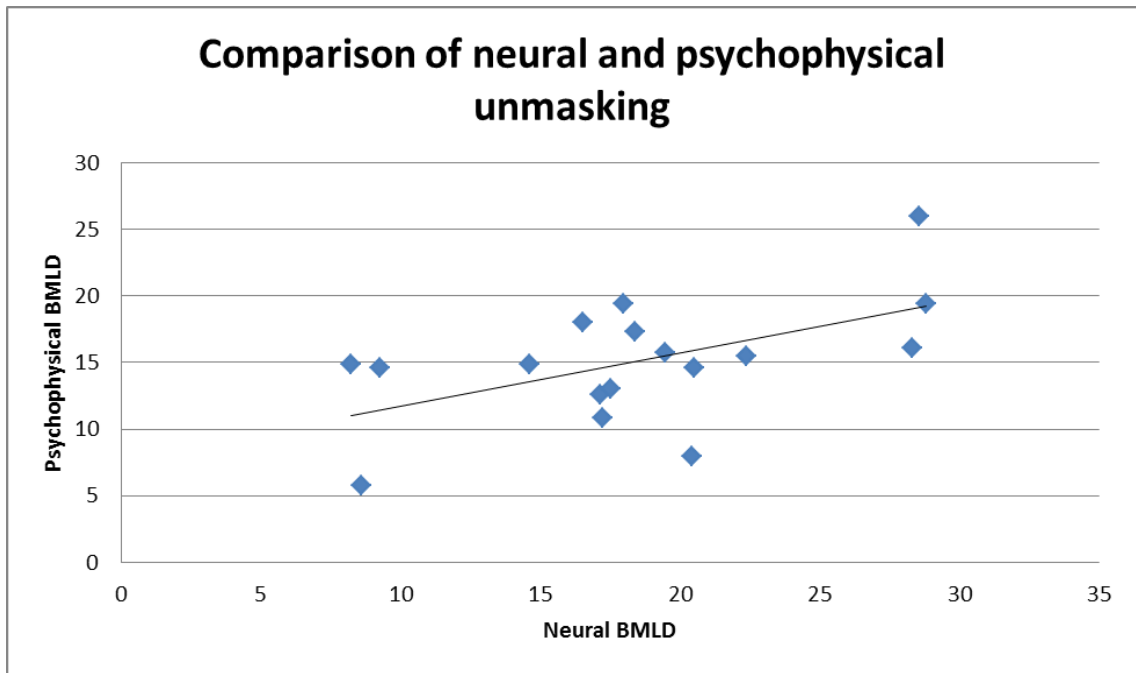


**Figure 5.12** Graph showing the linear trend of the correlation between the psychophysically derived BMLD and the neural BMLD extracted from the amplitude values at source. A Pearson-product-moment correlation coefficient shows a significant correlation between the two variables ( $r=0.586$ ,  $n=17$ ,  $p=0.013$ ).

The correlation of the psychophysical BMLD values with the neural BMLD values taken from the source level amplitude from all triggers is significant. There is a degree of individual variability in the individual correlations between the psychophysical and the neural BMLDs, however, the significance of the test shows that neural BMLD appears to be a moderate predictor of psychophysical BMLD. See Appendix 2 for a table of psychophysical and neural BMLD values.

## 5.4 Discussion

### 5.4.1 Key findings

The aim of this study was to explore whether a passive MEG stimulus designed to elicit specific neural evoked responses could be used as an alternative to the psychophysical BMLD measure to estimate binaural hearing abilities.

The results of this study show that the psychophysical and neural unmasking values, extracted from the difference between the dichotic and diotic source amplitude values for each individual, show a significant, albeit moderate, correlation. No other correlations yielded a significant result, including sensor level amplitude and latency values, and source level latency values.

#### **5.4.2 Measuring the BMLD**

Traditionally the BMLD is measured using the threshold values for dichotic and diotic tones that can be detected over background noise. In MEG, detection of a tone is usually measured using an evoked response, which provides a useful measure not only of whether or not the tone is heard, but also how loud it is perceived to be. Measurements of evoked responses rely on a high SNR of the response over the background noise of brain activity, making threshold measurements very difficult. For this reason, a traditional measurement of the BMLD is not easily obtainable in MEG, hence an alternative method must be derived. This chapter explored the possibility of whether or not the binaural unmasking effect can be measured in MEG without determining threshold values.

Amplitude and latency of the N1m were both considered as potential indices of binaural unmasking, due to their predictable morphological changes associated with the tone intensity perception needed for the unmasking effect. Results from this study indicate that the neural evoked amplitude value derived from the difference between the dichotic and diotic response amplitudes summed for all four tone intensities provides a statistically significant correlate with the psychophysical BMLD value. This computation does not rely on the threshold of the signal, instead deriving the BMLD value from responses to suprathreshold stimuli.

#### **5.4.3 Overall effects of hemisphere**

MEG measurements were taken at sensor and source level from both the left and right hemispheres in all participants where possible. Statistical testing showed that there was no significant difference between the left and right hemisphere evoked response amplitudes, however it was clear that the right hemisphere was not always dominant in terms of amplitude and latency as predicted.

It has been shown in previous studies that there tends to be a strong right hemisphere lateralization for tones (e. g. Gabriel et al., 2004; Roberts et al., 2000; Huotilainen et al., 1998). In their study of tones in the free field, Burke et al. (1994) found that tones presented in the left hemispace of the free field, were localised more accurately than in the right hemispace, indicating a contralateral hemispheric advantage. Despite the strong evidence for right hemisphere lateralization of evoked responses to tones, there is also evidence that there is a hemispheric asymmetry in overall myelination, in favour of the left hemisphere (Anderson et al., 1999; Sigalovsky et al., 2006; Schönwiesner et al., 2005; Zatorre & Belin, 2001). Increased myelination enables faster speed of processing. The results presented in this chapter indicate no significant effect of hemisphere, however it can be seen from the MNE estimates that individuals tend to have one hemisphere that is dominant. There is no clear explanation for this, however this pattern of results mirrors the findings of Chait et al. (2004) and Hertrich et al. (2004), neither of whom found a lateralization effect for tones. Fujiki et al. (2002) used frequency tagging to separate the ipsi- and contralateral responses in both hemispheres to binaurally presented tones. They demonstrated that when presenting binaural sounds, the right hemisphere responses were suppressed in both hemispheres as opposed to monaural presentation. In contrast, the left hemisphere responses were suppressed for ipsi- but not for contralateral tones presented binaurally. These results indicate that there should be a left hemisphere dominance for contralateral sounds.

#### **5.4.4 Response morphology**

The adult timeseries data shown here show a 'classic pure tone response' (Chait et al., 2004), namely the M50, M100 and M150 are clearly visible, with the M100 being the largest peak. It is known that the N1 is modulated by attention (Näätänen, 1990), and Chait (2004) has extended this finding to show that this M100 response seems to only occur for a new object of attention, i. e. a tone, and does not occur just for noise alone. When measuring just noise onset, Chait et al. found a peak at M70 and M150 with no M100, with both of these peaks demonstrating a M50 spatial distribution. A different inter-aural phase configuration will yield an M100 as it is a new attentional object. Interestingly Chait et al. found no lateralization for a tone, which reflects the data presented in this

chapter in the sense that there was not a consistent hemisphere to which the tone lateralized, but there was a trend for a larger response in one hemisphere or the other in most participants. Chait et al. did find a lateralization for inter-aural configurations of noise in the right hemisphere, which the author attributed to a right hemisphere dominance for detection of slow modulations in noise (Poeppe, 2003; Zatorre et al., 2002).

Expanding on the notion of attention and its effect on the M100, responses to speech sounds have been shown to lateralize to the left hemisphere only when they are attended to, when presented passively there is no effect of lateralization (Poeppe et al., 1996). With regards to the data in this chapter, the participants were not instructed to attend to the stimuli, however this is very hard to control for, as it is not always possible to know if they are attending to the stimulus or not. In this study a visual stimulus was provided to help keep alertness but also to provide an alternative item of interest for the participant rather than attending to the auditory stimulus. This could be an interesting avenue for further exploration of the M100 in relation to the BMLD.

#### **5.4.5 The BMLD**

The data presented in this chapter suggest that a measure of the BMLD can be found using evoked responses in MEG. At group level the M100 characteristics reflect the expected trend of an increase in amplitude and decrease in latency with a louder tone (Näätänen & Picton, 1987; Stufflebeam et al., 1998; Picton, 1977) in most instances. This trend is evident in the group data presented here for amplitude and latency, which provides validation for the sensor evoked responses and also the timeseries data. In terms of relating the psychophysical BMLDs to the MEG data, the timeseries amplitudes shown in this chapter show a correlation between the two values. Previous work has only shown that the BMLD shows a correlation with a neural value to a certain extent (Fowler & Mikami 1992b; Fowler & Mikami, 1995; Kevanishvili & Lagidze, 1987; Galambos & Makeig, 1992b). Galambos & Makeig (1992b) undertook a study investigating tonepip SSRs and their relationship to the masking level difference, and the results showed that the amplitude changes found in the SSRs did not consistently match the participant perception of the tonepips. In their earlier experiments,

Fowler & Mikami (1992a,b) used EEG to measure the P2 BMLD. The first study results showed that the behavioural MLD saturates at high SNRs confirming previous psychophysical observations (Henning, 1973), yet the neural BMLD thresholds showed a linear increase with an increase in noise. There were only 5 subjects in this study, so in their next study they showed with 15 participants that there were no significant differences in the threshold of the behavioural BMLD and the BMLD of P1, N1, P2 and N2. Their conclusion was that the behavioural BMLD was a similar process to the late potential BMLD. Further, Epp et al. (2013) found a correlate of the BMLD and CMR using EEG. The author measured the N1 and P2 using both paradigms and found that the BMLD could be measured using both N1 and P2, however CMR could only be measured using the P2. This would imply that the P2 was a more robust response that responded to different types of binaural unmasking, however as shown in Chapter 3 of this thesis, the P2 is not always measurable reliably in MEG for all participants. Therefore, using the N1m to measure the BMLD is more appropriate in this case. The results of this study add weight to the findings of EEG that there is a link between behavioural BMLD and neural BMLD when measured at the cortical source.

#### **5.4.6 Limitations of the analysis method**

One main advantage of using a distributed dipole model such as MNE, is that it provides an indication of the spread of activity and allows visualisation of the strength of activity in the different vertices within that area. MNE has been criticised as a method due to the fact that it does not provide a single peak of activity (Grech et al., 2008), but instead measures the strength of dipoles at each vertex on the dipole grid. This is not necessarily a limitation however, as it is not exactly clear whether or not the auditory response consists of simply one dipole or many dipole activations close together in location. As has been shown previously, single dipole model localization may not be suitable for modelling the auditory response in children (Pang et al., 2003), so it is worthwhile investigating alternative techniques in order to be able to extract the binaural response data in an initial adult cohort. The M100 is localised to the floor of the Sylvian fissure (Lutkenhoner & Steinstrater, 1998), however the supratemporal plane has been shown to be variable between

individuals (Campain & Minckler, 1976), so choosing the appropriate vertex for each individual within this region is a valid method of measurement.

#### **5.4.7 Limitations of the study design**

Rather than presenting the tones at the same level for all participants, it may have been advantageous to calibrate the levels to each individual threshold as has been done in previous work (Sasaki et al., 2005). This was not possible in this instance as the software used did not allow a large enough range of tones to be presented if the levels were to vary between people. Therefore, it was decided to utilise a suprathreshold range of tones for each person. The range of tones needed to be within certain limits, as psychophysics has shown that at high SNRs the effects of inter-aural phase of the signals are small (Henning, 1973).

It may be natural to assume that the psychometric function obtained from the evoked responses in MEG would be the same as in psychophysics, and for this reason calibrating the tone and noise levels to individual thresholds would be important. Sasaki et al. (2005) used this method in their study of neural BMLD, however after measuring the source location using dipoles, they then reported the amplitude of the response using sensor data rather than presenting source timeseries data, as in this thesis. The reason why they did not report source amplitudes remains unclear. The psychophysics literature shows that the thresholds for dichotic and diotic stimuli eventually asymptote at large stimulus amplitudes, rendering the inter-aural phase relation negligible (Henning, 1973). It might be expected that this pattern would be reflected in the amplitudes of the evoked responses or timeseries data, however this does not occur for the suprathreshold stimuli presented in this thesis. Presenting the tones at a suprathreshold level for all participants instead allows for a clear evoked response to be measured at the different intensities of tone without them being occluded by background noise when close to threshold level.

#### **5.4.8 Recommendations for further research**

In the context of this study, further research could involve exploration of alternative methods of measuring binaural hearing, such as binaural pitch. When broadband noise is presented to both ears, a slight difference in configuration between the inter-aural noise can elicit the percept of pitch. An example of such a method is Huggin's pitch (HP), (Cramer and Huggins, 1958), involving a broadband noise presented diotically, with only a narrowband section phase-inverted in one ear. The literature has previously compared Huggin's pitch to the binaural masking level difference as a means of measuring binaural hearing. Interestingly it has been shown that Huggin's pitch and the BMLD may not be directly related; (Nitschmann et al., 2010) found that some participants did not hear Huggin's pitch but did have a BMLD, implying that binaural hearing is complex and there is not one single factor of impairment. Further investigation into the extent of this using the techniques presented in this chapter would provide more information about the nature of the difference in these mechanisms.

# Chapter 6:

---

## Measuring the neural BMLD in typically developing children

### 6.1 Introduction

This chapter will report results of the measurement of the BMLD in a group of typically developing children. It will begin with a rationale for the study, followed by a summary of the developmental trajectory of the auditory response and binaural development. Both sensor and source level findings will be reported, with a consideration of the differences in the two age groups of the participants (10-12 years, and 16-17 years). Findings will be discussed in the context of previous literature and the effectiveness of the MEG stimulus paradigm for measurement of the BMLD in children.

Psychophysics involves a time-consuming number of repetitions of the same stimulus, therefore a certain level of cognition is necessary on the part of the participant to perform adequately. It can be difficult to engage children in this kind of task in the first place, but also there is evidence to suggest that children are not able to perform as efficiently as adults in general during psychophysical listening tasks (e.g. Allen & Wightman, 1994; Hartley et al., 2000; Werner & Boike, 2001). The reason for children's poorer performance is debated in the literature, as it is not clear whether to it is attributable to cognitive factors such as selective attention, or physiological factors such as neural immaturity, or perhaps a mixture of a number of factors.

#### 6.1.1 Auditory response development

The auditory evoked response changes throughout childhood, until it starts to take a more adult morphology around early adolescence. It has been shown that larger morphological and anatomical changes take place before the age of 8 (Toninquist-Uhlén et al., 1995), after which time only smaller changes take place. The N1P2 response complex appears around the age of 9 (Toninquist-Uhlen et al,

2003), however the latency and amplitude of the response differs slightly from the adult. An early study by Goodin et al., (1978) identified that the latency of the N1 decreases and amplitude increases with age, up until the age of 14-16 years when it becomes stable.

Between the ages of 10-12 years, auditory processing undergoes important development. It is around this time that a clear N1 wave appears (Bishop et al., 2007; Moore & Linthicum, 2007; Picton & Taylor, 2007). Bishop et al. (2007) undertook a reanalysis of ERPs from a selected sample of previous studies. They identified 3 classes of maturation, the ages 5-12 years, 13-16 years, and adulthood. There was no developmental progression within these age bands. In contrast to this, Poulsen et al. (2007) measured the M100 at the onset of a tone in an adult cohort aged 19-45, and their result indicated that the latency of the response continues to decrease with age throughout adulthood.

#### **6.1.1.1 EEG**

First described by Wolpaw & Penry (1975), the T-complex refers to the set of neural components that make up the middle and long latency auditory ERP at the vertex, consisting of small negativity Na, large positivity Ta and larger negativity Tb. The T-complex also appears in the temporal lobes, and the different hemispheric components of the T-complex have their own developmental trajectories, for example Pang & Taylor (2000) reported that the left hemispheric Na component matured before the age of 3, and the right hemispheric Na matured around 7-8 years. The authors explained this hemispheric difference with reference to the stimulus type, as speech stimuli evoked responses developed in the left hemisphere earlier than the right hemisphere, before the development of tonal responses.

The peak of the auditory evoked response occurs at the vertex due to the bilateral response in the primary auditory cortices (Hari et al., 1980). Tonnquist-Uhlen et al. (1995) created topographic maps of auditory responses in children aged between 8-16 years using a 500Hz pure tone burst, which was presented separately to the two ears. The maps showed a fronto-lateral localisation for the N1.

It is generally accepted that the T-complex components are equivalent to some of the components of the N1 response in EEG, consisting of N1a, N1b and N1c respectively. N1b is the component more commonly referred to as the N100 (Näätänen & Picton, 1987), as it occurs at approximately 100ms and is the component with the largest amplitude. Despite this notion of the T-complex and N1 complex being the same, Ponton et al. (2002) undertook a study demonstrating a difference in orientation between the T-complex components and the N1 components using dipole modelling, the results of which indicate that they are separate responses due a difference not only in maturation but also localisation.

EEG may not be suitable for measurement of the auditory responses due to the difficulty in separating the hemispheric responses associated with that particular technique. Oades et al. (1988) found very late N100s in control children in EEG, a finding they attribute to contribution from other N1 components, highlighting the need to use brain space rather than sensor space to visualise evoked components (Edgar et al., 2003). In light of this, there is a need to examine the developmental trajectory of the auditory response in each hemisphere separately (Ferri et al., 2003). As previously described, MEG provides a suitable method to examine the responses in source space and also to visualise each hemisphere separately.

In their review of previous studies into auditory development as part of their study of central auditory evoked responses in EEG, Bishop et al. (2011) identified two models of auditory development, the stability model and the incremental model. The stability model predicts that maturation of the auditory response is a complete process and by middle childhood the response is fully mature. The incremental model predicts that auditory development proceeds in a step-wise fashion, and that certain levels of processing are established before others, for example development of speech discrimination continues into adolescence. There is some discrepancy in the literature about which of these models might be more valid, despite the existence of evidence for both models. Continuing their study of EEG evoked responses in children, Bishop et al. (2011) found that temporal and fronto-central maturation occurred over different developmental trajectories. Namely, temporal sites demonstrated lateralisation of responses and no developmental change in

the low-frequency phase-resetting of the response, whereas fronto-central sites showed a change in low-frequency over the course of development but showed no lateralisation.

#### **6.1.1.2 MEG**

Development of the auditory response has been studied using MEG, although to a lesser extent than EEG at present. MEG only measures the activity tangential to the cortical surface and so reflects the first component described by Näätänen and Picton (1987) as occurring on the supra-temporal plane of the auditory cortex, considered one of the 'true' N1 components.

It is generally accepted that the evoked responses seen in MEG are correlates of the responses recorded using EEG (Huotilainen et al., 1998), so the literature on EEG and MEG will be considered in the same manner here. Using MEG, Kotecha et al. (2009) recorded the latencies of the responses evoked in children by pure tones. They found consistent responses of M50, M70 and M100 in children. All three responses shortened their latency with age, the M50 decreased in amplitude with age whereas the M100 increased in amplitude with age, and the M70 increased in amplitude until the age of 12-14, after which time it started to decrease again. The results here are in concordance with Paetau et al. (1995) who found a biphasic response in children, with peaks at 70ms and 140ms in EEG. Kotecha et al. (2009), claim that the M50 and M70 are easily localisable in children but not in adults, however other studies have shown that this is possible (e. g. Godey et al., 2001). Evidence for a difference in the morphology between adult and child responses has been found by Paetau et al. (1995). Adults showed a triphasic response, with the middle peak identifiable as the M100, whereas in children, the response was biphasic with the peaks appearing around 100ms and 260ms in children up to the age of 12. However at longer ISIs, the child responses became more adult-like (Paetau et al., 1995; Sussman et al., 2008).

Developmental studies have shown that M100 latencies systematically decrease up to the ages of 14-16 years (Goodin et al., 1978; Fuchigami et al., 1993). Further, the dynamic range relating to latency also has a developmental trajectory, between tone frequencies of 200-1000Hz (Gage et al., 2003b), namely the difference in latency between the two tone frequencies increases with age.

### **6.1.2 Auditory system development**

Most of the structure of the auditory system is in place at birth, with only the cortical layers to complete development during childhood (Moore & Linthicum, 2007). Similarly, the pinna and external ear canal are formed during early gestation, but do not reach an adult-like phase of development until the age of around 9 years (Keefe & Levi, 1996; Wright, 1997). The middle ear power transfer shows a developmental difference between infants and adults (Keefe et al., 1993). (Hall, 2000) provides a summary of the development of the auditory pathway.

### **6.1.3 Factors affecting children's performance**

#### **6.1.3.1 Attention**

Fatigue or lapses in sustained attention can increase the number of incorrect perceptual decisions made, which then results in inaccurate threshold estimation per se during a psychophysical task. Wightman & Allen (1992) used simulated data to demonstrate that general inattention during a proportion of trials of an adaptive psychophysical task led to higher thresholds and a flatter psychometric function. The results were comparable to the actual results found in child data, providing strong support for the theory that sustained attention, or lack of it, is a large contributing factor in accurate psychophysics. In further support of this argument, Oh et al. (2001) measured children's pure tone signal detection with and without maskers. They found that children experienced an increase in masked threshold masking effect when the masker and target were spatially separated in frequency. As this effect is not seen in adults, it indicates that children are more easily distracted by a distractor tone that is presented at a spatially separated frequency (Werner & Bargones, 1991). Oh et al. (2001) argue that this is an effect of informational masking as opposed to energetic masking, and that children utilise a wider range of auditory filters when processing signals amongst distracting sounds. Informational masking refers to masking that occurs when the masker is changing or uncertain, and may form part of a tone-in-noise masker effect in relation to frequency discrimination (Lutfi, 1990).

In opposition to the inattention argument, some studies have shown that lapses in attention will not have an effect large enough to justify the masked threshold differences witnessed between children and adults (e. g. Schneider & Trehub, 1992; Viemeister & Schlauch, 1992; Werner & Bargones, 1992). Wightman & Allen (1992) showed that an inattention rate of 30% will shift the psychometric function by only 2-3dB, therefore indicating that inattention alone is not the sole cause for the size of difference in adult and child thresholds.

Children appear to have shallower psychometric slopes than adults, and the reason for this remains largely unknown (Buss et al., 2006). Buss et al. (2006) proposed the possibility of an internal noise hypothesis, stating that children may have certain characteristics which lead to their poorer performance than adults in discrimination tasks. The hypothesis indicates that these characteristics are likely to be neurally-based, however the authors concede that there may be other behavioural factors such as lack of motivation or change of strategy which may also lead to poorer performance than adults. A later study showed Buss et al. (2009) testing this internal noise hypothesis using psychometric functions, with the premise that greater internal noise will lead to a shallower psychometric function slope in children. Their findings supported this prediction, with children yielding significantly shallower psychometric functions than adults. However, the actual nature of internal noise remains unclear.

#### **6.1.3.2 Neural immaturity**

Development of cortical responses co-occurring with growing efficiency in psychophysical performance might lead to the conclusion that it is immaturity of auditory neural responses that make it difficult for children to complete an auditory task reliably. Olsho et al. (1987) conclude that immaturity of the auditory system could be the cause of frequency threshold differences between adults and infants. However, this is only one factor that might contribute to children's poor performance in the auditory discrimination tasks. Other influences may consist of cognitive aspects of development such as poorer memory, which has been shown to be important in adult psychophysics to gain a reliable result (Jesteadt and Sims, 1975). The nature of the psychophysical

task here requires some memory capability, as there is a need to compare one trial with another consecutively.

Some authors argue that children's poorer performance than adults in auditory discrimination tasks is not due to sensory or cognitive factors but instead due to behavioural differences. For example Werner & Marean (1996) showed that some much younger observers are able to complete the psychophysical tasks satisfactorily, leading to the hypothesis that very early development of sensory factors gives children the potential to perform adequately. Despite this, Buss et al. (2009) conclude that children's poorer performance is not due to fluctuations in attention or listening strategy, as their findings indicate that the psychometric function remains stable over blocks of trials when comparing interleaved adaptive paradigms. If the children had lost attention for a block of trials this would be reflected in variance in the staircase trial performance.

As has been described, there are a number of reasons why children may perform more poorly in an auditory psychophysical task than adults. The effect of errors in behavioural tasks is so detrimental to accurate BMLD estimation that it would seem advantageous to create a scenario where the BMLD can be measured without the need for any behavioural task. The M100 provides a potentially suitable measure for this kind of percept. Measurement of the M100 provides its own challenges in children, as the response does not fully develop to an adult level of maturity until the age of 14-16 years (Goodin et al., 1978). However, the M100 first appears around the age of 9 (Toninquist-Uhlen et al., 2003), so it should be possible to measure the BMLD using this response in the same way as has been described for adults in the previous chapter.

#### **6.1.4 Stimulus effects on the auditory response**

##### **6.1.4.1 ISI**

Studies have shown that the ISI of the stimulus can have stark effects on the child auditory response morphology. Since the N1 has a longer latency in children than adults, the ISI of the stimulus must take this into account. Further, there is also evidence that a long ISI is necessary to fully elicit the childhood N1 (Paetau et al., 1995; Gomes et al., 2001; Ceponiene et al., 1998). Ceponiene et al.

(1998) found that a 350ms ISI elicited biphasic response with peaks at P100 and N250 in children aged 7-9 years, but an ISI longer than 700ms elicited response with additional peaks of N160, and N460. The authors suggested that the N160 was a correlate of the adult auditory N1 (Ceponiene et al., 1998).

#### **6.1.4.2 Frequency**

Frequency has an effect on the auditory evoked response in both adults and children. In general, there is an earlier M100 response to higher frequency than lower frequency tones (Gage et al., 2003b; Roberts et al., 2000). Children exhibit relatively longer latencies for both M50 and M100 as a function of frequency compared to adults (Cardy, 2004). It is possible that this effect is due to tonotopicity differences in adults and children. Further, childhood thresholds for tones of different frequencies have been shown to mature (i. e. reach adult levels) at different rates. Lower frequency tone thresholds (0.4-1kHz) mature more slowly by the age of 10 years, whereas high frequency tones thresholds (2-4kHz) mature by age 8 (Trehub et al., 1988).

#### **6.1.4.3 Masker**

The masker bandwidth and SNR have been shown to have an effect on the child auditory response. Hall & Grose (1990) measured MLDs in children aged 3-9 years using both a 300Hz wide and 40Hz wide masker. They found that up to the age of 6, MLDs increased with the 300Hz wide masker. Older children show similar MLDs to adults at a wider masker bandwidth (Hall & Grose, 1990). With a 40Hz-wide masker, MLDs were smaller in children than adults, which the authors posit as due to immaturity in central auditory processing as opposed to peripheral processing. Other studies also show that young children have smaller MLDs in general than adults (Hutchings, et al., 1992; Nozza, 1987; Nozza et al., 1988).

Grose et al. (1997) looked specifically at the effect of masker and signal bandwidth on the child MLD. Results suggest that the younger the participant, the wider the masker bandwidth must be to observe MLDs of adult magnitude. The authors suggest that the reason for this could be related to

the spectral properties of the signal and masker (Grose et al., 1997). Namely, that the younger children may require a larger difference in spectra between the signal and masker before adult-level BMLDs are found, as they are not able to access the binaural cues present in narrow-band masker fluctuations as easily as adults (Eddins, 1996). In adults, it has been found that binaural cues can be utilised more effectively when they fluctuate slowly (Grantham & Wightman, 1978) so narrowband noise maskers yield larger BMLDs as the binaural cues fluctuate more slowly than in wideband noise (Zurek & Durlach, 1987).

There is some disparity in the EEG literature regarding the amplitude and latency of the N100 during the crucial developmental phase. This could be due to the fact that measurement of the vertex N100 is potentially confounded as it has been established that this ERP consists of contributions from a number of neural generators (Rojas et al., 1998), and so could be made up of different evoked potentials that vary in their developmental trajectory. Previous studies have shown that different N1 components are likely to arise from differing sources (Gomes et al., 2001) and their summation at the vertex may be misleading.

#### **6.1.5 Practical considerations when recording children using MEG**

In MEG, head size and movement are both crucially important to quality data acquisition. Ideally, the head needs to be as close to the inside of the dewar helmet as possible, however when recording children, this position can be difficult to obtain and also maintain. The size of the head of a child can mean that the sensors are far away from the scalp, leading to a lower SNR. This problem may be compounded by a large amount of movement by the child while in the scanner, which although can be compensated for during post-processing, is a disruption during the recording. One advantage of MEG is that the problems associated with the attainment of reliable psychophysics measures are ameliorated. Lapses of attention and concentration should not influence the data collected as the participants are not instructed to attend to the stimuli. Fatigue may be a cause of alpha artefact contamination, however this can be reduced with the introduction of a visual stimulus.

### **6.1.6 Finding the BMLD**

There are a few recent studies that have looked into the developmental trajectory of spatial release from masking, especially with regards to speech, but not many that have considered the binaural masking level difference per se. Van Deun et al. (2010) studied a number of aspects of spatial speech perception in development, including spatial release from masking, head shadow, summation and squelch. These are all mechanisms that utilise differing inputs between the two ears to improve signal detection over background noise. Some of these mechanisms, such as the head shadow effect, rely on external changes to the sound prior to it reaching the inner ears. This can be difficult to implement as it can be hard to control in a laboratory environment, particularly in MEG where in-ear headphones are a requirement. In this study, van Deun et al. (2010) found that children over the age of 6 years gained a positive benefit from spatially separated noise, but under this age no effect was seen. The type of masker and measurement at certain points of the envelope can also have an effect on the masking level difference. Hall et al. (2004) studied the difference between the MLD at the envelope minima and maxima of a 50Hz wide masker. Results indicated that there was a binaural advantage associated with the minima more than the maxima of the masker, with older children able to utilise the binaural cues proffered by the envelope minima more effectively than younger children.

### **6.1.7 Aim**

The main aim of this chapter is to investigate the effectiveness of the BMLD stimulus in a group of control children through measurement of morphological characteristics of the M100.

## **6.2 Method**

### **6.2.1 Participants**

10 children were recorded between the ages of 7 and 17. They were recruited via members of staff at the University, and also through community engagement activities. All recruitment procedures were approved by the Ethics Committee of the School of Life and Health Sciences at Aston University.

Consent was gained from parents, and from children over 12, and assent from children under the age of 12 years. Screening forms were completed by parents. The youngest participant was unable to stay still enough to keep their head inside the MEG dewar helmet, and was also unable to complete the psychophysics, so they were excluded from the study. One MEG dataset could not be used in the study as this 11-year old participant's data had an extremely low SNR due to very noisy channels which could not be rectified in post-processing. Table 5.1 shows that in total nine participants took part, seven of whom were able to complete the psychophysics task, and eight of whom were able to provide neuroimaging data.

Participant	1	2	3	4	5	6	7	8	9
Age	12	12	10	17	17	16	17	12	11
Psychophysics?	X	X	Y	Y	Y	Y	Y	Y	Y
MEG?	Y	Y	Y	Y	Y	Y	Y	Y	X

**Table 6.1** Participant demographics and data acquisition.

### 6.2.2 Psychophysics procedure

Children were asked to undertake the psychophysics protocol as previously described in Chapter 5. They found this a harder task than the adults so they were continuously encouraged to complete the testing, although two children did not complete the test. All psychophysics took place in the soundproof room as previously described in Chapter 2.

### 6.2.3 MEG procedure

All children underwent the same preparation procedure as the adults for the MEG acquisition. They were asked if they would like to bring their own choice of DVD along prior to the appointment and some children did choose to do this. Sometimes it was useful to present the child with a video of their choice while they were having their head digitised outside the scanner to help them keep still during the polhemus procedure. A stronger emphasis was placed on watching the silent DVD during

the recording to keep the children focused. Often a parent would sit in with the child during the recording to help keep them calm and focused on the task, the parent would also remove all metal items before entering the shielded room.

#### **6.2.4 Stimulus**

The stimulus used for child recordings was shorter than the one used for the adult recordings through the reduction in the number of triggers presented. This was with the intention of shortening the duration of the recording, as the children found it harder to keep alert and still for a longer amount of time. The stimulus for the child recordings consisted of 3 tones in both dichotic and diotic conditions, at the levels of 20.3, 17.6, and 13dB above the background noise level of 70dB. The stimulus generally lasted for 7 minutes, as there was an inbuilt random (Gaussian distribution) jitter of up to 100ms at each ISI of 1 second.

The analysis protocol for this study was the same as previously described in the adult data chapter. The data for the children was in general more noisy than for the adults, so rather than a 0.5-30Hz filter, a bandpass filter of 4-30Hz was applied to all child datasets. Following this, the analysis protocol was the same as previously described.

### **6.3 Results**

#### **6.3.1 Sensor data**

Example sensor data for the younger and older child group are shown in Figures 6.1 and 6.2.

The sensor averages show a distinct difference between the dichotic and diotic averages for both the younger and older child examples shown here.

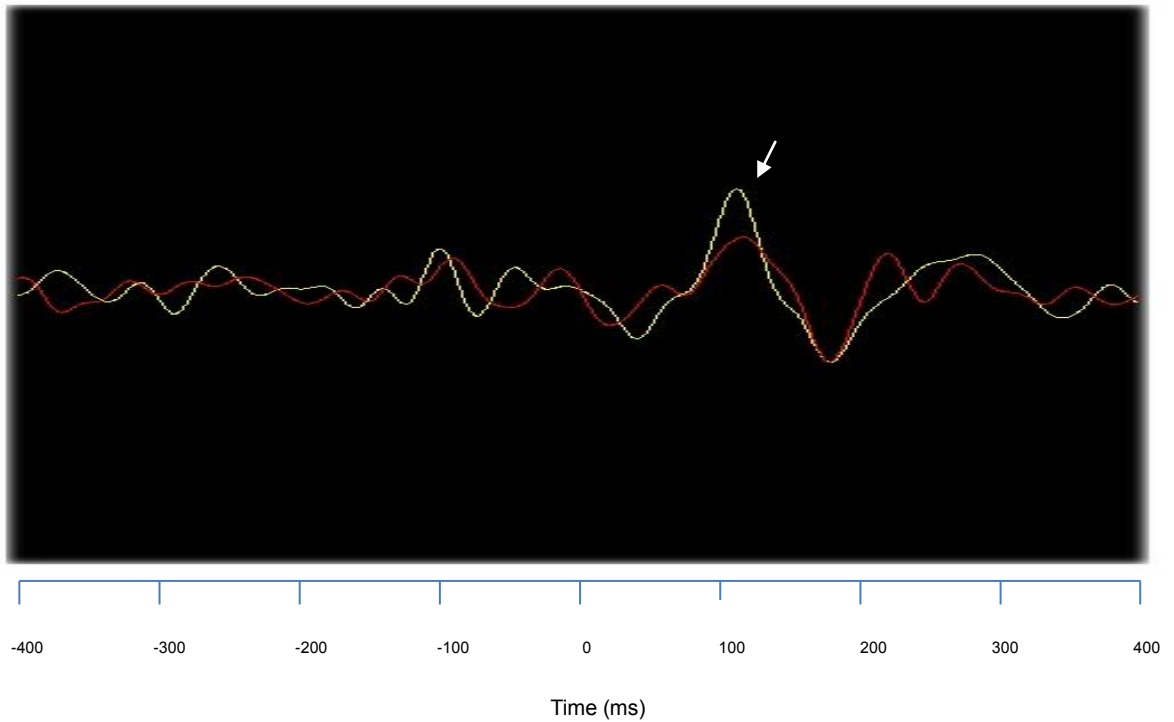


**Figure 6.1** Evoked average for an example younger child showing the difference between the loudest dichotic and diotic responses. The yellow line shows the dichotic response and the red line shows the diotic response to the loudest masked tone. The arrow indicates the M100 response taken from a group of channels in the right temporal lobe, showing the relative difference between the dichotic and diotic M100 responses.

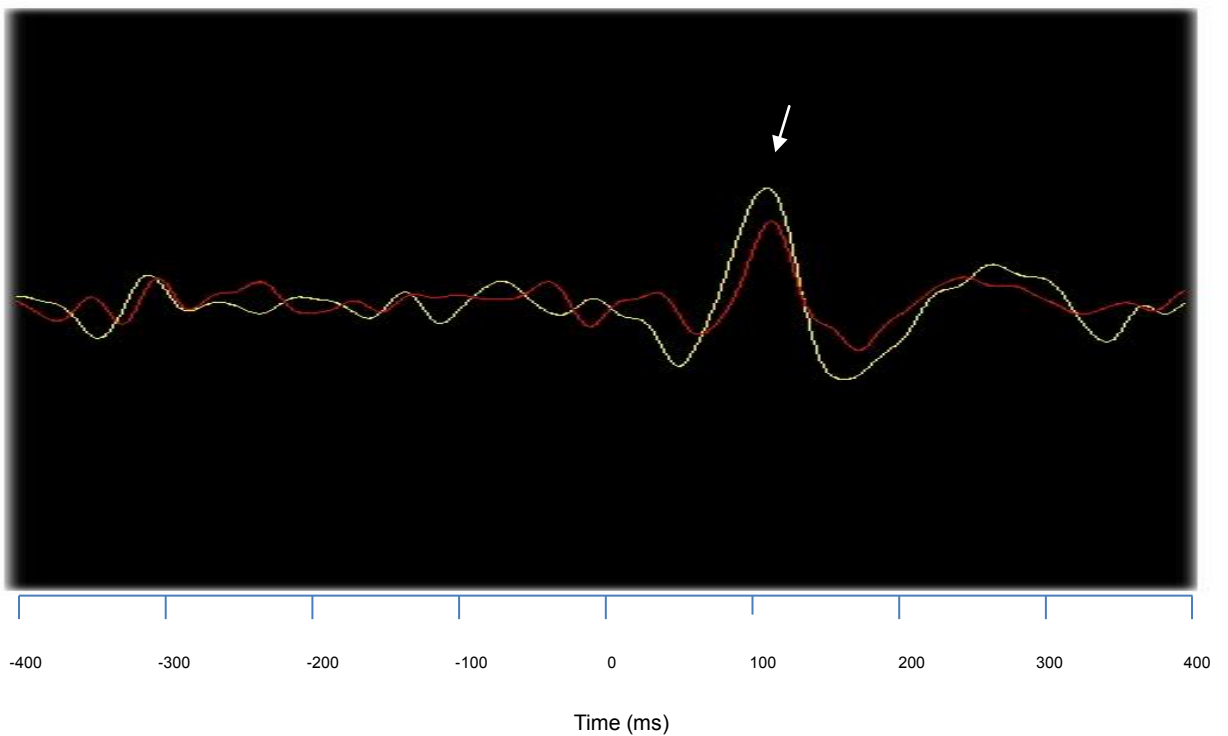


**Figure 6.2** Evoked average for an example older child showing the difference between the loudest dichotic and diotic responses. The yellow line shows the dichotic response and the red line shows the diotic response to the loudest masked tone. The arrow indicates the M100 response taken from a group of channels in the right temporal lobe, showing the relative difference between the dichotic and diotic M100 responses.

The child data has a tendency to contain more baseline noise than adult data, so the evoked responses are not as clearly visible, as the lower amplitude responses are occluded by noise. For this reason, only the values taken from the loudest dichotic and diotic trigger will be considered in computation of the BMLD.

This method was also used to evaluate the adult unmasking effect, however there was not a significant correlation between the neural values and the psychophysical BMLD. The method can instead be used to give an indication of the extent of binaural unmasking on an individual basis.

The individual evoked amplitude values are represented in Figure 6.3 for the younger child group and Figure 6.4 for the older child group. These are presented individually as the variation is too large to show the data effectively when scaled.

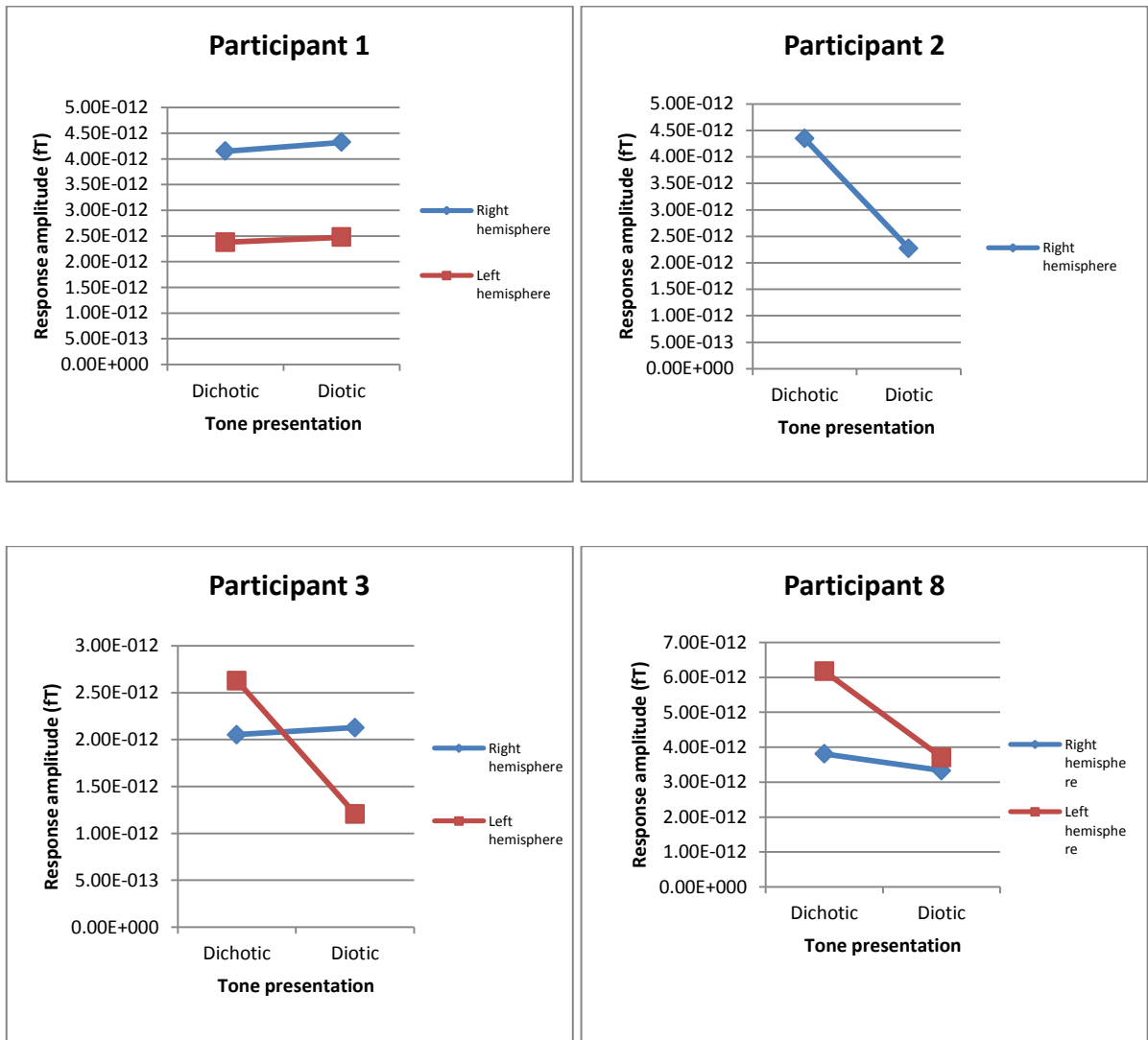


**Figure 6.3.** Evoked amplitude values for four younger children, showing values for the loudest dichotic and diotic tone stimulus over noise for both hemispheres. Data is shown for each member of the younger child group individually. Participant 2 did not have any evoked responses that were significantly above background noise in the left hemisphere.

The younger child group show an unclear pattern of results regarding their sensor averages for the loudest dichotic and diotic tone. The expected pattern of a decrease in response amplitude as a function of decrease in tone amplitude is only present in Participant 8 for both hemispheres. Participant 1 shows the opposite pattern and Participants 2 and 3 show the expected pattern in one hemisphere only.

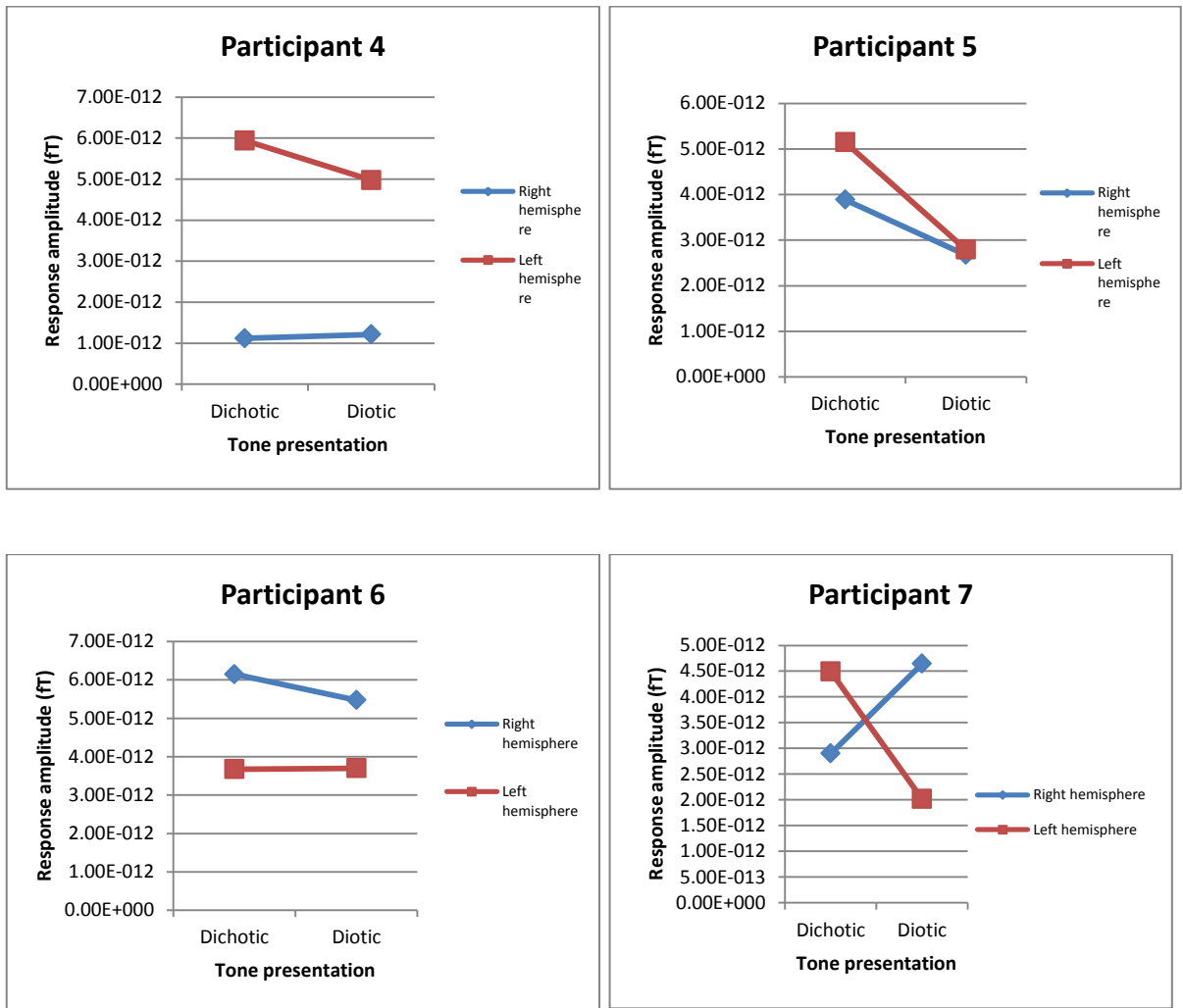


**Figure 6.4** Evoked amplitude values for four older children, showing values for the loudest dichotic and diotic tone stimulus over noise for both hemispheres. Data is shown for each member of the older child group individually.

The older child group show a more consistent pattern of results than the younger group, however Participant 7 appears to have a negative BMLD in the right hemisphere as the amplitude of the response increases with the diotic tone. The remaining participants show at least one hemisphere showing the expected increase in response amplitude with increase with tone intensity.

The latency values for both young and old participants are presented together in Figure 6.5.

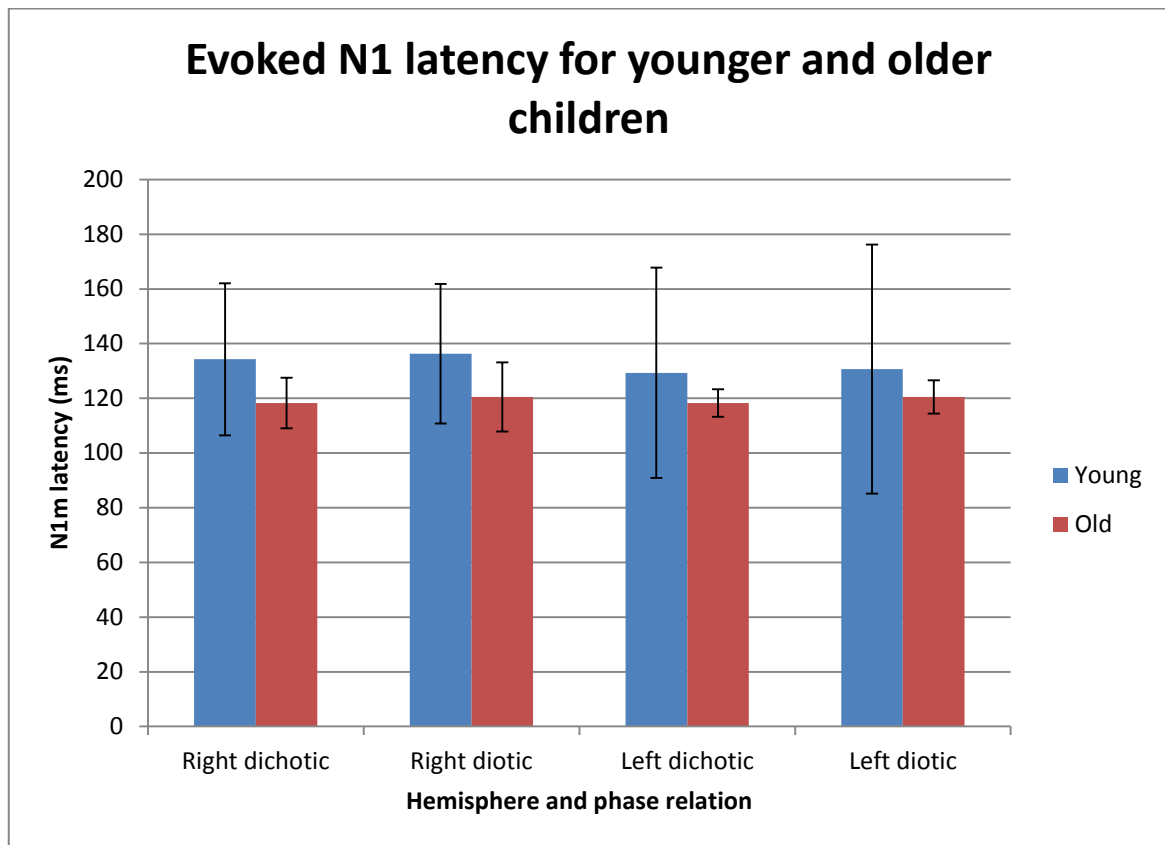


**Figure 6.5** Mean evoked latency values for the loudest dichotic and diotic tone stimulus over noise, taken from both hemispheres. N = 4 younger children (right hemisphere) and 3 younger children (left hemisphere) and N= 4 older children.

There was no significant difference between the right dichotic latencies for young (M=122, SD=33.23) and old (M=117, SD=9.69) children,  $t(6)=.303$ ,  $p=.772$ . There was no significant difference between the right diotic latencies for young (M=127, SD=36.82) and old (M=121, SD=11.53) children,  $t(6)=.324$ ,  $p=.757$ . There was no significant difference between the left dichotic latencies for young (M=139, SD=23.89) and old (M=119, SD=9.6) children,  $t(5)=1.535$ ,  $p=.185$ . There was no significant difference between the left diotic latencies for young (M=141, SD=25.24) and old (M=121, SD=7.37) children,  $t(5)=1.525$ ,  $p=.188$ .

### 6.3.2 Inverse estimates

The dSPM MNE estimates can be seen in Figure 6.6 for the younger child group and Figure 6.7 for the older child group.

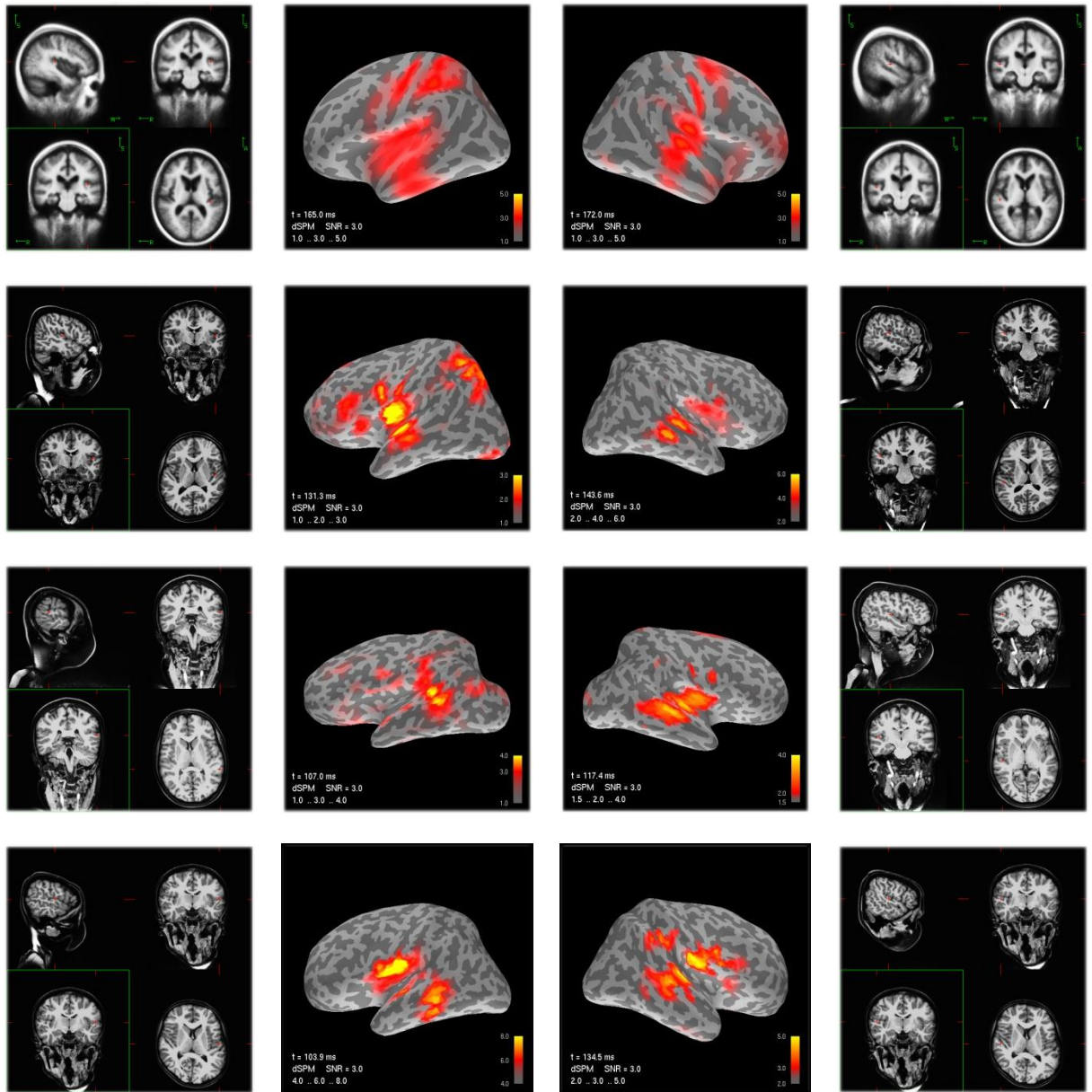


**Figure 6.6.** dSPM estimates for the younger group of participants (1, 2, 3 & 8), in response to the loudest dichotic trigger, shown for both hemispheres. The central two columns show the dSPM estimates and the outer columns show the anatomical MRIs indicating the vertex chosen for analysis. The MRIs are presented in radiological view. Each MNE estimate is shown with a threshold that suitably demonstrates the spread of activity, and also the latency at which the distribution of activity was shown to be strongest. An adequate freesurfer reconstruction could not be acquired for the first participant at the top due to poor image contrast resolution, so the freesurfer average brain was used for this participant.

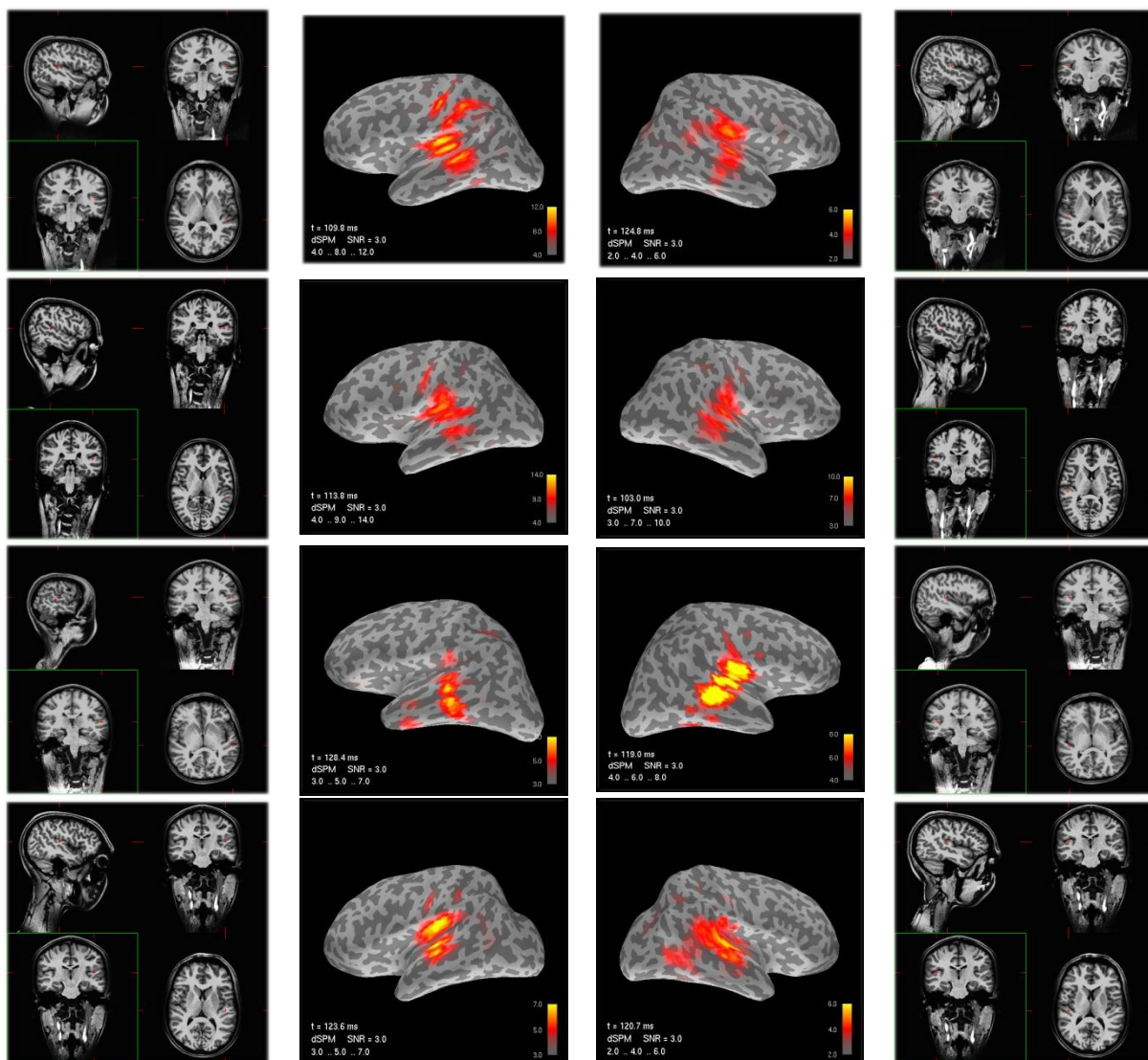
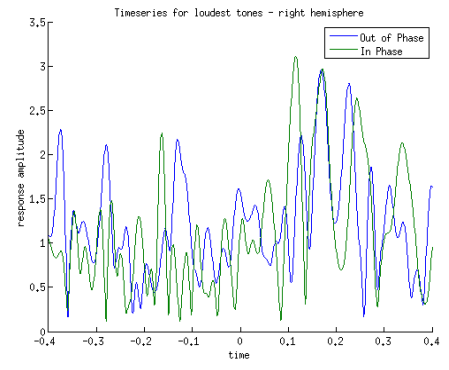
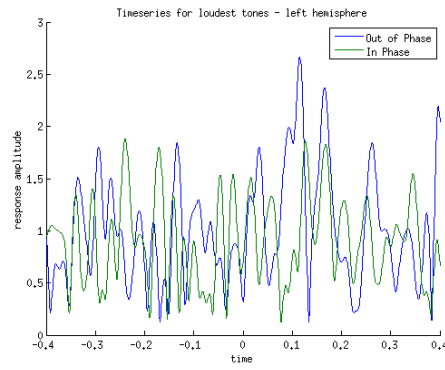


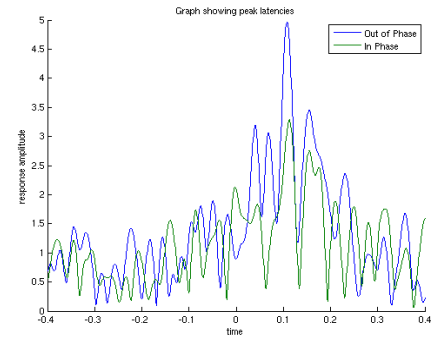
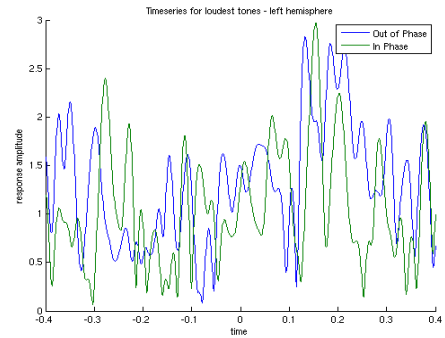
**Figure 6.7.** dSPM estimates for the older group of participants (4, 5, 6, & 7), in response to the loudest dichotic trigger, shown for both hemispheres. The central two columns show the dSPM estimates and the outer columns show the anatomical MRIs indicating the vertex chosen for analysis. The MRIs are presented in radiological view. Each MNE estimate is shown with a threshold that suitably demonstrates the spread of activity, and also the latency at which the distribution of activity was shown to be strongest.

The dSPM estimates derived from the MNE software show that the auditory activity is localised to the auditory cortex in all individuals. Participant one of Figure 6.6 shows a low threshold of activity due to a lot of noise in the baseline data, as well as a poor resolution MRI that could not be reconstructed correctly using the Freesurfer protocol. In this instance the ‘fsaverage’ option was utilised (Fischl, 2012) which still shows a spread of activation in the expected area despite low amplitude of activity. Figures 6.8 and 6.9 show the reconstructed timeseries data for each individual child in the younger and older child group respectively, for the loudest dichotic and diotic trigger, in both hemispheres.

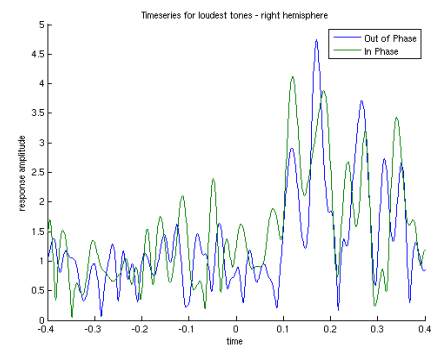
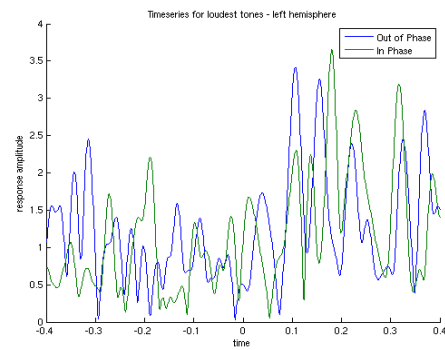
1



2



3



8

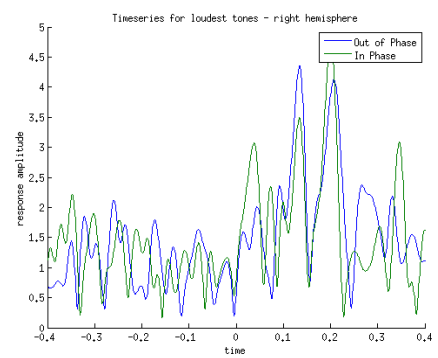
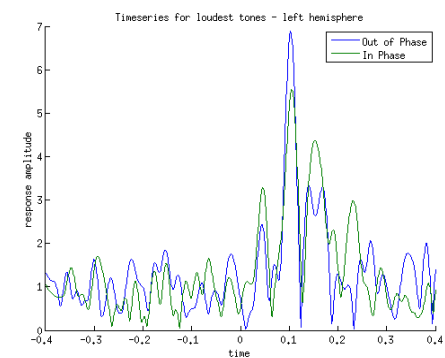


**Figure 6.8** Overlaid timeseries data extracted from MNE for the left and right hemispheres of the group of younger children (participants 1,2,3 and 8). The plots are reconstructed in Matlab using the MNE timeseries sample points. The blue line represents the loudest dichotic stimulus, and the green line represents the loudest diotic stimulus. The left column shows the left hemisphere response, and the right column shows the right hemisphere response.

As can be seen in the evoked timeseries data for the younger group of child participants, BMLDs can be witnessed in most of the participant hemispheres separately. Participant one shows very noisy data, with the evoked response only just visible. There is a BMLD in the left hemisphere, but in the right hemisphere there appears to be a negative BMLD. Participant two shows noisy data in the left hemisphere, with a small evoked response, but the right hemisphere is cleaner with a much clearer evoked response indicating the presence of a BMLD. Participant three shows a clear M100 with a BMLD on the left, but in the right hemisphere, there is a negative BMLD at the M100 latency, followed by a BMLD response around 200ms. An example of the sensor level M100 response for the right hemisphere is shown below (Figure 6.9). Participant eight shows a large M100 evoked response amongst a low level of background noise in the left hemisphere, with a clear BMLD. In the right hemisphere there is a slightly different pattern, with a more noisy response but a clear BMLD at the M100. This participant shows negative BMLDs both before and after the M100 peak in both hemispheres. The older child evoked timeseries' are shown in Figure 6.10.

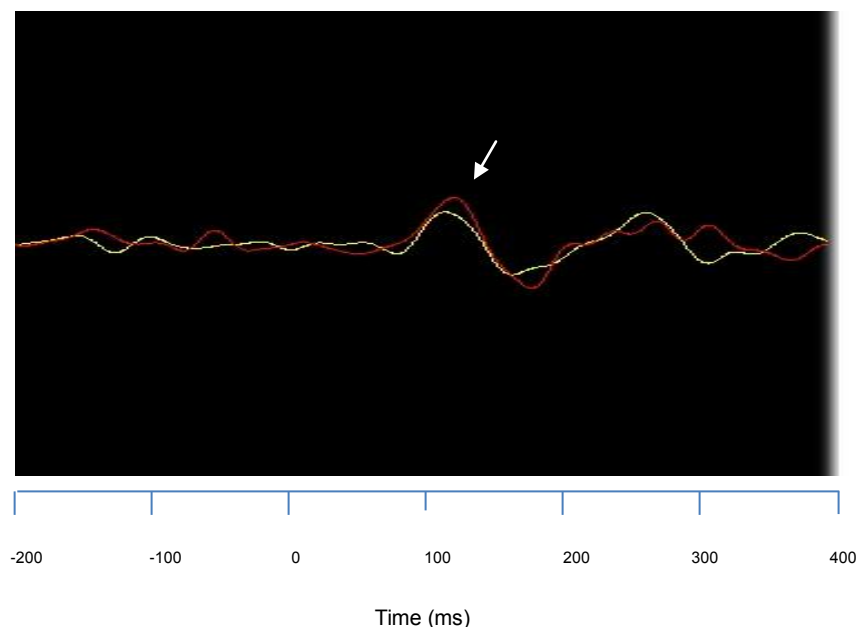
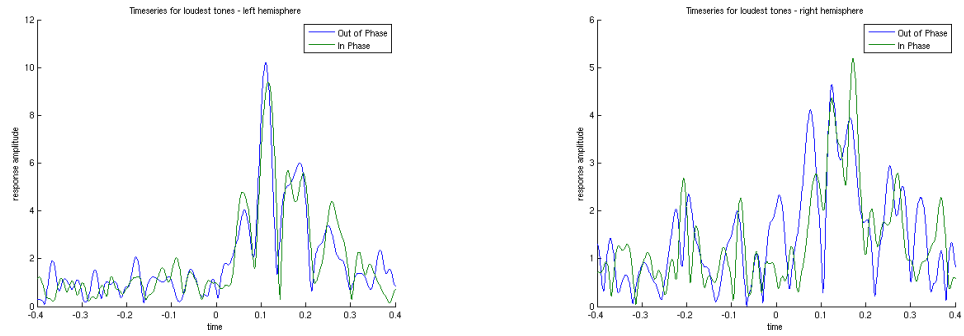
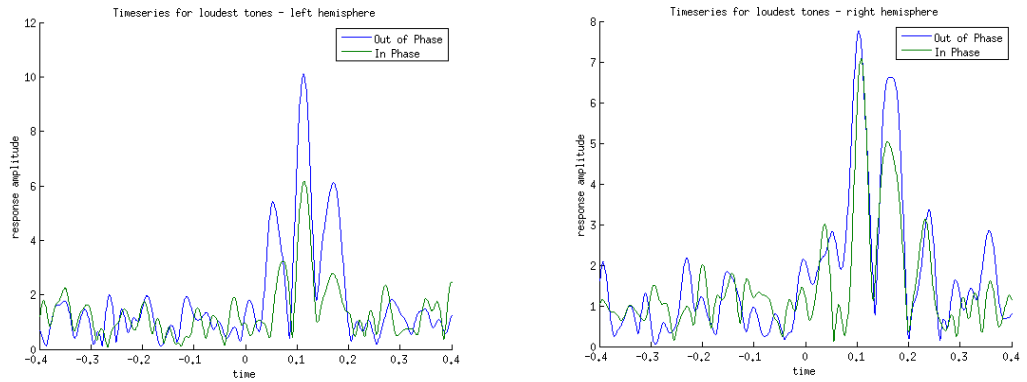


**Figure 6.9** Sensor level evoked response taken from the right temporal lobe for participant 3, using MNE software. The yellow line represents the response to the dichotic stimulus, and the red line denotes the response to the diotic stimulus. The M100 is labelled with an arrow, showing the relative difference between the dichotic and diotic M100 responses. As can be seen there is an effect of a negative BMLD, showing that it is not an effect of incorrect orientation reconstruction in source data.

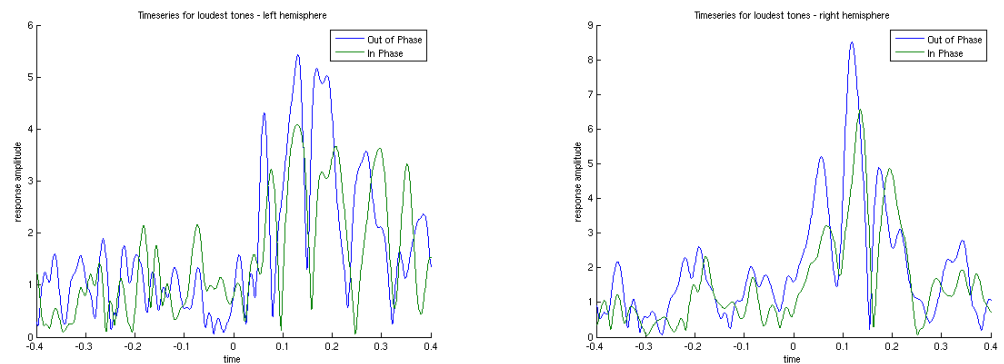
4



5



6



7

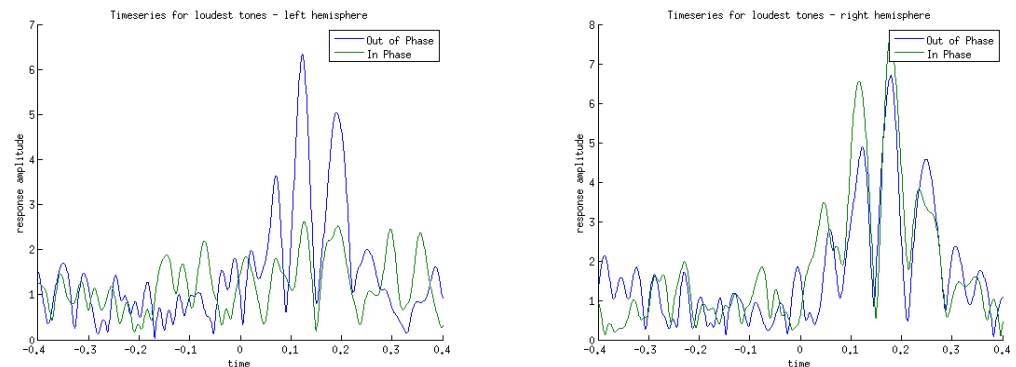


**Figure 6.10** Overlaid timeseries data extracted from MNE for the left and right hemispheres of the group of older children. The plots are reconstructed in Matlab using the MNE timeseries sample points. The blue line represents the loudest dichotic stimulus, and the green line represents the loudest diotic stimulus. The left column shows the left hemisphere response, and the right column shows the right hemisphere response.

In Figure 6.10, the evoked responses for the older group of child participants are shown. Participant four shows a large, clear evoked response but with a relatively small BMLD in the left hemisphere and a somewhat more unclear pattern of results in the right hemisphere. The M100 here is not easily distinguishable but it is taken to be the response occurring just after 100ms with the small BMLD, rather than the previous peak. Participant five displays a clear evoked response and BMLD in the left hemisphere, mirrored in the right hemisphere by a smaller amplitude and smaller BMLD response. This participant clearly shows the developmental pattern of a relatively large M50 peak (Kotecha et al, 2009). Participant six shows a clear triphasic response pattern in both left and right hemispheres with a clear BMLD in the response component around 100ms. Participant seven shows a very large BMLD in the left hemisphere with a clear triphasic pattern, however the right hemisphere shows a negative BMLD with a less clear evoked response component that could be considered to be an M100 response. To confirm that this effect is not due to incorrect orientation reconstruction at source level, an image of the sensor level data for this participant is included below (Figure 6.11) showing a negative BMLD for the right hemisphere.

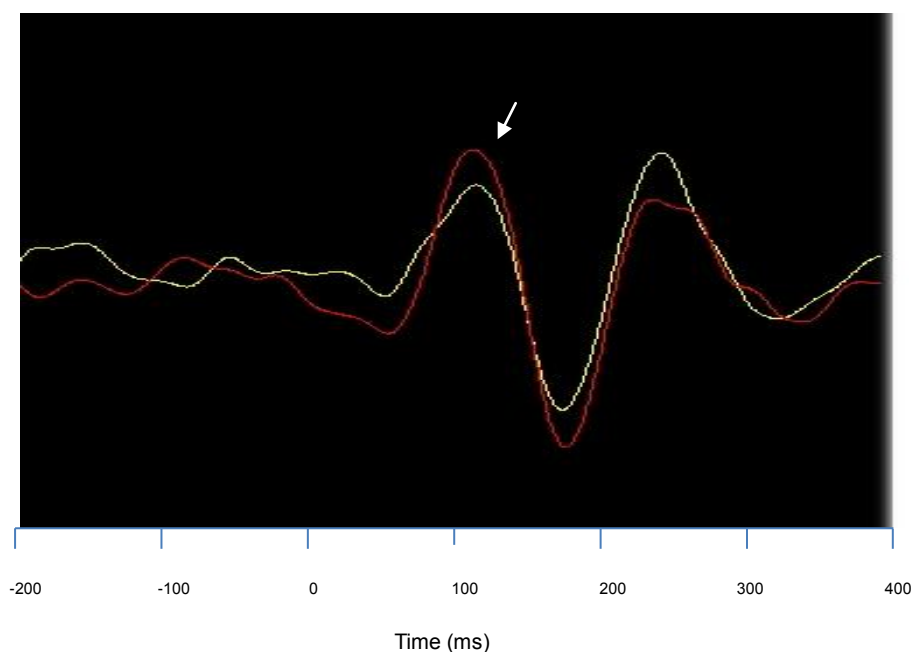


**Figure 6.11** Sensor level evoked response taken from the right temporal lobe for participant 7, using MNE software. The yellow line represents the response to the dichotic stimulus, and the red line denotes the response to the diotic stimulus. The M100 is labelled with an arrow, showing the relative difference between the dichotic and diotic M100 responses. As can be seen there is an effect of a negative BMLD.

Figure 6.11 demonstrates that there is a negative BMLD at sensor level when also found at source level for participant seven, confirming that this is not due to incorrect orientation reconstruction.

### 6.3.2.1 Timeseries amplitude and latency

Figures 6.12 and 6.13 show the timeseries amplitudes for the younger and older group of children respectively.

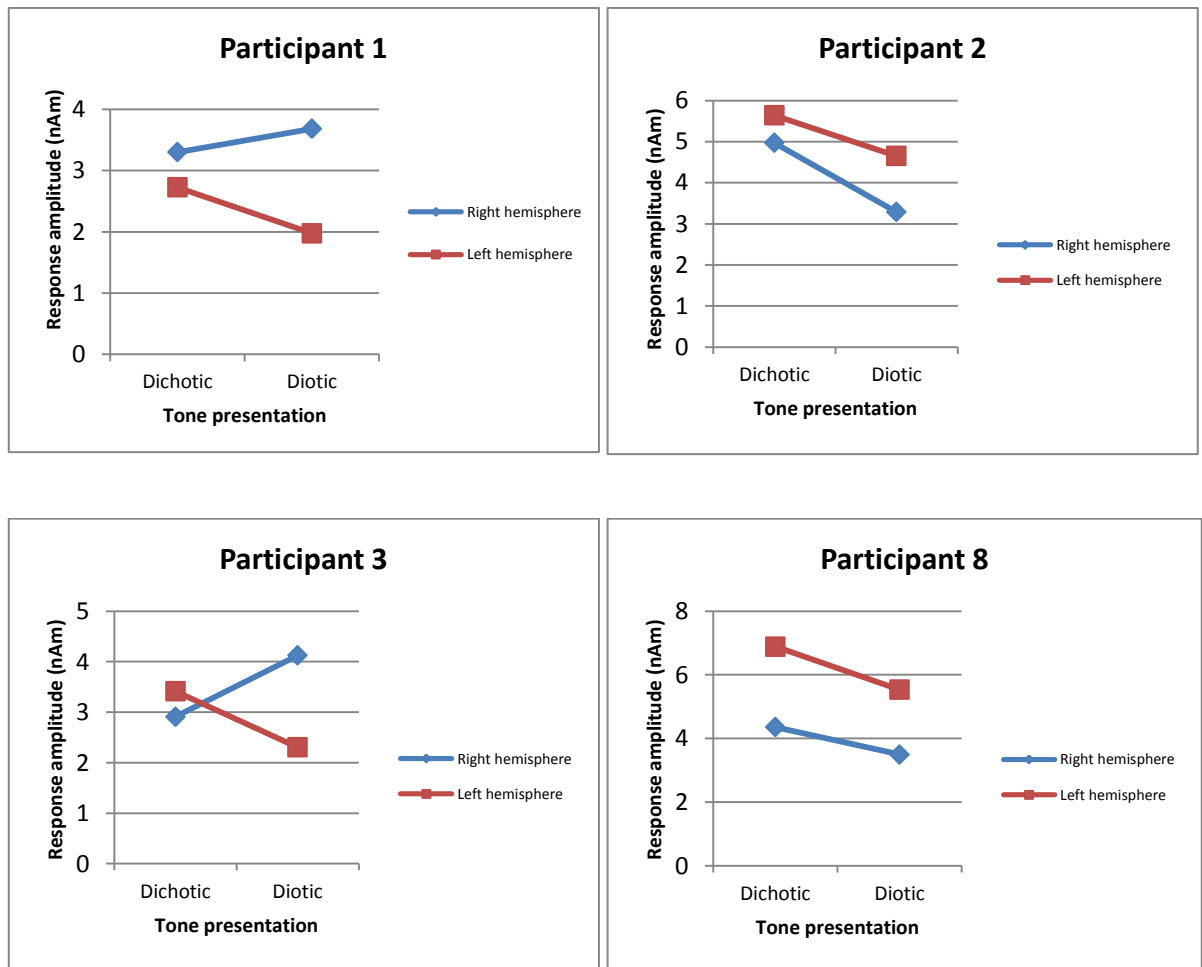


**Figure 6.12** Evoked amplitude values for four younger children, showing values for the loudest dichotic and diotic tone stimulus over noise for both hemispheres. Data is shown for each member of the younger child group individually.

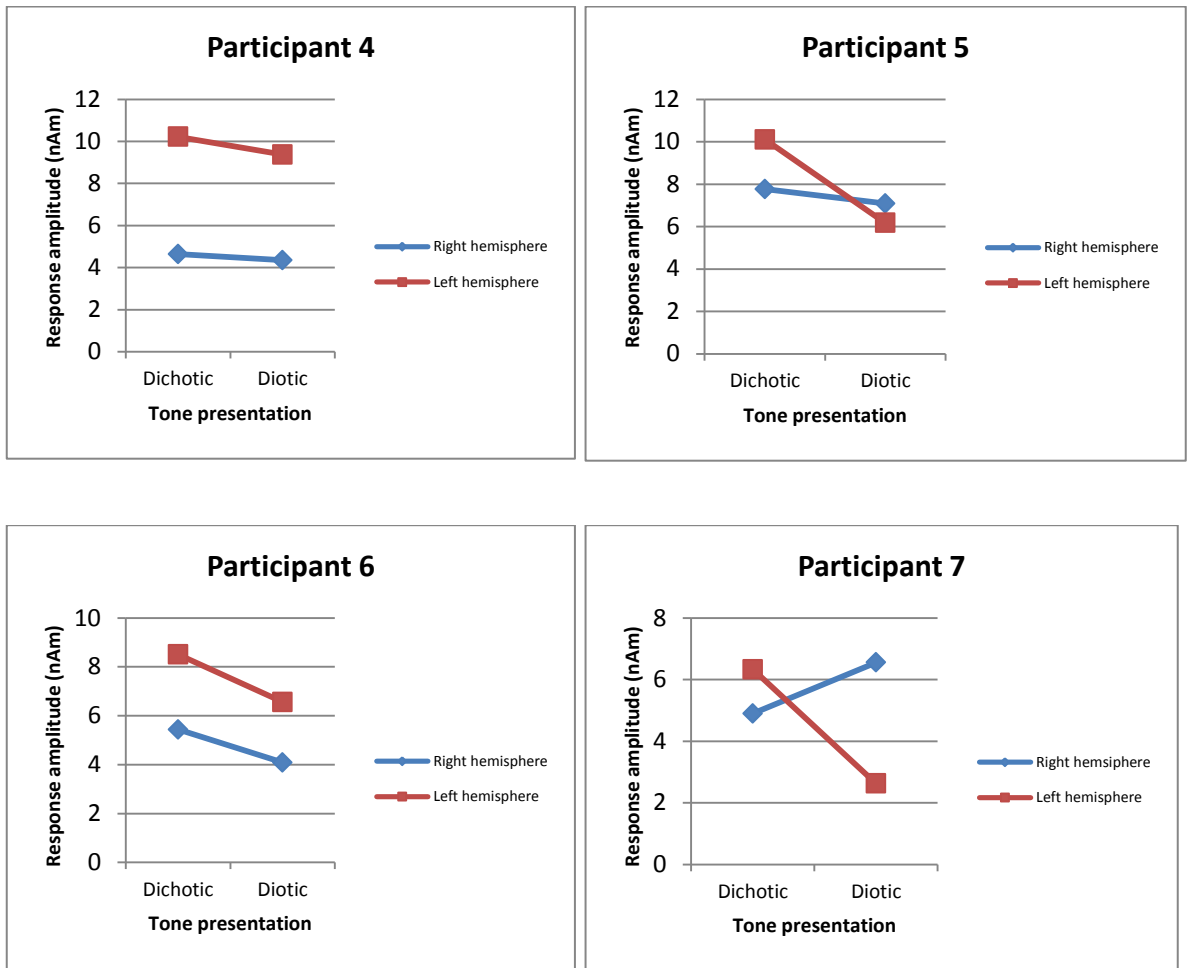


**Figure 6.13** Evoked amplitude values for four older children, showing values for the loudest dichotic and diotic tone stimulus over noise for both hemispheres. Data is shown for each member of the older child group individually.

When compared to the sensor data, the amplitude values extracted from the timeseries more frequently show the expected pattern of a higher response amplitude for the dichotic stimulus than the diotic stimulus in both age groups. There is a trend for the left hemisphere values to be higher than those in the right hemisphere, particularly in the dichotic condition where this is true for all older child participants.

The timeseries latencies for both groups and hemispheres are shown in Figure 6.14.

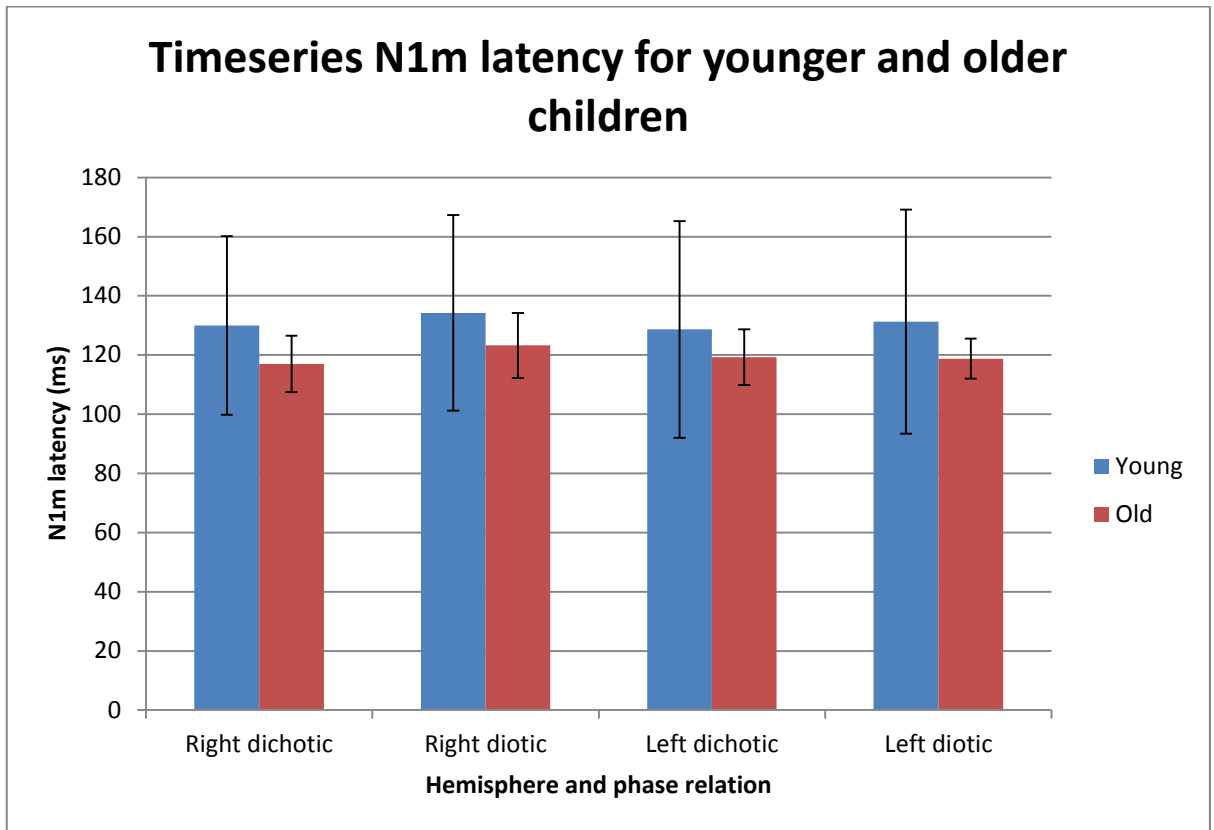


**Figure 6.14** Mean raw latency values for the younger and older children taken from the MNE timeseries data. The error bars show the 95% confidence intervals. N=4 young and 4 older children

There was no significant difference between the right dichotic latencies for young ( $M=130$ ,  $SD=30.77$ ) and old ( $M=117$ ,  $SD=9.69$ ) children,  $t(6)=.806$ ,  $p=.451$ . There was no significant difference between the right diotic latencies for young ( $M=134$ ,  $SD=33.77$ ) and old ( $M=123$ ,  $SD=11.24$ ) children,  $t(6)=.618$ ,  $p=.559$ . There was no significant difference between the left dichotic latencies for young ( $M=129$ ,  $SD=32.35$ ) and old ( $M=119$ ,  $SD=9.61$ ) children,  $t(5)=-.556$ ,  $p=.596$ . There was no significant difference between the left diotic latencies for young ( $M=131$ ,  $SD=33.47$ ) and old ( $M=119$ ,  $SD=6.89$ ) children,  $t(2)=.641$ ,  $p=.584$ . Tables 6.2 and 6.3 show the raw amplitude and latency values extracted from the MNE timeseries data for the younger and older child group respectively.

*Age group 11-12 years*

<i>Participant ID</i>	<i>Left hemisphere Amplitude(nAm)</i>		<i>Right hemisphere Amplitude(nAm)</i>		<i>Left hemisphere Latency (ms)</i>		<i>Right hemisphere Latency (ms)</i>	
	<i>Dichotic</i>	<i>Diotic</i>	<i>Dichotic</i>	<i>Diotic</i>	<i>Dichotic</i>	<i>Diotic</i>	<i>Dichotic</i>	<i>Diotic</i>
1	2.73	1.98	3.3	3.68	172	182	165	169
2	5.64	4.65	4.97	3.29	n/a	n/a	108	113
3	3.41	2.3	2.91	4.13	118	120	106	108
8	6.89	5.54	4.36	3.49	103	105	134	134

**Table 6.2** Amplitude and latency values extracted from the timeseries data for the younger child group, demonstrating the difference between the largest dichotic and largest diotic tones.

*Age group 16-17 years*

<i>Participant ID</i>	<i>Left hemisphere Amplitude (nAm)</i>		<i>Right hemisphere Amplitude (nAm)</i>		<i>Left hemisphere Latency (ms)</i>		<i>Right hemisphere Latency (ms)</i>	
	<i>Dichotic</i>	<i>Diotic</i>	<i>Dichotic</i>	<i>Diotic</i>	<i>Dichotic</i>	<i>Diotic</i>	<i>Dichotic</i>	<i>Diotic</i>
4	10.21	9.38	4.64	4.36	110	116	124	124
5	10.12	6.17	7.76	7.08	113	114	103	108
6	8.5	6.56	5.43	4.09	118	135	131	129
7	6.33	2.63	4.89	6.56	123	126	123	116

**Table 6.3** Amplitude and latency values extracted from the timeseries data for the older child group, demonstrating the difference between the largest dichotic and largest diotic tones.

### 6.3.3 Computing the BMLD

It was particularly difficult to obtain psychophysical data in the younger children. Two of the five younger children's psychophysical BMLDs were unobtainable due to their inability to complete the task, and one who could do the psychophysics had MEG data that was not usable due to excessive channel noise. For raw psychophysical threshold values please see Appendix 3. The neural BMLD value for amplitude was computed by subtracting the raw diotic amplitude value from the dichotic value in both hemispheres and summing them. The same procedure was followed for the neural latency value, except the dichotic value was subtracted from the diotic value instead. A low sample number of six means that statistical correlation testing between the psychophysical BMLD and the neural BMLD values is not appropriate. However, the timeseries amplitude values indicate the presence of an unmasking effect, which can also be seen clearly in the timeseries data from Figures 6.8 and 6.10.

			<i>Sensor data</i>		<i>Timeseries data</i>	
<i>Participant</i>	<i>Age</i>  <i>(years)</i>	<i>Psychophysical</i>  <i>BMLD</i>	<i>Amplitude</i>  <i>BMLD</i>  <i>(fT at E-012)</i>	<i>Latency</i>  <i>BMLD (ms)</i>	<i>Amplitude</i>  <i>BMLD (nAm)</i>	<i>Latency</i>  <i>BMLD (ms)</i>
1	12	N/A	-0.269	9	0.37	14
2	12	N/A	2.07	4	2.67	5
3	10	1.123	1.34	-5	-0.1036	4
4	17	21.7	0.872	3	1.12	6
5	17	21.6	3.57	-1	4.62	6
6	16	15.92	0.649	16	3.29	15
7	17	18.4	0.733	0	2.05	-4
8	12	15.93	2.94	4	2.2	2
9	11	15.64	N/A	N/A	N/A	N/A

**Table 6.4** Psychophysical BMLD values of the whole sample population with available data compared with the amplitude and latency unmasking values extracted from sensor and source data.

## **6.4 Discussion**

This chapter describes the effectiveness of the passive MEG stimulus when testing normally developing child participants. The main conclusion to be drawn from these data is that the passive MEG measure can provide an indication of the extent of unmasking with no need for psychophysical testing.

### **6.4.1 Morphology**

#### **6.4.1.1 Latency**

Previous work has suggested that child responses have a biphasic morphology that tend to show a peak around 70ms and another around 140ms (e. g. Paetau et al., 1995). This was not immediately apparent in the data reported here. The younger group of children showed a high level of baseline noise in the data, but they did have a peak around or just after 100ms, which concurs with other reports of the developing auditory response (e. g. Kotecha et al., 2009). The developmental trajectory of the auditory evoked field is known to show a later M100 for children than adults, which then becomes shorter with maturation of the auditory response (Ponton et al., 1996; Wunderlich et al., 2006).

#### **6.4.1.2 Amplitude**

N1 and P2 peaks are not always visible in children under the age of 12 years (Albrecht et al., 2000; Ponton et al., 2000), however in this study the N1m was always identifiable despite the low SNR. The older group of children showed an adult-like response, comparable to data from the previous chapter in morphology, amplitude and latency. In contrast the younger children showed smaller amplitude values, which could be attributable to their heads being further from the MEG sensors.

Results in anatomical MRI data indicate that structural development aspects of auditory maturation may take place over an extended period (Sowell et al., 1999; Thompson et al., 2000), and so evoked peaks in child auditory data may not be representative of the underlying component structure (Luck, 2005). It is natural to assume that when a waveform does not contain a particular peak, then the

generator of that component is inactive, however this may not necessarily be the case (Gilley et al., 2005). Ponton et al. (2000) suggest that it is possible for the N1 to be masked by P2 phase cancellation. Another reason that child waveforms may appear different to adult waveforms, especially in source localisation, is that the generators are in the same location as for adults, but at different ages, certain generators are more dominant than others (Albrecht et al., 2000; Ceponiene et al., 2002; Ponton et al., 2002).

A number of studies have shown that the M50 is dominant in children and could be used as an alternative to the M100 in indexing auditory development (Cardy et al., 2004; Kotecha et al., 2009). This would be something to investigate further with a larger cohort of children with a wider age range. It would be appropriate to consider using the M50 as an index to auditory development in younger children, however it would still not be appropriate for measurement of the BMLD as previous research has shown that middle latency responses do not demonstrate unmasking at the cortical level in both EEG and MEG (Fowler & Mikami, 1996; Kevanishvili & Lagidze, 1987; Levanen & Sams, 1997).

#### **6.4.2 Group data**

The group data show a high degree of variation in amplitude and latency between participants, particularly in the younger group. There are a number of reasons why this may occur in child data. It is more difficult to make sure the child's head is properly inside the MEG helmet, meaning that the SNR of the brain activity may be variable between participants. Also, the proximity of the child's body to the sensors often results in an ECG artefact that can be difficult to remove from the data using standard post-processing programs. Children may find themselves more physically uncomfortable in the chair, as occasionally their shoulders touch the bottom of the helmet, which can lead to EMG artifacts from tension in the neck muscles. Different head sizes, movement, lack of alertness, blinking and other bodily artifacts can all be detrimental to the process of obtaining clean data. It is notoriously difficult to accurately localise the auditory response in children using dipoles

(Pang et al., 2003), and so using a distributed source localization technique such as MNE allows examination of a wider area of the region of interest.

Another reason for high variability in the group data could be due to large variation in neural synchronisation caused by undeveloped connections in certain brain regions (Tonnquist-Uhlen, 1995). The data in this chapter would seem to support this theory, as the variability in the amplitude and latency responses in the older child group is lower than the younger child group. However, it must be taken into account that children in the younger group are also more likely to differ in physical size due to different developmental rates, a factor of which may be the gender of the participant. It is known that boys and girls grow at different rates. The younger group of neuroimaging participants contained 3 boys and 1 girl, whereas the older group consisted only of boys.

#### **6.4.3 Binaural Masking Level Difference**

The psychophysical MLDs found in this study are large compared to previous findings. For example, Roush & Tait (1984) reported MLD values for a 500Hz tone for children aged between 6-12 years. Their BMLDs ranged from 10-14dB, with no significant change within this age range. Sweetow & Reddell (1978) also reported BMLD values in children aged 4-12 and adults, of 6-8dB for speech and 9-10dB for pure tones. The reason for the larger BMLDs in this chapter could be due to a number of factors. For example, larger BMLDs could be as a result of children not completing the task reliably, perhaps by not responding correctly whether they hear the signal over the masking noise or not (Allen & Wightman, 1992). The larger BMLDs recorded here could also be an effect of noise bandwidth, although this effect is not clear cut. It has been reported that children have smaller MLDs at wider bandwidths (Hall et al., 2007), and also that they have larger MLDs at wider bandwidths (Grose et al., 1997), highlighting an area of uncertainty within the literature. Hall et al. (2007) attribute the smaller MLDs at wider bandwidths to a short signal duration which leads to misplacement of the binaural temporal window. The effect of using a longer signal duration increases the child MLD in a wideband masker (Hall et al., 2007). Grose et al. (1997) suggested that the

perceptual similarity between the signal and masker may be important for detection, in that the more dissimilar the signal and masker the larger the MLD. The authors found that children had smaller MLDs when there was signal presented over a narrowband masker, and thought this effect could be due to the narrow-band nature of both the signal and masker. However, when testing this theory of perceptual similarity, Grose et al. (1997) found that the effect was not present when using a wide band signal and masker, suggesting that noise bandwidth may have a larger effect on the size of the MLD than perceptual similarity of the noise and signal.

The argument for the effect of noise bandwidth is further supported by Hall & Grose (1990), who used both a 300Hz wide masker and a 40Hz wide masking band over a 500Hz tone. Results showed that the wider noise band yielded MLD values that increased up to the age of 5-6 years, at which point they were equivalent to adult values. On the other hand the 40Hz wide masker yielded smaller MLDs that did not reach adult levels by the age of 5-6 years. The authors explain the relatively poorer MLDs in children as less efficient processing of inter-aural time and amplitude differences. These could be coded precisely in the periphery, however may be more inefficiently coded in the central auditory structures (Hall & Grose, 1997).

#### **6.4.4 Neural BMLD validity**

The sample size in this study is too small to be subjected to statistical testing, however the values extracted from the difference between the dichotic and diotic values at amplitude and latency level show good face validity as a correlate of the psychophysical BMLD. Two participants exhibited negative BMLDs in one hemisphere, visible at sensor and source level using the MEG stimulus. The psychophysical BMLD for the older participant (participant 7) was in the normal range, which would suggest normal binaural unmasking abilities. The psychophysical BMLD for the younger of the two (participant 3) was very low, see Table 6.4, indicating that the MEG measure can indicate poor binaural unmasking abilities in some circumstances. Overall, the passive MEG measure allows for

assessment of whether or not a binaural unmasking effect is taking place using the M100 evoked field.

# Chapter 7

---

## **Binaural hearing in epilepsy: 10 case studies**

### **7.1 Introduction**

This chapter will introduce ten cases of patients with epilepsy and assess their binaural hearing abilities using the same method as described previously. The types of epilepsy presented include temporal lobe, motor and frontal lobe. First a summary of binaural hearing with relation to epilepsy will be presented and the effects of neuronal disruption in different brain areas will be considered in terms of spatial hearing and the evoked M100 response. Following this, each patient case will be presented one at a time and discussed.

Epilepsy is a neurological condition affecting more than 65 million people worldwide, with prevalence being higher for babies and children than adults in the developing world (Ngugi et al., 2010). The term 'epilepsy' in fact refers to a broad range of symptoms of overactivity of neurons (seizures) in various brain areas. There are two types of seizure, generalized and partial seizures, with the latter accounting for 60% of all adult seizures (Engel, 2001). A partial seizure involves epileptiform activity in only one hemisphere or localized to a specific region, whereas generalized seizures involve the whole brain.

Epilepsy can have detrimental effects on the function of a cortical area (van Rijckevorsel, 2006). This functional disruption could affect sensory perception. The literature demonstrates that there is a change in perception of sound location in the presence of a temporal lobe lesion (e.g. Kotelenko et al., 2007; Altman et al., 1987). This type of spatial hearing reflects the ability to separate a signal from a background masking noise. If epileptic activity is disruptive to the binaural hearing mechanism, the patient could have difficulties in determining a target signal from background noise.

In a classroom environment, this could translate into an inability to hear a teacher over the background noise, which in turn can be a risk factor for decreasing academic performance (ASHA, 2005). In this situation, measurement of the extent of binaural unmasking in patients is important, particularly when this measurement cannot be gained from a behavioural psychophysical task which is often the case in patient populations (Korostenskaja et al., 2013).

### **7.1.1 Epilepsies**

#### **7.1.1.1 Temporal lobe epilepsy**

The temporal lobe is the site of the primary auditory cortex, which is essential for localizing sound sources in space, particularly in the right hemisphere (Zatorre & Penhune, 2001). The most common form of epilepsy occurs in the temporal lobe, accounting for 50% of all cortical cases (Korotov & Kuryshov, 1998; Zemskaya, 1998). Temporal lobe epilepsy can occur in either or both hemispheres, however it has been shown that seizures in the right temporal lobe have a detrimental effect on binaural hearing, whereas seizures located in the left temporal lobe do not (Kotelenko et al., 2000). In their study of patients with different forms of epilepsy, Kotelenko et al. (2000) investigated temporal lobe epilepsy and the effect it had on spatial hearing. Their findings showed that the degree of binaural hearing impairment was reliant not only upon the extent and localization of an epileptic site, but also the surrounding areas that showed epileptiform activity. Despite this, epileptic activity was shown to have a less detrimental effect on spatial hearing than an organic lesion such as a tumour or cyst in the same region (Kotelenko et al., 2000) as the authors suggest these types of lesion may increase the amount of convulsive activity occurring in the surrounding regions. Focal lesions within the temporal lobe can lead to general deficits in auditory processing (Meneguello et al., 2006; Griffiths et al., 1997) with particular difficulty in localising sound stimuli (Altman et al., 1987; Kotelenko et al., 1996) or detecting movement of sound stimuli (Kotelenko et al., 2007).

#### **7.1.1.2 Benign rolandic epilepsy**

Rolandic epilepsy is the most common epilepsy in children, with a peak of activity at 8-9 years, but many children grow out of it around the age of 15-18 years (Holmes, 1993), hence it is often referred

to as 'benign'. Rolandic epilepsy occurs near to the central sulcus in the parietal lobe, and generally consists of centrottemporal spiking occurring overnight (Boatman et al., 2008). Despite the epileptic activity occurring in areas outside of the primary auditory cortex, BRE patients have been shown to perform worse than age-matched controls in distinguishing speech from background noise (Staden et al., 1998; Boatman et al., 2008). As the spikes occur overnight, Liasis et al. (2006) investigated the possibility that disruption caused by overnight spiking activity may have long-term effects on language processing during the day. The results of this study indicated that patients with unilateral spikes had abnormally large evoked N1s in the contralateral hemisphere, in contrast to the symmetrical evoked component seen in the control group. Further, no asymmetry in this component was seen when the epileptic activity was bilateral, (Liasis et al., 2006).

#### ***7.1.1.3 Frontal epilepsy***

Frontal lobe epilepsy (FLE) is the second most common type of partial epilepsy after temporal lobe epilepsy in children (Manford et al., 1992). Age of onset is around 4-7 years, and children with the disorder often demonstrate cognitive and behavioural impairments (Braakman et al., 2012). Very few studies have considered impairments in auditory processing with relation to frontal lobe epilepsy, however it is possible that the attention deficits present in FLE may impact on auditory selective attention and the ability to utilise binaural mechanisms.

#### ***7.1.1.4 Landau-Kleffner syndrome***

Originally described in 1957, Landau-Kleffner syndrome is an aphasia thought to originate from epileptic activity within the auditory cortex (Fandino et al., 2011). It is an acquired condition, usually beginning in childhood between 3-7 years (Landau & Kleffner, 1998) with the epileptic activity often subsiding at adolescence, although communication can still be severely affected long into adulthood if not permanently. Despite normal early development, LKS can abruptly impair a child's verbal and auditory abilities, often starting with receptive impairment followed by expressive impairment. Physiologically speaking LKS is thought to originate from hyperexcitability of cortical areas due to a

lack of neuronal inhibition, where there is also an increase in glucose consumption (Maquet et al., 1995).

### 7.1.2 Medications

There are a number of epilepsy medications which are commonly used to treat or prevent epileptic seizures. Table 7.1 describes the medications prescribed to the patients in this study with a bit of information about their usage and potential side effects.

Name	Type of drug	Disorders	Side-effects
Lamotrigine (Lamictal)	Anticonvulsant drug used in epilepsy and bipolar disorder. Also used in treating clinical depression.	For epilepsy – used to treat focal seizures, primary and secondary tonic-clonic seizures, and seizures associated with Lennox-Gastaut syndrome	Life-threatening skin reactions e. g. Stevens-Johnson syndrome, DRESS syndrome, and toxic epidermal necrolysis
Oxcarbazepine (Trileptal)	Anticonvulsant and mood stabiliser.	Used to treat epilepsy, anxiety and mood disorders.	Dizziness, drowsiness, blurred vision, fatigue.
Topiramate (Topamax)	Anticonvulsant	Epilepsy, Lennox-Gestaut syndrome. Also used for weight loss.	Cognitive side effects may be more common than with Lamotrigine (Blum et al., 2006). Dizziness, weight loss
Sodium valproate	Anticonvulsant and mood stabiliser	Epilepsy, anorexia nervosa, panic attacks	Tiredness, tremors, nausea, vomiting. High risk of birth defects in pregnancy.
Levetiracetam (Keppra)	Anticonvulsant	Epilepsy	Usually well tolerated. May cause drowsiness, weakness, unsteady gait, fatigue.
Carbamazepine (Tegretol)	Anticonvulsant and mood stabiliser	Epilepsy, bipolar disorder, trigeminal neuralgia	Drowsiness, headaches, migraines, motor co-ordination impairment

**Table 7.1** Typical epilepsy medications and side effects.

### **7.1.3 M100 in epilepsy**

#### **7.1.3.1 Latency effects**

Studies have indicated that auditory M100 latencies are delayed in the presence of temporal lobe epilepsy (Damasio & Damasio, 1979; Seri et al., 1998; Kubota et al., 2007). In an early study, Damasio & Damasio (1979) measured the N1 latency in response to dichotic listening in epilepsy patients. There was a trend towards a response delay in the hemisphere contralateral to the ear of stimulus presentation, however this effect was not significant.

More recently, Kubota et al. (2007) found a significant delay in the M100 in adults with epileptic foci located in the primary auditory cortex. The auditory N1 in the brainstem also shows a delayed response to speech-in-noise stimuli (Li et al., 2007), whereby wave V in the left ear showed longer latencies for patients with partial seizures than controls. This finding agrees with previous work by (Verleger et al., 1997) who also investigated the latency of the N1 in patients with partial seizures and found that they were delayed at cortical level.

#### **7.1.3.2 Amplitude effects**

The effect of epilepsy on M100 amplitude is less clear. Some studies have shown that the M100 amplitude is reduced when epileptic activity is present (Korostenskaja et al., 2010). In this study Korostenskaja et al. (2010) measured M100 amplitudes in cases of intractable epilepsy, with findings that amplitudes of M100, M150 and M200 were reduced in both hemispheres. However, in their study the authors did not differentiate between types of complex partial seizure, so it is unclear what type of epilepsy may have caused their main effect. Another study found reduction in amplitude of auditory N1 at the vertex in the presence of temporal lobe epilepsy, with the left hemisphere spikes having a greater effect on the N1 in terms of a smaller amplitude and longer latency than spike activity in the right hemisphere (Seri et al., 1998). In contrast to these findings, Ford et al., (2001) found that epilepsy does not affect the amplitude of the N1, however N1 amplitudes were reduced in schizophrenic patients. Interestingly, there was an effect of latency delay in these epilepsy patients

(the majority of whom had temporal lobe seizures) but not schizophrenic patients (Ford et al., 2001). As evidence seems to demonstrate that latency can be more affected by epilepsy and epilepsy medication, only M100 amplitude will be considered in the results of this study.

### **7.1.3.3 Effects of medication**

Anti-epileptic medication can have an effect on the auditory evoked response morphology. An EEG study examining the effect on the N1 latency in 48 normal volunteers showed mixed effects for different drugs (Akaho, 1996). Using an auditory oddball task presented at two different tone intensities (30dB SPL and 70dB SPL), Akaho (1996) found a prolonged N1 latency at the louder tone intensity and a reduction in N1 amplitude at the quieter tone intensity for the volunteers taking carbamazepine. Also, a prolonged N1 latency was found for participants taking phenytoin at the quieter tone intensity, however a shortened N1 latency was found for this tone intensity for those participants taking valproate, a finding which the author is unable to explain.

### **7.1.4 Aim**

The aim of this chapter is to individually examine 10 patient cases of epilepsy in terms of the effect on their binaural perception, measured using the M100 evoked response.

## **7.2 Method**

### **7.2.1 Participants**

Participants were all patients who had been referred to the ABC for a MEG assessment as part of their ongoing epilepsy treatment pathway. Ten patients with different types of epilepsy and lesions were recorded. Paediatric patients (ages 8-17) were prioritised for binaural hearing measurement for the purposes of this research, however 4 adult patients were also recorded, including two 18 year olds.

### **7.2.2 Stimulus**

The MEG stimulus used was the same as the stimulus used for the control children in Chapter 6.

No psychophysical data was collected on these patients.

### **7.2.3 MEG data collection**

Data were collected on the Elekta Neuromag system as outlined in the General Methods chapter. The patients were primarily visiting the ABC for other measurements such as language mapping and somatosensory tests that would ultimately contribute towards the planning for their surgery. For this reason, the auditory BMLD measurement was only undertaken if it was deemed suitable and the patient seemed comfortable enough following the other necessary measurements. The actual procedure was the same as outlined in Chapter 6.

### **7.2.4 Analysis**

The analysis procedure for this study was the same as described in the previous chapter, however each patient was considered separately rather than in a group comparison. The data were band-pass filtered between 4-30Hz due to high levels of noise and movement. The data were visually screened for abnormal inter-ictal spike activity. The M100 response was taken to be the largest response in the dichotic condition occurring between 80-150ms after trigger onset.

## **7.3 Results**

The patient data are presented individually including images depicting the sensor level responses, MNE source locations and source model timeseries. Following this, table 7.2 summarises the amplitude values for the dichotic and diotic M100 responses for each patient.

### **7.3.1 Patient number: 1**

**Age** 8

**Context/Background** This patient had a global developmental delay, especially in speech. They were also Dyspraxic and had ASD. Initially it was thought that this patient had Landau-Kleffner Syndrome in their right hemisphere, however there was no sign of regression.

**Medications** N/A

#### **Conclusions**

This patient exhibits a strong evoked response including a binaural unmasking effect in both hemispheres, as can be seen in Figure 7.1.

The source model shows an unexpected localisation for the right temporal auditory activity. The activity distribution would be expected to localise to the floor of the Sylvian fissure, however in this patient, the activity localises more laterally. The source data were taken from the peak of the activity distribution shown, and still demonstrate an unmasking effect in this area. The epileptic activity was isolated to the right hemisphere, which could have impacted on the distribution of neuronal activity.

The left hemisphere responses are larger in general but the right hemisphere shows a larger difference between the diotic and dichotic stimuli, indicating greater binaural unmasking in the right hemisphere.

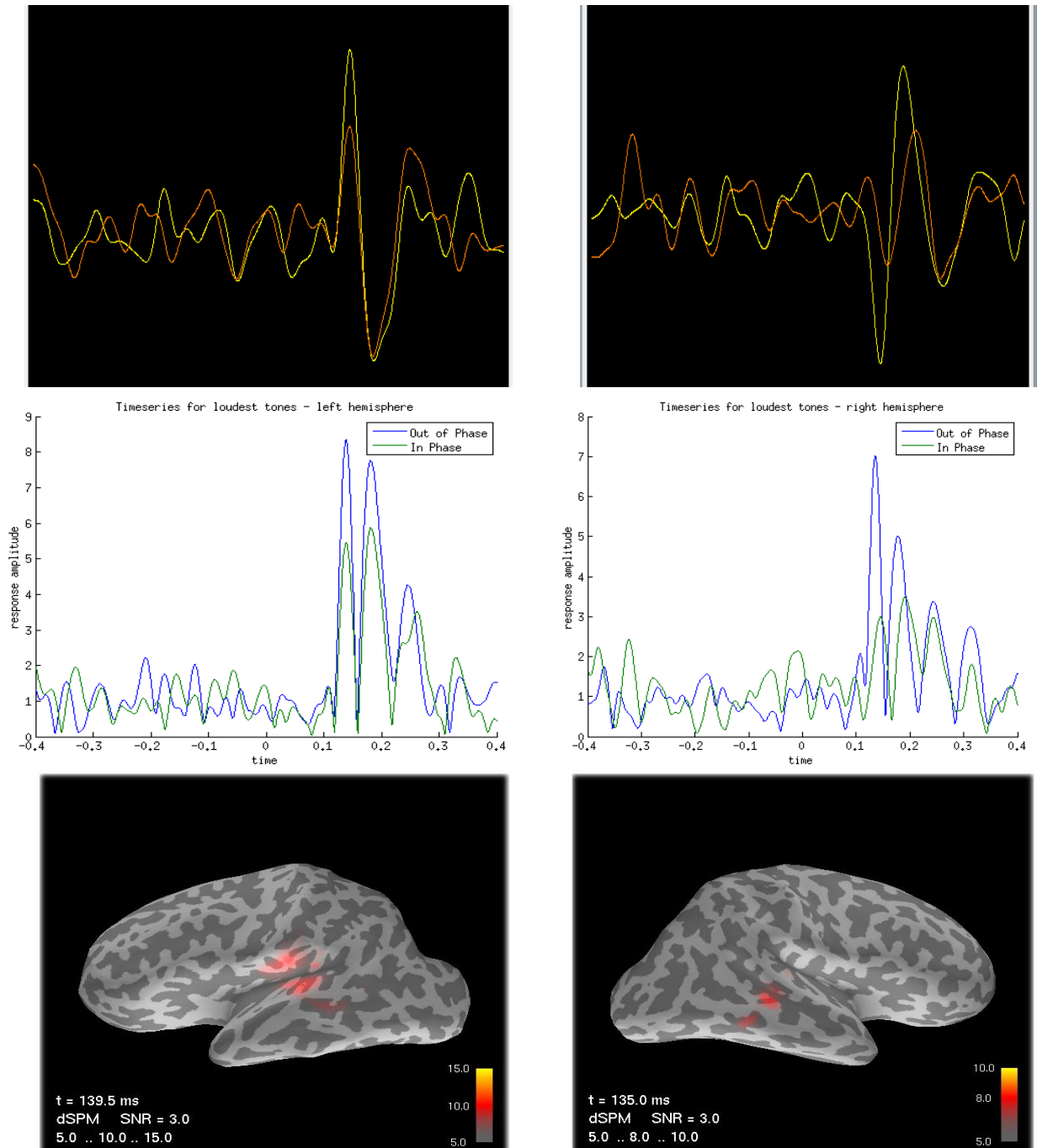


**Figure 7.1.** Patient 1 sensor averages (top), Matlab timeseries plots (middle) and dSPM estimates (bottom) for the left (left column) and right (right column) hemisphere responses to the loudest dichotic and diotic triggers. Sensor averages show the dichotic response in yellow and the diotic condition in orange, and are taken from a temporal channel group for the left and right hemispheres. Sensor amplitudes are shown for relative purposes. Averages were filtered between 4-30Hz. dSPM estimates were thresholded to show the distribution of activity clearly. Matlab timeseries plots used the sample point data from the dSPM estimate and show the amplitude in nAm..

### **7.3.2 Patient number: 2**

**Age** 36

**Context/Background** The MRI and PET are shown to be normal. An EEG test showed abnormality in the right anterior temporal lobe. Seizures have been localised to the frontal lobe.

**Medications** N/A

#### **Conclusions**

The sensor and source level evoked responses in this patient show an asymmetry between the left and right hemispheres for the M100, as can be seen in Figure 7.2. The left hemisphere responses are smaller in amplitude overall, and do not show as large contrast between the peaks as can be seen in the right hemisphere.

The first peak occurring after 100ms after the trigger has been taken as the M100, however in the left hemisphere there is a clear peak occurring just before this which could be taken to be a late M50. A middle latency response of this relative size is unusual in a participant of this age (see Chapter 6) which could indicate immaturity of the neural responses in this hemisphere. This peak response shows little binaural unmasking in the left hemisphere, however the right hemisphere response shows a large unmasking effect for this peak response, which could be due to abnormal activity as opposed to a genuine unmasking effect.

The source waveforms indicate that there is a larger evoked response, and also a larger binaural unmasking effect in the right hemisphere. The clinical EEG showed abnormal activity in the right temporal lobe, however the exact nature of this abnormality is not known. However, abnormal neuronal activity could be linked with an atypical response localisation if the abnormal activity does not produce a stable average. An average evoked response provides the high SNR needed for localisation by the minimum norm estimate (Hämäläinen, 1994). The evoked activity seen here could be the average of the activity within the surrounding areas. The fact that there appears to be a spread of activity means that using a distributed source model is a suitable method for examining the evoked responses in cases where there may be neuronal disruption.

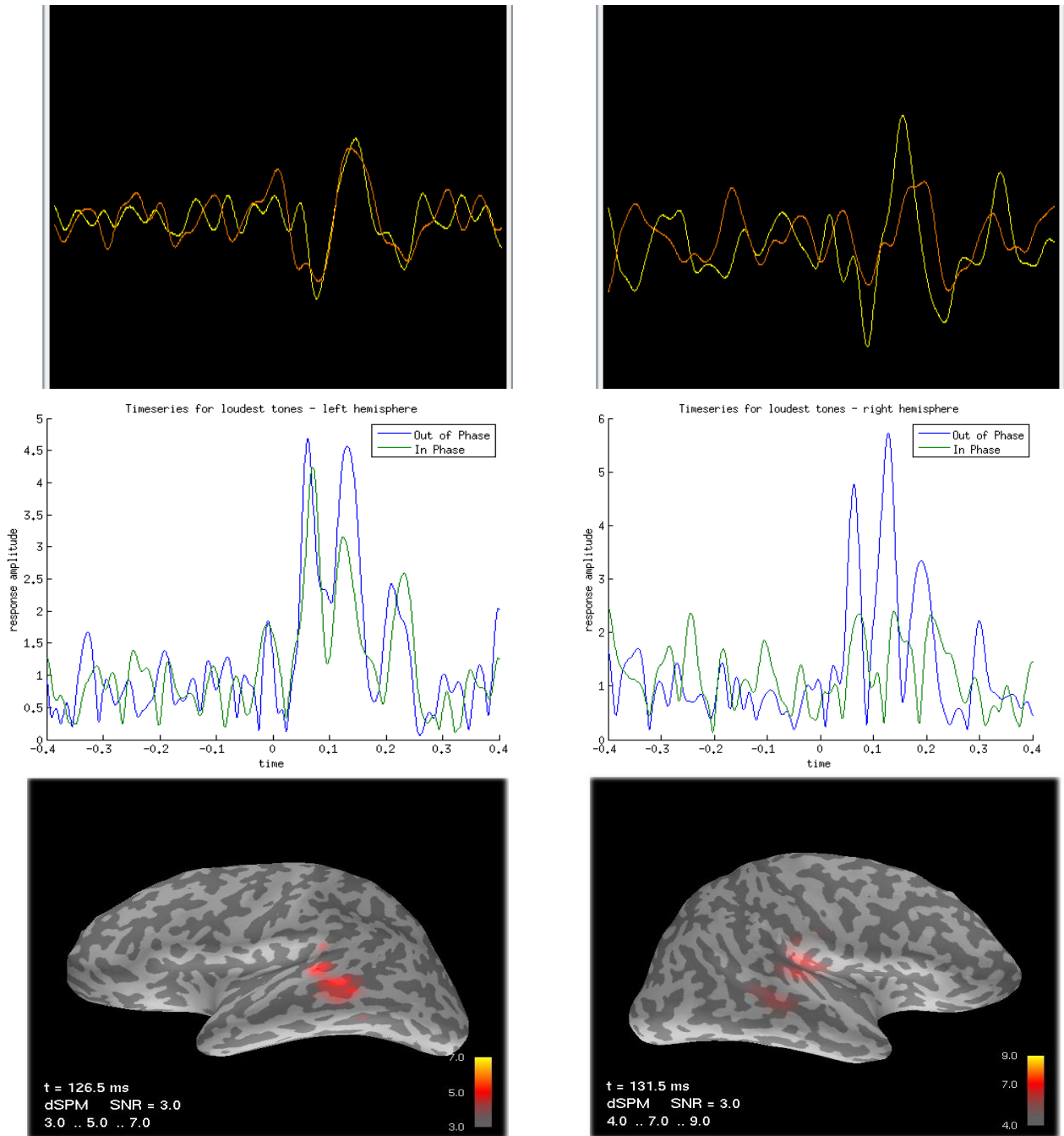


**Figure 7.2.** Patient 2 sensor averages (top), dSPM estimates (bottom) and Matlab timeseries plots (middle) for the left (left column) and right (right column) hemisphere responses to the loudest dichotic and diotic triggers. Sensor averages show the dichotic response in yellow and the diotic condition in orange and are taken from a temporal channel group for the left and right hemispheres. Sensor amplitudes are shown for relative purposes. Averages were filtered between 4-30Hz. dSPM estimates were thresholded to show the distribution of activity clearly. Matlab timeseries plots used the sample point data from the dSPM estimate and show the amplitude in nAm..

### **7.3.3 Patient number: 3**

**Age** 17

**Context/Background** This patient had visuo-motor difficulties, with a left occipital lobe lesion. They have Aspergers syndrome, and a recorded IQ measure of 103.

**Medications** Lamotragine, Oxcarbazepine

#### **Conclusions**

The evoked responses in this patient show an unusual pattern (Figure 7.3). The baseline is relatively noisy, particularly in the right hemisphere. There is a small evoked response in the right hemisphere at sensor level, so the use of a source model is proving effective in improving the SNR of the evoked response. There is little difference in the amplitudes for the dichotic and diotic tones in either hemisphere, indicating a lack of binaural unmasking. The left hemisphere peak occurring just before 80ms shows a large difference in the dichotic and diotic M100 response amplitudes, however the diotic component of the response falls below the baseline level of noise. This patient shows little unmasking in the temporal region, which is interesting considering the patient had a lesion in the occipital region.

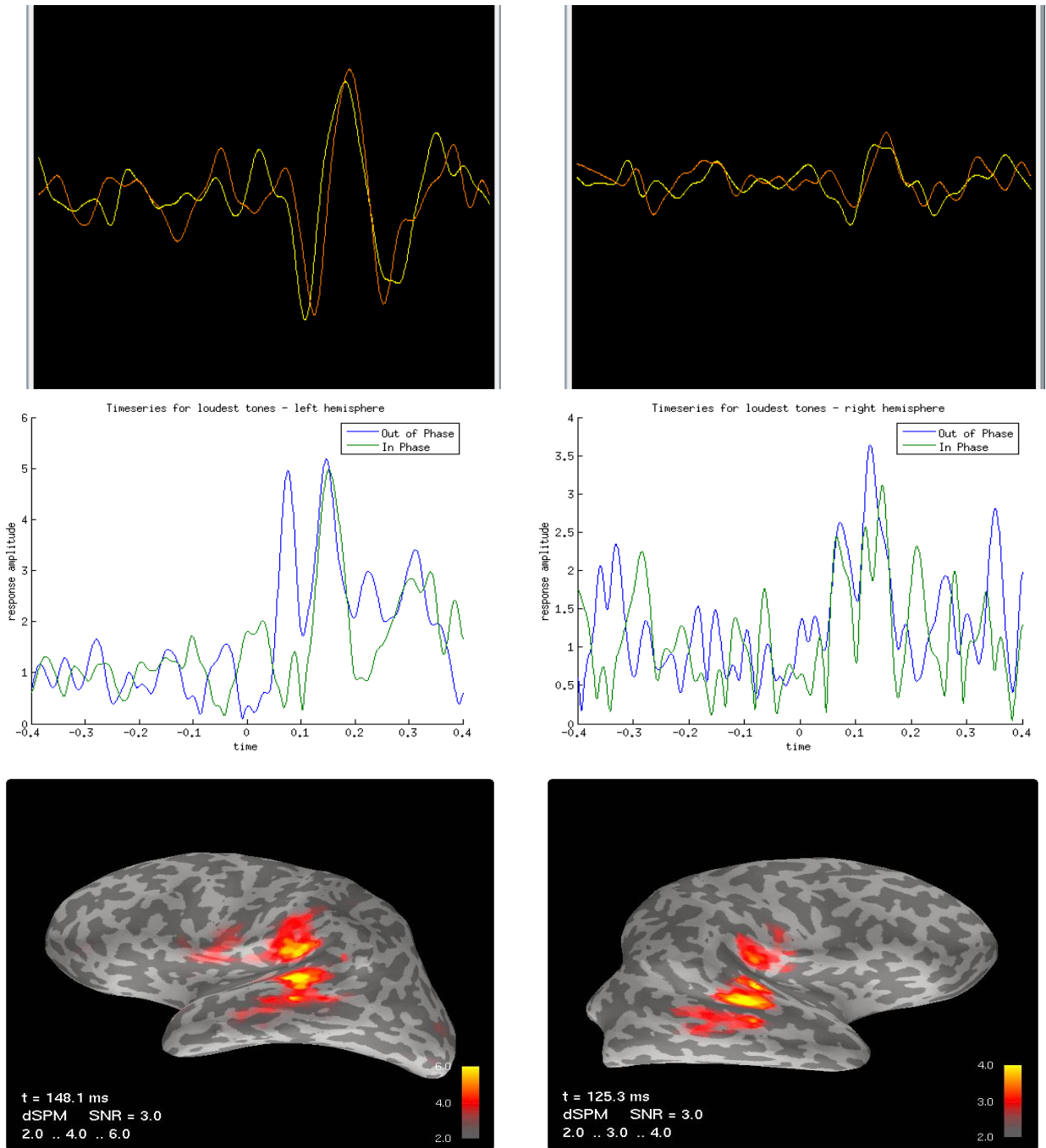


**Figure 7.3.** Patient 3 sensor averages (top), dSPM estimates (bottom) and Matlab timeseries plots (middle) for the left (left column) and right (right column) hemisphere responses to the loudest dichotic and diotic triggers. Sensor averages show the dichotic response in yellow and the diotic condition in orange and are taken from a temporal channel group for the left and right hemispheres. Sensor amplitudes are shown for relative purposes. Averages were filtered between 4-30Hz. dSPM estimates were thresholded to show the distribution of activity clearly. Matlab timeseries plots used the sample point data from the dSPM estimate and show the amplitude in nAm..

### **7.3.4 Patient number: 4**

**Age** 18

**Context/Background** This patient has shown spike and wave activity lateralised to the right temporal lobe.

**Medications** Lamotrigine, Tapirorate

#### **Conclusions**

In Figure 7.4, source timeseries waveforms show very small power in terms of the minimum norm estimate, the thresholds are very low and there is a lot of noise in the baseline. The sensor level data shows clear evoked responses in both hemispheres, which is reflected in the source model data, despite the noisy baseline. The left hemisphere shows an evoked response at the latency of 76ms, which will be used in the analysis of this patient as there is no alternative response, which is unusual in itself for a person of this age. There appears to be an effect of binaural unmasking in both hemispheres, although the right evoked response is slightly larger in amplitude than the left. It is possible that this patient's medication is affecting their evoked responses visible as a reduction in M100 amplitude, making it difficult to see the response over the background noise.

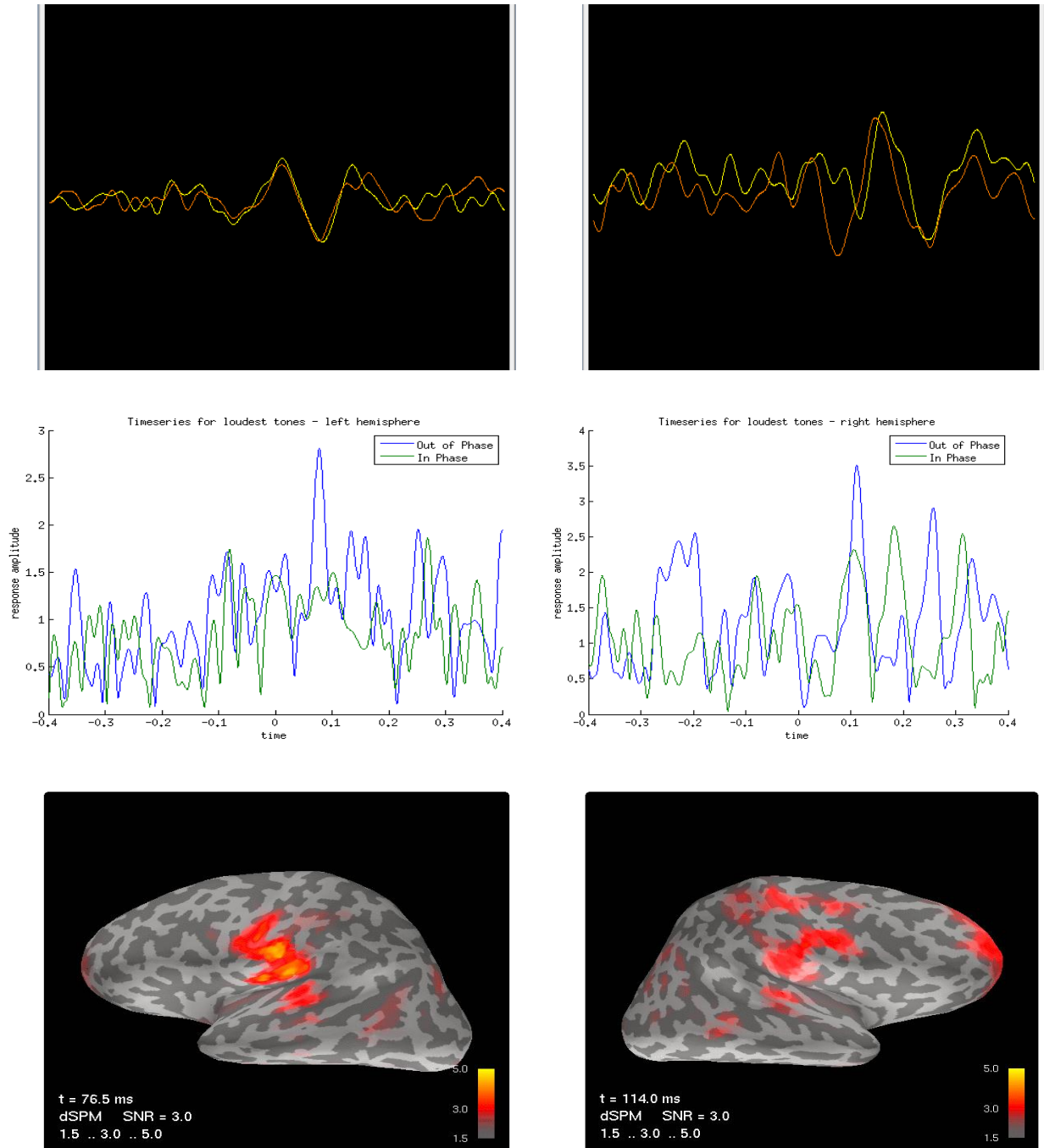


**Figure 7.4.** Patient 4 sensor averages (top), dSPM estimates (bottom) and Matlab timeseries plots (middle) for the left (left column) and right (right column) hemisphere responses to the loudest dichotic and diotic triggers. Sensor averages show the dichotic response in yellow and the diotic condition in orange and are taken from a temporal channel group for the left and right hemispheres. Sensor amplitudes are shown for relative purposes. Averages were filtered between 4-30Hz. dSPM estimates were thresholded to show the distribution of activity clearly. Matlab timeseries plots used the sample point data from the dSPM estimate and show the amplitude in nAm..

### **7.3.5 Patient number: 5**

**Age** 16

**Context/Background** This patient has Hydrocephalus and had a shunt in the left hemisphere. In this analysis the freesurfer 'fsaverage' average brain was used because a suitable reconstruction could not be obtained.

The patient had visual damage, alongside severe learning difficulties.

**Medications** Sodium valproate, Levetiracetum

### **Conclusions**

The use of an average brain here shows the response occurring in the parietal region of the brain, this is from where the auditory data were taken (Figure 7.5) The sensor level montage showed the auditory response occurring very frontally, so the unusual source localisation of the auditory response in the MNE reconstruction is not due to the fact an average brain was used. The timeseries data show a typical auditory evoked response in both hemispheres, with the left hemisphere M100 response having a larger amplitude and higher SNR than in the right hemisphere. The patient had a shunt in their left hemisphere, however this is the hemisphere with the stronger auditory response. Both hemisphere responses show a binaural unmasking effect at source level.

It is possible that the unusual location of this response is linked to the disruption of the neuronal activity, or it could be another response altogether. The morphology of the response mirrors that of the older child group in the previous chapter, particularly in the left hemisphere, indicating that it is the auditory evoked response. The results show that it is possible to measure binaural unmasking in a cortical area that is not the usual source of auditory evoked responses.

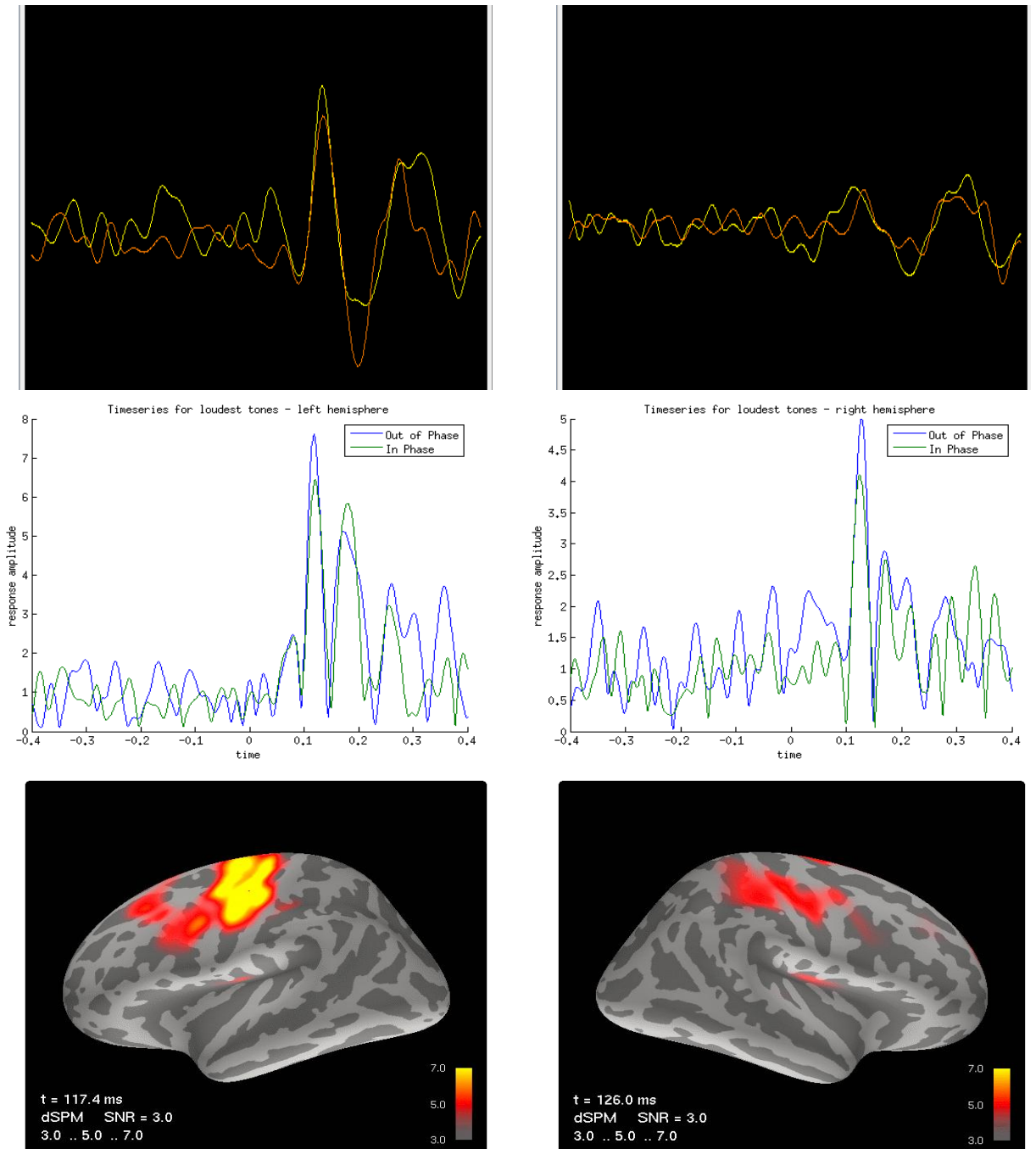


**Figure 7.5.** Patient 5 sensor averages (top), dSPM estimates (bottom) and Matlab timeseries plots (middle) for the left (left column) and right (right column) hemisphere responses to the loudest dichotic and diotic triggers. Sensor averages show the dichotic response in yellow and the diotic condition in orange and are taken from a temporal channel group for the left and right hemispheres. Sensor amplitudes are shown for relative purposes. Averages were filtered between 4-30Hz. dSPM estimates were thresholded to show the distribution of activity clearly. Matlab timeseries plots used the sample point data from the dSPM estimate and show the amplitude in nAm..

### **7.3.6 Patient number: 6**

**Age** 18

**Context/Background** This patient had lesions in the right parietal lobe, accompanied by stiffening of the left arm. There were not many epileptic spikes recorded in the data. An anatomical MRI shows additional lesions throughout the brain, but mostly based centrally.

**Medications** Levetiracetum

#### **Conclusions**

The sensor and source level evoked M100s in both hemispheres are within the normal range for latency and amplitude at an adult level, to be expected for a patient of this age (Figure 7.6). This patient also exhibits the pattern of the three peaked response, with the middle, and largest, peak being the M100 component of interest. Both hemisphere responses show a clear effect of binaural unmasking, with the right hemisphere response amplitude being slightly larger.

This dataset shows a good example of fairly clean data from a patient, which can be used in comparison with others. There was no temporal lobe epileptiform activity in this patient, which could be the reason why the binaural response is well defined in the auditory cortex.

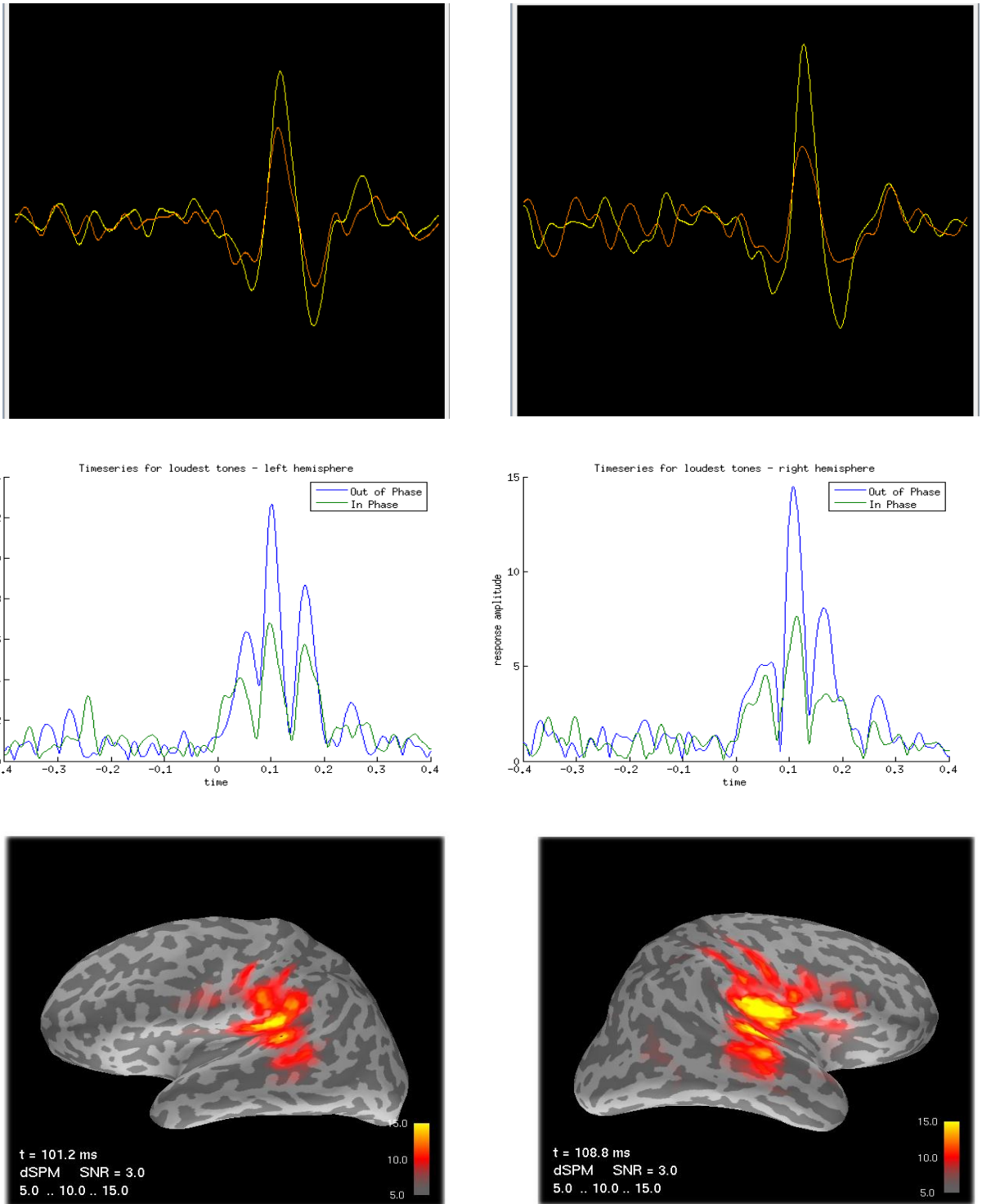


**Figure 7.6.** Patient 6 sensor averages (top), dSPM estimates (bottom) and Matlab timeseries plots (middle) for the left (left column) and right (right column) hemisphere responses to the loudest dichotic and diotic triggers. Sensor averages show the dichotic response in yellow and the diotic condition in orange and are taken from a temporal channel group for the left and right hemispheres. Sensor amplitudes are shown for relative purposes. Averages were filtered between 4-30Hz. dSPM estimates were thresholded to show the distribution of activity clearly. Matlab timeseries plots used the sample point data from the dSPM estimate and show the amplitude in nAm..

### **7.3.7 Patient number: 7**

**Age** 27

**Context/Background** This patient shows normal development. They had a vascular tumour in the right frontal lobe, accompanied by motor seizures.

**Medications** N/A

#### **Conclusions**

The evoked responses at sensor level are clear, however they do not show a very large binaural unmasking effect (Figure 7.7). The unmasking effect at source level is much larger, is present in both hemispheres, and the evoked responses are clearly visible over the baseline. The right hemisphere shows a larger M50 and P200 than the left hemisphere, which is similar in morphology to the older control paediatric responses from Chapter 6. This is in concordance with the location of the lesion in this patient. They had a vascular tumour in the right frontal lobe alongside motor seizures, which could have impacted on the development of the evoked response in this hemisphere leading to an immature response morphology.

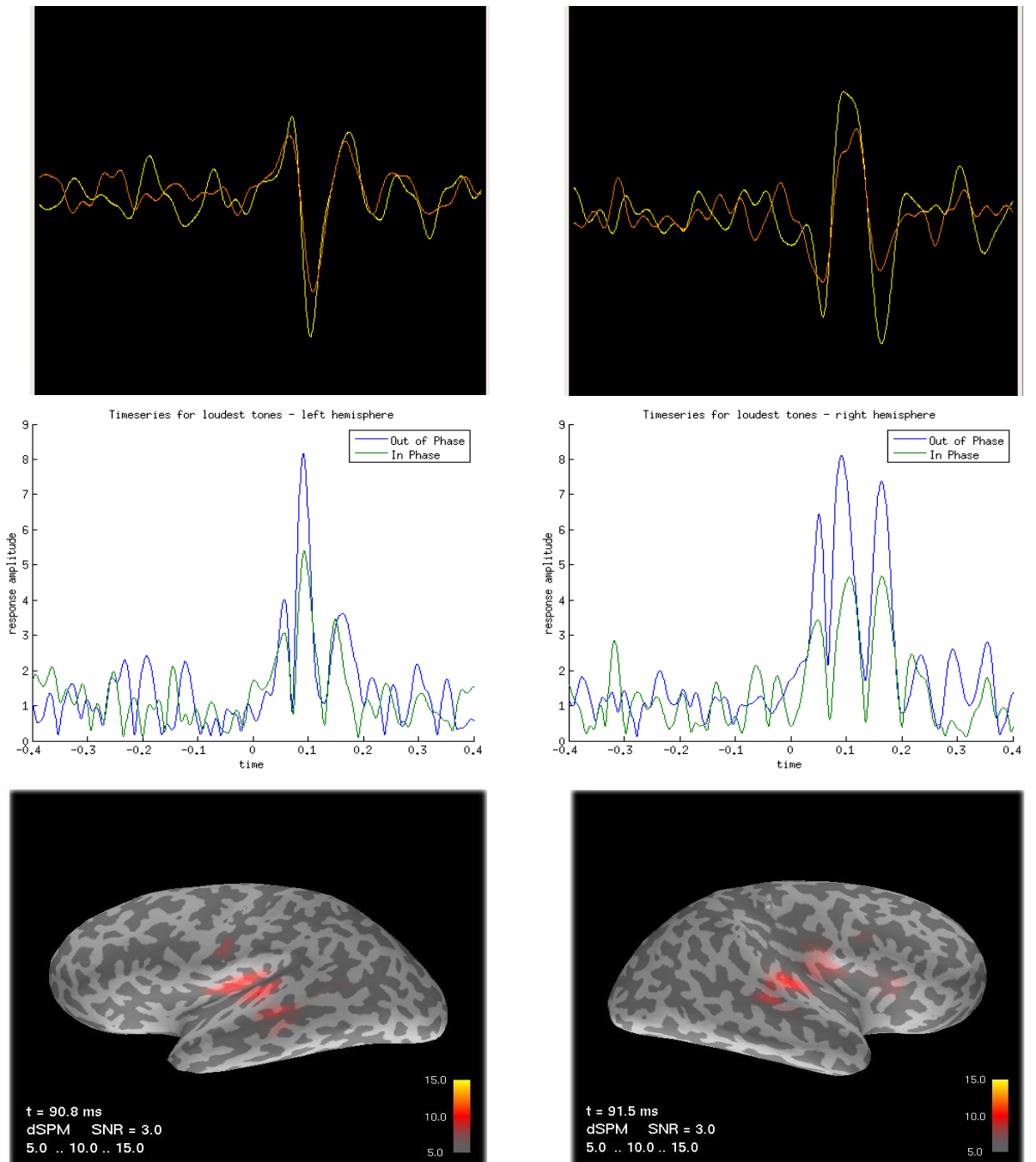


**Figure 7.7.** Patient 7 sensor averages (top), dSPM estimates (bottom) and Matlab timeseries plots (middle) for the left (left column) and right (right column) hemisphere responses to the loudest dichotic and diotic triggers. Sensor averages show the dichotic response in yellow and the diotic condition in orange and are taken from a temporal channel group for the left and right hemispheres. Sensor amplitudes are shown for relative purposes. Averages were filtered between 4-30Hz. dSPM estimates were thresholded to show the distribution of activity clearly. Matlab timeseries plots used the sample point data from the dSPM estimate and show the amplitude in nAm..

### **7.3.8 Patient number: 8**

**Age** 10

**Context/Background** This patient shows focal epilepsy in the left frontal lobe and right parietal lobe. A PET scan showed a reduced uptake of substances in the left prefrontal cortex. They had problems with attention and working memory, and very poor motor function.

**Medications** Levetiracetam, Carbamazepine

#### **Conclusions**

This patient would not be capable of undertaking a psychophysical task, however the source waveforms show a distinct unmasking effect, particularly in the left hemisphere, which is not visible from the sensor amplitudes (Figure 7.8). The sensor level data would suggest that the SNR of the signal is greater in the right hemisphere, however the source model data shows a much larger response amplitude in the left hemisphere with a greater SNR. For a patient of this age it might be expected to see a larger M50 and M200 however neither of these are clearly visible in the left hemisphere.

The left hemisphere shows a cleaner baseline than the right hemisphere at source level, demonstrating the benefits of using source measures of evoked responses to gain further insights into the extent of binaural hearing effectiveness

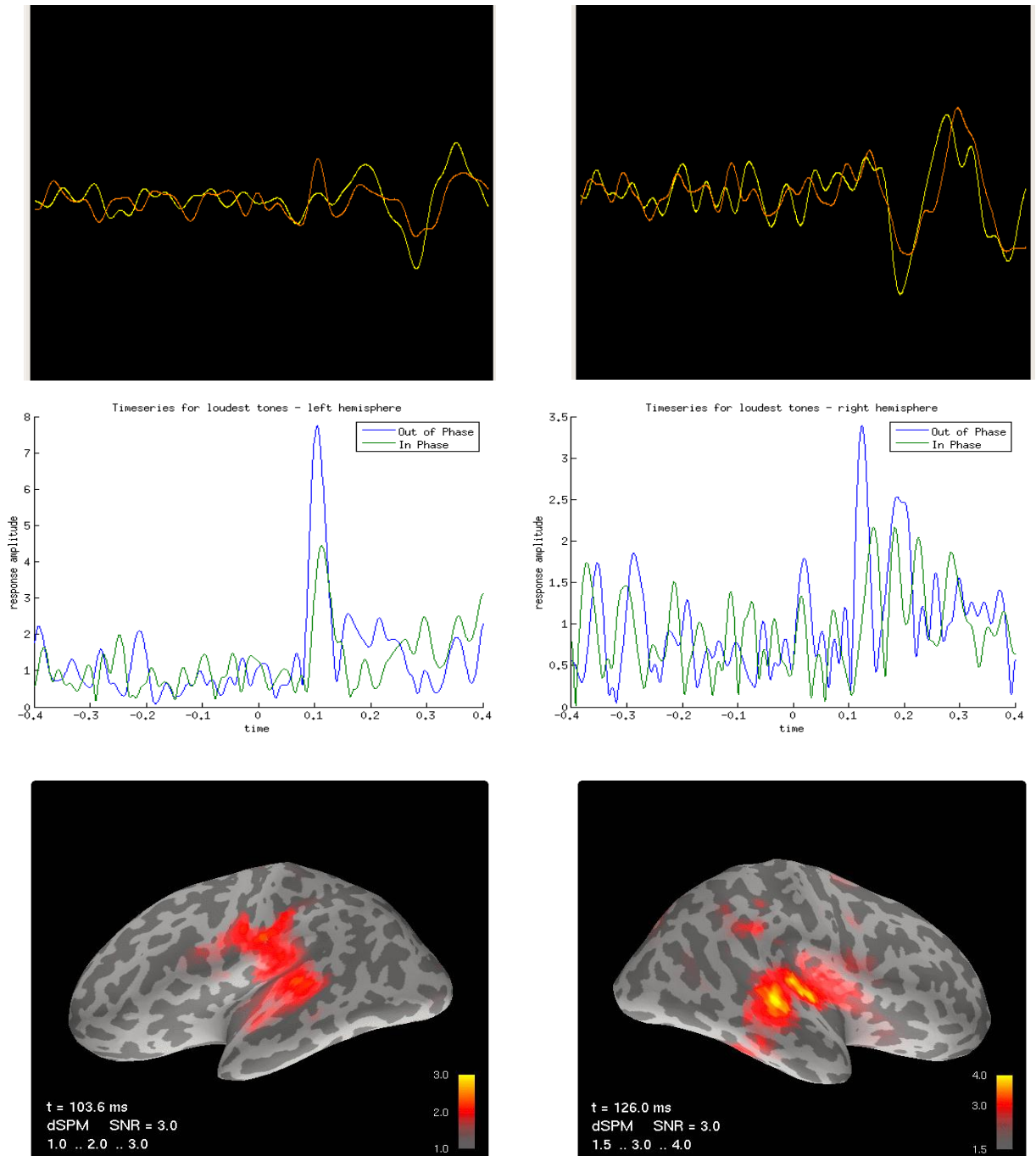


**Figure 7.8.** Patient 8 sensor averages (top), dSPM estimates (bottom) and Matlab timeseries plots (middle) for the left (left column) and right (right column) hemisphere responses to the loudest dichotic and diotic triggers. Sensor averages show the dichotic response in yellow and the diotic condition in orange and are taken from a temporal channel group for the left and right hemispheres. Sensor amplitudes are shown for relative purposes. Averages were filtered between 4-30Hz. dSPM estimates were thresholded to show the distribution of activity clearly. Matlab timeseries plots used the sample point data from the dSPM estimate and show the amplitude in nAm..

### **7.3.9 Patient number: 9**

**Age** 13

**Context/Background** This patient had neurofibromatosis II, an inherited syndrome whereby the patient develops non-malignant tumours around cranial nerve VIII, the main auditory nerve. They can hear a soft whisper in both ears but they have a right ear hearing abnormality. The patient also experiences parietal seizures. Only the right hemisphere could be modelled in this patient, using an average brain.

**Medications** Tegretol, Lamictal

### **Conclusions**

It was not possible to extract any auditory data from the left hemisphere of this patient due to unforeseen interference that occluded the auditory response. However, the source localisation technique allowed us to view the timeseries of the evoked response at the source location through maximization of the signal in the right hemisphere.

The right hemispheric response shows a clear M100 despite a noisy baseline at source level. Due to the larger baseline variations in the dichotic condition, the small BMLD effect witnessed at the evoked response is not reliable. The sensor level response does not show a difference in amplitude between the dichotic and diotic tones during the pre-trigger period, and shows no BMLD effect. It is possible that this patient's lesions could have affected temporal coding in the auditory nerve, meaning their hearing based on excitation-pattern is functioning correctly but they struggle to undertake tasks requiring timing. If this is the case, then it could be predicted that they would experience problems with low-frequency pitch but not high-frequency pitch, as at higher frequencies the binaural system utilises cues related to level differences between the ears as opposed to timing differences (Blauert, 1985; Litovsky et al., 1999).

Again this patient would not be able to undertake a psychophysical task, so using this method of determining the extent of binaural unmasking is very valuable.

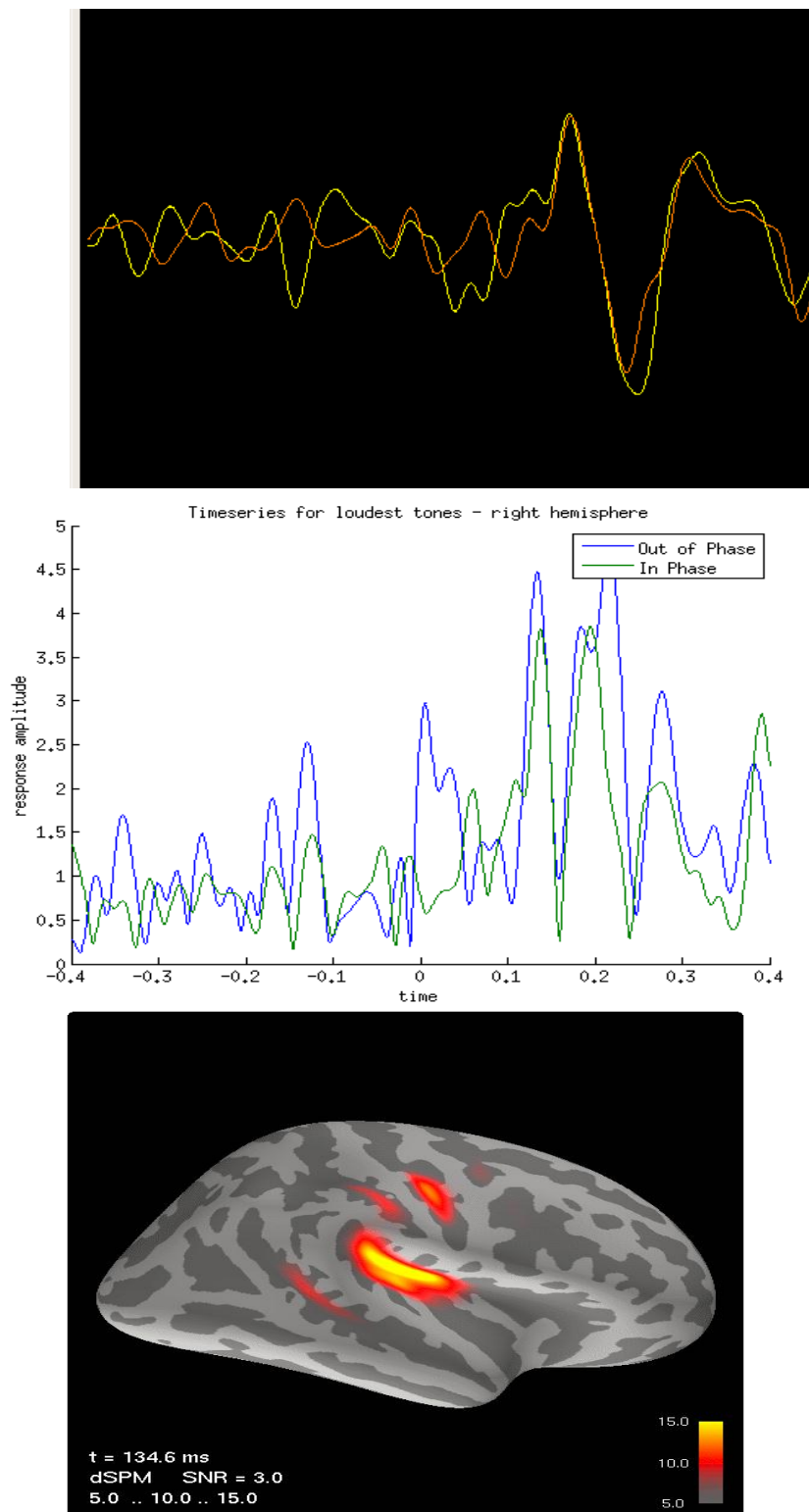


**Figure 7.9.** Patient 9 sensor averages (top), dSPM estimates (bottom) and Matlab timeseries plots (middle) for the right hemisphere responses to the loudest dichotic and diotic triggers. Sensor average shows the dichotic response in yellow and the diotic condition in orange and are taken from a temporal channel group for the hemisphere. Sensor amplitudes are shown for relative purposes. Averages were filtered between 4-30Hz. dSPM estimates were thresholded to show the distribution of activity clearly. Matlab timeseries plots used the sample point data from the dSPM estimate and show the amplitude in nAm.

### **7.3.10 Patient number: 10**

**Age** 16

**Context/Background** This patient has seizures starting in the right frontal lobe, with a slower uptake of substances in the right hemisphere using PET. They also have a specific memory impairment. The patient has a possible lesion in the right middle frontal gyrus.

**Medications** Carbamazepine

#### **Conclusions**

These data (Figure 7.10) exhibit good clear M100 responses at both sensor and source level, at a normal latency. The sensor level data show a small unmasking effect in the right hemisphere and a slightly larger effect in the left hemisphere, the pattern of which is mirrored in the source waveform data. This patient has abnormalities in the right hemisphere, which may account for the less effective binaural unmasking in this hemisphere. However, at source level, the auditory evoked response in the right hemisphere is larger than in the left which reflects normal auditory processing.

The left and right hemispheres show a different morphology of peaks, which could be due to an effect of the medication. Despite this, each peak showed a binaural unmasking effect which indicates that the M100 is not the only component of use in determining the effectiveness of unmasking in MEG.

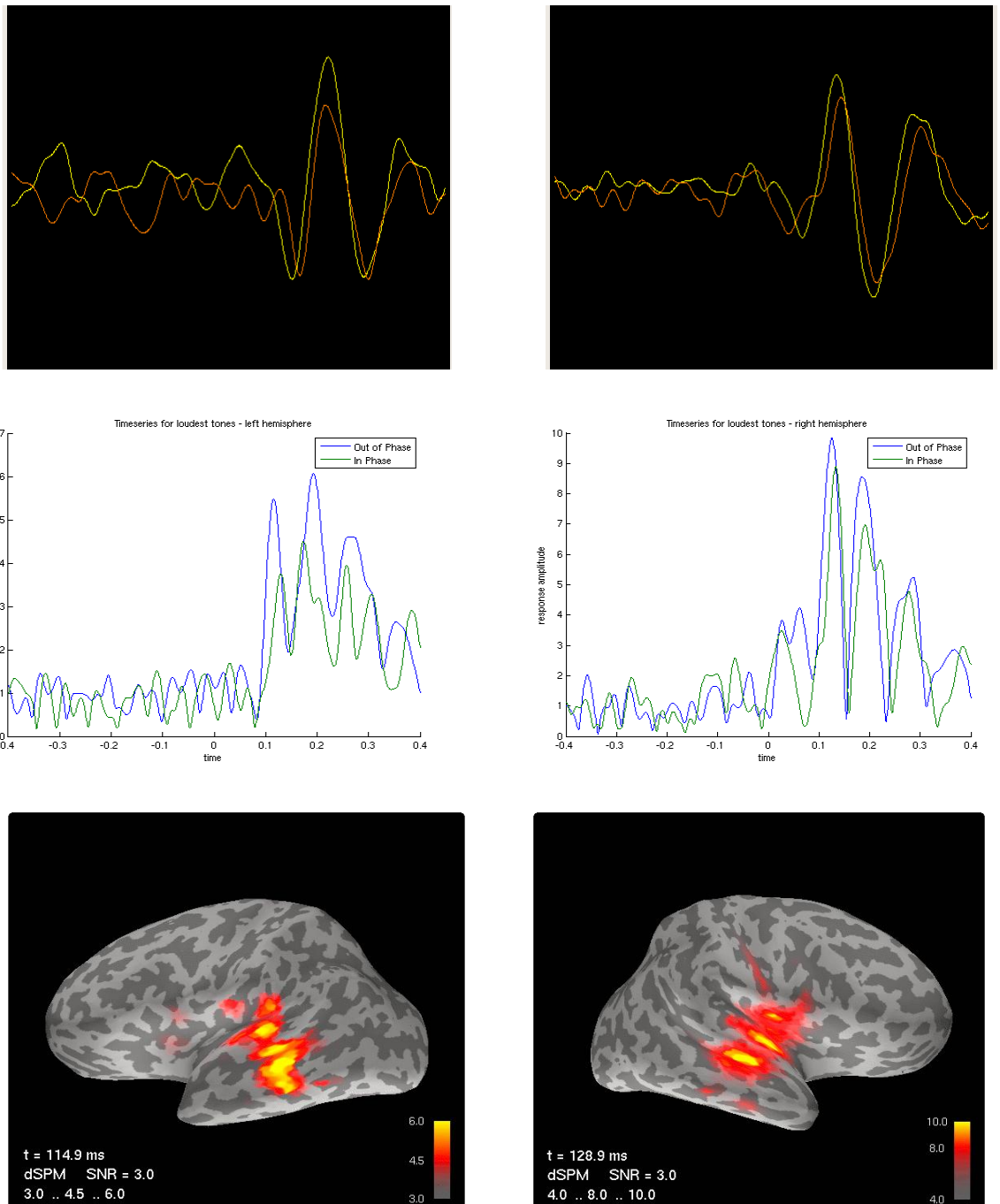


**Figure 7.10.** Patient 10 sensor averages (top), dSPM estimates (bottom) and Matlab timeseries plots (middle) for the left (left column) and right (right column) hemisphere responses to the loudest dichotic and diotic triggers. Sensor averages show the dichotic response in yellow and the diotic condition in orange and are taken from a temporal channel group for the left and right hemispheres. Sensor amplitudes are shown for relative purposes. Averages were filtered between 4-30Hz. dSPM estimates were thresholded to show the distribution of activity clearly. Matlab timeseries plots used the sample point data from the dSPM estimate and show the amplitude in nAm..

## 7.4 Summary of patient data

Patient	Age	Epilepsy	Medication	Left hemisphere M100 amplitude			Right hemisphere M100 amplitude		
				Dichotic	Diotic	Difference	Dichotic	Diotic	Difference
1	8	Temporal	N/A	8.34	5.44	2.9	7.03	2.98	4.05
2	36	Temporal and frontal	N/A	4.56	3.15	1.41	5.72	2.40	3.32
3	17	Occipital	Lamotragine, Oxcarbazepine	5.19	4.97	0.22	3.64	3.11	0.53
4	18	Temporal and frontal	Lamotragine, Topiramate	2.8	1.49	1.31	3.51	2.32	1.19
5	16	Parietal/temporal	Sodium valproate, Levetiracetum	7.6	6.44	1.16	4.99	4.11	0.88
6	18	Parietal	Levetiracetum	12.66	6.81	5.85	14.5	7.62	6.88
7	27	Frontal	N/A	8.16	5.39	2.77	8.1	4.66	3.44
8	10	Frontal and parietal	Carbamazepine, Levetiracetum	N/A	N/A	N/A	3.39	2.16	1.23
9	10	Parietal epilepsy and neurofibromatosis II	Tegretol, Lamictal	N/A	N/A	N/A	4.48	3.82	0.66
10	16	Frontal	Carbamazepine	5.48	3.75	1.68	9.84	8.89	0.95

**Table 7.2** Summary of patient data showing demographics, epilepsy and medication, and amplitude and latency values for N1m.

## **3.5 Discussion**

The aim of this chapter was to present a series of case studies examining the effect of epileptiform activity and other lesions on the binaural unmasking effect. Patients of a range of ages with different kinds of epilepsy were recorded in the study, including frontal, temporal, parietal and motor epilepsy.

Deficit studies have shown that a generalized abnormality in one hemisphere can have a negative effect on binaural hearing abilities (e. g. Efron et al., 1983; Ruff et al., 1981). Ortiz et al. (2009) undertook a study of 38 subjects with epilepsy, without knowledge of epilepsy-type other than if it was partial or generalised epilepsy. The paradigm involved a dichotic non-verbal listening test, whereby the participants had to concentrate on the sound at only one ear while ignoring the sound at the other. The findings indicated that both partial and generalized epilepsy patients had deficits in their dichotic listening, derived from a higher number of errors than would be observed in a normal population (Ortiz et al., 2009). These results indicate that epileptiform activity occurring outside of the auditory cortex can also affect dichotic listening and the binaural mechanism. When considering the evoked responses of the patients in this chapter, binaural unmasking and location of epilepsy do not seem to be related, see table 7.2 for a summary.

### **3.5.1 Evoked responses**

Every patient presented in this chapter shows an M100 response in one or both hemispheres, however the M50 and M200 are not always present in every participant, a pattern which agrees with previous literature (Kanno et al., 2006; Jacobsen et al., 1992). For descriptions of the M50 and M200 responses please see Chapters 6 and 3 respectively.

In some cases here, the M50 appears to show binaural unmasking, for example patient 3 shows a large unmasking effect for the M50, but not for the M100 in the left hemisphere. Initially, it might be questioned whether these peaks are actually the M50 and M100, however the right hemisphere shows the same pattern of peak morphology in this patient, yet this hemisphere shows unmasking is present for the M100 and not for the M50. In this instance, the validity of the unmasking occurring in

the left hemisphere might be questioned, as it could occur due to interference from the left occipital lobe lesion. As previously described, lesions can cause disruption to a wider area of cortex than simply epileptiform activity alone (Kotelenko et al., 2000). Additionally, patients 6 and 7 both show unmasking in the left hemispheric M50, with patient 7 showing even larger M50 unmasking in the right hemisphere. Patient number 6 displays unmasking in the left M50 response, but less so in the right hemispheric M50. Ultimately, despite the M50 sometimes showing unmasking, this effect could be limited in its usefulness due to the possibility of it occurring because of neuronal disruption, and also the fact that the M100 tends to show a larger effect anyway.

In the data in this chapter, where an M200 response is visible, usually an unmasking effect can be witnessed. One exception is in the right hemisphere of Patient 3, where the timeseries of the response to the diotic stimulus is clearly visible as an M200, whereas the dichotic counterpart to this cannot be clearly seen in the data. A similar case occurs in the left hemisphere of Patient 2. A clear M200 cannot be seen in Patient 4, agreeing with previous findings that this response is not robustly witnessed in all participants, unlike the M100 (Kanno et al., 2000). Patient 5 shows clear unmasking in the M100, but no unmasking is seen in the M200 or M50 in this patient. As expected overall, the M100 is the component response that consistently appears as an evoked response after presentation of an auditory stimulus in patients with disruption to their neuronal activity. In summary, the M100 is an appropriate component to use in studying the implementation of the binaural unmasking paradigm.

### **3.5.2 Hemispheric effects**

Previous literature would suggest that the right hemisphere shows a greater M100 response than the left (Kanno et al., 2000). In their study of lesional and non-lesional patients, Mazzucchi et al. (1985) used a stimulus consisting of dichotic tones. Their findings showed that the dominant hemisphere changed with regards to the location of the lesion, i. e. the hemisphere without the lesion was dominant in terms of binaural unmasking (known as the lesion effect). In contrast, in patients that had abnormal neuronal activity in either hemisphere, but without any lesions visible using a CT scan,

the unmasking was enhanced in the hemisphere with the abnormality (the paradoxical effect), also seen by Roeser et al. (1972). This paradoxical effect can be seen in patient case numbers 1 and 2, where the epileptic activity in the right hemisphere occurs alongside a larger unmasking effect in that hemisphere compared to the left. Patient 3 shows a left hemisphere lesion however there does not appear to be a larger unmasking effect in the right hemisphere as might be expected according to the lesion effect (Mazzucchi et al., 1985).

### **3.5.3 Types of epilepsy**

With regards to temporal lobe epilepsy, seizures occurring exclusively in the right temporal lobe can affect binaural hearing, however when they occur only in the left temporal lobe they do not always adversely affect binaural hearing abilities (Kotelenko et al., 2000). In contrast to these findings, (Kimura, 1961) demonstrated that damage to the left temporal lobe was detrimental to binaural hearing performance, regardless to which hemisphere the sound was presented. The results seen for the patients studied here do not always agree with this premise. Patient 1 exhibited epileptiform activity in the right temporal lobe, which was originally thought to be Landau-Kleffner syndrome, however they still showed a robust binaural unmasking effect in both hemispheres. LKS is a developmental language disorder, and language processing occurs predominantly in the left temporal lobe. In the case of this patient it would appear that epileptiform activity in the right hemisphere is involved in the detriment to language development. In cases like this, lesions can lead to dominance transferring to the other hemisphere through inter-hemispheric plasticity, as shown by Tanriverdi et al. (2009) in a PET study.

Contrary to other types of epilepsy, research has suggested that benign rolandic epilepsy in fact shows no significant differences in N1 amplitude and latency compared with controls (Boatman et al., 2008). In this study Boatman et al. (2008) recorded patients that were not on medication, and displayed impairments in non-primary auditory cortex, identifying a possible association between these impairments and the centro-temporal spiking associated with BRE. The authors suggest one explanation for this could be down to poor selective attention, which is difficult to measure using

behavioural measures due to attentional confounds associated with these (Boatman et al., 2008). In the data studied in this chapter, poor selective attention may be attributed to certain patients, for example patient 9 experienced parietal seizures, alongside a right ear hearing abnormality despite being able to hear a soft whisper in both ears. The timeseries data here suggest little binaural unmasking taking place, which could be linked to difficulties with selective attention.

#### **3.5.4 Effects of medication**

According to Ozmenek et al. (2008) there are potential long-term effects of medication, which would imply that if a patient had previously been medicated for epilepsy, there might still be effects that are present in the morphology of their auditory responses. Some of the patients in this chapter are being treated with various anti-convulsant medication (patients 3, 4, 5, 6, 8, 9, 10) and others are not (patients 1, 2, 7). As described in the introduction, epilepsy medication has been shown to have an effect on the latency of auditory evoked responses, and so amplitude has been the evoked response characteristic studied in this chapter. However, amplitude has been shown to be affected in some cases when patients are on medication. A reduction in amplitude of the N1m has been noted during medication with zorazepam (Rosburg et al., 2004), suridone and alprazolam (Semlitsch et al., 1995), and benzodiazepines (Sinton et al., 1986). In contrast, no N1 amplitude reduction was found by (Nakagome et al., 1998) when measuring the effect of triazolam, however there was an overnight effect of reduction of the MMN. Overall, the literature shows that latency is more affected by the effects of medication, and also by epilepsy itself, whereas amplitude is only affected by medication in some cases.

#### **3.5.5 Potential effects of attention**

It has been shown previously that the N1m amplitude can be affected by top-down processes such as attention (Hillyard & Kutas, 1983; Hari et al., 1989; Woldorff et al. 1993). Further, attention plays an important role in central auditory tasks (Harris, 1994), including dichotic speech perception, with laterality also being affected (Hiscock & Stewart, 1984). In cases of temporal epilepsy, attraction

effects may lead to 'hyperfunctioning' in that hemisphere (Mazzucchi & Parma, 1978), with an attentional bias being suggested as a potential reason for this asymmetry (Mazzucchi & Parma, 1978).

### **3.5.6 Evaluation of methods**

Visualisation of the timeseries of binaural unmasking has demonstrated that source model analysis can show visual inspection shows a clear binaural unmasking effect where there is a lesser effect seen at sensor level (i. e. patients 2, 4, 5, 6, 8 and 9). The reason for this is that source model analysis allows for artefact reduction, giving a higher SNR for the average, a processing step that is particularly important for data collected on participants belonging to atypical populations (Korostenskaja et al., 2013).

Using the minimum norm method has been particularly suitable for a number of patient cases presented in this chapter. MNE allows visualisation of the distribution of activity, and if that activity is disrupted in the expected area, in this case the Sylvian fissure, then the analysis program allows for examination of activity in the surrounding area easily. An advantage of MNE is that it does not rely on a priori knowledge of source location (Hämäläinen & Hari, 2002), but knowledge of the expected area can be advantageous in these situations.

# Chapter 8:

---

## Discussion

Binaural hearing is a mechanism that is very useful to us in our day-to-day lives. Some population groups may have difficulties with their binaural hearing due to developmental disorders or cortical abnormalities. In such cases, it is useful to be able to measure their binaural unmasking abilities. Binaural unmasking is a mechanism that is relatively simple to measure using a paradigm known as the binaural masking level difference.

Traditionally, the BMLD has been measured using a behavioural measure, however this type of task involves a level of cognitive input that is not always accessible to certain population groups, such as those with cortical abnormalities, or children. Hence, there is a need for a passive way to measure the binaural masking level difference to gain a sense of the efficiency of binaural unmasking without the need for cognitive input from the participant. The overall aim of this thesis was to develop a BMLD stimulus for use in MEG.

When measuring neural activity in MEG, the evoked sensor data is useful, however it does not provide information about the source of the neural activity. This can be achieved through the use of a source model, which provides a number of advantages over sensor level data. Source models are able to reduce the artefact contamination through suppression of activity from the surrounding area, something which is useful for child MEG data. Source models are also able to separate the hemispheric activity without interference from signal leakage. Chapter 3 focused on determining an appropriate source model technique to localise the response of interest, the N1m.

MEG provides a method of neural measurement allowing for source localisation of the evoked response without any interference from the skull or scalp. The auditory N1m is a widely researched response, using a variety of source localisation techniques. Chapter 3 focused on the study of three of these different analysis techniques, namely, ER beamformer, dipole fitting and minimum-norm

estimation. Each of these techniques has been used to localise the auditory response, however they have their own individual advantages and disadvantages.

A simple binaural click paradigm was used as the auditory stimulus, with the aim of eliciting a clear N1m and P2m for use in source modelling. The sources of the N1m and P2m have been shown to be elicited in the planum temporale and Heschl's gyrus respectively in previous literature (Lutkenhoner & Steinstrater, 1998). The results of this study do not show a significant difference between the N1m and P2m localisations in any of the techniques used, as might be expected. However, the dipole fit showed a less accurate localisation than the beamformer and MNE, possibly due to its focality (Pang et al., 2003). The beamformer and MNE showed good localisations overall with the smaller variability than the dipole fits, and both confer advantages over dipole fitting in terms of noise reduction and a lack of location bias. MNE confers the further advantage of allowing the user to view each vertex timeseries separately within a region of interest.

Previous work has indicated that the P2m is not always visible in every participant (Jacobson et al., 1992), a pattern which is shown here in both the beamformer and dipole fits. MNE shows the P2m in every participant, however the localisation of the P2m in MNE is not always accurate as the source appears too deep. Hence the N1m was chosen as the response to be examined using MNE in further studies within this thesis.

Measurement of the BMLD has been regularly undertaken using psychophysics, however not many studies have attempted to measure the extent of unmasking using a passive measure such as MEG. The N1m provides a suitable index for measurement of the BMLD, due to its characteristic morphological changes as a function of tone intensity, which is a key stimulus component in a BMLD paradigm. Chapter 4 considered the stimulus attributes and parameters that combine to make an effective BMLD stimulus for use in MEG. Stimulus components such as type and level of noise, validity and salience of tone, and parameters such as number of averages and ISI can all have an effect on the evoked response. Ultimately a stimulus was designed using a 500Hz wide Gaussian white noise as a background masker, centred on 500Hz and presented at 70dB SPL. The tone stimuli

consisted of a 500Hz sinusoidal tone with a duration of 50ms and a 5ms rise and fall time. The tone is presented diotically and dichotically 180 degrees out-of-phase. Each tone is presented randomly at four different tone levels of 20.3, 17.6, 15.2, and 9.1dB above the background noise level, for 100 trials at an ISI of 1s with up to 100ms random jitter.

Chapter 5 focused on testing the BMLD paradigm using an adult cohort of 17 participants. The main findings from this study show that there is a significant correlation between the individual psychophysical BMLD values and the values of the neural correlate extracted from the amplitude difference between the evoked N1m responses to the dichotic and diotic stimuli. One aim of the chapter was to explore the possibility of using either the N1m amplitude or latency as an index of binaural unmasking. Both amplitude and latency exhibit the characteristic changes associated with a change in tone perception, namely a louder tone stimulus eliciting an evoked N1m of higher amplitude (Keidel & Spreng, 1965; Adler & Adler, 1989) and shorter latency (Picton et al., 1977; Forss et al., 1993). Ultimately the amplitude measured from the source timeseries provided a significant correlation with the psychophysical BMLD value.

Chapter 6 describes the implementation of the passive BMLD paradigm with a cohort of typically developing children. The findings from the adult study showed that it is possible to find a correlation between the psychophysical BMLD and neural BMLD. However, the method used to extract the neural BMLD in the adult chapter could not be used for the child data due to the large level of baseline noise, which occluded the smaller evoked responses. Instead, the responses to the loudest dichotic and diotic triggers were used to evaluate the extent of the unmasking taking place. When comparing the values computed in this manner for the neural BMLD with the psychophysical BMLD value, there is no significant relationship, however there is a good concordance between the values on an individual level. The results here indicate that the passive MEG measure is able to indicate the extent of binaural unmasking in children using source level N1m amplitudes for the loudest dichotic and diotic tones.

Abnormalities in the cortical neurons can lead to impaired binaural hearing abilities, however using psychophysics to measure the extent of this impairment is not always possible. When participants are unable to undertake a psychophysical task at all, the use of the MEG stimulus to measure their binaural unmasking abilities provides a useful indicator of binaural hearing efficiency. The patients presented in this thesis in Chapter 7 have a range of epilepsies, including temporal lobe epilepsy. Abnormal activity in the temporal lobe can lead to impaired binaural unmasking abilities (Kotelenko et al., 2000). One aim of this chapter was to investigate the effect of different types of epilepsy on the effectiveness of binaural unmasking in patients. The results of Chapter 7 show that the patients that did not show an unmasking effect at sensor level, did show unmasking at source level, highlighting the benefits of using a source space approach to identify the efficiency of unmasking.

Previous work has shown that the binaural unmasking effect can be measured using sensor MEG data in adults (Sasaki et al., 2005), and other work has provided evidence that source modelling can be used to visualise auditory timeseries data (Lee, et al. 2014), however this thesis provides the original contribution of using a source modelling approach to visualise the extent of binaural unmasking in participants that require a passive stimulus, due to their age or developmental difficulties. The source modelling approach provides a measure that can uncover a binaural unmasking effect which is not visible at the sensors (see Chapter 7), nor is obtainable using a psychophysical task. Limitations of this study may include the fact that, as thresholds are not measured, a traditional BMLD value cannot be achieved by definition. However, in paediatric or patient participant groups, the practicalities of obtaining threshold data may become a challenge in itself. By using suprathreshold stimuli, the evoked N1m can be visualised more easily, and the difference between the dichotic and diotic stimuli can be computed to uncover any unmasking effect present. As psychophysical BMLDs are not obtainable in these populations, any measure of binaural unmasking provides valuable information about their abilities to hear a signal over a background masking noise.

A passive measure of binaural unmasking in MEG has a great deal of potential for use with a large variety of participant groups. The concept of the BMLD in this thesis relies on the interaural phase

difference of the masked tone, which essentially relies on detection of timing differences between the ears. Investigating the binaural unmasking abilities of different participant groups that are known to have deficits in timing could be a useful future direction for this work. Timing deficits related to speed of processing are thought to be a factor in the developmental disorder of dyslexia (Goswami, 2011). Investigating dyslexic children's binaural unmasking abilities without the need for them to undertake a psychophysical task could provide further information related to speed of processing and timing deficits.

## List of References

- Adjamian, P. et al., 2004. Co-registration of magnetoencephalography with magnetic resonance imaging using bite-bar-based fiducials and surface-matching. *Clinical Neurophysiology*, 115, pp.691–698.
- Adler, G. & Adler, J., 1989. Influence of stimulus intensity on AEP components in the 80- to 200-millisecond latency range. *Audiology : official organ of the International Society of Audiology*, 28, pp.316–324.
- Akaho, R., 1996. The effects of antiepileptic drugs on cognition in normal volunteers. *Psychiatry Clin Neurosci*, 50(2), pp.61-9.
- Alain, C. et al., 2009. Noise-induced increase in human auditory evoked neuromagnetic fields. *The European journal of neuroscience*, 30(1), pp.132–42.
- Alain, C. & Tremblay, K., 2007. The Role of Event-Related Brain Potentials in Assessing Central Auditory Processing. *Journal of the American Academy of Audiology*, 18, pp.573–589.
- Albrecht, R., Suchodoletz, W. & Uwer, R., 2000. The development of auditory evoked dipole source activity from childhood to adulthood. *Clin Neurophysiol*, 111, pp.2268–2276.
- Allen, P. & Wightman, F., 1994. Psychometric functions for children's detection of tones in noise. *Journal of speech and hearing research*, 37, pp.205–215.
- Allen, P. & Wightman, F., 1992. Spectral pattern discrimination by children. *Journal of speech and hearing research*, 35, pp.222–233.
- Altman, J.A. et al., 1987. Lateralization of a moving auditory image in patients with focal damage of the brain hemispheres. *Neuropsychologia*, 25(2), pp. 435-42.
- Anderson, B., Southern, B.D. & Powers, R.E., 1999. Anatomic asymmetries of the posterior superior temporal lobes: a postmortem study. *Neuropsychiatry, neuropsychology, and behavioral neurology*, 12, pp.247–254.
- ANSI, 1997. S3.5, Methods for calculation of the speech intelligibility index (American national standards institute, New York).
- American Speech-Language-Hearing Association, 2005. (Central) auditory processing disorders. ASHA Working Group Technical Report.
- Baule, G.M. & McFee, R. 1963. Detection of the magnetic field of the heart. *Am. Heart J.*, 66(7), pp.95-6.
- Barnes, G.R. et al., 2006. A verifiable solution to the MEG inverse problem. *NeuroImage*, 31, pp.623–626.
- Beutelmann, R., Brand, T. & Kollmeier, B., 2010. Revision, extension, and evaluation of a binaural speech intelligibility model. *The Journal of the Acoustical Society of America*, 127(4), pp.2479–97.
- Bi, J. & Ennis, D.M., 1998. Sensory thresholds: concepts and methods. *Journal of Sensory Studies*, 13(2), pp.133-148.

- Bilecen, D. et al., 2002. Amplitude of the human auditory cortex: an fMRI study. *Neuroimage*, 17, pp.710–718.
- Billings, C. J. et al., 2010. Cortical encoding of signals in noise: effects of stimulus type and recording paradigm. *Ear Hear.* 32, pp. 53-60.
- Bishop, D.V.M. et al., 2007. Maturation of the long-latency auditory ERP : step function changes at start and end of adolescence. *Dev Sci.*, 5, pp.565–575.
- Blauert, J., 1985. Spatial Hearing: The Psychophysics of Human Sound Localization by Jens Blauert. *The Journal of the Acoustical Society of America*, 77, p.334.
- Blum, D. et al., 2006. Cognitive effects of lamotrigine compared with topiramate in patients with epilepsy. *Neurology*, 67(3), p.400-406.
- Boatman, D.F. et al., 2008. Cortical auditory dysfunction in benign rolandic epilepsy. *Epilepsia*, 49(6), pp.1018–1026.
- Bourbon, W.T. & Jeffres, L.A. 1965. Effects of bandwidth of masking noise on detection of homophasic and anti-phasic tonal signal. *Journal of the Acoustical Society of America*, 37, p.1180
- Braakman, H.M.H. et al., 2012. Original article Cognitive and behavioural findings in children with frontal lobe epilepsy. *European Journal of Paediatric Neurology*, 16(6), pp.707–715.
- Brandewie, E. & Zahorik, P., 2010. Prior listening in rooms improves speech intelligibility. *The Journal of the Acoustical Society of America*, 128(1), pp.291–9.
- Bregman, A.S., 1990. *Auditory Scene Analysis: The Perceptual Organization of Sound*, Cambridge: MIT Press
- Bronkhorst, A.W. & Plomp, R., 1988. The effect of head-induced interaural time and level differences on speech intelligibility in noise. *The Journal of the Acoustical Society of America*, 83, pp.1508–1516.
- Burgess, A.P., 2012. Towards a Unified Understanding of Event-Related Changes in the EEG: The Firefly Model of Synchronization through Cross-Frequency Phase Modulation. *PLoS ONE*, 7(9), e45630. doi: 10, 1371/journal.pone.0045630
- Burke, K.A., Letsos, A. & Butler, R.A., 1994. Asymmetric performances in binaural localization of sound in space. *Neuropsychologia*, 32, pp.1409–1417.
- Buss, E., Hall, J.W. & Grose, J.H., 2006. Development and the role of internal noise in detection and discrimination thresholds with narrow band stimuli. *The Journal of the Acoustical Society of America*, 120(5), p.2777.
- Buss, E., Hall, J.W. & Grose, J.H., 2009. Psychometric functions for pure tone intensity discrimination: slope differences in school-aged children and adults. *The Journal of the Acoustical Society of America*, 125(2), pp.1050–8.
- Buss, E., Hall, J.W. & Grose, J.H., 2003. The masking level difference for signals placed in masker envelope minima and maxima. *The Journal of the Acoustical Society of America*, 114, pp.1557–1564.

- Caird, D., Goettl, K.H. & Klinke, R., 1980. Interaural attenuation in the cat, measured with single fibre data. *Hearing Research*, 3, pp.257–263.
- Campaigne, R. & Minckler, J. 1976. A note on the gross configurations of the human auditory cortex. *Brain Lang.*, 3(2), pp.318-23
- Cansino, S., 2006. 'Mapping the Functional Organization of the Human Auditory Cortex', in F. J. Chen (Ed.), *Progress in Brain Mapping Research*, Ed. F. J. Chen, New York: Nova Science, pp. 81-121
- Cardy, J.E.O. et al., 2004. Prominence of M50 auditory evoked response over M100 in childhood and autism. *Neuroreport*, 15(12), pp.0–3.
- Carlyon, R.P. et al., 2001. Effects of attention and unilateral neglect on auditory stream segregation. *Journal of experimental psychology. Human perception and performance*, 27, pp.115–127.
- Ceponiene, R., Cheour, M. & Näätänen, R., 1998. Interstimulus interval and auditory event-related potentials in children: Evidence for multiple generators. *Electroencephalography and Clinical Neurophysiology - Evoked Potentials*, 108, pp.345–354.
- Chait, M., Poeppel, D. & Simon, J.Z., 2006. Neural response correlates of detection of monaurally and binaurally created pitches in humans. *Cerebral cortex (New York, N.Y. : 1991)*, 16(6), pp.835–48.
- Chait, M., Simon, J.Z. & Poeppel, D., 2004. Auditory M50 and M100 responses to broadband noise: functional implications. *Neuroreport*, 15, pp.2455–2458.
- Chatterjee, M. & Robert, M.E., 2001. Noise enhances modulation sensitivity in cochlear implant listeners: Stochastic resonance in a prosthetic sensory system? *Journal of the Association for Research in Otolaryngology*, 2, pp.159–171.
- Cherry, E.C., 1953. Some experiments on the recognition of speech, with one and with 2 ears. *Journal of the Acoustical Society of America*, 25, pp.975–979.
- de Cheveigné, A. 2005. Pitch perception models. In: C. Plack, A.J. Oxenham, R.R. Fay & A.N. Popper (Eds.) *Pitch - neural coding and perception*. New York: Springer, pp. 169-233
- Cheyne, D. et al., 2007. Event-related beamforming : A robust method for presurgical functional mapping using MEG. *Clinical Neurophysiology*, 118, pp.1691–1704.
- Cicmil, N. et al., 2014. Localization of MEG human brain responses to retinotopic visual stimuli with contrasting source reconstruction approaches. *Frontiers in Neuroscience*, 8, pp.1-16.
- Cohen, D., 1972. Magnetoencephalography: detection of the brain's electrical activity with a superconducting magnetometer. *Science (New York, N.Y.)*, 175, pp.664–666.
- Cohen, D., Edelsack, E.A. & Zimmerman, J.E., 1970. Magnetocardiograms taken inside a shielded room with a superconducting point-contact magnetometer. *Applied Physics Letters*, 16, pp.278–280.
- Cohen, M.F. & Schubert, E.D., 1991. Comodulation masking release and the masking-level difference. *The Journal of the Acoustical Society of America*, 89(6), pp.3007–8.
- Coles, M.G.H. & Rugg, M.D., 1995. 1 Event-related brain potentials : an introduction. *Electrophysiology of Mind*, 61, pp.1–26.

- Cramer, E.M. & Huggins, W.H., 1958. Creation of Pitch through Binaural Interaction. *The Journal of the Acoustical Society of America*, 30, p.413.
- Crowley, K.E. & Colrain, I.M., 2004. A review of the process of the evidence for P2 being an independent component process: age, sleep and modality. *Clinical Neurophysiology*, 115, pp.732–744.
- Culling, J.F., Hodder, K.I. & Toh, C.Y., 2003. Effects of reverberation on perceptual segregation of competing voices. *The Journal of the Acoustical Society of America*, 114, pp.2871–2876.
- Dale, A.M. et al., 2000. Neurotechnique Mapping : Combining fMRI and MEG for High-Resolution Imaging of Cortical Activity. *Neuron*, 26, pp.55–67.
- Damasio, H. & Damasio, A., 1979. “Paradoxical” ear extinction in dichotic listening: possible anatomic significance. *Neurology*, 29, pp.644–653.
- David, O., Harrison, L. & Friston, K.J., 2005. Modelling event-related responses in the brain. *NeuroImage*, 25, pp.756–770.
- Davis, H. et al. 1966. The slow response of the human cortex to auditory stimuli: recovery process. *Clin Neurophysiol.*, 21(2), pp.105-113
- Delgutte, B., 1990. Physiological mechanisms of psychophysical masking: observations from auditory-nerve fibers. *The Journal of the Acoustical Society of America*, 87(2), pp.791–809.
- Van Deun, L., van Wieringen, A. & Wouters, J., 2010. Spatial speech perception benefits in young children with normal hearing and cochlear implants. *Ear and hearing*, 31(5), pp.702–13.
- Durlach, N.I., 1963. Equalization and Cancellation Theory of Binaural Masking-Level Differences. *The Journal of the Acoustical Society of America*, 35, p.1206.
- Durlach, N.I. et al., 2003. Note on informational masking (L). *The Journal of the Acoustical Society of America*, 113(6), p.2984.
- Durlach, N.I. & Colburn, H.S. 1978. Binaural phenomena. In: E.C. Carterette & M.P. Friedman (Eds.). *Handbook of perception*. New York: Academic Press. pp.365-466
- Eddins, D.A., 1996. Temporal cues in monaural and binaural detection and discrimination. *J. Acoust. Soc. Am.*, 99, p.2471
- Edgar, J. et al., 2003. Interpreting abnormality: an EEG and MEG study of P50 and the auditory paired-stimulus paradigm. *Biological Psychology*, 65(1), pp.1–20.
- Efron, R. et al., 1983. Central auditory processing. III. The “cocktail party” effect and anterior temporal lobectomy. *Brain and language*, 19, pp.254–263.
- Egan, J.P., 1965. Masking-level differences as a function of interaural disparities in intensity of signal and of noise. *The Journal of the Acoustical Society of America*, 38, pp.1043–1049.
- Ehrenstein, W.H. & Ehrenstein, A., 1999. Psychophysical methods. In: U. Windhorst & H. Johansson (Eds.) *Modern Techniques in Neuroscience Research*. Berlin: Springer-Verlag. pp.1211-1241.
- Elberling, C. et al., 1982. Auditory magnetic fields from the human cerebral cortex: location and strength of an equivalent current dipole. *Acta neurologica Scandinavica*, 65, pp.553–569.

- Engel, J., 2001. A proposed diagnostic scheme for people with epileptic seizures and with epilepsy: report of the ILAE Task Force on Classification and Terminology. *Epilepsia*, 42(6), pp.796-803
- Epp, B., Yasin, I. & Verhey, J.L., 2013. Objective measures of binaural masking level differences and comodulation masking release based on late auditory evoked potentials. *Hearing Research*, 306, pp.21–28.
- Eulitz, C. et al., 1995. Magnetic and electric brain activity evoked by the processing of tone and vowel stimuli. *The Journal of Neuroscience*, 15(4), pp.2748–2755.
- Fandino, M. et al., 2011. Landau-Kleffner syndrome: a rare auditory processing disorder series of cases and review of the literature. *Int J Pediatr Otorhinolaryngol*, 75, pp.33–38.
- Fechner, G.T., 1860. Elemente der Psychophysik. *The British Journal of Statistical Psychology*, 13(1), pp.1-10.
- Ferguson, M.O. et al., 1998. Chronic conductive hearing loss in adults: effects on the auditory brainstem response and masking-level difference. *Archives of otolaryngology--head & neck surgery*, 124, pp.678–685.
- Ferri, R. et al., 2003. The mismatch negativity and the P3a components of the auditory event-related potentials in autistic low-functioning subjects. *Clin Neurophysiol.* , 114, pp.1671–1680.
- Festen, J.M. & Plomp, R., 1990. Effects of fluctuating noise and interfering speech on the speech-reception threshold for impaired and normal hearing. *The Journal of the Acoustical Society of America*, 88(4), pp.1725–36.
- Fischl, B., 2012. FreeSurfer. *NeuroImage*, 62, pp.774–781.
- Fletcher, H., 1940. Auditory patterns. *Reviews of Modern Physics*, 12, pp.47–65.
- Ford, J.M. et al., 2001. N1 and P300 abnormalities in patients with schizophrenia, epilepsy, and epilepsy with schizophrenialike features. *Biological Psychiatry*, 49, pp.848–860.
- Forss, N. et al., 1993. Temporal integration and oscillatory responses of the human auditory cortex revealed by evoked magnetic fields to click trains. *Hearing research*, 68, pp.89–96.
- Fowler, C.G. & Mikami, C.M., 1992a. The late auditory evoked potential masking-level difference as a function of noise level. *Journal of speech and hearing research*, 35, pp.216–221.
- Fowler, C.G. & Mikami, C.M., 1992b. Effects of noise bandwidth on the late-potential masking level difference. *Electroencephalography and Clinical Neurophysiology*, 84, pp.157-163.
- Fowler, C.G. & Mikami, C.M., 1995. Binaural phase effects in the auditory brainstem response. *Journal of the American Academy of Audiology*, 6, pp.399-406.
- Fowler, C.G. & Mikami, C.M., 1996. Phase effects on the middle and late auditory evoked potentials. *Journal of the American Academy of Audiology*, 7, pp.23–30.
- Fuchigami, T. et al., 1993. Auditory event-related potentials and reaction time in children: evaluation of cognitive development. *Dev Med Child Neurol*, 35, pp.230–237.
- Fujiki, N. et al., 2002. Human cortical representation of virtual auditory space: Differences between sound azimuth and elevation. *European Journal of Neuroscience*, 16, pp.2207–2213.

- Gabriel, D. et al., 2004. Effect of stimulus frequency and stimulation site on the N1m response of the human auditory cortex. *Hearing research*, 197, pp.55–64.
- Gage, N.M. & Roberts, T.P., 2000. Temporal integration: reflections in the M100 of the auditory evoked field. *Neuroreport*, 11(12), pp.2723–6.
- Gage, N.M., Siegel, B., Callen, M. & Roberts, T. P. L., 2003b. Cortical sound processing in children with autism disorder : an MEG investigation. *Auditory and vestibular systems*, 14(16), pp. 2047-51
- Galambos, R. & Makeig, S., 1992a. Physiological studies of central masking in man. I: The effects of noise on the 40Hz steady-state response. *The Journal of the Acoustical Society of America*, 92(5), pp.2683-90.
- Galambos, R. & Makeig, S., 1992b. Physiological studies of central masking in man. II: Tonepip SSRs and the masking level difference. *The Journal of the Acoustical Society of America*, 92(5), pp.2691–2697.
- Gazzaniga, M.S. 1995. *The cognitive neurosciences*. Cambridge:MIT Press
- Giard, M.H. et al., 1994. Dissociation of temporal and frontal components in the human auditory N1 wave: a scalp current density and dipole model analysis. *Electroencephalography and clinical neurophysiology*, 92, pp.238–252.
- Gibson, D.J., Young, E.D. & Costalupes, J.A., 1985. Similarity of dynamic range adjustment in auditory nerve and cochlear nuclei. *Journal of neurophysiology*, 53, pp.940–958.
- Gilley, P.M. et al., 2005. Developmental changes in refractoriness of the cortical auditory evoked potential. *Clin Neurophysiol*, 116, pp.648–657.
- Gilmore, C.S., Clementz, B.A. & Berg, P., 2009. Hemispheric differences in auditory oddball responses during monaural versus binaural stimulation. *International Journal of Psychophysiology*, 73, pp.326–333.
- Godey, B. et al., 2001. Neuromagnetic source localization of auditory evoked fields and intracerebral evoked potentials: A comparison of data in the same patients. *Clinical Neurophysiology*, 112, pp.1850–1859.
- Gomes, H. et al., 2001. Spatiotemporal maturation of the central and lateral N1 components to tones. *Developmental Brain Research*, 129, pp.147–155.
- Goodin, D.S. et al., 1978. Age-related variations in evoked potentials to auditory stimuli in normal human subjects. *Electroencephalography and Clinical Neurophysiology*, 44, pp.447–458.
- Goswami, U., 2011. A temporal sampling framework for developmental dyslexia. *Trends in Cognitive Sciences*, 15(1), pp.3-10.
- Grantham, D., 1995. Spatial hearing and related phenomena. In *Hearing*. pp. 297–345.
- Grantham, D.W. & Wightman, F.L., 1978. Detectability of varying interaural temporal differences. *The Journal of the Acoustical Society of America*, 63(2), pp.511–23.
- Gravel, J.S., Wallace, I.F. & Ruben, R.J., 1996. Auditory consequences of early mild hearing loss associated with otitis media. *Acta oto-laryngologica*, 116, pp.219–221.

- Grech, R. et al., 2008. Review on solving the inverse problem in EEG source analysis. *Journal of neuroengineering and rehabilitation*, 5, p.25.
- Green, D.M. & Swets, J.A., 1966. *Signal detection theory and psychophysics*, New York:John Wiley & Sons
- Griffiths, T.D. et al., 1997. Spatial and temporal auditory processing deficits following right hemisphere infarction. A psychophysical study. *Brain*, 120, pp.785–794.
- Grose, J.H., Iii, J.W.H. & Dev, M.B., 1997. MLD in Children : Effects of Signal and Masker Bandwidths. *J Speech Lang Hear Res.*, 40, pp.955–959.
- Gutschalk, A. et al., 2004. Temporal dynamics of pitch in human auditory cortex. *NeuroImage*, 22(2), pp.755–66.
- Hall, D.A. & Plack, C.J., 2007. The human “pitch center” responds differently to iterated noise and Huggins pitch. *Neuroreport*, 18, pp.323–327.
- Hall, J.W. & Grose, J.H., 1990. The masking-level difference in children. *Journal of the American Academy of Audiology*, 1, pp.81–88.
- Hall, J.W. et al., 2004. Developmental effects in the masking-level difference. *Journal of speech, language, and hearing research*, 47, pp.13–20.
- Hall, J.W., Buss, E. & Grose, J.H., 2007. The binaural temporal window in adults and children. *The Journal of the Acoustical Society of America*, 121, pp.401–410.
- Hall, J.W., Haggard, M.P. & Fernandes, M. A., 1984. Detection in noise by spectro-temporal pattern analysis. *The Journal of the Acoustical Society of America*, 76(1), pp.50–6.
- Hall, J.W., 2000. Background Science Development of the Ear and Hearing. *Journal of Perinatology*, 20(8), pp.11–19.
- Hall, J.W. et al., 1998. The masking-level difference in low-noise noise. *J. Acoust. Soc. Am.*, 103(5), pp.2573–2577.
- Hämäläinen, M.S. et al., 1993. Magnetoencephalography—theory, instrumentation, and applications to noninvasive studies of the working human brain. *Reviews of Modern Physics*, 65, pp.413–497.
- Hämäläinen, M.S. & Hari, R., 2002. Magnetoencephalographic characterization of dynamic brain activation: basic principles, and methods of data collections and source analysis. In: A.W.Toga & J.C. Mazziotta (Eds.) *Brain mapping, the methods*, 2<sup>nd</sup> ed. Amsterdam: Academic Press, pp.227-253.
- Hämäläinen, M.S. & Ilmoniemi, R.J., 1994. Interpreting magnetic fields of the brain: minimum norm estimates. *Medical & biological engineering & computing*, 32, pp.35–42.
- Hannley, M., Jerger, J.F. & Rivera, V.M., 1983. Relationships among auditory brain stem responses, masking level differences and the acoustic reflex in multiple sclerosis. *Audiology : official organ of the International Society of Audiology*, 22, pp.20–33.
- Hari, R. 1983. Auditory evoked magnetic fields of the human brain. *Revue de laryngology*, 104, pp.143-151

- Hari, R. et al., 1980. Auditory evoked transient and sustained magnetic fields of the human brain localization of neural generators. *Experimental Brain Research*, 40, pp.237–240.
- Hari, R. et al., 1982. Interstimulus interval dependence of the auditory vertex response and its magnetic counterpart: implications for their neural generation. *Electroencephalography and clinical neurophysiology*, 54, pp.561–569.
- Hari, R. et al., 1989. Neuromagnetic responses of human auditory cortex to interruptions in a steady rhythm. *Neuroscience letters*, 99, pp.164–168.
- Hari, R. & Mäkelä, J.P., 1988. Modification of neuromagnetic responses of the human auditory cortex by masking sounds. *Exp Brain Res*, 71(1), pp.87-92
- Harris, J., 1994. Brain lesions, central masking, and dichotic speech perception. *Brain and language*, 46, pp.96–108.
- Hartmann, W. M., 1998. *Signals, Sound and Sensation*. New York:Springer-Verlag
- Hartley, D.E. et al., 2000. Age-related improvements in auditory backward and simultaneous masking in 6- to 10-year-old children. *Journal of speech, language, and hearing research*, 43, pp.1402–1415.
- Hauk, O., 2004. Keep it simple : a case for using classical minimum norm estimation in the analysis of EEG and MEG data. *Most*, 21, pp.1612 – 1621.
- Hawkins, H. & Stevens, S. S., 1950. The masking of pure tones and of speech by white noise. *Journal of the Acoustical Society of America*, 25(2), pp.6-13.
- Hawley, M.L., Litovsky, R.Y. & Culling, J.F., 2004. The benefit of binaural hearing in a cocktail party: Effect of location and type of interferer. *The Journal of the Acoustical Society of America*, 115(2), p.833.
- Heil, P., Rajan, R. & Irvine, D.R.F., 1994. Topographic representation of tone intensity along the isofrequency axis of cat primary auditory cortex. *Hearing Research*, 76, pp.188–202.
- Helmholtz, H., 1853. Ueber einige Gesetze der Vertheilung elektrischer Ströme in körperlichen Leitern mit Anwendung auf die thierisch-elektrischen Versuche. *Ann. Phys. Chem.*, 89, pp.211–233, 353–377.
- Henning, G.B., 1973. Effect of interaural phase on frequency and amplitude discrimination. *The Journal of the Acoustical Society of America*, 54(5), pp.1160–78.
- Henning, G. B., Zwicker, E., 1984. Effects of the bandwidth and level of noise and of the duration of the signal on binaural masking-level differences. *Hearing Research*, 14(2), pp.175-178.
- Herdman, A.T. et al., 2003. Determination of activation areas in the human auditory cortex by means of synthetic aperture magnetometry. *Source*, 20, pp.995–1005.
- Hertrich, I. et al., 2004. Time course and hemispheric lateralization effects of complex pitch processing: Evoked magnetic fields in response to rippled noise stimuli. *Neuropsychologia*, 42, pp.1814–1826.
- Hillyard, S.A. et al., 1971. Evoked Potential Correlates of Auditory Signal Detection. *Science*, 172, pp.1357–1360.

- Hillyard, S.A. & Kutas, M., 1983. Electrophysiology of cognitive processing. *Annual review of psychology*, 34, pp.33–61.
- Hine, J. & Debener, S., 2007. Late auditory evoked potentials asymmetry revisited. *Clinical neurophysiology : official journal of the International Federation of Clinical Neurophysiology*, 118, pp.1274–1285.
- Hirsh, I.J., 1948. The Influence of Interaural Phase on Interaural Summation and Inhibition. *The Journal of the Acoustical Society of America*, 20, p.592.
- Hirsh, I.J., 1950. The Relation between Localization and Intelligibility. *The Journal of the Acoustical Society of America*, 22(2), p.196.
- Hiscock, M. & Stewart, C., 1984. The effect of asymmetrically focused attention upon subsequent ear differences in dichotic listening. *Neuropsychologia*, 22, pp.337–351.
- Hofman, P.M., Riswick, J.G.A. Van & Opstal, A.J. Van, 1998. Relearning sound localization with new ears. *Nature Neuroscience*, 1(5), pp.417–421.
- Holmes, G.L., 1993. Benign focal epilepsies of childhood. *Epilepsia*, 34 (Suppl3), pp.S49-S61.
- Houtsma, A.J.M., 1972. The Central Origin of the Pitch of Complex Tones: Evidence from Musical Interval Recognition. *The Journal of the Acoustical Society of America*, 51, p.520.
- Howard, M.A. et al., 2000. Auditory cortex on the human posterior superior temporal gyrus. *The Journal of comparative neurology*, 416, pp.79–92.
- Howard, M.F. & Poeppel, D., 2009. Hemispheric asymmetry in mid and long latency neuromagnetic responses to single clicks. *Hearing Research*, 257, pp.41–52.
- Huang, M.X. et al., 2006. Vector-based spatial-temporal minimum L1-norm solution for MEG. *NeuroImage*, 31(3), pp.1025–37.
- Huang, M.X., Mosher, J.C. & Leahy, R.M., 1999. A sensor-weighted overlapping-sphere head model and exhaustive head model comparison for MEG. *Physics in medicine and biology*, 44, pp.423–440.
- Huffman, R.F. & Henson, O.W., 1990. The descending auditory pathway and acousticomotor systems: Connections with the inferior colliculus. *Brain Research Reviews*, 15, pp.295–323.
- Huotilainen, M. et al., 1998. Combined mapping of human auditory EEG and MEG responses. *Electroencephalography and clinical neurophysiology*, 108, pp.370–379.
- Hutchings, M.E., Meyer, S.E. & Moore, D.R., 1992. Binaural masking level differences in infants with and without otitis media with effusion. *Hearing research*, 63, pp.71–78.
- Hyde, M. 1997. The N1 response and its applications. *Audiol. Neurootol.*, 2(5), pp.281-307
- Imada, T. et al., 1997. The silent period between sounds has a stronger effect than the interstimulus interval on auditory evoked magnetic fields. *Electroencephalography and Clinical Neurophysiology*, 102, pp.37–45.
- Jacobson, G.P. et al., 1992. Occurrence of auditory evoked field (AEF) N1M and P2M components in a sample of normal subjects. *Ear and Hearing*, 13(6), pp.387–395.

- Jansen, B.H. et al., 2003. Phase synchronization of the ongoing EEG and auditory EP generation. *Clinical Neurophysiology*, 114, pp.79–85.
- Jeffress, L.A., 1971. Detection and Lateralization of Binaural Signals. *International Journal of Audiology*, 10, pp.77–84.
- Jeffress, L.A., Blodgett, H. C. & Deatherage, B. H., 1952. The Masking of Tones by White Noise as a Function of the Interaural Phases of Both Components. I. 500 Cycles. *The Journal of the Acoustical Society of America*, 24(5), p.523.
- Jenkins, J. et al., 2011. The elicitation of audiovisual steady-state responses: Multi-sensory signal congruity and phase effects. *Brain Topography*, 24, pp.134–148.
- Jesteadt, W. & Sims, S.L. , 1975. Decision processes in frequency discrimination. *J. Acoust. Soc. Am.*, 57, pp.1161-1168
- Jiang, D., McAlpine, D. & Palmer, A.R., 1997. Detectability index measures of binaural masking level difference across populations of inferior colliculus neurons. *The Journal of neuroscience : the official journal of the Society for Neuroscience*, 17, pp.9331–9339.
- Kanno, A. et al., 2000. Middle and long latency peak sources in auditory evoked magnetic fields for tone bursts in humans. *Neuroscience Letters*, 293, pp.187–190.
- Kawase, T. et al., 2000. Effects of contralateral noise on measurement of the psychophysical tuning curve. *Hearing Research*, 142, pp.63–70.
- Keefe, D.H. et al., 1993. Ear-canal impedance and reflection coefficient in human infants and adults. *The Journal of the Acoustical Society of America*, 94, pp.2617–2638.
- Keefe, D.H. & Levi, E., 1996. Maturation of the middle and external ears: acoustic power-based responses and reflectance tympanometry. *Ear and hearing*, 17, pp.361–373.
- Keidel, W.D. & Spreng, M., 1965. Neurophysiological evidence for the Stevens power function in man. *The Journal of the Acoustical Society of America*, 38, pp.191–195.
- Kevanishvili, Z. & Lagidze, Z., 1987. Masking level difference: an electrophysiological approach. *Scandinavian audiology*, 16, pp.3–11.
- Kidd, G. et al., 1998. Release from masking due to spatial separation of sources in the identification of nonspeech auditory patterns. *The Journal of the Acoustical Society of America*, 104, pp.422–431.
- Kiebel, S.J. et al., 2007. Variational Bayesian inversion of the equivalent current dipole model in EEG/MEG. *NeuroImage*, 39(2), pp.728-41
- Kingdom, F.A.A. & Prins, N., 2010. *Psychophysics: A practical introduction*. London:Academic Press.
- Kimura, D., 1961. Some effects of temporal-lobe damage on auditory perception. *Canadian journal of psychology*, 15, pp.156–165.
- Klein, M.A. & Hartmann, W.M., 1981. Binaural edge pitch. *The Journal of the Acoustical Society of America*, 70, pp.51–61.

- Korostenskaja, M. et al., 2010. Neuromagnetic evidence of impaired cortical auditory processing in pediatric intractable epilepsy. *Epilepsy Research*, 92, pp.63–73.
- Korostenskaja, M. et al., 2013. Passive testing of cognitive function in epileptic children unwilling or unable to cooperate: comprehensive summary of non-invasive neurophysiological approaches. *Pediatrics and Therapeutics*, 4(1), p.2161-0665.
- Korotkov, A.G. & Kuryshov, V.N., 1998. The effect of stereotactic treatment on the memory of patients with drug-resistant temporal epilepsy. *Russian-American Symposium on Clinical and Social Aspects of Epilepsy*, St. Petersburg, p98.
- Kosaki, H. et al., 1997. Tonotopic organization of auditory cortical fields delineated by parvalbumin immunoreactivity in macaque monkeys. *Journal of Comparative Neurology*, 386, pp.304-316.
- Kotecha, R. et al., 2009. Modeling the Developmental Patterns of Auditory Evoked Magnetic Fields in Children. *PLoS ONE*, 4(3) e4811.
- Kotelenko, L.M., Fed'ko, L.I. & Shustin, V. A., 2000. The comparative characteristics of spatial hearing in patients with different forms of cortical epilepsy. *Fiziologija cheloveka*, 26(2), pp.30–6.
- Kotelenko, L.M., Fed'ko, L.I. & Shustin, V. a., 2007. The subjective auditory space of epileptic patients with lesions in both the temporal cortical area and the hippocampus. *Human Physiology*, 33(5), pp.539–545.
- Kotelenko, L.M. et al., 1996. The role of the cortical and mediobasal brain structures in perception of moving sound images. *Sens. Sist.*, 10(2), p.38.
- Kubota, Y. et al., 2007. Delayed N100m latency in focal epilepsy associated with spike dipoles at the primary auditory cortex. *Journal of clinical neurophysiology : official publication of the American Electroencephalographic Society*, 24, pp.263–270.
- Kuriki, S. & Murase, M., 1989. Neuromagnetic study of the auditory responses in right and left hemispheres of the human brain evoked by pure tones and speech sounds. *Experimental brain research. Experimentelle Hirnforschung. Experimentation cerebrale*, 77, pp.127–134.
- Landau, W.M. & Kleffner, F.R., 1957. Syndrome of acquired aphasia with convulsive disorder in children. *Neurology*, 51, p.1241-49
- Langford, T.L., 1984. Responses elicited from medial superior olivary neurons by stimuli associated with binaural masking and unmasking. *Hearing Research*, 15, pp.39–50.
- Lavikainen, J. et al., 1994. Auditory stimuli activate parietal brain regions: a whole-head MEG study. *Neuroreport*, 6, pp.182–184.
- Lee, A.K.C. et al., 2014. Using neuroimaging to understand the cortical mechanisms of auditory selective attention. *Hearing Research*, 307, pp.111–120.
- Licklider, J. C. R., 1948. The influence of interaural phase relations upon the masking of speech by white noise. *J. Acoust. Soc. Am.*, 20, p.150.
- Litovsky, R.Y. & McAlpine, D., 2010. 'Physiological correlates of the precedence effect and binaural masking level differences', in D. R. Moore, A. Rees & J. Palmer, *The Oxford Handbook of Auditory Science: The Auditory Brain*, Oxford: Oxford University Press.

- Von Leupoldt, A. et al., 2010. Cortical sources of the respiratory-related evoked potential. *Respiratory Physiology and Neurobiology*, 170, pp.198–201.
- Levanen, S. & Sams, M., 1997. Disrupting human auditory change detection: Chopin is superior to white noise. *Psychophysiology*, 34, pp.258–265.
- Levitt, H., 1971. Transformed up-down methods in psychoacoustics. *The Journal of the Acoustical Society of America*, 49(2), p.Suppl 2:467+.
- Li, L. et al., 2007. Primary investigation of central auditory function in patients with temporal lobe epilepsy. *Chinese journal of otorhinolaryngology head and neck surgery*, 42, pp.664–668.
- Liasis, A. et al., 2006. Evidence for a neurophysiologic auditory deficit in children with benign epilepsy with centro-temporal spikes. *J. Neural. Transm.*, 113, pp.939-949.
- Licklider, J.C.R., 1948. The Influence of Interaural Phase Relations upon the Masking of Speech by White Noise. *The Journal of the Acoustical Society of America*, 20, p.150.
- Liégeois-Chauvel, C. et al., 1994. Evoked potentials recorded from the auditory cortex in man: evaluation and topography of the middle latency components. *Electroencephalography and clinical neurophysiology*, 92, pp.204–214.
- Liegeois-Chauvel, C., Musolino, A. & Chauvel, P., 1991. Localization of the primary auditory area in man. *Brain*, 114 ( Pt 1A), pp.139–151.
- Litovsky, R.Y. et al., 1999. The precedence effect. *The Journal of the Acoustical Society of America*, 106(4 Pt 1), pp.1633–54.
- Loveless, N. et al., 1989. Evoked responses of human auditory cortex may be enhanced by preceding stimuli. *Electroencephalography and Clinical Neurophysiology*, 74, pp.217–227.
- Luck, S.J., 2005. *An introduction to the event-related potential technique*. Cambridge: The MIT Press.
- Lutfi, R.A., 1990. How much masking is informational masking? *The Journal of the Acoustical Society of America*, 88, pp.2607–2610.
- Lütkenhöner, B. et al., 2003. Localization of primary auditory cortex in humans by magnetoencephalography. *NeuroImage*, 18, pp.58–66.
- Lütkenhöner, B. & Steinsträter, O., 1998. High-precision neuromagnetic study of the functional organization of the human auditory cortex. *Audiology and Neuro-Otology*, 3, pp.191–213.
- Makeig, S. et al., 2002. Dynamic brain sources of visual evoked responses. *Science (New York, N.Y.)*, 295, pp.690–694.
- Mäkelä, J.P., 1988. Contra- and ipsilateral auditory stimuli produce different activation patterns at the human auditory cortex. A neuromagnetic study. *Pflugers Arch.* 412(1-2), pp.12–16.
- Mäkelä, J.P. et al., 1993. Functional differences between auditory cortices of the two hemispheres revealed by whole-head neuromagnetic recordings. *Human Brain Mapping*, 1, pp.48–56.
- Manford, M. et al., 1992. National General Practice Study of Epilepsy (NGPSE): partial seizure patterns in a general population. *Neurology*, 42, pp.1911-17

- Maquet, P. et al., 1995. Regional cerebral glucose metabolism in children with deterioration of one or more cognitive functions and continuous spike-and-wave discharges during sleep. *Brain*, 118, pp.1497–1520.
- Martin, B.A., Tremblay, K.L. & Korczak, P., 2008. Speech evoked potentials: from the laboratory to the clinic. *Ear & Hearing*, 29, pp.285–313.
- Mazzucchi et al., 1985. Hemispheric prevalence changes in partial epileptic patients on perceptual and attentional tasks. *Epilepsia*, 26, pp.279-390.
- Mazzucchi, A. & Parma, M., 1978. Responses to dichotic listening tasks in temporal epileptics with or without clinically evident lesions. *Cortex; a journal devoted to the study of the nervous system and behavior*, 14, pp.381–390.
- Meneguello, J. et al., 2006. Auditory processing in patients with temporal lobe epilepsy. *Braz. J. Otorhinolaryngol.*, 72(4), 496-504.
- Merrifield, W.S. et al., 2007. Hemispheric language dominance in magnetoencephalography : Sensitivity , specificity , and data reduction techniques. *Methods*, 10, pp.120–128.
- Merzenich, M.M. & Brugge, J.F., 1973. Representation of the cochlear partition of the superior temporal plane of the macaque monkey. *Brain research*, 50, pp.275–296.
- Middlebrooks, J.C., Makous, J.C. & Green, D.M., 1989. Directional sensitivity of sound-pressure levels in the human ear canal. *The Journal of the Acoustical Society of America*, 86, pp.89–108.
- Moore, B.C. J. & Vickers, D.A., 1997. The role of spread excitation and suppression in simultaneous masking. *The Journal of the Acoustical Society of America*, 102, pp.2284–2290.
- Moore, B. C. J., 2008. *Cochlear hearing loss: physiological, psychological and technical issues*, 2<sup>nd</sup> Ed. Chichester: John Wiley & Sons Ltd.
- Moore, B.C.J., 2008. Basic auditory processes involved in the analysis of speech sounds. *Philosophical Transactions of the Royal Society B: Biological Sciences*, 363, pp.947–963.
- Moore, B.C.J., 2004. Dead regions in the cochlea: conceptual foundations, diagnosis, and clinical applications. *Ear and hearing*, 25, pp.98–116.
- Moore, D.R., 1991. Anatomy and physiology of binaural hearing. *Audiology*, 30, pp.125–34.
- Moore, D.R., 2007. Auditory processing disorders: Acquisition and treatment. *Journal of Communication Disorders*, 40, pp.295–304.
- Moore, J.K. & Linthicum, F.H., 2007. The human auditory system: a timeline of development. *International journal of audiology*, 46, pp.460–478.
- Moss, F., Ward, L.M. & Sannita, W.G., 2004. Stochastic resonance and sensory information processing: a tutorial and review of application. *Clin Neurophysiol*, 115, pp.267–281.
- Näätänen, R., 1990. The role of attention in auditory information processing as revealed by event-related potentials and other brain measures of cognitive function. *Behavioral and Brain Sciences*, 13, pp.201–233.

- Näätänen, R. & Picton, T., 1987. The N1 wave of the human electric and magnetic response to sound: a review and an analysis of the component structure. *Psychophysiology*, 24, pp.375–425.
- Nakagome, K. et al., 1998. Overnight effects of triazolam on cognitive function: An event-related potentials study. *Neuropsychobiology*, 38, pp.232–240.
- Ngugi, A.K. et al., 2010. Estimation of the burden of active and life-time epilepsy: A meta-analytic approach. *Epilepsia*, 51, pp.883–890.
- Nitschmann, M., Verhey, J.L. & Kollmeier, B., 2010. Monaural and binaural frequency selectivity in hearing-impaired subjects. *International journal of audiology*, 49(5), pp.357–67.
- Noffsinger, D., Martinez, C.D. & Schaefer, A.B., 1982. Auditory brainstem responses and masking level differences from persons with brainstem lesion. *Scandinavian audiology. Supplementum*, 15, pp.81–93.
- Norman-Haignere, S., Kanwisher, N. & McDermott, J.H., 2013. Cortical pitch regions in humans respond primarily to resolved harmonics and are located in specific tonotopic regions of anterior auditory cortex. *The Journal of Neuroscience*, 33, pp.19451–69.
- Nozza, R.J., 1987. The binaural masking level difference in infants and adults: Developmental change in binaural hearing. *Infant Behavior and Development*, 10, pp.105–110.
- Nozza, R.J., Wagner, E.F. & Crandell, M.A., 1988. Binaural release from masking for a speech sound in infants, preschoolers, and adults. *Journal of speech and hearing research*, 31, pp.212–218.
- Oades, R.D.I. et al., 1988. Event-related potentials in autistic and healthy children on an auditory choice reaction time task. *International Journal of Psychophysiology*, 6, pp.25–31.
- Ogura, Y. & Sekihara, K., 1993. Relationship between dipole parameter estimation errors and measurement conditions in magnetoencephalography. *IEEE Transactions on Biomedical Engineering*, 40, pp.919–924.
- Oh, E.L., Wightman, F. & Lutfi, R.A., 2001. Children's detection of pure-tone signals with random multitone maskers. *The Journal of the Acoustical Society of America*, 109, pp.2888–2895.
- Okamoto, H. et al., 2007. Left hemispheric dominance during auditory processing in a noisy environment. *BMC Biology*, 5, p.52.
- Olsho, L.W., Koch, E.G. & Halpin, C.F., 1987. Level and age effects in infant frequency discrimination. *The Journal of the Acoustical Society of America*, 82, pp.454–464.
- Ortiz, K.Z. et al., 2009. Nonverbal dichotic test in epilepsy. *Neuropsychologia*, 3(2), pp.108–113.
- Oxenham, A.J. & Plack, C.J., 1998. Suppression and the upward spread of masking. *The Journal of the Acoustical Society of America*, 104, pp.3500–3510.
- Ozmenek, O.A. et al., 2008. The role of event related potentials in evaluation of subclinical cognitive dysfunction in epileptic patients. *Acta neurologica Belgica*, 108, pp.58–63.
- Paetau, R. et al., 1995. Auditory evoked magnetic fields to tones and pseudowords in healthy children and adults. *J. Clin. Neurophysiol.*, 12, pp.177–185.

- Pang, E.W. et al., 2003. Localization of auditory N1 in children using MEG : source modeling issues. *International Journal of Psychophysiology*, c, pp.27–35.
- Pang, E.W. & Taylor, M.J., 2000. Tracking the development of the N1 from age 3 to adulthood: an examination of speech and non-speech stimuli. *Clinical Neurophysiology*, 111, pp.388–397.
- Pantev, C. et al., 1989. Neuromagnetic evidence of an amplitopic organization of the human auditory cortex. *Electroencephalography and clinical neurophysiology*, 72, pp.225–231.
- Pantev, C. et al., 1995. Specific tonotopic organizations of different areas of the human auditory cortex revealed by simultaneous magnetic and electric recordings. *Electroencephalography and Clinical Neurophysiology*, 94, pp.26–40.
- Pardo, P.J., Mäkelä, J.P. & Sams, M., 1999. Hemispheric differences in processing tone frequency and amplitude modulations. *Neuroreport*, 10(14), pp. 3081-6.
- Pascual-Marqui, R.D., 2002. Standardized low-resolution brain electromagnetic tomography (sLORETA): technical details. *Methods and findings in experimental and clinical pharmacology*, 24 Suppl D, pp.5–12.
- Pekkonen, E. et al., 1995. Automatic auditory discrimination is impaired in Parkinson's disease. *Electroencephalography and clinical neurophysiology*, 95, pp.47–52.
- Penagos, H., Melcher, J.R. & Oxenham, A.J., 2004. A Neural Representation of Pitch Saliency in Nonprimary Human Auditory Cortex Revealed with Functional Magnetic Resonance Imaging. *Trends in Cognitive Sciences*, 24(30), pp.6810 – 6815.
- Pfurtscheller, G. & Lopes Da Silva, F.H., 1999. Event-related EEG/MEG synchronization and desynchronization: Basic principles. *Clinical Neurophysiology*, 110, pp.1842–1857.
- Phillips, D.P., 1988. Effect of tone-pulse rise time on rate-level functions of cat auditory cortex neurons: excitatory and inhibitory processes shaping responses to tone onset. *Journal of neurophysiology*, 59, pp.1524–1539.
- Phillips, D.P., 1990. Neural representation of sound amplitude in the auditory cortex: Effects of noise masking. *Behavioural Brain Research*, 37, pp.197–214.
- Phillips, D.P. & Hall, S.E., 1986. Spike-rate intensity functions of cat cortical neurons studied with combined tone-noise stimuli. *The Journal of the Acoustical Society of America*, 80, pp.177–187.
- Phillips, D.P. & Kelly, J.B., 1992. Effect of Continuous Noise Maskers on Tone-evoked Potentials in Cat Primary Auditory Cortex Tone Pulse Amplitude ( dB SPL ). *Cerebral Cortex*, 2, pp. 134-140
- Picton, T.W. et al., 1977. Evoked-potential audiometry. *J. Otolaryngol.*, 6, pp.90-119.
- Picton, T.W. & Taylor, M.J., 2007. Electrophysiological evaluation of human brain development. *Developmental neuropsychology*, 31, pp.249–278.
- Poeppl, D. et al., 1996. Task-induced asymmetry of the auditory evoked M100 neuromagnetic field elicited by speech sounds. *Cognitive Brain Research*, 4, pp.231–242.
- Poeppl, D., 2003. The analysis of speech in different temporal integration windows: Cerebral lateralization as 'asymmetric sampling in time.' *Speech Communication*. pp. 245–255.

- Ponton, C. et al., 2002. Maturation of human central auditory system activity: separating auditory evoked potentials by dipole source modeling. *Clinical Neurophysiology*, 113, pp.407–420.
- Ponton, C.W. et al., 1996. Maturation of human cortical auditory function: differences between normal-hearing children and children with cochlear implants. *Ear Hear.*, 17, pp.430–437.
- Poulsen, C., Picton, T.W. & Paus, T., 2007. Age-Related Changes in Transient and Oscillatory Brain Responses to Auditory Stimulation in Healthy Adults 19–45 Years Old. *Cereb Cortex*, 17(6), pp. 1454-67.
- Pumplin, J. 1985. Low-noise noise. *J. Acoust. Soc. Am.*, 78, pp.100-4
- Quraan, M.A. et al., 2011. Detection and localization of hippocampal activity using beamformers with MEG: A detailed investigation using simulations and empirical data. *Human Brain Mapping*, 32, pp.812–827.
- Rayleigh, Lord, 1907. XII. On our perception of sound direction. *Philosophical Magazine Series 6*, 13, pp.214–232.
- Reite, M. et al., 1994. Auditory M100 component 1: relationship to Heschl's gyri. *Cognitive Brain Research*, 2, pp.13–20.
- Van Rijckevorsel, K., 2006. Cognitive problems related to epilepsy syndromes, especially malignant epilepsies. *Seizure*, 15, pp.227–234.
- Rita, R., Rinne, T. & Näätänen, R., 2002. Maturation of cortical sound processing as indexed by event-related potentials. *Clinical Neurophysiology*, 113, pp.870–882.
- Roberts, T.P. et al., 2000. Latency of the auditory evoked neuromagnetic field components: stimulus dependence and insights toward perception. *Journal of clinical neurophysiology*, 17, pp.114–129.
- Robinson, S. E. & Vrba, J. 1998. Functional neuroimaging by synthetic aperture magnetometry (SAM). In: T. Yoshimoto, M. Kotani, S. Kuriki, H. Karibe, N. Nakasoto (Eds.). *Recent advances in biomagnetism*. Sendai: Tohoku University Press. pp.302-5
- Roeser, R. et al., 1972. Effects of intensity on dichotically presented digits. *J Auditory Res.*, 12, pp.184-186.
- Rojas, D.C. et al., 1998. Developmental changes in refractoriness of the neuromagnetic M100 in children. *Neuroreport*, 9(7), pp.1543–7.
- Romani, G.L., Williamson, S.J. & Kaufman, L., 1982. Tonotopic organization of the human auditory cortex. *Science*, 216, pp.1339-1340
- Rosburg, T. et al., 2004. Effects of lorazepam on the neuromagnetic mismatch negativity (MMNm) and auditory evoked field component N100m. *Neuropsychopharmacology*, 29(9), pp. 1723-33.
- Roush, J. & Tait, C.A., 1984. Binaural fusion, masking level differences, and auditory brainstem responses in children with language-learning disabilities. *Ear and Hearing*, 5, pp.37-41
- Ruff, R.M., Hersh, N.A. & Pribram, K.H., 1981. Auditory spatial deficits in the personal and extrapersonal frames of reference due to cortical lesions. *Neuropsychologia*, 19, pp.435–443.

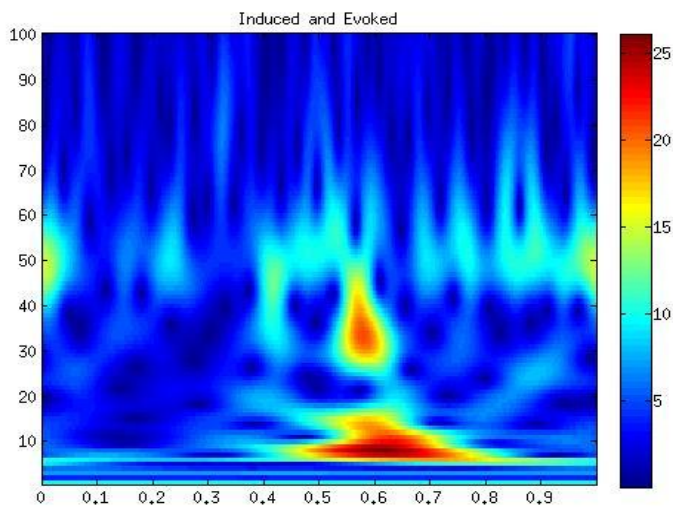
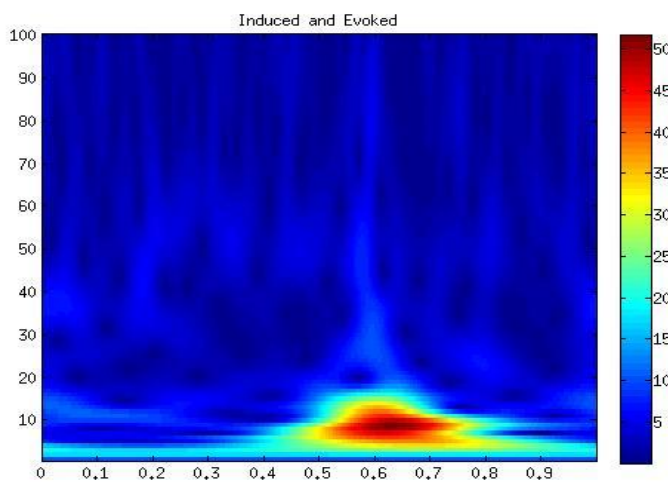
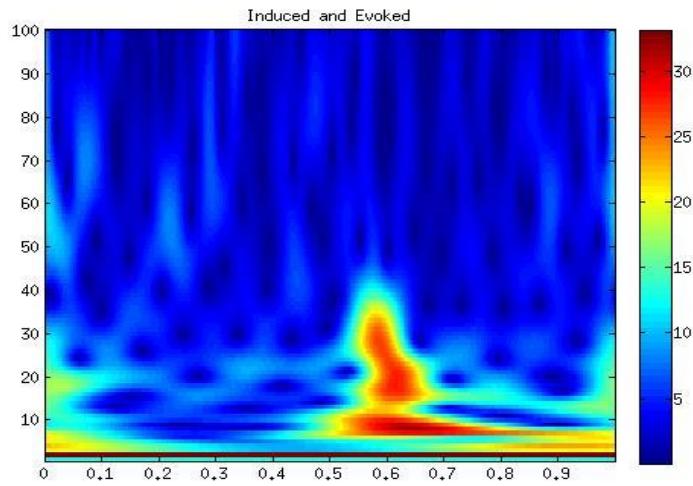
- Sasaki, T. et al., 2005. Neuromagnetic evaluation of binaural unmasking. *NeuroImage*, 25(3), pp.684–9.
- Schneider, B.A. & Parker, S., 1990. Intensity discrimination and loudness for tones in broadband noise. *Perception & psychophysics*, 47, pp.92–94.
- Schneider, B.A. & Trehub, S.E., 1992. Source of developmental change in auditory sensitivity. In: L.A. Werner & E.W. Rubel (Eds.) *Developmental psychoacoustics*, Washington D.C.: American Psychological Association, pp.3-46
- Schönwiesner, M., Rübsamen, R. & von Cramon, D.Y., 2005. Hemispheric asymmetry for spectral and temporal processing in the human antero-lateral auditory belt cortex. *Eur J Neurosci.*, 22(6), pp. 1521-8.
- Sedley, W. et al., 2012. Gamma band pitch responses in human auditory cortex measured with magnetoencephalography. *NeuroImage*, 59, pp.1904–1911.
- Seither-Preisler, A. et al., 2004. Interaction between the neuromagnetic responses to sound energy onset and pitch onset suggests common generators. *European Journal of Neuroscience*, 19, pp.3073–3080.
- Semlitsch, H. V, Anderer, P. & Saletu, B., 1995. Acute effects of the anxiolytics suriclone and alprazolam on cognitive information processing utilizing topographic mapping of event-related brain potentials (P300) in healthy subjects. *Eur Clin J Pharmacol*, 49(3), pp.183-91.
- Seri, S., Cerquiglini, A. & Pisani, F., 1998. Spike-induced interference in auditory sensory processing in Landau-Kleffner syndrome. *Electroencephalography and clinical neurophysiology*, 108, pp.506–510.
- Shahin, A.J., 2011. Neurophysiological influence of musical training on speech perception. *Frontiers in psychology*, 2, p.126.
- Sigalovsky, I.S., Fischl, B. & Melcher, J.R., 2006. Mapping an intrinsic MR property of gray matter in auditory cortex of living humans: a possible marker for primary cortex and hemispheric differences. *NeuroImage*, 32, pp.1524–1537.
- Sinton, C.M. et al., 1986. Modulation of auditory evoked magnetic fields by benzodiazepines. *Neuropsychobiology*, 16, pp.215–218.
- Sowell, E.R. et al., 1999. Localizing age-related changes in brain structure between childhood and adolescence using statistical parametric mapping. *NeuroImage*, 9, pp.587-597.
- Spillman, L. & Ehrenstein, W.H. 1996. From neuron to Gestalt: mechanisms of visual perception. In: R. Gregor & U. Windhorst (Eds.). *Comprehensive human physiology*. Berlin:Springer, pp.861-893.
- Staden, U. et al., 1998. Language dysfunction in children with rolandic epilepsy. *Neuropediatrics*, 29, pp.242-248.
- Stern, R.M. & Trahiotis, C., 1998. Binaural mechanisms that emphasize consistent interaural timing information over frequency. In: A. R. Palmer, A. Rees, A.Q. Summerfield & R. Meddis (Eds.) *Psychophysical and Physiological Advances in Hearing*. London: Whurr, pp.384-395
- Stufflebeam, S.M. et al., 1998. Peri-threshold encoding of stimulus frequency and intensity in the M100 latency. *Neuroreport*, 9(1), pp.91–4.

- Stufflebeam, S.M., Poeppel, D. & Roberts, T.P., 2000. Temporal encoding in auditory evoked neuromagnetic fields: stochastic resonance. *Neuroreport*, 11, pp.4081–4085.
- Suga, N & Manabe, T., 1982. Neural basis of amplitude-spectrum representation in auditory cortex of the mustached bat. *Journal of Neurophysiology*, 47, pp.225-255
- Sussman, E. et al., 2008. The maturation of human evoked brain potentials to sounds presented at different stimulus rates. *Hearing Research*, 236, pp.61–79.
- Sweetow, R.W. & Reddell, R.E., 1978. The use of masking level differences in the identification of children with perceptual problems. *Journal of the American Audiology Society*, 4, pp.52-56.
- Talairach, J. & Tournoux, P., 1988. *Co-Planar Stereotaxis Atlas of the Human Brain*, New York: Thieme
- Talavage, T.M. et al., 2004. Tonotopic organization in human auditory cortex revealed by progressions of frequency sensitivity. *Journal of neurophysiology*, 91, pp.1282–1296.
- Taniguchi, I. & Nasu, M., 1993. Spatio-temporal representation of sound intensity in the guinea pig auditory cortex observed by optical recording. *Neuroscience Letters*, 151, pp.178–181.
- Tanriverdi, F. et al., 2009. Evaluation of cognitive performance by using P300 auditory event related potentials (ERPs) in patients with growth hormone (GH) deficiency and acromegaly. *Growth Hormone and IGF Research*, 19, pp.24–30.
- Taulu, S. & Kajola, M., 2005. Presentation of electromagnetic multichannel data: The signal space separation method. *Journal of Applied Physics*, 97(12), pp. 124905-124905-10
- Taulu, S. & Simola, J., 2006. Spatiotemporal signal space separation method for rejecting nearby interference in MEG measurements. *Physics in medicine and biology*, 51, pp.1759–1768.
- Tiihonen, J., Hari, R., Hämäläinen, M.S., 1989. Early deflections of cerebral magnetic responses to median nerve stimulation. *Electroencephalogr. Clin. Neurophysiol.*, 74, pp.290-296
- Thompson, P.M. et al., 2000. Mathematical/computational challenges in creating deformable and probabilistic atlases of the human brain. *Human Brain Mapping*, 9, pp.81-92.
- Tonnquist-Uhlen, I. et al., 2003. Maturation of the human central auditory system activity: the T-complex. *Clinical Neurophysiology*, 114, pp.685–701.
- Tonnquist-Uhlén, I., Borg, E. & Spens, K.E., 1995. Topography of auditory evoked long-latency potentials in normal children, with particular reference to the N1 component. *Electroencephalography and clinical neurophysiology*, 95(1), pp.34–41.
- Treuhub, S.E. et al., 1988. Auditory Sensitivity in School-Age Children. *Journal of Experimental Child Psychology*, 46, pp.273–285.
- Turetsky, B., Raz, J. & Fein, G., 1990. Representation of multi-channel evoked potential data using a dipole component model of intracranial generators: application to the auditory P300. *Electroencephalography and clinical neurophysiology*, 76, pp.540–556.
- Uusitalo, M.A. & Ilmoniemi, R.J., 1997. Signal-space projection method for separating MEG or EEG into components. *Medical and Biological Engineering and Computing*, 35(2), pp. 135-140.

- Vasama, J.P. et al., 1995. Effects of intensity variation on human auditory evoked magnetic fields. *Acta Otolaryngol*, 115, pp.616–621.
- Van Veen, B.D. et al., 1997. Localization of brain electrical activity via linearly constrained minimum variance spatial filtering. *IEEE transactions on bio-medical engineering*, 44(9), pp.867–80.
- Verleger, R. et al., 1997. Event-related potentials suggest slowing of brain processes in generalized epilepsy and alterations of visual processing in patients with partial seizures. *Cognitive Brain Research*, 5, pp.205–219.
- Viemeister, N.F. & Schlauch, R.S., 1992. Issues in infant psychoacoustics. In: L.A. Werner & R.W. Rubel (Eds.) *Developmental psychoacoustics*, Washington D.C.:American Psychological Association, pp.191-210
- Virtanen, J. et al., 1998. Replicability of MEG and EEG measures of the auditory N1/N1m-response. *Electroencephalography and Clinical Neurophysiology*, 108, pp.291–298.
- Ward, L.M. et al., 2006. Neural synchrony in stochastic resonance, attention, and consciousness. *Canadian journal of experimental psychology*, 60, pp.319–326.
- Weber, D.L., 1983. Do off-frequency simultaneous maskers suppress the signal? *The Journal of the Acoustical Society of America*, 73, pp.887–893.
- Werner, L.A. & Bargones, J.Y., 1991. Sources of auditory masking in infants: distraction effects. *Perception & psychophysics*, 50, pp.405–412.
- Werner, L.A. & Bargones, J.Y., 1992. Psychoacoustic development of human infants. In: C. Rovee-Collier & L. Lipsitt (Eds.) *Advances in infancy research*, Norwood:Ablex, pp.103-45
- Werner, L.A. & Boike, K., 2001. Infants' sensitivity to broadband noise. *The Journal of the Acoustical Society of America*, 109, pp.2103–2111.
- Werner, L.A. & Marean, G.C., 1996. *Human auditory development*. Boulder: Westview Press
- Wetherill, G.B. & Levitt, H., 1965. Sequential estimation of points on a psychometric function. *The British journal of mathematical and statistical psychology*, 18, pp.1–10.
- Wickens, T.D., 2002. *Elementary signal detection theory*, Oxford: Oxford University Press.
- Wightman, F.L., 1969. Binaural masking with sine-wave maskers. *The Journal of the Acoustical Society of America*, 45(1), pp.72–8.
- Wightman, F.L., 1992. & Allen, P., 1992. Individual differences in auditory capability among preschool children. In: L.A. Werner & E.W. Rubel (Eds.) *Developmental psychoacoustics*, Washington D.C.: American Psychological Association, pp.113-133
- Wightman, F. L., McGee, T. & Kramer, M., 1977. Factors influencing frequency selectivity in normal and hearing-impaired listeners. In E. F. Evans & J.P. Wilson (Eds.) *Psychophysics and Physiology of Hearing*. London:Academic.
- Witton, C. et al., 2012. Sensory thresholds obtained from MEG data: Cortical psychometric functions. *NeuroImage*, 63, pp.1249–1256.

- Woldorff, M.G. et al., 1993. Modulation of early sensory processing in human auditory cortex during auditory selective attention. *Proceedings of the National Academy of Sciences of the United States of America*, 90, pp.8722–8726.
- Wolpaw, J.R. & Penry, J.K., 1975. A temporal component of the auditory evoked response. *Electroencephalography and Clinical Neurophysiology*, 39(6), pp.609–620.
- Wong, W.Y.S. & Stapells, D.R., 2004. Brain stem and cortical mechanisms underlying the binaural masking level difference in humans: an auditory steady-state response study. *Ear and hearing*, 25, pp.57–67.
- Woods, D.L., Hillyard, S.A. & Hansen, J.C., 1984. Event-related brain potentials reveal similar attentional mechanisms during selective listening and shadowing. *Journal of experimental psychology. Human perception and performance*, 10, pp.761–777.
- Wright, C.G., 1997. Development of the human external ear. *J. Am. Acad. Audiol.*, 8(6), pp.379-82
- Wunderlich, J.L., Cone-Wesson, B.K. & Shepherd, R., 2006. Maturation of the cortical auditory evoked potential in infants and young children. *Hearing Research*, 212, pp.185–202.
- Yost, W.A., 1997. The cocktail party problem: Forty years later, in R.H. Gikey & T.R. Anderson (Eds.) *Binaural and Spatial Hearing*. Hillsdale, NJ: Lawrence Earlbaum Associates, pp. 329-348
- Zatorre, R.J. & Belin, P., 2001. Spectral and temporal processing in human auditory cortex. *Cerebral cortex*, 11, pp.946–53.
- Zatorre, R.J., Belin, P. & Penhune, V.B., 2002. Structure and function of auditory cortex: Music and speech. *Trends in Cognitive Sciences*, 6, pp.37–46.
- Zatorre, R.J. & Penhune, V.B., 2001. Spatial localization after excision of human auditory cortex. *Journal of Neuroscience*, 21, pp.6321–6328.
- Zemskaya, A.G., 1998. Polymorphism of the Clinical Course, Diagnosis and Surgical Treatment of Mono- and Multi- focal Epilepsy in Children. *Russian-American Symposium on Clinical and Social Aspects of Epilepsy*, St. Petersburg, p.98
- Zeng, F.G., Fu, Q.J. & Morse, R., 2000. Human hearing enhanced by noise. *Brain Research*, 869, pp.251–255.
- Zurek, P.M. & Durlach, N.I., 1987. Masker-bandwidth dependence in homophasic and antiphase tone detection. *The Journal of the Acoustical Society of America*, 81, pp.459–464.
- Zwicker, E., 1970. Masking and psychological excitation as consequences of the ear's frequency analysis, in R. Plomp & G. F. Smorenburg (Eds.) *Frequency analysis and periodicity detection in hearing*, Leiden:Sijthoff, pp. 376-394.
- Zwicker, E. & Henning, G.B., 1984. Binaural masking-level differences with tones masked by noises of various bandwidths and levels. *Hearing research*, 14, pp.179–183.
- Zwicker, E. & Henning, G.B., 1985. The four factors leading to binaural masking-level differences. *Hearing research*, 19(1), pp.29–47.

## Appendix 1



Example spectrograms exhibiting pilot data to define time-frequency bins for the ER-beamformer. Each division on the x-axis represents 100ms, with 0.5 representing the trigger onset. Most of the power lies within the expected time range for the N1m, and within the lower frequency bands.

## Appendix 2

Participant	Psychophysical BMLD	Sensor M100 Amplitude difference (fT)		Sensor M100 Latency (ms)		Source M100 Amplitude difference (nAm)		Source M100 Latency (ms)	
		Loudest trigger	All triggers	Loudest trigger	All triggers	Loudest trigger	All triggers	Loudest trigger	All triggers
1	16.12	$8.83 \times 10^{-12}$	$1.58 \times 10^{-11}$	15	95	8.39	33.73	36	147
2	18.05	$2.08 \times 10^{-12}$	$1.16 \times 10^{-11}$	-3	21	1.03	21.78	-3	4
3	15.5	$3.31 \times 10^{-12}$	$-9.38 \times 10^{-13}$	5	92	9.89	22.82	-2	67
4	26	$4.67 \times 10^{-12}$	$9.48 \times 10^{-12}$	9	60	9.31	39.31	11	41
5	19.37	$5.12 \times 10^{-12}$	$1.7 \times 10^{-11}$	-17	77	7.41	25.02	8	62
6	17.28	$5.81 \times 10^{-12}$	$6.27 \times 10^{-12}$	-6	48	6.37	24.62	5	55
7	12.62	$7.15 \times 10^{-12}$	$1.83 \times 10^{-11}$	3	50	7.33	23.22	1	28
8	14.87	$1.01 \times 10^{-12}$	$5.22 \times 10^{-12}$	34	20	2.89	16.25	17	-35
9	14.62	$1.32 \times 10^{-12}$	$5.37 \times 10^{-12}$	3	-12	2.79	13.97	-3	29
10	5.8	$2.71 \times 10^{-12}$	$4.29 \times 10^{-12}$	24	-25	4.02	9.03	44	82
11	10.87	$8.16 \times 10^{-12}$	$1.31 \times 10^{-11}$	-15	33	6.27	19.93	-8	-39
12	7.99	$7.32 \times 10^{-12}$	$1.65 \times 10^{-11}$	5	78	6.99	28.26	-2	13
13	15.75	$3.51 \times 10^{-12}$	$1.16 \times 10^{-11}$	23	136	5.82	24.91	29	106
14	19.37	$4.06 \times 10^{-12}$	$1.39 \times 10^{-11}$	19	105	10.24	26.73	18	-46
15	13	$4.04 \times 10^{-12}$	$1.22 \times 10^{-11}$	2	-145	5.29	24.21	3	30
16	14.62	$2.22 \times 10^{-12}$	$1.07 \times 10^{-11}$	14	53	4.32	24.54	11	59
17	14.87	$3.92 \times 10^{-12}$	$6.18 \times 10^{-12}$	6	-5	3.72	11.03	-6	-31

Table showing the computed neural values for unmasking. Amplitude was calculated by subtracting the diotic M100 value from the dichotic value for sensor and source amplitude values. Both the full set of triggers and just the loudest dichotic and diotic trigger were computed. Latency was calculated by subtracting the dichotic from the diotic latency value for sensor and source data in the same manner.

### Appendix 3

<i>Participant</i>	<i>Noise threshold</i>	<i>SpiNo threshold</i>	<i>SONO threshold</i>
3	0.007521	0.06388	0.0727
4	0.00159	0.007	0.085
5	0.00065	0.0049	0.059
6	0.00166	0.024	0.15
7	0.00142	0.011	0.091
8	0.00166	0.02396	0.1499
9	0.0009	0.0107	0.0648

Table shows the psychophysical thresholds obtained for child participants, see Chapter 6.